N and P removal from wastewater: a novel approach by developing innovative media augmented by sequencing batch reactor technology (SBR-CBA)

A thesis

submitted in partial fulfilment

of the requirements for the Degree of

Doctor of Philosophy

at

Lincoln University

by

Parsa Mohajeri

Lincoln University

2020

Pre-Publication of Parts of this Thesis

A patent application has been registered and is under legal review at the moment. The novelty has been approved from AJPark.

Chapter 2 - a manuscript from this section has been submitted as follows:

Mohajeri, P., Smith, C. M., Chau, H. W., & Lehto, N. (2020). Nitrate and Phosphorus Removal Methods from Groundwater and Wastewater: A Review Based on the Biological and Adsorption Methods. *Environmental Chemical Engineering*. In review.

Chapter 3 - a manuscript from this section has been published as follows:

Mohajeri, P., Smith, C. M., Chau, H. W., & Lehto, N. (2020). Powdered ALLODUST/ALLOCHAR Augmented Single Batch Aerobic Reactor (SiBAR) for High Concentration Phosphorous Removal from Agricultural Wastewater. *Journal of Water Process Engineering*, **36**, 101301.

Chapter 4 - a manuscript from this section has been published as follows:

Mohajeri, P., Smith, C. M., Chau, H. W., & Lehto, N. (2020). Optimising the Phosphate Adsoption/Desorption Capacity of a Novel Media from Agricultural Wastewater: ALLODUST. WaterNZ Conference and Expo, Hamilton, New Zealand, November 2020.

Chapter 5 - a manuscript from this section has been published as follows:

Mohajeri, P., Smith, C. M., Chau, H. W., & Lehto, N. (2020). ALLODUST Augmented Activated Sludge Single Batch Anaerobic Reactor (AS-SBAnR) for High Concentration Nitrate Removal from Agricultural Wastewater. *Science of the Total Environment*, **752**, 141905.

Chapter 6 - a manuscript from this section has been submitted as follows:

Mohajeri, P., Smith, C. M., Chau, H. W., & Lehto, N. (2020). Nitrate and Phosphorous Removal from Waterbodies by Floating Treatment Wetland (FTWs) Using *Carex virgata*. *International Journal of Phytoremediation*, in review.

Abstract of a thesis submitted in partial fulfilment of the requirements for the Degree of Doctor of Philosophy .

Abstract

N and P removal from wastewater: a novel approach by developing innovative media augmented sequencing batch reactor technology (SBR-CBA)

by

Parsa Mohajeri

The agriculture sector has many challenges: how to feed a growing global population, and also to mitigate negative impacts on the environment. How can we protect the environment, while producing food and fibre in a sustainable way? Discharge of different contaminants from agricultural, industrial and residential sources threatens the surrounding environment and ecosystems. One of the biggest environmental issues facing New Zealand, and our planet Earth, is N and P contamination of freshwater. Two novel methods in water process engineering were identified and evaluated in this PhD:

1. A powdered media was developed from locally sourced soil minerals and byproducts of the wood processing industry. After use, the novel media can be used as a soil conditioner. The physiochemical properties of ALLODUST were adjusted for the target contaminants. It provided a high area for adsorption and active sites for binding phosphate along with a desirable surfaces and pores for the denitrifier biofilm development. It was able to convert nitrate and phosphate applied to the system in concentrations up to 120 mg L^{-1} and 300 mg L^{-1}, respectively, into passive forms. Field monitoring, regulation guidelines from Environment Canterbury, consultancies reports, and government publications suggest that the media would be suitable for waste water treatment in most commonly encountered NZ conditions.

2. The bioreactor has been designed and constructed with a focus on on user-friendly operation and cost effective components. The bioreactor's agitation system was designed with a novel aeration and stirring design at the bottom of the reactor, which can save a significant amounts of energy, during the operation of the technology.

In Chapter 3, two novel media were developed and the phosphate adsorption capacity of each was determined. In order to explain the adsorption mechanism, a series of the physiochemical experiments along with a morphology study were used. ALLODUST and ALLOCHAR consisted of allophanic soil mineral material sourced from either Horotiu soil or Craigieburn soil , two unique soils that are known to contain allophane minerals. Central Composite Design and Response Surface Methodology were used to design the experiment and model the nature of the response surface of the novel media in the experimental design and to analyze the optimum operational conditions. A Single Batch Aerobic Reactor with Couple Bottom Aertion was consturcted at lab scale. The reactor design was optimized for three ranges of P contamination: 1-50 mg L^{-1} (low range); 51-175 (mid-range); and 176-300 (high range). The ALLODUST novel media demonstrated a higher P adsorption capacity compared to the ALLOCHAR media and Allophane compound itself. The ALLODUST adsorbent dosage of 3 g L^{-1} was the optimum: being able to remove 100% of P up to 50 mg L^{-1} in 30 minutes with the lowest aeration rate (1.5 L min^{-1}) and remove 76% of P up to 300 mg L^{-1} in 450 minutes with the highest aeration rate (7.5 L min^{-1}).

In Chapter 4, the phosphate adsorption results from chapter 3 were optimised. The ALLODUST was designed to be able to neutralise phosphate concentrations representative of contamination from diffuse- and point sources. An elution experiment was used to investigate the adsorption cycle capacity of the media. Both Freundlich and Langmuir adsorption isotherms were used to describe the adsorption behavior of the ALLODUST with phosphate contaminated water. The BET experiment could support the high adsorption capacity of the ALLODUST while the total pore volume was increased by 70% compared to Horotiu soil itself. After seven continuous cycles, ALLODUST could still adsorb a high concentration of the phosphorous with only 13% desorption. The BET experiment could support the high adsorption capacity of the ALLODUST while the total pore volume was increased by 70%

compared to Horotiu soil itself. This result can prove the high adsorption capacity of the ALLODUST in a fixed mode which the legacy phosphorous release could be expected in the lowest amount when it's been used as a filter for the drainage pipes, fluidized media for the reactors, or floating media on the phosphorous contaminated lakes.

In Chapter 5, the mechanisms that underpin the reduction of nitrate concentrations and nitrous oxide (N_2O) emission were investigated in the presence of ALLODUST in an activated sludge process. Two anaerobic-aerobic batch reactors were developed, where the coupled bottom aeration method was used for efficient agitation and aeration in the aerobic reactor. The reactor was run at high nitrate concentrations (110 mg L^{-1}), under anaerobic conditions at low- to long-term contact times (2, 12, and 22 h), while the aerobic period was constant for all the experimental designs (2 h). ALLODUST retained its integrity and stability over the long-term operation. The allophanic soil material is a porous media with a high soil microbial population in anaerobic respiration. Also sawdust will provide an additional habitat for microbial colonization. Surface protonation by a chemical-acidic treatment lead to the development of positive surface charge density and also provided more microsites and nanosites which enhanced the specific surface area favourable for the microorganism's growth. Ions, water, and organic compounds can be retained by the polar sites on the surface. The very low N_2O concentration that was observed in the reactors containing ALLODUST might be the result of N_2O diffusion back into the aqueous phase from the headspace, during the denitrification process. So, it will be available to the bacterial communities on the media's surface for the reduction to N_2 by denitrifiers. The high specific surface area, pore sizes and the porous structure of the media could enhance the N_2O emission control. ALLODUST retained its integrity and stability over the long-term operation. Low ALLODUST concentrations (5.95 g L^{-1}) removed 87% of the NO^-_3-N from the wastewater within 12 h. Further exploration revealed that the same amount of the media was optimal for decreasing N_2O emissions from the anaerobic activated sludge reactor by 80%.

In Chapter 6, the nutrient uptake efficiency of Carex virgata was monitored. The main aim of this chapter was to investigate what rate of N and P concentration can enter a wastewater treatment pond after completing the removal processes in chapters 3-5 and how the Carex virgata can contribute to

the treatment process as a Floating Treatment Wetland system. A mesocosm batch experiment was performed at three different N and P concentrations, where 20 buckets were planted with Carex virgata and then the plants were left to grow for three months. The nitrate and phosphorous removal experiment was conducted in three ranges of contamination. Low-range buckets were set up by adding 10 mg d^{-1} L^{-1} NO_3-N and 0.5 mg d^{-1} L^{-1} PO_4-P. These amounts were 20 mg d^{-1} L^{-1} NO_3-N and 1 mg d^{-1} L^{-1} PO_4-P for average range and 30 mg d^{-1} L^{-1} NO_3-N and 1.5 mg d^{-1} L^{-1} PO_4-P for high-range. The role of the plant uptake in the FTW treatment system was the major in uptake the nitrate and phosphate from wastewater. i.e, 87% of TN and 82% of TP removal resulted from plant uptake.

In Chapter 7, an overall discussion and conclusion of all the chapters is presented.

Keywords: Water process engineering, Wastewater treatment, Water management, Nutrient contamination, Nitrate, Phosphate, Adsorption, Biological reduction.

Acknowledgements

Firstly, I would like to express my sincere gratitude to my supervisor Dr. Carol Smith for the continuous support of my Ph.D study and related research, for her patience, motivation, and immense knowledge. Her guidance helped me in all the time of research and writing of this thesis. I really grateful for all the time she spent discussing the idea to make it mature at different stages.

Many thanks also to my co-supervisors, Dr. Henry Chau and Dr. Niklas Lehto for their valuable advice and support during this PhD research. They've been always reachable and helpful during my research when I needed advice.

I highly appreciate the funding and support from Lincoln University. I also would like to thanks all the technical and analythical staff at Lincoln University specially Neil. Smith and Nigel Beale who helped make my project work possible. I also appreciate all the service and support I received from the University of Canterbury, Department of Chemical and Process Engineering, Mechanical Engineering, and Physical and Chemical Sciences for providing me access to the analytical labs and instruments.

To my wife Mahya, I couldn't make it happen witout you and your support during the past three years. You've been always here with me and faced all the challenges same as me. But, you made it easy with your support, patience, and enthusiasm.

Table of Contents

List of Tables

List of Figures

List of Abbreviations

ACF-LaOH	Lanthanum Hydroxide-Spiked Activated Carbon Fibre
AD	Autotrophic Denitrification
ANOVA	Analysis of Variance
ANZECC	Australian and New Zealand Environment and Conservation Council
APHA	The American Public Health Association
AS-SBAnR	Activated Sludge Single Batch Anaerobic Reactor
ATP	Adenosine Triphosphate
ATP	Adenosine Triphosphate
BD	Biological Denitrification
BP	Biological Process
BPR	Biological Phosphorous Removal
CA	Craigieburn Allophane
CBA	Couple Bottom Aeration
CCD	Central Composite Design
CEC	Cation Exchange Capacity
CPC	Cetylpyridinium Chloride
CTAB	Cetyl Trimethyl Ammonium Bromide
DI	Deionized Water
DO	Dissolved Oxygen
DOC	Dissolved Organic Carbon
DOE	Design of Experiment
DPAOs:	Denitrifying Phosphorus Accumulating Organisms
EBPR	Enhanced Biological Phosphorous Removal
EC	Electrical Conductivity
ED	Electro dialysis
EDS	Energy Dispersive X-Ray Spectroscopy
EEC	European Economic Community
EPA	The Environmental Protection Agency
FT-IR	Fourier-Transform Infrared Spectroscopy
FTWs	Floating Treatment Wetlands
GAO	Glycogen Accumulating Organisms
GC	Gas Chromatography
GHG	Green House Gas
HD	Heterotrophic Denitrification
HDPyCl	Hexadecylpyridinium Chloride
HTx:	Hydrotalcites
IEP	Ion-Exchange Process
MCL	Maximum Contaminant Level
NBOM	Non-biodegradable organic matters
NIWA	The National Institute of Water and Atmospheric Research
NZVI	Nano Zero-Valent Iron oxide
PAOs	Phosphorus Accumulating Organisms
PCA	Powdered Craigieburn Allophane
PEI	Polyethylenimine
PHAs	Polyhydroxyalkanoates
PFR	Piston Flow Reactor

PVA	Powdered Volcanic Allophane
RAS	Returned Activated Sludge
RO	Reverse Osmosis
RSM	Response Surface Methodology
SBR	Sequencing Batch Reactor
SEM	Scanning Electron Microscope
SiBAR	Single Batch Aerobic Reactor
VA	Volcanic Allophane
VFAs	Volatile Fatty Acids
WAS	Waste Activated Sludge
WHO	World Health Organization
WLFs	Water Level Fluctuations
XRD	X-ray powder diffraction
XRF	X-ray fluorescence

Chapter 1

Introduction

1.1 Background

Nitrate and Phosphorus contamination of surface water and groundwater is a global issue; and there is a primary need to reduce the potential for eutrophication. This issue is mandated and common in many countries specially relating to the agriculture industry and has simulated significant research interest. Understanding the current methods of nitrate and phosphorus removal from water and wastewater, the influences of process conditions and performances of various research findings are all vital for choosing the best technique to enable remediation of waters contaminated with N and P. In this thesis, engineered processes of N and P removal from wastewater are discussed. Several industrial methods are available to remove N and P from water: including biological treatment; membrane processes; ion-exchange; chemical precipitation; and adsorption. Nitrate removal from wastewater can be accomplished through microbial mechanisms while most of the prevailing phosphorus removal techniques utilize adsorption based technology. A comparative study is needed to provide a better understanding of the advantages and disadvantages of these techniques to choose the best strategy when faced with high concentrations of both N and P in water and wastewater.

The specific focus of my research is the remediation of wastewater discharge from an agricultural source, by developing a wastewater process method for the target contaminants. I have used a fertiliser distribution yard as an example agricultural source. I have used a combination of bioreactor technology, floating treatment wetlands, and mathematical modelling. The fertiliser company has a resource consent to discharge wastewater from their distribution depot, to 1.6 ha of land, adjacent to their distribution yard. The wastewater contains various species of nitrate, phosphate and there may be other species as yet undetermined which could include heavy metals and some hydrocarbons. The fertiliser company has consent to discharge up to 200 kg N/ha/yr. Wastewater (containing the wash downs from the distribution yard) is collected in a treatment pond and discharged to the land. Currently, they have occasions during the year when they have to pay to transport the

wastewater off site, as they can't dispose of the excess wastewater volume and its associated N content, within the conditions of the resource consent.

The significance of finding a solution to this challenge is that there are many similar fertiliser distribution depots in New Zealand, where constraints to wastewater discharge exist. In addition, there are other land management practices impacting on surface water quality and nitrate concentration (Foote et al., 2015). So, the issue of surface and ground water quality as related to nitrate contamination is an environmental issue of concern, both in Canterbury, New Zealand and globally(Fernández et al., 2017). Finding a near market solution to an existing problem such as this will allow us to explore the potential of applying our research findings to other fertilizer depots and land management practices associated with surface water quality, both in Canterbury and in New Zealand. The challenge is to find a (sustainable) way to remove the N and P from the wastewater. The collaboration between university and the industry is increasingly perceived as a strategy to enhance innovation through knowledge exchange. The main aim of this research revolves around designing a sustainable method for removing N and P from wastewater prior to land application. The tangible research outputs will thus contribute to our knowledge around mitigating excess nutrient flux to soils. It will allow us to move towards solving a significant environmental problem associated with the primary production sector in New Zealand.

1.2 Research Objectives

The objectives of this PhD research programme were to:

- Develop new and innovative material (low tech and cost effective) which combine OM and soil derived mineral material compounds: referred to thereafter as ALLODUST.

- Design a lab-scaled reactor and run the developed ALLODUST in order to remove different P and N concentrations from aqueous solution. Model and optimise the system using mathematical and numerical designing software.

- Operate the reactor in sequence with a mesocosm experiment with a NZ native plant to quantify the contribution of plants uptake to N and P removal in a FTW system.

- Evaluate the combined effectiveness of innovative materials and plant sequestration in a FTW system to determine the minimum contact time required for effective wasteater treatment.

1.3 Research Hypothesis

1. Incorporation of allophane with organic matter (as innovative materials called ALLODUST and ALLOCHAR) and single batch aerobic reactor (SiBAR) will remove high concentration of phosphate from wastewater in a low contact time.

2. The use of an innovative material (ALLODUST or ALLOCHAR) and activated sludge single batch anaerobic reactor (AS-SBAnR) will reduce nitrate-nitrogen concentration in wastewater at an optimal and at a low contact time and energy consumption.

3. Native wetland plant (*Carex virgata*) has an optimum uptake capacity to be used as a FTW system plantation and is able to remove excess nitrate-nitrogen and phosphate contamination in effluent out of the designed treatment system in a pond system (point source).

1.4 Thesis Structure

This thesis is divided into 7 chapters. The first chapter provides an overview of the thesis topic and the second chapter provides a review of the relevant literature. The next four chapters contain a short introduction and a materials and methods section, and then presents and discusses the results of the experiments conducted. The seventh chapter summarises the overall findings of this thesis and provides directions for future research. The final chapter presents the industrial design plans. The experimental road map presented in Figure 1.1.

Chapter 1

This chapter gives a general overview of the topic of this thesis, the research objectives, and an outline of the thesis structure.

Chapter 2

This chapter summarises the background knowledge in a literature review and provides the reasoning and justification for the research conducted in this PhD thesis.

Chapter 3

- This chapter evaluates the P adsorption process of the system. The media preparation and lab scaled reactor design is presented and the efficiency of the developed system is determined using different concentrations of P.

Chapter 4

- The process optimisation and isotherms for P adsorption are presented in this chapter. Several physiochemical experiments which are effective in the adsorption/desorption capacity (cycle) are discussed.

Chapter 5

- This chapter evaluates the Nitrate reduction process system by applying different variables. The N_2O emission from the system during the denitrification process is analysed.

Chapter 6

- This chapter presents the mesocosm experiment and phytoremediation process involved in the FTW system. In order to model the FTW, the N and P uptake capacity of a native plant was determined.

Chapter 7

- This chapter summarises the results from chapters 3-6 and provides recommendations for future study on the topic.

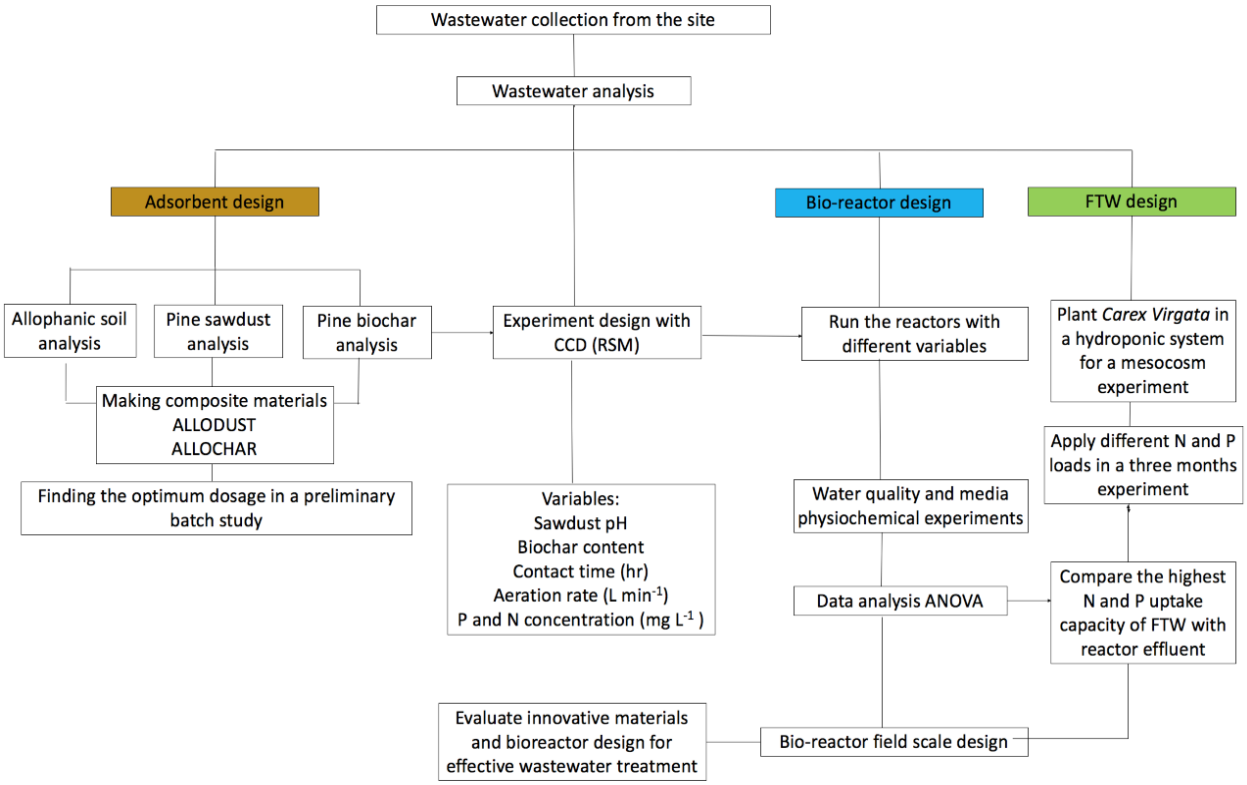

Figure 1.1 Experiment road map.

Chapter 2

Literature review

2.1 Introduction

Discharge of different contaminants from industrial and residential sources threatens the surrounding environment and ecosystems. Anthropogenic activities cause different organic and inorganic contamination of soil and water and of the world's largest source of freshwater which is groundwater (Karan et al., 2014; Smith et al., 2016). The application of groundwater has increased for irrigation, industrial use and drinking purposes over the recent years and it's a vital source for mankind in future years (Smith et al., 2016). Much research is being done on the different technologies to prevent soil and water contamination: by decreasing the bioavailability of contaminants through the adjustment of natural processes, rather than chemical treatment technologies. Stabilization and solidification (H. Liu et al., 2017; L. Wang et al., 2015; B. Zhang et al., 2016), adsorption (Rouquerol et al., 2013; Sanjay et al., 2013), and leaching (Buj et al., 2010; Neupane & Donahoe, 2013) are the main parameters that determine the efficiency of any treatment system. High concentrations of nitrate has been recorded in many parts of the world and it's become a global issue which requires policy and technological intervention to mitigate its impacts on the environment and human health.

Nitrogen could be considered as one of the fundamental pollutants in water which contributes to dissolved oxygen levels, eutrophication effects (excessive richness of nutrients) and toxicity of receiving water bodies. It causes over-simulation of growth of aquatic plants and algae. Excessive growth can clog water intakes and use up DO as they decompose and block light. Both organic and inorganic nitrogen exist in wastewaters (Wu et al., 2009). Total nitrogen is defined as the sum of inorganic and organic nitrogen in wastewater (Ahmed & Lan, 2012). Ammonia nitrogen (NH_3-N), nitrite (NO_2-), nitrate (NO_3-), nitrogen (N_2), nitrous oxide (N_2O) and nitric oxide (NO_2) in soluble or gas form are common inorganic nitrogen in wastewater (Saeed & Sun, 2012).

Nitrate is an anionic pollutant which is possibly the most widespread groundwater contaminant in the world due to its high water solubility. It's the most oxidized form of combined nitrogen for oxygenated systems. Nitrate is stable and chemically unreactive, and

as a part of the nitrogen cycle. Nitrate poses a serious threat to drinking water supplies; when the environmental conditions are favourable, high nitrate content in water promotes eutrophication (Cheng et al., 1997; Y. H. Huang & Zhang, 2004). Several kinds of human activities such as intensive use of fertilizers in agriculture, have led to the higher NO_3^- contamination of ground and surface water sources. High NO_3^- concentrations in drinking water sources pose risks to the environment and public health especially in infants (methemoglobinemia or blue baby syndrome), and the potential formation of carcinogenic nitrosamines. The U.S. Environmental Protection Agency (U.S. EPA) has set a maximum contaminant level (MCL) of 10 mg L^{-1} of NO_3^- in drinking water. Recent model estimates suggest that only 68.2% of NZ river concentration meet the Australian and NZ Guidelines for Fresh and Marine Water Quality (ANZECC) trigger values of nitrate contamination for slightly disturbed upland ecosystems (upland and lowland) of 11.3 mg L^{-1} (as NO_3-N) (ANZECC, 2000). There are several consented and permitted activities in New Zealand for which their discharges contain high concentrations of nutrients; specifically nitrate-nitrogen and phosphate which leaches to the environment. According to a report by Environment Canterbury (Loe, 2012) the highest N numbers belonged to meat and food processing wastewater with 1140 N(t/yr), while super intensive farming and centralised sewage effluent discharges leached the highest amount of P with 150 (t/yr). The total number for N leached from permitted activities discharges was 3135 (t/yr) and 508 (t/yr) for phosphate. The most affected zones by nutrient discharges in the Canterbury region was Ashburton-Rakaia (1078 tN/yr), Ashburton (630 tN/yr), and Selwyn-Waihora (472 tN/yr) respectively. Different contaminant sources contain N and P concentrations which can be a real challenge for a treatment system. The effluent from an on-site sewage system will have concentrations of approximately 60 (gN/m^3) and 15 (gP/m^3). For farm dairy effluent, concentrations would be 0.44 (kgN/m^3) and 0.07 (kgP/m^3) (Loe, 2012).

Water remediation technologies from nitrate is classified in two main categories: Biochemical nitrate and physical (adsorption) nitrate removal (King et al., 2012). Chemical and biochemical methods are designed to reduce nitrate to the other states of nitrogen, e.g. ammonia or a more innocuous form as nitrogen gas. Nitrite, nitrogen dioxide, and nitrous oxide may also be produced, depending on the treatment variables and conditions (Equation 2.1 – 2.3) (Huno et al., 2018; Obiri-Nyarko et al., 2014). On the other hand, nitrate removal methods involve physical processes. These technologies do not necessarily involve any alteration of the

chemical state of nitrate ions; the waste and adsorbents used in these technologies are separately disposed. By considering the removal efficiency, simplicity and cost effective aspects of a treatment, biological nitrate removal is recognized as a preferred method over physiochemical methods (J.-H. Kim et al., 2008). Biological nitrate removal carried out through sequential nitrification (aerobic) and denitrification (anaerobic) can be considered to be the most suitable treatment method for nitrate removal (equation 2.1 - 2.3). However, ammonia nitrogen cannot be degraded by common biological treatment methods. Adsorption by natural adsorbent such as zeolite has been highly cited for ammonia nitrogen removal via cation exchange; and a high concentration of nitrogen (especially in the ammonia form) is well known as a microorganism growth inhibitor (J.-H. Kim et al., 2008). But there is a lack of research for the adsorbent used to remove nitrate from the water. On the other hand, a low concentration of nitrogen in wastewater can prevent microorganisms producing enzymes for organic compound degradation (Ahmed & Lan, 2012). So, several factors are effective to choose the best strategy for the nitrate removal from water.

$$4NH_4 + 7O_2 \longrightarrow 4NO_2^- + 4H^+ + 6H_2O \quad (2.1)$$

$$2NO_2 + O_2 \longrightarrow 2NO_3^- \quad (2.2)$$

$$NO_3^- \longrightarrow NO_2^- \longrightarrow NO \longrightarrow N_2O \longrightarrow N_2 \quad (2.3)$$

Phosphates enter the surface and groundwater bodies from agricultural fertilizer run-off, discharge of effluents, biological wastes and residues (Bowes et al., 2015). Phosphates can also enter surface water bodies due to the runoff of phosphorous-rich sediment (Miller, 2013). Industrial effluents related to corrosion and scale control, chemical processing, and the use of detergents and surfactants contribute significantly to the phosphate content in the water bodies. After being dissolved in water, these are converted to orthophosphates at different rates depending upon their types, the temperature of the water, and the pH. Excessive phosphorus in effluents from wastewater treatment plants has been regarded as a significant cause of eutrophication. When excess phosphate enters water supply systems, it can cause severe health problems such as kidney damage and osteoporosis. To further prevent eutrophication, the U.S. EPA set stringent limits for total phosphorus in natural waters, i.e., 0.1 mg L^{-1} for rivers and 0.05 mg L^{-1} for rivers draining into lakes. Also ANZECC trigger values for the total phosphorus is 0.026 mg L^{-1} for upland rivers and 0.033 mgL^{1} for lowland rivers.

Phosphorus as one of the macro elements essential for organism growth and biosynthesis processes. Furthermore, its concentration during the digestion process of organic pollutants has a specific effect on enhancing the efficiency of biogas production (Khanal, 2008; Pearce & Chertow, 2017). Release through biological phosphorus removal shows a linear correlation with organic carbon (OC) (Ra et al., 2000). Adsorption by natural adsorbents such as zeolite is a highly recognized method of phosphorus removal from wastewater. Due to its specific effect on microorganisms and algal growth and unique role in adsorption of anions through bridging mechanisms on natural adsorbent like zeolite, P is a critical element in any biological treatment system. Also, targeted P-removal from wastewater has become increasingly common in large treatment plants while the potential negative impacts of P release from small treatment plants and also P present in the groundwater has been underestimated (Bowes et al., 2015).

So, a knowledge gap exists to find a sustainable and reliable method to adsorb P and remove (or reduce) N in wastewater treatment systems and from groundwater. The main N and P removal technologies are biological process (BP), Ion-exchange process (IEP), reverse osmosis (RO), electro dialysis (ED), chemical precipitation, and adsorption. But the fact is that all have advantages, disadvantages, and limitations. This review presents a list of nitrate and phosphorus removal technologies based on the biological and adsorption, the removal capacities and mechanisms and will critically discuss the challenges of each.

2.2 Biological process (BP)

2.2.1 Nitrate biological denitrification (BD)

Biological denitrification has been known as a cost effective and a promising method of biological nitrate removal (elimination). Biological nitrate removal can be classified as assimilation into biomass and dissimilation into nitrogen gas and is driven by either autotrophic or heterotrophic microorganisms. Autotrophic microorganisms use inorganic carbon, from sources such as CO_2 and HCO_3- and inorganic matter, such as H_2, reduced sulphur, and Fe^{2+}, as carbon sources and electron donors respectively. On the other hand, the heterotrophic microorganisms need an organic carbon source as electron donor in order to grow rapidly and use the nitrate as an electron acceptor (Huno et al., 2018). The additional carbon source adding to the system can be considered as a secondary pollution. The microalgae and cyanobacteria are the photoautotrophs which use light as an energy source

to eliminate the nitrates. Low amount of biomass generation, non-polluting, and being cost effective are the reasons which made the autotrophic nitrate elimination as an attractive area for the researchers (D. Chen, Dai, et al., 2016). The sulphur-based and hydrogen-based denitrification processes have attracted substantial attention amongst the other autotrophic technologies (D. Chen, Dai, et al., 2016; Z. Wang et al., 2017).

Biological denitrification (BD) due to its selective nitrate reduction to the harmless nitrogen gas without the need for post treatment and any disposal stream and remineralization stage is the most effective and commonly applied technologies. BD is a nitrate elimination process which can occur under anaerobic conditions with minimum sludge production (Shrimali & Singh, 2001; Soares, 2000). There are a couple of drawbacks for this method; the most important one being the contamination risk of the treated water with the denitrifying microorganisms and their metabolic byproducts (C. Liu et al., 2014). Also, the long hydraulic retention time due to the denitrification process is the other criticism to this method(Shrimali & Singh, 2001).

Depending on the source of contaminated water, the BD method can be operated in different ways. The water target could be a groundwater source as a drinking water supply, a contaminated stream or lake which is affected by surrounding agricultural fields, or a contaminated industrial pond. The groundwater bioremediation can be directly performed underground in an aquifer which is an *in-situ* process or can be pumped and transferred to a bioreactor above the ground which in known as an *ex-situ* process (USEPA, 2013). The dynamics of nitrate contamination of groundwater and its attenuation in the subsurface porous unconfined/confined rocks is a complex biogeochemical process which is affected by different variables. The mineral kinetics of water-rock interaction is the other factor which can influence the groundwater chemistry under different conditions (Bourke et al., 2019; Huno et al., 2018; Yidana et al., 2012). An in-situ treatment method is only applicable in a limited number of geological conditions because of the risk of clogging, and slow flow rates in aquifers. Also, substrate distribution control is so complicated due to the inhomogeneity and lack of isotropy of aquifers (Della Rocca et al., 2007). Above ground denitrification is a suitable method for wastewater treatment of contaminated ponds included suspended growth and attached growth (fixed film). In the case of fixed film denitrification, a high surface area is favorable in order to provide a good surface for biofilm growth by microorganism attachment

to the media (Mohseni-Bandpi et al., 2013; Soares, 2000). These media are included in fluidized bed reactors, packed bed reactors, membrane bioreactors, and bio-filters composed of sand, anthracite, activated carbon, calcium carbonate, and sulphur (Aslan & Turkman, 2006; Vasiliadou et al., 2006; X. Wang et al., 2013). The fluidized bed enables a greater denitrification rate per volume; clogging and channelling problems are not of concern. So, fluidized reactor is preferable compared to membrane and packed bed reactors. It's noteworthy that to prevent the breakthrough of the biomass as well as post-filtration requirements for removing contaminants which are carried by gas flow, the fluidized reactors need more process control. Cleaning the system, such as a centrifugal pump, hydrocyclone, and a screen for removing excess biomass and returning the cleaned sand to the reactor are all factors which need to be considered while employing this removal method (Di Capua et al., 2017; Kapoor & Viraraghavan, 1997; Soares, 2000).

So, after choosing the reactor type which could be a fluidized bed or fixed bed reactor, the other important factor is the biomass support which could be performed by ethanol, methanol, acetate, cotton, hydrogen, sulphur, and natural gas. They are used as substrates for microbial denitrification in several researches (Greenan et al., 2009; Schipper et al., 2010; Soares, 2000) . Denitrification bioreactors provide the bacteria with an organic carbon source (the initial amount is important) in a nitrate-enriched (initial concentration is important) and oxygen-poor environment and controlling the HRT, temperature, and pH.

2.2.1.1 Assimilatory and dissimilatory nitrate reduction

Assimilation is nitrate uptake by the cell growth while dissimilation refers to nitrification and denitrification. The reduction of nitrate to (ammonium) and ammonia in the absence of NH_4^+ - N and independent of the dissolved oxygen (DO) concentration is assimilatory nitrate reduction. It occurs for cell synthesizes and during the growth of all forms of microbes including heterotrophs and autotrophs (Krapp et al., 2014; Rezvani et al., 2019). Heterotrophs need a large amount of energy from organic matter degradation which results in a high yield of biomass and the assimilation of a significant amount of nitrogen. Also, nitrate can be assimilated by heterotrophic microorganisms but ammonium is preferable as a nitrogen source when it's present. Conversion of nitrogen to biomass is an important removal method which Kelso et al. showed that around 50% of nitrogen purged from groundwater can be converted to biomass in the presence of certain organic substrates (Kelso et al., 1999).

Autotrophs convert CO_2 to more organic complex forms that are suitable for cell synthesis by using a large amount of energy (equation 2.4 and 2.5). During this process a low biomass yield per unit of acquired energy is produced and hence they have low nitrogen requirements (Rezvani et al., 2019).

Autotrophs reaction:

$$(NH_4^+ \text{ or } NO_3^-) + CO_2 + \text{Autotrophs} \xrightarrow{\text{Energy}} \text{Cell protein (Organic N)} + H_2O \quad (2.4)$$

$$0.04\ NO_3^- + 0.18\ CO_2 + 1.04\ H^+ + e \longrightarrow 0.04\ C_5H_7O_2N + 0.39\ H_2O \quad (2.5)$$

In chemoautotrophs the energy can be provided by either inorganic matter, such as hydrogen, reduced sulphur, and iron and by light in photoautotrophs such as microalgae and cyanobacteria. Ammonium is the preferable form of nitrogen for almost the vast majority of the microorganisms but several species of bacteria and all species of the microalgae are able to reduce nitrate to ammonium for biomass growth (Burghate & Ingole, 2014). Dissimilatory nitrate reduction or denitrification is reduction of the nitrate to nitrogen gas, new cell biomass, and hydroxyl ion which leads to an increase in pH, which is not a concern in denitrification process. Nitrate serves as a terminal electron acceptor instead of oxygen and causes the generation of adenosine triphosphate (ATP). These electrons provided by specific

Inorganic and organic electron donors in both autotrophs and heterotrophs (Ashok & Hait, 2015; Lew et al., 2012). In denitrification, nitrate and nitrite are consumed as electron acceptors for the oxidation of organic and inorganic electron donors which involves energy conservation by increasing the substrate level phosphorylation reaction (equation 2.6). The organisms gain the energy by electron transformation from donor to acceptor and they apply that for the synthesis of new cell mass and the maintenance of the existing one. All these reactions happen only in the lack of oxygen and under anaerobic conditions while denitrification can happen due to a number of species of bacteria in the aerobic condition (Burghate & Ingole, 2014). *Paracoccus* is a variety of bacteria which can survive in different environments and can operate the denitrification process under aerobic conditions.

$$NO_3^- \longrightarrow NO_2^- \longrightarrow NO \longrightarrow N_2O \longrightarrow N_2 \quad (2.6)$$

The reduction process of nitrate to nitrogen gas is complete denitrification. Each step is catalysed by a specific enzyme system and performed by different microorganisms (equations 2.7 – 2.10) (Lew et al., 2012).

$$NO_3^- + 2e + 2H^+ \longrightarrow NO_2^- + H_2O \quad (2.7)$$

$$NO_2^- + 2e + 2H^+ \longrightarrow 0.5\ N_2O + 0.5\ H_2O + OH^- \quad (2.8)$$

$$0.5\ N_2O + e + H^+ \longrightarrow 0.5\ N_2 + 0.5\ H_2O \quad (2.9)$$

$$NO_3^- + 5e + 5H^+ \longrightarrow 0.5\ N_2 + 2\ H_2O + OH^- \quad (2.10)$$

For reduction of nitrate to the nitrogen gas, five electrons are required which is provided by specific organic and inorganic donors. Also from equation 10, for every mole of nitrate that is reduced, 1 mol of hydroxyl ion is released and new cell biomass and increasing in the pH level are the other products of the denitrification (Ashok & Hait, 2015).

2.2.1.2 Heterotrophic nitrate removal

Nitrate removal by biological denitrification is mostly facilitated by heterotrophic bacteria which need an organic carbon source such as methanol, ethanol, glucose, or acetate. Methanol is most widely used at a lower cost compared to the other carbon sources but produces a lower bacterial cell yield (Hamlin et al., 2008; Weigelhofer & Hein, 2015). The alternative organic carbon sources are volatile fatty acids, shredded newspaper, wheat straw, unprocessed short fibre cotton, atrazine, natural methane gas, elemental sulphur, and sugar (glucose syrup) (Aslan & Turkman, 2006).

Pseudomonas and *Bacillus* are the most common heterotrophic denitrifiers which degrade organic carbon to obtain energy for growth and reproduction (Brezonik, 2013). In order for cell synthetisation, respiration and anabolism to occur, both nitrate and organic carbon need to be included in the process (Rezvani et al., 2019). In a denitrification process with the presence of methanol as the carbon source, nitrate is reduced to nitrogen gas, and methanol is converted to water and carbon dioxide during the respiration reaction (Burghate & Ingole, 2014; Mohseni-Bandpi et al., 2013). The following equations (2.11-2.17) describe nitrate dissimilation in heterotrophs in the case of the sodium acetate stoichiometric relation:

$$NO_3^- + 2H^+ + 2e^- \longrightarrow NO_2^- + H_2O\ (\text{reduction}) \quad (2.11)$$

$$CH_3COO^- + 2H_2O \longrightarrow 2CO_2 + 7H^+ + 8e^- \text{ (oxidation)} \quad (2.12)$$

$$4NO_3^- + H^+ + CH_3COO^- \longrightarrow 4NO_2^- + 2CO_2 + 4H_2O \quad (2.13)$$

$$8NO_2^- + 32H^+ + 24e^- \longrightarrow 4N_2 + 16H_2O \text{ (reduction)} \quad (2.14)$$

$$3CH_3COO^- + 6H_2O \longrightarrow 6CO_2 + 21H^+ + 24e^- \text{ (oxidation)} \quad (2.15)$$

Combined: (if in acidic conditions)

$$3CH_3COO^- + 8NO_2^- + 11H^+ \longrightarrow 4N_2 + 10H_2O + 6CO_2 \quad (2.16)$$

If this is happening in basic conditions:

$$3CH_3COO^- + 8NO_2^- + 11H_2O \longrightarrow 4N_2 + 10H_2O + 6CO_2 + 11OH^- \quad (2.17)$$

In a complete cycle of the denitrification under anoxic conditions, nitrogen gas is the product of the process. If the system does not operate under optimum conditions, N_2O will be produced. The effective factors during the denitrification process are (C/N) ratio, sludge age, HRT, organic carbon source, organic loading rate, dissolved oxygen (DO), pH, and temperature. All these parameters can affect the N_2O production in BD (Brenner & Argaman, 1990). (C/N) ratio seems to be the most effective factor in BD and a high amount of carbon source in the influent can lead to the production of inert nitrogen gas N_2 rather than the greenhouse gas N_2O. On the other hand, the excessive amount of carbon in the influent will affect the water quality and when there is an excess amount of unused carbon source in the environment, the treated water quality might not be subjected to chemical oxygen demand (COD) or biological oxygen demand (BOD) limitations. In order to minimize the N_2O and organic carbon production in the effluent it's important to ensure the optimum amount of C/N ratio in BD system.

According to the stoichiometric relationship for the BD process the optimal C/N ratio can be theoretically calculated. For reduction of 1 g of NO_3^-, 0.238 g of CH_3COONa is required. However, the actual amount required by the heterotrophs for a denitrification process

appears to be higher than that obtained from theoretical calculations (Mohseni-Bandpi et al., 2013). The Na^+ would just be a spectator ion, so would be present but wouldn't affect (or be affected by) the reaction. In other words, it doesn't change and is still there after the reaction has occurred. C/N ratio is dependent on the form of carbon source, the stoichiometric relationship and the dependence of the amount of denitrified nitrogen. The concentration of the carbon source in the medium in the stoichiometric relation is linear (Mohseni-Bandpi et al., 2013).

2.2.1.3 Autotrophic nitrate removal

Autotrophic microorganisms and organisms use inorganic matter and oxidizes this to gain energy by transferring the released electron to an acceptor such as nitrate. The denitrifiers use this energy for their metabolism and growth (Table 2.1). The *T.denitrificans* (T: *Thiobacillus*) and *T. thioparus* are the most effective microorganisms to remove the nitrate through the denitrification process by using a reduced sulphur compound (S^{2-} , $S_2O_3^-$, and S^0) as electron donor (Rezvani et al., 2019). Autotrophic denitirification is most likely to happen in the presence of T*. dinitrificans* (Brettar et al., 2006). The other kinds of autotrophic bacteria are *Micrococcus denetrificans* and *Paracoccus denitrificans*, which oxidize H_2 by using nitrate as electron acceptor. It's noteworthy that a number of autotrophics can grow heterotrophically in the absence of an inorganic carbon source by using organic carbon (Kurt et al., 1987).

Table 2.1 Autotrophic nitrate denitrifier's characteristics (Justin & Kelly, 1978; Shrimali & Singh, 2001).

Autotrophic denitrificans	e donor	e acceptor	inorganic carbon source
Paracoccus	Hydrogen	Nitrate	CO_2, HCO_3^-
Thiobacillus	Sulphur/Reduced sulphur compounds	Nitrate	CO_2, HCO_3^-
Gallionella	ferrous iron	Nitrate	CO_2, HCO_3^-
Leptotrix	ferrous iron	Nitrate	CO_2, HCO_3^-
Sphaerotillus	ferrous iron	Nitrate	CO_2, HCO_3^-
Ferrobacillus	ferrous iron	Nitrate	CO_2, HCO_3^-

Autrotrophic denitrifiers have been divided to two main groups; hydrogen-based process in which hydrogen gas is used as the electron donor and sulphur-based process where the

sulphur compounds have been used as the energy source (Table 2.2) (K.-C. Lee & Rittmann, 2002; Moon et al., 2006).

Table 2.2 Physiological properties of autrotrophic denitrifiers (Aslan & Turkman, 2006; Mohseni-Bandpi et al., 2013; Oh et al., 2001).

growth condition	purely mineral medium
Energy source	inorganic substance / hydrogen and sulphur compounds
Carbon source	carbon dioxide and bicarbonate
-Organic substances are not needed, they slow the growth of the autotrophic bacteria (they are not able to decompose organic substances)	

Autohydrogenotrophic denitrification has several advantages compared to the other methods. Cost-effectiveness, low biomass yield, and being a clean technology (as it uses H_2 gas which makes no interference to the biological process stability and there is no need for any post treatment (no acid formation) are a number of the reasons to utilise autohydrogenotrophic bacteria as the denitrification agent. On the other hand, the hydrogen gas supply and the high flammability of hydrogen gas has always been a concern when using this technology (Karanasios et al., 2010; Sakakibara & Kuroda, 1993). In order to convert 1 mg nitrate to dinitrogen, 0.35 mg hydrogen gas is needed theoretically while the practical value is higher (Karanasios et al., 2010). The bio-electrochemical reactors (BER) are able to provide a desirable environment for the autohydrogenotrophic bacteria on the surface of the cathode and can stimulate the culture by an electric current (Karanasios et al., 2010). The reactor types, nitrate loading, C/N ratio, HRT, pH, gas flow rate, temperature, and the sulphur form are the effective parameters and the operational details on the nitrate removal system performance by sulphur and hydrogen based autotrophic bacteria (D. Chen, Yang, et al., 2016; Zhou et al., 2011).

The nitrate removal from groundwater was recently studied by (Taşkın & Cuci, 2019) using a hydrogen-based membrane biofilm reactor. Different hydrogen pressure and HRT was applied to the system at constant nitrate concentration which was 10 mg L^{-1}. The highest hydrogen pressure which was 5 psi, showed the most efficient nitrate removal by 98% while dropping HRT from 12h to 1h didn't affect the system performance. Also, (D. Chen, Yang, et al., 2016) previously studied the effect of a number of operational details on the removal efficiency in autohydrogenotrophic denitrificans. They showed that the optimum pH which inhibited the

system from nitrite accumulation was 6.0-7.0. The removal efficiency increased by 74% while the temperature increased from 20 °C to 35 °C. The presence of biomass was a positive effect which led to 100% removal of nitrate in just 3h. C/N ratio was not an effective factor itself but caused an increase in the system pH which inhibited the reductase's activity to hinder the denitrification process.

In sulphur-based autrotrophic denitrification process, sulphur is oxidized to sulphate as the electron donor and nitrate is reduced to nitrogen gas as electron acceptor. Sulphur and its compounds can be used by the microorganisms for the cell synthesis (Brettar et al., 2006). In research conducted by (Duyar et al., 2018) about removal of nitrate from wastewater which contained 1200 and 1500 mg L^{-1} of COD and SO_4^{2-} respectively, an anaerobic baffled reactor (ABR) was used to remove COD, sulphide, nitrogen (25–1500 mg NH_4^+-N/L), and nitrate (60–300 mg NO_3-N L^{-1} d^{-1}). The autrotrophic denitrification occurred by using the produced sulphide in the initial compartment. Optimum nitrate loading rate was determined as 146 mgNO_3-N L^{-1} d^{-1} at molar N/S ratio of 0.42, corresponding with 100% nitrate, 83% sulphate, and 79% COD removals. In addition, the optimum S/N ratio in this system was 0.42. Thiosulphate is a more effective electron donor than sulphur. The ecological floating beds (EFBs) used by (Sun et al., 2020) which were enriched by sodium thiosulphate, and mixed donors of sodium acetate and sodium thiosulphate. The result showed that both autotrophic and mixtrophic denitrification efficiency was 100%, and ranged from 4 to 43% when the electron donor was not present in the treatment. Also, it was proved that sodium acetate could drop the sulphate concentration in the effluent along with nitrogen oxide emission from the system. The main disadvantage of the sulphur-based autrotrophic denitrification is that it produces 7.54 mg sulphate per one mg of nitrate removal and acid, while thiosulphate generated 35% more sulphate in the system. It's important to consider that the trigger value for the sulphate in drinking water is 250 mg L^{-1} (Uçar et al., 2016). In order to drop the acidity of the treated water an alkalinity source needs to be added to the system and the most common one is limestone because it is cost-effective and increases effluent hardness (Uçar et al., 2016). In order to utilise the sulphur-based autrotrophic denitrification with the highest efficiency it's essential to control alkalinity source and sulphur type/size as the smaller granules can provide higher specific surface area and enhance the denitrification process but tend to clog the system and cause gas entrapment (Rezvani et al., 2019). Also S/N ratio must

be controlled since at low ratios, nitrite accumulation occurs because of the limit in the nitrate to dinitrogen conversion (Figure 2.1).

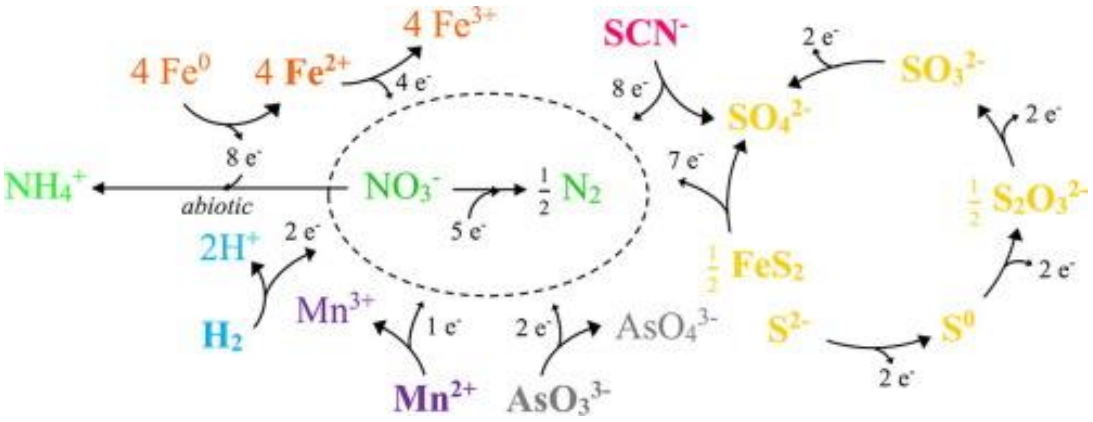

Figure 2.1 Electron donors for autorotrophic denitrifiers (Di Capua et al., 2019).

In summary, biological denitrification (BD) is conducted by heterotrophic or autotrophic organisms. Heterotrophic organisms have a higher denitrification capacity but the process needs an additional organic carbon source as the electron donor in the removal system; while autotrophic denitrification happens in the presence of hydrogen gas or sulphur compounds (Mohseni-Bandpi et al., 2013; Rezvani et al., 2019; Soares, 2000). Excess carbon in drinking water is undesirable because of its trihalmethane formation and causes pipe corrosion and affects the taste and odour quality of the treated water (Y.-T. Huang et al., 2016; Schipper et al., 2010). Dissolved organic carbon (DOC) is the other by-product in the heterotrophic denitrification process and the concentration ranges from 0 to 45 mg L^{-1}. (Robertson, 2010). Moreover, an insufficient amount of the organic carbon causes nitrite accumulation (Uçar et al., 2016) which needs a post treatment chlorination to be oxidized. Another challenge in using the heteotrophic denitrification pathway is to control the process and variables for complete denitrification to occur otherwise nitrous oxide (N_2O) will be emitted from the system and this is a significant greenhouse gas. This situation usually happens at a low pH and in the presence of excess organic carbon (Sanchez Gomez & Minamisawa, 2019). The other negative aspect of the presence of excess organic carbon is methane production by the anaerobic digestion (Davis, 2018). The biomass production during the heterotrophic denitrification (HD) is two times and nitrous oxide emission is 6 times higher than the autotrophic denitrification (AD) (Z. Wang et al., 2017). During denitrification process in both AD and HD, the hydroxyl group can be released, which causes an increase in the pH of the effluent. In this case, the pH is adjusted

by adding acid in HD, while there is no need for a post treatment in AD as the presence of carbon dioxide prevents the shift of pH to the alkaline state (Kapoor & Viraraghavan, 1997).

2.2.2 Biological phosphorus removal (BPR)

Microorganisms can utilize the phosphorus in energy transfer and for cell synthesis. This process (BPR) utilizes microorganisms to remove P. In this process, different fractions of phosphorus are accumulated by the microorganisms. Human waste, industrial wastewater and agriculture are the main sources of P. In wastewater, there are mainly three forms of phosphorus:

- **Organic phosphate**: Phosphate which is combined with an organic compound.
- **Polyphosphate**: Large molecules containing many individual molecules of orthophosphate.
- **Orthophosphate**: The simplest form consisting of individual molecules of phosphate.

Microorganisms readily assimilate orthophosphate. When organic phosphate and polyphosphate are present in wastewater, most of the microorganisms are associated with the orthophosphate during the biological activities. Total phosphorus is the sum of the dissolved and particulate phosphorous. Particulate phosphorous is removed using a physical removal method like filters and sedimentation. Soluble phosphorous can be removed using biological processes, as the microorganisms are able to accumulate phosphorus. These microorganisms called phosphorus accumulating organisms (PAOs). *Canadidatus Accumulibacter Phosphatis* is the most widely studied PAO with a well understood taxonomy; it is the most prevalent PAO in the EBPR systems (Martin et al., 2006; Oehmen et al., 2007). Under anaerobic conditions, PAOs convert organic matter to Polyhydroxyalkanoates (PHAs) which are energy-rich carbon compounds. The breakdown of the polyphosphate can provide the energy for the organic matter conversion which causes an increase of the phosphate concentration in the solution. Under aerobic conditions, this energy is restored by phosphate uptake in the system (Figure 2.2).

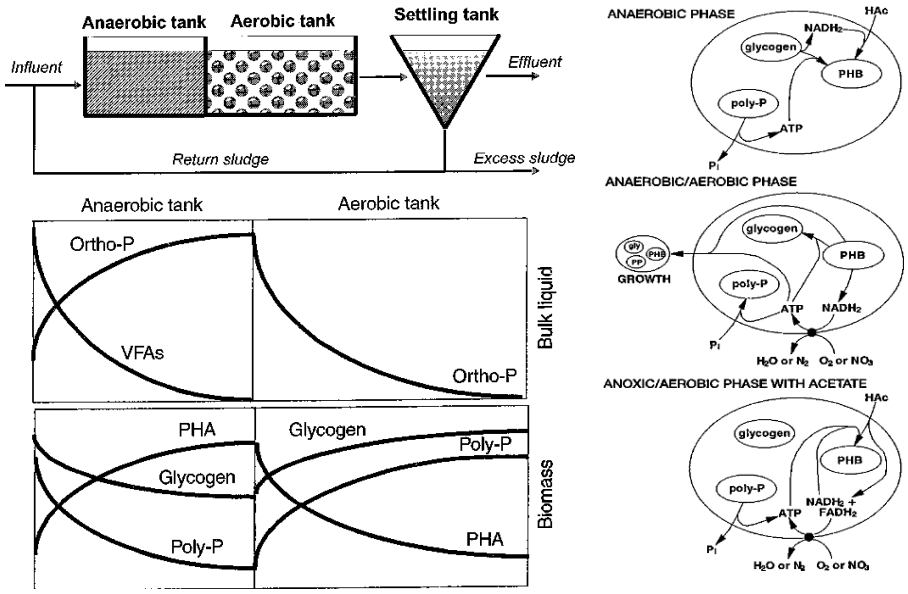

Figure 2.2 Biological phosphorous removal process (Van Loosdrecht et al., 1997).

2.2.2.1 Volatile fatty acids

The PAOs grow best on volatile fatty acids (VFAs), which is their preferred food source. So, in a BPR system, it is important to ensure that it contains adequate amounts of the PAOs food source. VFAs are the smallest molecules into which organic material can be broken down. Fermentation is the main process by which VFAs can be formed in the collection system, primary clarifiers or fermentation tank. These components are present in a number of treatment designs. VFAs primarily consist of acetic acids and propionic acids (Figure 2.3).

In BPR systems, for each g of P that is removed, 7-10 g of the VFAs is required. Chemical addition is another alternative approach to provide enough PAOs if the system is not able to produce the food source itself.

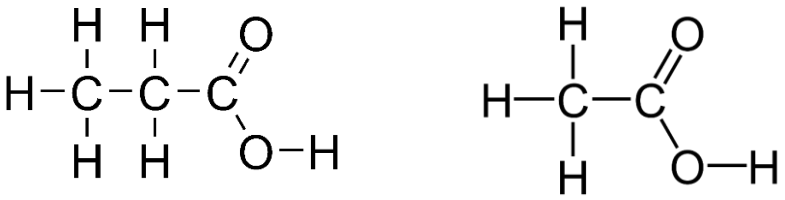

Propionic acid – CH_3CH_2COOH Acetic acid – CH_3COOH

Figure 2.3 Propionic acid and Acetic acid structure.

There are several operational details in a bioreactor treatment system which can affect the VFAs including that which influences the PAOs population and BPR efficiency. The most significant process is the interference of returned activated sludge (RAS) which is rich in nitrate due to the fermentation process in the anaerobic reactor. Another significant process is using the air lift pumps to return the activated sludge which can then introduce oxygen to the anaerobic zone and impair the process. During the treatment design there are two main controllable processes which can led to a higher VFAs concentration. These are:

- Storing the sludge in a higher blanket for a longer time in the first clarifier which can produce more VFAs through enhanced fermentation.

- Preventing the ingress of oxygen into the effluent channel (water turbulence in anaerobic zone).

2.2.2.2 PAO's – Anaerobic condition

The stored polyphosphate is the main source of energy for the PAO's in taking up and storing food under the anaerobic conditions. During this process the polyphosphate breaks down to orthophosphate molecules. Because of the negative charge of the orthophosphate molecules, they can't cross cell membranes. So, they need to bond to a cation which is present in the system and can be neutralized during bonding. Magnesium and potassium are the main cations present in sufficient quantities in domestic wastewater. The process of bonding and passing through the cell membrane is called phosphorus release; which in addition, causes the release of magnesium and potassium in the water.

The minimum requirements in order to operate a BPR system are:

- Sufficient organic carbon in the system.

- Well-sized anaerobic zone (BOD_5 / TP = 20/1, Hydraulic retention time (HRT) = 1 h – To avoid the secondary P release due to the absence of the VAFs, Solid retention time (SRT) = 2 days) – Enough time for the EBPR.

- Presence of sufficient cations in the system to facilitate P release.

2.2.2.3 PAO's – Aerobic condition

The PAO's exhibit non-inhibited uptake behavior under aerobic conditions. They take up orthophosphate (more than what they released under the anaerobic condition) using the energy from the oxidation of organic matter by nitrate or dissolved oxygen (or accumulated PHA is oxidized by an electron acceptor) and convert it to the polyphosphate which they store in their cells (Nicholls & Osborn, 1979). The *Acintobacteria sp* are the PAOs which carry out the non-inhibited P uptake in a EBPR system (Oehmen et al., 2007). It's acknowledged that they generally accumulate more complex carbon sources, such as amino acids and proteins under anaerobic conditions as an unidentified substance (Günther et al., 2009). Then, in order to removing the phosphorus from the system, it is essential to remove the waste activated sludge (WAS). The cycling of wastewater between aerobic and anaerobic zones can act in favor of the PAO's for their cell growth.

The glycogen accumulating organisms (GAO), can compete with PAOs to take up and metabolize the VAFs in the anaerobic zone but not accumulate P (Cydzik-Kwiatkowska & Zielińska, 2016). High SRT, high temperature (>28), long anaerobic zone, waste with low TKN content, periods of intermittent low BOD load and low pH in the aerobic zone are the parameters which lead to providing favorable conditions for the growth of GAOs over PAOs and that also cause poor system performance in P removal (Oehmen et al., 2007). To design and operate a bio-P removal system there are conditions (Table 2.3.) which must be considered, in order to ensure optimal P removal efficiency.

Table 2.3 Optimum Biological phosphorous removal system condition.

Condition	Value	Target
Mixed liquor condition	Sequential anaerobic and aerobic	for PAO's cell growth
VFAs - anaerobic	7-10 mg L^{-1} / 1 mg P	to providing enough VFAs
BOD_5/ TP - anaerobic	20:1	to providing enough VFAs
MLSS - aerobic	Waste it	to avoid secondary release of P
HRT- anaerobic	1 h	to avoid secondary release of P
SRT- anaerobic	2 days	to avoid secondary release of P
DO - anaerobic	minimize	to avoid interfere with fermentation
NO_3^- - anaerobic	minimize	to avoid interfere with fermentation
pH - aerobic	>7.2	to avoid growth of GAOs

2.2.2.4 Enhanced biological phosphorus removal (EBPR)

The plug flow mode reactor or piston flow reactor (PFR) was the first model in which EBPR was observed to operate at a high rate, in non-nitrifying plants. An anaerobic zone was followed by an extended aerobic zone, in which the sludge returned to the anaerobic reactor after the second clarifier. In conventional treatment systems (nitrification and denitrification) an initial anaerobic stage which is nitrate free was designed to ensure EBPR (Phoredox). This P removal method is considered to be a cost effective and a sustainable method compared to chemical treatments (Acevedo et al., 2012; T. T. Nguyen et al., 2013). However, due to its complicated operational details and process controlling, EBPR is unreliable when down scaled and used in decentralized treatment projects (N. Brown & Shilton, 2014).

There are several configurations for BPR which all involve anaerobic and aerobic zones. They are designed to minimize the nitrate return to the anaerobic zone which interfere with fermentation. Moreover, when the main concern of the wastewater contamination is nitrate-nitrogen, these configurations can be employed for N and P removal by using some modifications and providing an appropriate carbon source. The DPAOs (denitrifying PAOs) can simultaneously carry out P removal by accumulation mechanisms and denitrification by using nitrate as the sole terminal electron acceptor for oxidation of PHA under anoxic conditions (R. J. Zeng et al., 2003). A/O, A^2O, UCT, JHB, and OD are the main enhanced biological phosphorus removal designs that have been used in conventional projects (Table 2.4).

The main challenge of the EBPR process is the biological process modification that is required (i.e. anaerobic –aerobic sequencing) and that the water quality and system performance is highly affected by the influent flow and the pollution concentration. Effluent P concentrations are determined by volatile fatty acid (VFAs) to total phosphorus ratio in the influent to anaerobic zone. So, the concentration of the VFAs should always be monitored to determine if the supplemental is required or not. Also, all the process can be affected by biological toxicity.

Table 2.4 Summary of designs and processes for enhanced biological phosphorous removal (EBPR).

EBPR	Technologies	System set-up	Specification
A/O	Anaerobic / Oxic Phoredox system in South Africa in 1974 and later patented in the United States under the name A/O	Similar to a conventional activated sludge process with an anaerobic zone at the head of the secondary train	Where ammonia removal is not required so nitrates are not being returned to the anaerobic zone
A^2O	Anaerobic/anoxic/oxic -	An anoxic zone is situated between the anaerobic and aerobic zones	Nitrate rich MLSS is returned from the end of the aerobic zone to the anoxic zone for denitrification prior to RAS being returned to the anaerobic zone
MB	Modified Bardenpho modification of the A^2O process	Additional anoxic and aerobic zones situated at the end of the secondary train	This was developed for additional nitrogen removal and consequently minimal nitrate return to the anaerobic zone.
UCT	University of Cape Town modification of the A^2O process	Returns both nitrate rich MLSS from the end of the aerobic zone and RAS from the secondary clarifier to the head of the anoxic zone for denitrification	Minimize nitrate return to the anaerobic zone
MUCT	modified University of Cape Town modified UCT configuration	Uses a second anoxic zone that receives the return of nitrate rich MLSS from the end of the aerobic zone	-
JHB	Johannesburg modification of the A^2O process	Has a separate anoxic zone on the RAS line for denitrification before return to the anaerobic zone	-

2.2.3 Sequencing Batch Reactors (SBR)

SBR perform all the necessary functions of nutrient removal in a single tank with variable water levels and timed aeration. This system requires a minimum of three tanks and advanced automation equipment to control the cycle times and phases. The SBR control systems allow the operation to be configured to operate as almost any other suspended growth reactor by adjusting the cycle phases between fill, mix, aerated, settle and decant. Sequencing batch biofilm reactors are considered a relatively innovative water treatment method (Mielcarek et al., 2015). A growth carrier is added to the react batch that can be fixed bed, moving bed, or in suspension. The advantages of this method is space saving through the use of single reactor tank and up two times higher biomass retention compared to the activated sludge system (Jabari et al., 2014) which makes this method one of the most reliable ones to be utilised in small scale operations.

Fixed bed biofilm reactor has been used in several scenarios, in which EBPR has been reported in different rates. Total P removal of > 90% observed in a lab scale reactor operated by Gieseke et al. (2002), and H. Yin et al. (2017), while a lower system efficiency between 70% to 90% was reported by Rahimi et al. (2011). Addition of carbon source or chemical precipitation have been suggested by X.-J. Wang et al. (2006) to achieve low P levels in the effluent. The maintenance of this system have been challenging regarding biomass removal and cleaning the system by backwash and this can impact the operation of the EBPR if not effectively implemented (Mielcarek et al., 2015). Also, a consistent P removal efficiency has not been reported in a full scale reactor and the PAO behaviour within the biofilms and different operational details and media is not known yet (Kesaano & Sims, 2014). The consistent efficiency of the system is one of the most important factors to ensure, together with optimum design method because of the tightly regulated environments and also the overarching water quality regulations from government agencies.

2.3 Adsorption process

The adsorption process is known as one of the most convenient removal processes due to its simplicity in design and ease of operation. This method has been used widely to remove different organic and inorganic contaminants from wastewater and also water bodies (Mohan

et al., 2014; Walcarius & Mercier, 2010) . Various sources of adsorbents has been used to remove different inorganic anions such as nitrate (Kalaruban et al., 2016; Khosravi et al., 2018; Mubita et al., 2019), fluoride (Dong & Wang, 2016; D. Kang et al., 2017; Nabbou et al., 2019), bromate (Ji et al., 2017; Y. Yang et al., 2019), and perchlorate (George et al., 2018; Sowmya et al., 2019) from wastewater. In order to achieve the optimum performance in an adsorption system, selecting the appropriate media for a specific contaminant is important. Different conventional and non-conventional adsorbents from different sources have been used in order to nitrate removal from water and wastewater. Natural sorbents, agricultural wastes, bio-sorbents, carbon-based sorbents, industrial waste sorbents, and miscellaneous adsorbents are the main categories of materials which have been applied to a treatment system for the nitrate removal. The adsorption and use of various media is a broad topic so a review of the function of the most popular media is presented.

There has been always a number of challenges ahead of the adsorption process. The most important one is a relatively expensive distillation process is required to the product recovery through microbiological, chemistry and thermal processes. The adsorbent regeneration and adsorbate recovery need additional processes which apply cost and challenges to the treatment system. Also, the adsorbent can be considered as a hazardous waste after losing the adsorption capacity and adsorbent regeneration process can add extra cost to the project.

2.3.1 Natural clay adsorbents

The hydrous aluminosilicates minerals that constitute the colloid fraction of materials such as soils, rocks, and sediment are known as clay. Clays can be formed from a combination of fine sized clay minerals and clay-sized particles of quartz, carbonate, metal oxides and the other minerals. The main mechanism and behavior of the clays when in contact with a pollutant is cation/anion exchange and adsorption.

2.3.1.1 Nitrate

Kaolin was used by Mohsenipour et al. (2015) for nitrate adsorption (45 – 450 mg L^{-1}) in an acidic environment (pH=2). The maximum adsorption capacity of the kaolin clay mineral was 25% at the highest contact time of 150 minutes and demonstrated that it can act as a natural nitrate scavenger in the environment. El Ouardi et al. (2015) showed that a local clay from Morocco (NC) could remove up to 72% of the nitrate (300 mg L^{-1}) from an aqueous solution by using only 1 g L^{-1} of adsorbent. The optimum adsorption happened in 240 min contact time.

In other research by Malakootian et al. (2019) nitrate could be removed up to a limit of 99% nitrate (50 mg L^{-1}) in 80 minutes by a natural clay carrying nano zero-valent iron oxide (NZVI). The optimum adsorbent dosage to achieve the highest removal capacity was 10 mg L^{-1} in an acidic environment. The calcium montmorillonite was thermoactivated by sulphuric and hydrochloric acids by Mena-Duran et al. (2007) in order to remove 40 mg L^{-1} nitrate from a solution. One g of the adsorbent could remove 22.28% of the nitrate by hydrochloric acid activation. Hydrotalcites (HTx) are the anionic clays which are the most favorable materials to adsorb anions. HTx with different ratios of the Mg/Al was prepared by Wan et al. (2012). They demonstrated that the calcined hydrotalcites with the Mg/Al ratio of 4 (CHT4) had the highest adsorption capacity by 34.36 mg N/g in 350 min. Several organoclays have been synthesized and used by researchers in recent years in order to compare them with the commercially available ones and achieve the maximum nitrate removal rates. Three types of the organoclays MCM-41 (hexagonal), MCM-48 (cubic), MCM-50 (layered) were synthesized by Seliem et al. (2013) and used as sorbents for nitrate. The removal efficiency of the synthesized clays compared to the commercially available Closite: Cloisite 10A. The highest nitrate uptake belonged to the Closite 10A with 0.359 meq g^{-1}. The selective nitrate removal of the synthesized organoclays was at a very high rate which could remove nitrate in the presence of the 10 times highest concentration of the other elements such as Cl^-, SO_4^{2-} , and CO_3^{2-}. Montmorillonite was modified by hexadecylpyridinium chloride (HDPyCl) to increase the CEC by four times. High selectivity nitrate removal in 4h was achieved by using 0.67 mmol g^{-1} of HDPy-montmorillonite (Bagherifam et al., 2014).

2.3.1.2 Phosphate

According to the different surface physical and chemical characteristics of the clay minerals, phosphate can be adsorbed by various mechanisms. Kaolinite and goethite which are often cemented together in a binary association used as a mixture (GKM) and also association (GKA), to enhance the soil phosphate adsorption capacity (Wei et al., 2014). Both goethite and kaolinite minerals are pH dependent and the adsorption capacity is highly dependent on the surface properties of the adsorbents. Wei et al. (2014) showed that goethite could adsorb higher amounts of the phosphate compared with the GKA, GKM, and kaolinite respectively. The main reasons were the higher specific surface area and external SSA and also being positively charged on the surface at the same pH of the other adsorbents. By considering the ligand exchange at surface hydroxyl sites as one of the main phosphate adsorption

mechanisms by the clays, goethite has a higher density of reactive hydroxyl sites (Fe-OH spread over entire surface) compared to the kaolinite (Al-OH are located at the edge of the crystal structure)(Borgnino et al., 2010; Landry et al., 2009). Montmorillonite's surface area and pore volumes enhanced by the Zr^{4+} and Zr^{4+} / Al^{3+} treatment. Zr^{4+} / Al^{3+} showed a more significant performance to adsorb phosphate by 17.2 mg P/g in an acidic condition. W. Huang et al. (2015) introduced the Zr^{4+} / Al^{3+} polyhydroxy-cations into the interlayers of the natural montmorillonite which adjusted more positive charges on the surface area (pH_{zpc}=9.2). It's been reported that the metal treatment of the clay minerals can boost their phosphate adsorption capacity which has been reported as up to 1.5 times more than the natural in some cases (Koilraj & Kannan, 2010; Tian et al., 2009). The inorganic-bentonite modification was conducted by Fe and Al (L.-g. Yan et al., 2010). The interlayer spacing and pore volumes were increased significantly; 4 g L-1 of the Al-bentonite at pH=3 could adsorb up to 60 mg L^{-1} phosphate in 6 hrs. In general, due to the fact that Al has an insensitivity to the change of redox condition, Al has been preferred for use compared to Fe (Boers et al., 1992). The electrostatic and ligand exchange was introduced as the main adsorption mechanism of the Al- bentonite (Chitrakar et al., 2006; Xue et al., 2009). Also, an increase in the pH of the solution proved the ion release during the ion exchange reaction. Phoslock® (lanthanum (La) modified bentonite), has been recognized as one of the most powerful media's to adsorb phosphate in an aqueous solution (Boers et al., 1992; Haghseresht et al., 2009; Reitzel, Jensen, et al., 2013; Robb et al., 2003; Ross et al., 2008; van Oosterhout & Lürling, 2013; Vopel et al., 2009). Phoslock®, was invented in Australia by the CSIRO. Meis et al. (2012) used 100:1 dosage of the Phoslock®: P concentration and proved that the media dosage was not sufficient to target the mobile P at sediment depth > 4cm in the shallow reservoir which they studied. Acidic conditions were reported as favourable for Phoslock® adsorption behaviour. Haghseresht et al. (2009) showed a 30% drop in adsorption capacity when the pH increased to 9.0 from 5.0. It was reported that Phoslock® can't control the SRP concentration higher than 0.047 mg P/l and the reason for this is the interaction between La and humic acids (Lürling & van Oosterhout, 2013; Reitzel, Jensen, et al., 2013) even in the ratio of 220:1 Phoslock® : P. After investigating Phoslock® performance in different lakes at different pH values, Reitzel, Andersen, et al. (2013) suggested using a minimum of 200:1 adsorbent dosage, since 100:1 was insufficient for even concentrations below 0.001 mg P L^{-1}. Moreover, pH dependency of the Phoslock® is reversible. So in recent years, researchers have tried to introduce a natural,

sustainable, stable and effective clay based media to adsorb phosphate from wastewaters. Mdlalose et al. (2019) achieved 82% adsorption of 100 mg L^{-1} concentration in an acidic (pH=3) condition during 24 hrs by use of Co modification of the bentonite clay. A zirconium/magnesium-modified bentonite (ZrMgBT) was used in an acidic (pH=3) environment with 4-30 mg L^{-1} of phosphate concentration (Y.-F. Lin et al., 2002). The optimum adsorption rate reported with 13.0 mg g^{-1} removal at pH=7 during a 24 hrs contact time and adsorbent dosage of 25 mg in a 50 ml solution volume. Ligand exchange between $HPO{-}4/HPO_2{-}4$in aqueous solution and hydroxyl group bound to zirconium (Zr-OH) on ZrMgBT was proposed as the main adsorption mechanism.

2.3.2 Carbon-based adsorbents

Materials derived from environmental wastes are a main source for the production of adsorbents due to their high carbon content (Demiral & Gündüzoğlu, 2010; Santana-Mayor et al., 2020; Xiaodong Yang et al., 2019). They have been broadly used in liquid and gas purification process to remediate a wide range of contaminants (Creamer & Gao, 2016). Carbon based adsorbents can be made from agricultural by-products, wood industry wastes, petroleum polymeric wastes, and coals (Başar, 2006). Usually, further chemical treatments applied during the adsorbent preparation are used to enhance the chemical and physical characteristics of the final product (Cho et al., 2011; Khalil et al., 2017; Xia et al., 2019).

2.3.2.1 Nitrate

One of the most important environmental wastes used for contaminant removal from aqueous solutions is activated carbon with a high carbon content. Several researchers have reported the preparation of low cost activated carbon mainly from agricultural wastes such as shells (coconut) and fruit stones (apricot) (Omotosho, 2016; Tsai & Jiang, 2018; Youssef et al., 2005). Chemical activated carbon by $ZnCl_2$ with the source of the sugar beet bagasse was used in a study with the nitrate concentration between 10 – 200 mg L^{-1} with the dosage of 20:1 AC : volume (Demiral & Gündüzoğlu, 2010). This research demonstrated that activation temperature is an effective factor in increasing the surface area and pore sizes; with a 35% (1826 m^2 g^{-1}) increase in the surface area by applying 700 °C compared to the 500 °C. $ZnCl_2$ acted as an effective agent not only in creating new pores, but also in widening existing pores from 1.87 to 2.22 nm (Hu et al., 2001). Maximum nitrate adsorption by activated $ZnCl_2$ was 41.2% in an acidic (pH=3) condition which provided increased positive charges on the surface

for electrostatic attraction (Chatterjee & Woo, 2009). Commercial granular activated carbon was modified by sodium hydroxide and cationic surfactant Cetyl trimethyl ammonium bromide (CTAB) (Mazarji et al., 2017). Four g L^{-1} of the prepared adsorbent was added to tubes contained 40 mg L^{-1} nitrate solution at pH=7 and then mixed for 2 h. However, the surface activation didn't have any significant effect on the pore sizes and the surface area. The maximum adsorption capacity of treated GAC was 21.51 mg N g^{-1}. The alkaline treatment followed by a cationic surfactant treatment was found to be significantly effective in the increase of the functional groups without any negative effect on the physicochemical properties of the adsorbent. Two different types of pine cones were used as the stock material to prepare activated carbon and the three different treatments; phosphoric acid activation, thermal, and urea were applied to develop and enhance the activated carbon nitrate adsorption capacity (Nunell et al., 2015). The optimum nitrate adsorption was achieved with a modification including a thermal treatment at 800 °C in an atmosphere of nitrogen, and a urea treatment followed by a consecutive heat treatment at 350 °C that could adsorb a maximum of 0.45 mmol g^{-1}. The main adsorption mechanism was a noticeable increase in nitrogen functionalities (amidine/amino)(Pietrzak et al., 2006) and basic functional group. A sequential modification of the activated carbon fibre (ACF) was conducted by different methods (Machida et al., 2019). Chemical vapour deposition at 800 °C was applied to ensure nitrogen element adjustment on the adsorbent surface, followed by a heat treatment at 950 °C which converted the nitrogen species into quaternary nitrogen. Additional pores developed on the activated carbon surface due to steam activation at 800 °C. The optimum nitrate adsorption was 0.7 mmol g^{-1} under acidic conditions (pH=3). The quaternary nitrogen (N-Q) sites on the high specific surface area played a major role in adsorbing nitrate. It was demonstrated that π-electrons on graphene sheet (without electron-withdrawing groups such as acidic functions and quaternary nitrogen (N-Q)) are the principal adsorption sites for nitrate on carbon based adsorbents (Ota et al., 2013).

2.3.2.2 Phosphate

Lanthanum hydroxide-spiked activated carbon fibre (ACF-LaOH) was used for phosphate removal from wastewater by the adsorption method. It was prepared based on the ultrasound-assisted chemical precipitation (L. Zhang et al., 2012). 2.5 g L^{-1} of adsorbent was added to a solution with 30 mg L^{-1} phosphate concentration. At the optimum condition (concentration of La^{3+} solution of 0.11 mol L^{-1}, ultrasonic power at 206 W, and ultrasonic time

of 7.3 min, respectively), 87.0% phosphate removal was achieved, with a combination of ligand exchange, electrostatic interaction and Lewis acid–base interaction the main adsorption mechanisms. Low pH was determined as a favourable factor effecting adsorption efficiency and associated mechanisms. Mg/Al-layered double hydroxides (Mg/Al-LDHs) modified biochar has also been used as an effective carbon based media to adsorb the phosphate from the aqueous solution (Ronghua Li et al., 2016). A high ratio of Mg/Al (4:1) resulted in an optimum adsorption capacity of the modified biochar with 81.83 mg P/g under acidic conditions (pH=3). Ion exchange, electrostatic attraction and surface inner-sphere complex formation are the main adsorption mechanisms of the modified biochar (derived from a sugarcane leaves). The presence of other inorganic anions (F^-: being the most effective one) in the solution had the greatest effect on the P adsorption efficiency when a low ratio of the Mg/Al (2:1) was used. S. Y. Lee et al. (2019) used 1.25 g L^{-1} rice husk-derived biochar which was functionalized by MgAl-calcined LDHs biochar to adsorb phosphate from different solutions contained 25 to 100 mg L^{-1} of the phosphate. They proposed that a lower Mg:Al molar ratio increased the charge density and hence phosphate adsorption; although this contradicts the research by Ronghua Li et al. (2016). Here, the reconstruction of the LDH structures during the phosphate (memory effect) adsorption and in addition, the inner and outer sphere complexes were proposed as the main phosphate adsorption mechanisms. It is apparent that the adsorbent's physical characteristics (surface area – pore size distribution (PSD)) are the important factors when in contact with high concentrations of phosphate (Kumar et al., 2017). In addition, mesopores (porous area>3nm) are responsible for phosphate adsorption at low concentrations (< 20 mg L^{-1}) while the high surface area resulting from the micropores were found to not contribute to phosphate adsorption.

2.3.3 Nano materials adsorbents

The nitrate and phosphate adsorption by the nanomaterials can happen through both the physical or chemical mechanisms. The innate surface area and external functionalization of the nanomaterials are the most effective factors in the nitrate adsorption efficiency (Mirkin et al., 1996). The other nanomaterial characteristics such as location of atoms on the surface, low internal diffusion resistance, and high surface binding energy are effective factors when reacting with nitrate (Khajeh et al., 2013). Nanomaterials reaction with nitrate can be summarized in two main categories; adsorption and reduction. The adsorption efficiency and

reducing capacity varies between different nanomaterials, for instance nanoparticles, nanotubes, nanofibers, nanoshells, nanoclusters, and nanocomposites.

2.3.3.1 Nitrate

Nanoparticles due to their high specific surface area and catalytic activity, are known as an alternative to conventional nitrate removal treatments. They can be found as metallic, semiconductor, or polymeric, in the range of 1-100 nm. Nanoparticles have been utilized in environmental remediation projects and can effectively remove different kinds of contaminants from soil and water (W.-T. Liu, 2006). Different coating and immobilization methods with the nano particles might be required; they have also been used as a standalone system to remove contaminants from aqueous solutions. Nano zero valent ion (NZVI) agglomerates readily in the system because of its colloidal characteristics. The immobilization agents which are used to support the nanomaterials in nitrate removal are SiO_2 (Ding et al., 2017); nanographene sheets (Salam et al., 2015); chelating resins; kaolin (Cai et al., 2014); NaY zeolite (R. J. Zeng et al., 2003); nanofibrous adsorbent(Eroglu et al., 2012); and exfoliated graphite(H. ZHANG et al., 2006) (Tyagi et al., 2018). (NZVI) has been widely used to reduce and adsorb nitrate from water and wastewater during the last decade. Its high surface area and catalytic activities allow it to act as a reducing agent and an adsorbent. The nitrate will reduce to ammonium, ammonia, nitrite and nitrogen gas while the NZVI acts as a reducing agent and adsorb nitrate on to surface. The nanomaterials which have been used to adsorb the nitrate are NZVI/NaY zeolite (Y. Zeng et al., 2017), Fe/polyphenol (T. Wang et al., 2014), nano alumina (Bhatnagar et al., 2010), and nano-ball allophane (Hagemann et al., 2017; Padilla & Henmi, 2002). The Fe, Cu/Fe, and Mn/Fe nanoparticles loaded on the NaY Zeolite (Na faujasite) by ion exchange and liquid phase reduction process by Y. Zeng et al. (2017) to increase the nitrate removal efficiency of the system by adsorption and reduction processes. They showed that metal@Y had a higher BET surface area compared to the NZVI and metal nanoparticles coated outer surface and embedded inner pores. Between all kinds of the metal@Y samples, C/F@Y showed a significant nitrate removal with a 4 g L^{-1} adsorbent dosage under a wide range of pH from acidic to alkaline. Iron played a major role in nitrate reduction, as did NaY zeolite in NH_4^+ adsorption. Thus, the zeolite in the metal@Y system decreases the NH_4^+ concentration which leads to a better conversion of nitrate/nitrite to the nitrogen gas. Nitrate was removed by 90% by CF@Y in 150 minutes up to 200 mg L^{-1} nitrate concentration and after 150 minutes of reaction the ammonia concentration increased while no nitrite was

detected. Eucalyptus (EL) and green tea was used to synthesize iron nanoparticles (GT-Fe) in order to enable nitrate removal from wastewater (T. Wang et al., 2014). Fe^0-iron oxide core-shell nano particles was the result of the synthesis, where the polyphenols formed as a capping/stabilizing agent. The nitrate removal efficiency of the GT-Fe and EL-Fe was 59.7% and 41.4% with the dosage of 1 g L^{-1} in 20 mg L^{-1} initial nitrate concentration solution respectively. The NZVI removed 87.6% of the nitrate under the same conditions during 120 min contact time. The reactivity of the GT-Fe was higher than the NZVI after a two months aging period in air; which is a benefit to the use of this adsorbent on a large scale. The removal mechanism of the GT-Fe was proposed to be an adsorption and co-precipitation by polyphenols capped Fe NPs supported by a reduction process involving the Fe^0 core. The redox reaction was negligible during the nitrate removal by GT-Fe nano particles.

Nano alumina is another nanoparticle which is used to adsorb nitrate from wastewater (Bhatnagar et al., 2010). 0.5 g L^{-1} of the nano alumina was used to adsorb up to 100 mg L^{-1} of nitrate in an acidic condition (pH=3.1). The high surface area with 151.7 m^2 g^{-1} and pore volume of 1.09 cm^3 g^{-1} were the unique properties of the nano alumina which enhanced nitrate adsorption. The 4.0 mg g^{-1} adsorption capacity of the nano alumina was observed and a two stage ligand exchange reaction between metal (Al) oxide and nitrate was introduced as the adsorption mechanism (Figure 2.4).

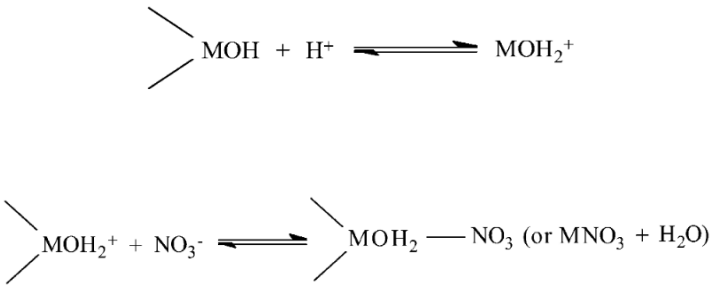

Figure 2.4 Ligand exchange reaction, reaction between nitrate ion and metal oxides (Cengeloglu et al., 2006).

Nano ball allophane has been used to adsorb nitrate and other anion contaminants from water (Table 2.5). Allophane samples with low Si/Al ratio are preferable to use in a nitrate removal system because of the high occurrence of aluminol groups (Al-OH, Al-OH_2). At high pH (Above 7.0) no nitrate adsorption was observed by Padilla and Henmi (2002). The highest nitrate adsorption occurred at the initial pH=3 which the nano balls have positive charges (Al-OH^+_2). So, a ligand exchange and anion exchange (nitrate exchange with perchlorate) reaction was proposed as the main nitrate adsorption mechanisms by nano allophane (Padilla & Henmi, 2002; Prado et al., 2006).

Table 2.5 Nanomaterials used to remove nitrate from aqueous solution.

Nanomaterial	Modification	pH	Dosage	Temperature	Contact time	Removal efficiency	References
Carbon-silicon nano composites	-	-	2 g L^{-1}	25.0	60 min	45.35% - 50 mg N/l	(Muthu et al., 2017)
Carbon nanotube (CNT) sheets	Oxidized - Nitrogen group functionalized	7.0	2.5 - 15 g L^{-1}	25.0	24 hr	90 % - 200 mg N/l	(Tofighy & Mohammadi, 2012)
Magnetic multi-walled carbon nanotubes	-	4.0	0.1 g L^{-1}	25.0	90 min	97.15 - 100 mg N/l	(Alimohammadi et al., 2016)
Chitosan nanofiber mats	Microalgae immobilized	6.0	-	25.0	16 days	87 % - 30 mg N/l	(Eroglu et al., 2012)
Chitosan/Al_2O_3/Fe_3O_4composite nanofibrous	-	3.0	2%	20.0	180 min	150 mg N/g	(Bozorgpour et al., 2016)
Nanoscale zerovalentiron (NZVI	Immobilized on SiO2–FeOOH core	3.0	4 g L^{-1}	25.0	150 min	99.84 % - 64 mg L^{-1}	(Ensie & Samad, 2014)
Polyethylene glycol/chitosan	-	3.0	0.3	25.0	60 min	50.68 mg g^{-1}	(Rajeswari et al., 2016)
Polyvinyl alcohol/chitosan	-	3.0	0.3	25.0	60 min	35.03 mg g^{-1}	(Rajeswari et al., 2016)
Chitosan /Zeolite Y/Nano ZrO_2 nanocomposite		3.0	20 g L^{-1}	35.0	60 min	1.95 mg g^{-1}	(Teimouri et al., 2016)
Chitosan-polystyrene-Zn nanocomposite		3.0	20 g L^{-1}	25.0	30 min	82.5 % - 10 mg L^{-1}	(Keshvardoostchokami et al., 2017)
Fe_3O_4/ZrO_2/chitosan	-	3.0		25.0	30 hr	89.3 mg g^{-1}	(Jiang et al., 2013)
lanthanum hydroxide doped onto magnetic reduced graphene oxide (MG@La)	-	4.0	12.5 mg L^{-1}	25.0	180 min	90%	(Nodeh et al., 2017)

2.3.3.2 Phosphate

Silver nanoparticle- activated carbon which was derived from tea residue has been used as a phosphate adsorbent agent (T. M. P. Nguyen et al., 2020). The AgNPs-TAC could adsorb up to 13.62 mg g^{-1} of the phosphate from a solution with 30 mg L^{-1} initial concentration during 150 min. The optimum condition was pH=3, and the ratio AgNPs/TAC of 3% w/w. The chemisorption through ligand exchange and surface complexes was introduced as the adsorption mechanism. A novel media, polyethylenimine (PEI)-grafted chitosan (CS) core-shell (called as Fe_3O_4/CS/PEI) magnetic nanoparticles was synthesized and used to adsorb phosphate from water. It could adsorb 48.2 mg g^{-1} of phosphate under acidic conditions (pH=3), and room temperature. The electrostatic attraction was the primary phosphate adsorption mechanism by Fe_3O_4/CS/PEI (C.-C. Fu et al., 2020). Humic acid coated magnetite nanoparticles (HA-MNP) was used for phosphate adsorption from water and could then be easily separated from solution by a magnet. These were 7-12 nm particles which could adsorb 28.9 mg g^{-1} of the phosphate (10 mg L^{-1}) at pH=6.0 through the chemisorption mechanism. Cellulose/graphene oxide hybrids embedded with Zr/La species was used in a phosphate treatment system in order to achieve enhanced removal. The adsorption efficiency was shown to be pH dependent which could remove 25.3 mg g^{-1} phosphate under acidic conditions. Lanthanum leach was noticeable in the presence of 150 mg L^{-1} humic acid at the rate of 2.1 mg L^{-1} while no Zr leach was observed. The Zr/La hydroxides were introduced as the main phosphate adsorption sites and mechanism (L. Zhang et al., 2019). The iron oxide nanoparticles were used as a phosphate adsorbent by Yoon et al. (2014). The maximum phosphate adsorption was 5.03 mg g^{-1} under 24 h contact time. The experimental conditions to reach the highest efficiency was 0.6 g L^{-1} adsorbent dosage and an initial phosphate concentration range of 2-20 mg L^{-1}. Also the acidic environment (pH=2-6) was favourable and the adsorption efficiency dropped to 0.33 mg g^{-1} under alkaline conditions. The main phosphate adsorption mechanism by iron oxide nanoparticles is attributed to ligand exchange (phosphate ions replacement with OH^- on the surface and phosphate inner-sphere complexes). A low-cost hydrothermal process was utilised to synthesize the amorphous zirconium oxide nanoparticles for use as the phosphate adsorbent in the aqueous environment. The highest adsorption capacity of the am-ZrO_2 nanoparticles (0.1 g L^{-1}) was of the order 99.01 mg g^{-1} under acidic conditions (pH= 2-6) and phosphate concentration at a range of 5-50 mg L^{-1} (initial concentration = 5-10 mg L^{-1}). The contact time to reach optimum adsorption rate was 1

h which was one of the fastest phosphate adsorption processes. The adsorption mechanism of phosphate onto am-ZrO_2 nanoparticles was deemed to follow the inner-sphere complexing mechanism, and the surface -OH groups played a major role in the phosphate removal. Also the adsorbed phosphate was released by NaOH solution and the material could be subsequently used for another adsorption process (Su et al., 2013). A CeO_2-functionalized Fe_3O_4@SiO_2 core-shell magnetic nanomaterial was prepared and used as a phosphate adsorbent by J. Liu et al. (2017). They used 0.5 g L^{-1} of the adsorbent in a solution containing 5-10 mg L^{-1} of phosphate and shaken for 48 h, at pH=6.2. The highest adsorption efficiency was 36.2 mg g^{-1}. Electrostatic interaction and ligand exchange were the adsorption mechanisms. The NaOH solution was used to regenerate the adsorbent and an external magnetic field was employed for separation after four adsorption-desorption cycles.

2.4 Approaches for simultaneous nitrate and phosphate removal

The removal of nitrate and phosphate in one system is a critical issue in water and wastewater treatment systems because further release of the nutrients in the treatment system can cause serious adverse effects in the water systems (Y.-S. Kim et al., 2012). The cross-flow micellar-enhanced ultrafiltration (MEUF) system was used by (B.-K. Kim et al., 2004) to remove nitrate and phosphate anions through an electrostatic adsorption mechanism along with an ultrafiltration. The cetylpyridinium chloride (CPC) was used as a cationic surfactant which formed micelles with positive charge on the surface and polyacrylonitrile membranes for the ultrafiltration stage to remove the micelles-pollutants complex (High contact time, low concentration). This removal system is a surfactant-based separation technique with a low energy.

Polymeric anion exchangers have been widely used for adsorbing nutrients such as nitrate and phosphate in aqueous solutions. They're cheap, easy access and commercially available. The resin ion exchangers are insoluble polymeric spheres which are sub-millimetre in size and hold ions loosely which means they can be easily exchanged with the ions which are the contaminants. Most of the resins (ion-exchange) are conventionally synthesized by polymerization and cross-linking of divinylbenzene monomers and styrene. The adsorption efficiency of the resins depends on the densities and specific type of ion-exchange groups (i.e., the amino group), the specific surface area, and the types of functional groups and counter-

ions. High capacity anion exchange resin was synthesized by Y.-S. Kim et al. (2012) with 33% higher density of functional groups compared to commercialized ones, to remove nitrate and phosphate simultaneously. A synthetic wastewater which contained 20 mg L^{-1} of nitrate and phosphate was continuously (flow rate = 30 ml/min) passed through a 100 ml column which contained 30 ml resin. The removal efficiency was 185.8 mg g^{-1} which was three times higher than commercialized resin (AMP16-OH). The disadvantages of this technology include potentially high water and chemical use, the inability to remove non ionized degradation products, and disposal of significant volume of dilute sodium salts and acids for the regeneration (Pan et al., 2019). The most important consideration is that the resin and regeneration requirements (high cost) vary in different wastewaters according to the ion selectivity property of the resins and each system must be custom designed.

Nitrate and phosphate can also be removed by zero-valent iron in the presence of hydrogen peroxide from acidic wastewaters. Acidic conditions need to be provided because of the sequential transformation of ZVI. The corrosion of the ZVI generates electrons which enable nitrate reduction (Yoshino et al., 2014). Then OH radical generates from the reaction of hydrogen peroxide and ferrous ion (ZVI corrosion) and phosphate participates with iron ions. 3.0 g L^{-1} ZVI could remove 1.6mM nitrate, 1.0 mM phosphate, and 9.0 mM hydrogen peroxide from a synthesized acidic wastewater and pH adjusted to 3.0 in 100, 15, and 15 min respectively. The major disadvantages of using ZVI include a narrow working pH, low reactivity due to its intrinsic passive layer, a reactivity loss with time due to the precipitation of metal hydroxides and metal carbonates, and low selectivity under anoxic conditions (Guan et al., 2015).

The pyrrhotite autotrophic denitrification biofilter (PADB) technology is the other method which was used by Ruihua Li et al. (2016) to simultaneously remove nitrate and phosphate from wastewater. The system included the natural pyrrhotite as the biofilter medium which inoculated with autotrophic denitrifiers from the anaerobic sludge. A synthetic wastewater contained 28 mg L^{-1} nitrate and 6 mg L^{-1} phosphate in the absence of organic matter passed through the PADB at HRT of 24 h and only 1.13 mg L^{-1} nitrate and 0.28 mg L^{-1} phosphate was remained in the effluent. The PADB is a simple, efficient and low cost method for simultaneous nitrate and phosphorous removal from the secondary effluent. Nitrate biological reduction and

phosphate adsorption on pyrrhotite was considered as the removal mechanism by PADB (Y. Zhang et al., 2019).

Magnesium-Mg-Al modified biochar (Mg-Al/BC) was prepared to enable the removal of ammonium, nitrate, and phosphate simultaneously from eutrophic water (Q. Yin, Wang, et al., 2018). The biochar was derived from a thermochemical treatment of soybean straw. 2 g L-1 of the biochar was added to a solution contained 50 mg L^{-1} ammonium, nitrate, and phosphate and the pH was fixed at 6.0. The maximum adsorption capacities for ammonium (0.70 mg g^{-1}), nitrate (40.63 mg g^{-1}), and phosphate (74.47 mg g^{-1}) were achieved for Mg–Al/BC, Al/BC, and Mg/BC, respectively for a 24h contact time. The positive charged ALOOH surface, Al/BC developed pores and the high surface area provided large adsorption sites to react and adsorb nitrate ions under acidic conditions (Q. Yin, Ren, et al., 2018). On the other hand, Mg/BC was a more positively charged biochar which could adsorb the phosphate by surface deposition and precipitation.

Zero valent iron and nickel were loaded on zeolite (Z-Fe/Ni) for simultaneous removal of nitrate and phosphate from aqueous solution. The Fe^0 was protected from oxidation on the zeolite. 0.5 g L-1 of Z-Fe/Ni reacted with 20 mg L^{-1} nitrate and 5.0 mg L^{-1} phosphate for 6 h contact time for a pH range 3.0 to 8.0. The system could remove 72.5% and 98% of nitrate and phosphate respectively under low pH which was favourable for nitrate and phosphate removal. The nitrate was removed by reduction and phosphate by adsorption on inner-sphere complexes (Y. He et al., 2018). Z-Fe/Ni showed larger surface area and dispersibility compared to the unsupported one. The presence of the nitrate could enhance the phosphate adsorption, while phosphate existence interfered with nitrate reduction by forming inner-sphere complexes and co-precipitation with iron hydroxide on Z-Fe/Ni surface.

Ultrafiltration (UF) membrane micro-reactor (MMR) was used for the first time by Q. Gao et al. (2019) for simultaneous removal of low concentrations of nitrate and phosphate. The amorphous Zr hydroxide and quaternary ammonium powder with poly (vinylidene fluoride) were blended and were structured the same as the conventional UF membrane with the same range of pore size. The wastewater contained 10 mg L^{-1} nitrate and 1 mg L^{-1} phosphate. The regeneration process was carried out by filtering 0.1 M NaCl solution for 20 min, followed by DI water for another 20 min at 0.1 MPa. The highest adsorption capacity of MMR were 9.66 mg g^{-}

^{1} and 15.58 mg g^{-1} for nitrate and phosphate respectively. The adsorption mechanism is ion exchange for both the nitrate and phosphate ions. This technology provides a high permeability and selectivity while low permeability is the main drawback of NF and RO technologies.

Siderite ($FeCO_3$) is a mineral which contains 48% iron with no sulphur or phosphorous. A sulphur-siderite (volume ratio sulphur-siderite = 1:3) autotrophic denitrification (SSAD) system was developed for simultaneous removal of nitrate and phosphate. The removal efficiency of the SSAD column system was 28 mg L^{-1} nitrate and 3.1 mg L^{-1} phosphate at 12 h HRT with no blocking during 401 days. The siderite could provide the inorganic carbon sources and pH buffer for sulphur autotrophic denitrification and sulphur acted as the electron donor to remove the nitrate from the water through the reduction. Phosphate was removed by iron phosphate precipitation mechanism.

2.5 Summary

According to the efficiency of the nitrate removal systems and the operational details, biological denitrification (BD) has been demonstrated to be more reliable and beneficial compared to the other developed technologies such as physicochemical methods in the recent years. The heterotrophic nitrate reduction showed a higher removal capacity while the autotrophic resulted in less by-product; this is one of the more important factors when selecting a treatment technology. Due to the clean nature of the hydrogen and the absence of by-products, the autohydrogenotrophic process is the most sustainable and efficient nitrate reduction technology at present. However, more research is needed to optimise the autohydrogenotrophic process in terms of the nutrient concentration, pH and temperature, and hydrogen – CO_2 flow rates. An engineered designed bioreactor can help to resolve the hydrogenotrophic technology limitations but to enable an economic solution the hydrogen and energy production from renewable energy resources is needed.

A wide range of technologies can achieve efficient phosphate removal but the energy cost, complexity, excessive maintenance are factors which make their use limited. The adsorption process has been shown to be the most efficient system to remove phosphate from aqueous solutions. According to the wide range of the adsorbents from different sources, there are several natural minerals which could adsorb phosphate in high concentration and recover a

large amount of it easily. The phosphate adsorption process is simple to design and easy to operate. Despite the extensive variety of nitrate and phosphate removal technologies, to find a reliable method to remove both nitrate and phosphate simultaneously has always been a challenge due to the limitations of nutrient concentration, HRT and contact time, and cost of the removal systems. Most of the technologies are limited in application with high nutrient concentrations, high HRT and contact time. More studies and research is needed in order to enhance the ability to deal with higher nutrient concentrations, reducing HRT, and also in making the process energy and resource sustainable.

This literature review identifies the following research and knowledge gaps in dealing with phosphate and nitrate in wastewater.

i. How an adsorbent can be developed from the natural sources without any chemical treatment for dealing with high concentration of phosphate with high adsorption capacity and low legacy desorption.

ii. How the physiochemical properties of the developed adsorbent can have an effect on its elution capacity.

iii. How the same adsorbent can work for nitrate at high concentrations and what is the effect of the adsorbent in nitrate reduction in a complete cycle with the lowest N_2O emission.

iv. What range of concentration of nitrate and phosphate can be released out of the reactors and which plants can uptake the rest in a floating treatment wetland system at a pond.

The following chapters will address these research gaps and will provide data and analyses around the efficiency of the developed material; in particular its ability to remove phosphate and nitrate from wastewater sources.

Chapter 3

Powdered ALLODUST/ALLOCHAR augmented single batch aerobic reactor (SiBAR) for high concentration phosphorous removal

3.1 Introduction

Adsorption is one of the most popular removal methods used for treating wastewaters containing agricultural nutrients. The challenge is that phosphorous concentration is very high in agricultural related industries and is higher than the adsorption capacity of the system. This chapter investigates the treatment of agricultural wastewater by developing and adding two novel media (ALLODUST, ALLOCHAR) to a Single Batch Aerobic Reactor (SiBAR). ALLODUST and ALLOCHAR consisted of allophanic soil mineral material sourced from either a Horotiu soil (Allophanic soil) or a Craigieburn soil (Allophanic Brown soil). Central Composite Design (CCD) and Response Surface Methodology (RSM) were utilized to design the experiment and model the nature of the response surface of the novel media in the experimental design and to analyze the optimum operational conditions.

Excessive application of different types of fertilizers in the agricultural industries, oxidation of nitrogenous waste products in human and animal excreta including septic tanks lead to contamination of surface and groundwater and has become a critical global issue (Seitzinger et al., 2010). Changes in land use and excessive use of artificial fertilisers are the main factor for the significant increase of phosphorus levels in groundwater over the past 20 years (Karanasios, Vasiliadou, Pavlou, & Vayenas, 2010). Phosphates enter surface water bodies as a result of agricultural fertilizer run-off, as well as the wastes which are derived from various biological sources. The wastes and effluents from chemical processing industrial sources is the other important source of phosphate contamination of surface water resources and waterways. Depending upon the type of contaminant, and the other environmental factors such as pH and temperature, orthophosphate can be a product following dissolution in surface water. Moreover, one of the main factors which causes eutrophication is the presence of the excessive phosphorus in the water treatment plants and also waterways. Kidney damage and

osteoporosis (Bouwer, 2000) are the main outcome of the phosphate presence in not acceptable concentrations in the water supply systems. Rigorous limits have been set from the U.S. EPA for total phosphorus concentration in water resources from the point of the waterways, 0.1 mg L^{-1} for rivers and 0.05 mg L^{-1} for rivers draining into lakes has been indicated to prevent further eutrophication. Also ANZECC trigger values for the total phosphorus is 0.026 mg L^{-1} for upland rivers and 0.033 mg L^{-1} for lowland rivers.

Phosphorus as one of the macro elements essential for organism growth and biosynthesis processes. Furthermore, the efficiency of the biogas production can be spiked by the presence of phosphorus in organic pollutant digestion processes (Khanal, 2008; Pearce & Chertow, 2017). Organic carbon (OC) content has a linear correlation with biological phosphorus removal which is reported in recent studies (Bashar et al., 2018; Q. He et al., 2018; Mielcarek et al., 2015). One of the recognized and sustainable phosphorus removal methods is adsorption through natural media and minerals. Phosphorous is a critical element in any biological water treatment, due to its effect on microorganisms and algal growth rate as well as conducting the anions adsorption by the bridging mechanism.

The chemical or physical interaction between a substance and a solid surface evolving mass transfer in a liquid phase is known as adsorption (Kurniawan et al., 2006; Mohajeri et al., 2018). Adsorption as an electrostatic process is a promising approach in the field of wastewater management and wastewater process engineering (Foo & Hameed, 2009). This technique can be utilised along with other mechanisms and even biological process can be supported by an adsorption mechanism (Mojiri & Branch, 2011). The physical and chemical characteristic of the anions and adsorbent and their interaction is the principle factor in the adsorption process. The other anion characteristics which can be effective in the selective adsorption mechanism efficiency are the solubility, ionic radius, hydration energy and bulk diffusion coefficient.

Emerging research indicates that allophanic soils may reduce phosphorous in wastewater (Mohammed Abdalla Elsheikh et al., 2018; Hagemann et al., 2017; Hashimoto et al., 2012; Prado et al., 2006). However, more information is required to understand the mechanisms involved and to quantify the effects more accurately. The Horotiu series (allophanic soils; Hewitt, 2010) and Craigieburn soils (typic allophanic brown soils; Hewitt, 2010) are some examples of New

Zealand soils with an allophanic component. The Horotiu is formed under the specific environmental conditions which the short-range order clay mineral allophane formed from weathering the volcanic glass within the soil material in North Island. Craigieburn occur where the feldspar-bearing greywacke and schist parent materials in the South Island high country have been highly weathered, resulting in the new formation of allophane. The alophane mineral has a very high affinity to adsorb phosphate. The other advantage of the presence of this mineral in a soil material is to help advancing the soil physical characteristics by enhancing the soil particles binding which make a low-density and permeable soil (Parsa et al., 2019).

Bio-sorption process has been widely used for contamination removal from wastewater such as using low-cost agricultural wastes and algae (Holan & Volesky, 1994; H. S. Lee & Volesky, 1997; Park et al., 2006). The agro-based materials became an alternative for chemical adsorbents during the recent years (Hashem et al., 2007). One of the most popular and readily available bio wastes is sawdust which has been used in different projects and researches (Schmidt & Clark, 2012). Also biochar is the other bio waste product which can be obtained from the carbonization of biomass. It can enhance the soil properties and has been used as a soil amendment in different projects (Lehmann & Joseph, 2009).

Recently, application of media filters for P removal from the water and wastewater has attracted a wide range of the research (Bashar et al., 2018; Beck et al., 1999; Benyoucef & Amrani, 2011; F. Fu et al., 2014; Y. Gao et al., 2018). The high concentration of phosphorus present in many agricultural industry effluents make most of the phosphorus technologies non-economic and not applicable in terms of the handling the elevated concentrations. So, in recent years research has focused on the introduction of a natural, sustainable, stable and effective clay based media to adsorb phosphate from wastewaters. The research reported in this chapter aims to examine the ability of a new, inexpensive developed media to adsorb P efficiency, under high concentration. Our study will also investigate the adsorption mechanism involved and a microstructure analysis of media before and after phosphorus adsorption.

3.2 Materials and Methods

3.2.1 Wastewater Sampling and Analysis

Ballance Agri-nutrients Ltd. has a resource consent to discharge wastewater from their Rolleston distribution depot, to 1.6 ha of land, adjacent to their distribution yard. The wastewater contains high concentrations of nitrate and phosphorus (110 mg L^{-1}N and 300 mg L^{-1} P). The fertiliser company has consent to discharge up to 200 kg N/ha/yr. Wastewater (containing the wash downs from the distribution yard) is collected in a treatment pond and discharged to the land (Figure 3.1). Currently, they have occasions during the year when they have to pay to transport the wastewater off site, as they can't dispose of the excess wastewater volume and its associated N content, within the conditions of the resource consent.

Figure 3.1 Wastewater sampling from the Ballance Agri-nutrients company pond.

Several wastewater samples were collected from the Ballance Agri-Nutrients fertiliser distribution yard, Rolleston, Canterbury for monitoring the wastewater characteristics. The samples from the pump, pond and the sump were collected in clean polycarbonate containers. The pond samples were collected from the centre and 35 cm depth from the surface and were immediately stored in a fridge at 4°C to prevent any changes in the sample properties due to the biological reactions (APHA 2005). The pH, temperature (°C), electrical conductivity (ms cm^{-1}), salinity (g L^{-1}), and TSS (%) were determined on site at the time of sampling. All the quality analysis was conducted in accordance with the Standard Methods for the Examination of Water and Wastewater (APHA 2005). The water characteristics is presented in Table 3.1 The phosphorus concentration was fixed in different batches by spiking K_2PO_4 in different concentration zones from 50 mg L^{-1} to 300 mg L^{-1}.

Table 3.1 Wastewater chemical characteristics.

Characteristics	Value
Total Suspended Solids (TSS)	37 mg L^{-1}
Nitrate-nitrogen	47 mg L^{-1}
Total Ammoniacal-N (TAN)	210 mg L^{-1}
Total Kjeldhal Nitrogen (TKN)	390 mg L^{-1}
Dissolved Reactive Phosphorus (DRP)	16.9 mg L^{-1}
Electrical Conductivity (EC)	780 µs cm^{-1}
Dissolved Oxygen (DO)	6.5 mg L^{-1}
Temperature	18.0 °C
pH	7.20

3.2.2 ALLODUST/ALLOCHAR preparation

Allophanic clay material from a Craigieburn Bw horizon (typic allophanic brown soil) and Horotiu Bw horizon (allophanic soil) (Hewitt, 2010) were collected from the Lake Coleridge area, South Island New Zealand and Ruakura Agricultural Centre, North Island respectively. Both the Craigieburn and Horotiu soils were sampled in the B horizon, which has the maximum accumulation of allophanic minerals for these soils. The soil samples had been air dried before using as an adsorbent and had been passed through a 2mm sieve and then stored in dry and cool conditions (Figure 3.2) (Isoyama & Wada, 2007).

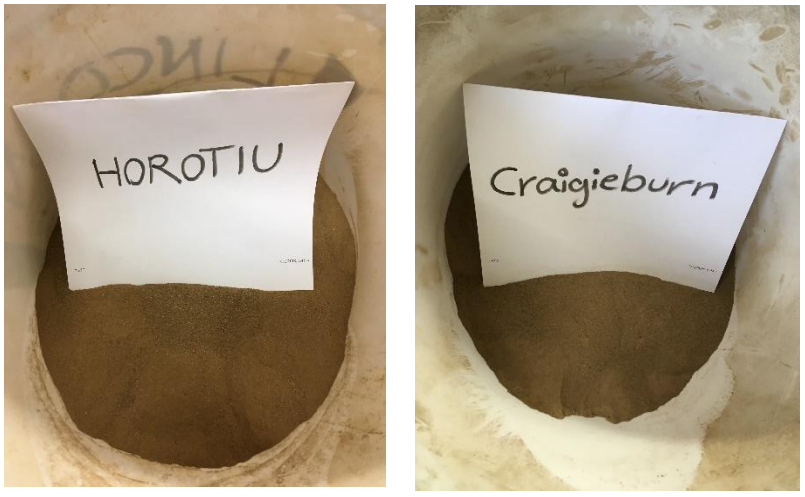

Figure 3.2 Air dried Horotiu and Craigieburn soils.

The sawdust (from *Pinus radiata*) was collected from SRS Ltd in Rolleston, Christchurch, New Zealand. The sawdust was oven dried at 70°C after washed with RO and then deionized water couple of times to a constant weight. To obtain a fine powder a coffee grinder was used to make

sawdust particles in 100-150 µm size (Figure 3.3) (P. Brown et al., 2000). In order to remove undesirable substances a solution of 0.5 M HCL was used at room temperature for 6 h (Doltabadi et al., 2016). The adsorbent was kept under airtight conditions until used in the experiments. The pH of both treated and untreated sawdust was determined. A ratio of 1:10 sawdust/water (W/V) solution was prepared to measuring the pH, using 5g of raw sawdust with 50mL deionized water.

Figure 3.3 sawdust resizing to use in ALLODUST and for the biochar production to use in the ALLOCHAR.

After determining the sawdust pH in 1:10 solid/water ratio, the sawdust was placed in separate glass beakers. The sawdust pH was adjusted to different ranges, using 0.1 M HCl solution. Specific amounts of 0.1 M HCl was added to the different glass beakers contained the sawdust and DI water with the pH meter probe located in the beaker. The addition of HCl drops continued until the pH stabilised at the same pH value. Then, the beakers were kept overnight in a room temperature environment and the pH measured 24 hrs after the pH adjustment (Figure 3.4). The pH treatment process stopped after observation of a fixed number for two consecutive days. The acidic-treated sawdust was then dried in a 70°C oven and was stored in a desiccator until used in the experiments (Argun et al., 2007).

Figure 3.4 Sawdust acid treatment.

The same stock of the collected sawdust was used for the pine biochar production. Particles less than 1 mm dried were pyrolyzed in an inert atmosphere at 550°C temperature. A steel container covered with aluminium foil was used as the sawdust container in the muffle furnace. A thermocouple controlled the consistency of the temperature (550°C - 8°C / min for 3 h) during the process (Figure 3.5).

Figure 3.5 Biochar stock used in the ALLOCHAR.

A series of innovative materials were prepared. Fresh "ALLOCHAR "(Allophane soil + biochar) and "ALLODUST"(Allophane + Sawdust) were prepared according to the different proportions of the allophanic soils, biochar and pH adjusted sawdust (Figure 3.6). H-ALLODUST and H-

ALLOCHAR refers to the the media with Horotiu base and C-ALLODUST and C-ALLOCHAR to Craigieburn base. Powdered Craigieburn Allophane (PCA), Powdered Volcanic Allophane (PVA: developed from the Horotiu soil), powdered pH adjusted pine sawdust (PPS), and powdered pine biochar (PPB) were utilized as media in the treatment system (75 µm < particle size <150 µm). A similar size range has used in recent studies (Aghamohammadi et al., 2007; Aziz, Aziz, & Yusoff, 2011).

Figure 3.6 Powdered ALLODUST preparation.

The mix design was prepared according to previous findings (Mohajeri et al., 2018; Mojiri et al., 2014). Allophanic soil materials, sawdust, biochar, silica powder, and Portland cement were mixed together. The white cement was used as the binder agent as it had a lower Fe content. The mix design and cost estimation of ALLOCHAR and ALLODUST are shown in Table 3.2. Based on this information, the estimated cost of ALLODUST and ALLOCHAR per ton are around NZ$700 respectively. The mixture was moulded using the ratio of the 0.45 water/solid. After 1 day, the mixed media was placed into water and cured for 3 days. Then, it was removed from the water and dried at room temperature for two days. The prepared media was subjected to XRD, XRF, FTIR for physiochemical analysis and SEM/EDS for morphological analysis in accordance with ASTM STP479, D8064, D5477-18 and C1723-16 respectively.

Table 3.2 Cost analysis of different developed adsorbents.

ALLODUST mix design			ALLOCHAR mix design		
Raw Materials	**Value (Kg)**	**Price/ton NZD**	**Raw Materials**	**Value (Kg)**	**Price/ton NZD**
Allophanic soils	459.40	-	**Allophanic soils**	459.40	-
pine sawdust	87.6	18	**Pine Biochar**	87.6	50
Silica powder	153.20	85	**Silica powder**	153.20	85
Portland Cement	300.0	600	**Portland Cement**	300.0	600
Water	30.0	-	**Water**	30.0	-
ALLODUST	1000	700	**ALLOCHAR**	1000	735

3.2.3 Bioreactor Design (Single Batch Aerobic Reactor -SiBAR with Couple Bottom Aeration -CBA)

Ten separate units of a Single Batch Aerobic Reactor (SiBAR) were used for the experiment. The SiBAR's consists of a transparent column made of Plexiglas for easier process controlling. UPVC was used for the base and cap parts of the reactors. In order to enhance the mixing efficiency of the air and water, the CBA (couple bottom aeration) method was used. By using the CBA aeration method the agitator was removed from the process design. Both the aeration and agitation were performed by CBA process. The total volume of the reactors was 2000 ml, with 1500 ml working volume. All ten reactors were run under the same environmental conditions and at the same time. Two air pumps were used for the aeration of the system. All the running details of the reactors were programmed into a data logger (Campbell Scientific CR850). In order to apply different aeration rates to the reactors, an air flow meter was used to adjust the air flow rate entering the system. This SiBAR allows both mixing and aeration processes. This experimental design was selected to allow for easy applicability and for simultaneous operation.

Different operational variables was considered in order to design an optimum treatment system. The sawdust pH (2, 4, and 6), aeration rate (0.5, 4, and 7.5 L min^{-1}), contact time (30, 240, and 450 min), and adsorbent dosage (3, 5, 7 g L^{-1}) in different phosphorous concentrations (50, 175, and 300 mg L^{-1}) were introduced to the system as the variables. To analyse the phosphorous removal process, four dependent parameters (P removal percentage, Chemical Oxygen Demand (COD), Electrical Conductivity (EC), and pH) were measured as the design responses. In all the reactor runs the timing of fill and mix (20 min), draw and idle (10 min), and

settle (90 min) were set as a constant value for all the reactors (Aziz, Aziz, & Yusoff, 2011; Mahvi et al., 2004); (Aziz et al., 2012).

3.2.4 Batch experiment

For each batch/shaking experiment, the optimum ALLODUST and ALLOCHAR dosage and mixed design for a range of time scales were determined. For batch/optimisation, the optimum adsorbent dosage and contact time were determined. The experiment was conducted in 50ml centrifuge tubes and shaken at different contact times. After the shaking was finished the samples were centrifuged for 10 minutes at 3500 rpm speed. The supernatants were analysed by the Smartchem 200 discrete analyser (Murphy & Reily 1962) method. The COD samples was prepared using COD digestion vials- high range, and employing the reactor digestion method from HACH-New Zealand (analysed by the HACH-DR 2800 spectrophotometer).

3.2.5 Scanning Electron Microscope (SEM)

The SEM was employed to examine the morphology of the soil and developed media before and after reaction with phosphorus. The soil and optimum developed media samples were coated with carbon by EMS 150T ES at 62A and 80 mm distance with three pulses @ 3 seconds/pulse. The morphology study was operated by SEM JEOL JSM 7000F at 5KV and WD6mm for imaging and WD10mm for EDS.

3.2.6 Experimental design (RSM-CCD)

In this research, central composite design (CCD) and the response surface methodology (RSM) method of DOE software (Stat – Ease) used mathematical and statistical techniques to model and analyse the responses of the materials to the experimental conditions. The design consists of k_2 factorial points completed by 2k axial points and a centre point, where k is the number of variables. Thereupon, the CCD and RSM methods were run in order to evaluate the association between the variables. Specifically, the pH of the sawdust, aeration rate, and contact time. Their responses (which were %P removal, COD. Also, the DO, EC, and pH) were recorded for each reactor. Thus, the objective of this design was to optimize the appropriate situation of operating

variables to predict the best value of responses; which was the removal of P contamination. This is summarised in equation 18:

$$\boldsymbol{Y} = (\boldsymbol{\beta_0} + \varepsilon) + \sum_{i=1}^{k} \boldsymbol{\beta_i X_i} + \sum_{i=1}^{k} \boldsymbol{\beta_{ii} X^2} + \sum_{i_i<j}^{k} \sum_{j}^{k} \boldsymbol{\beta_{ij} X_i X_j} + \cdots + \boldsymbol{e} \quad (3.1)$$

where Y is the response; Xi and Xj are the variables; β_0 is a constant coefficient; β_j, β_{jj}, and β_{ij} are the interaction coefficients of linear, quadratic and second-order terms, respectively; k is the number of studied factors; and e is the error.

3.3 Results and Discussions

3.3.1 Phosphorous removal analysis

Figure 3.7 illustrates the suitability of the system under different conditions. Desirability of P removal in the highest system proficiency – highest P removal, lowest contact time – is 1 while the adsorbent dosage is minimum. Also, it can be concluded that the highest P removal occurred when the system contained the minimum adsorbent dosage. The removal efficiencies of ALLODUST (Sawdust $_{pH:2}$) are presented in Table 3.3 and Figure 3.7.

Table 3.3 Experiment design of the batch study to find the optimum adsorbent dosage.

	Variables			Responses
Run	**P Concentration (mg L^{-1})**	**Adsorbent dosage (g L^{-1})**	**Contact time (min)**	**P removal (%)**
1	30	5	360	94.5
2	50	5	360	88
3	50	7	120	80
4	30	5	120	96
5	10	3	600	100
6	30	5	360	95
7	30	5	360	95
8	30	7	360	92
9	30	5	360	94.5
10	30	5	360	95
11	10	7	120	99
12	50	3	120	87
13	50	3	600	85
14	50	7	600	82
15	30	3	360	97
16	30	5	600	95
17	10	7	600	98.7
18	10	5	360	99.5
19	10	3	120	100

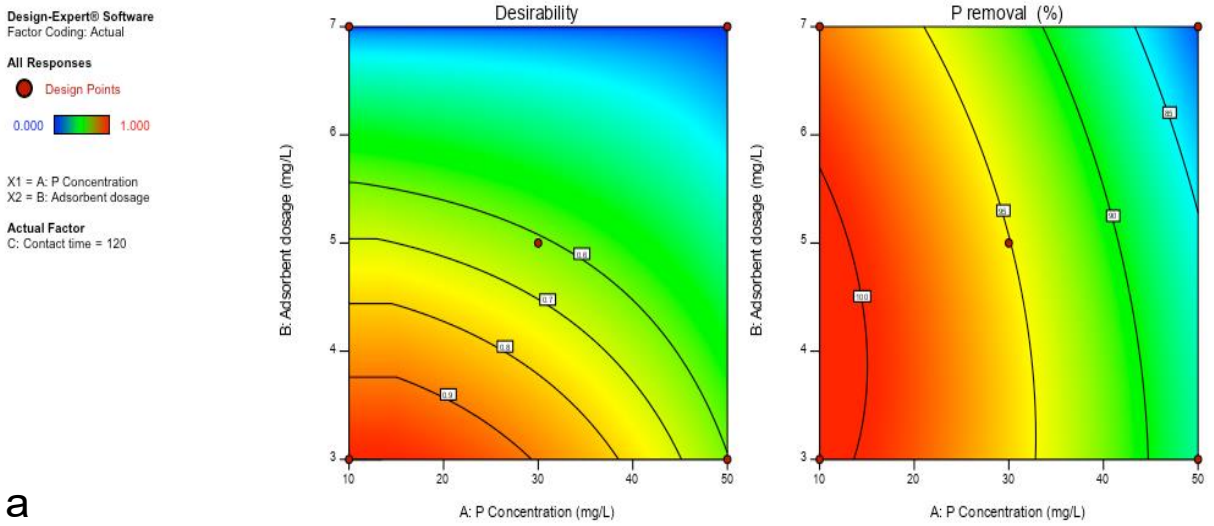

a

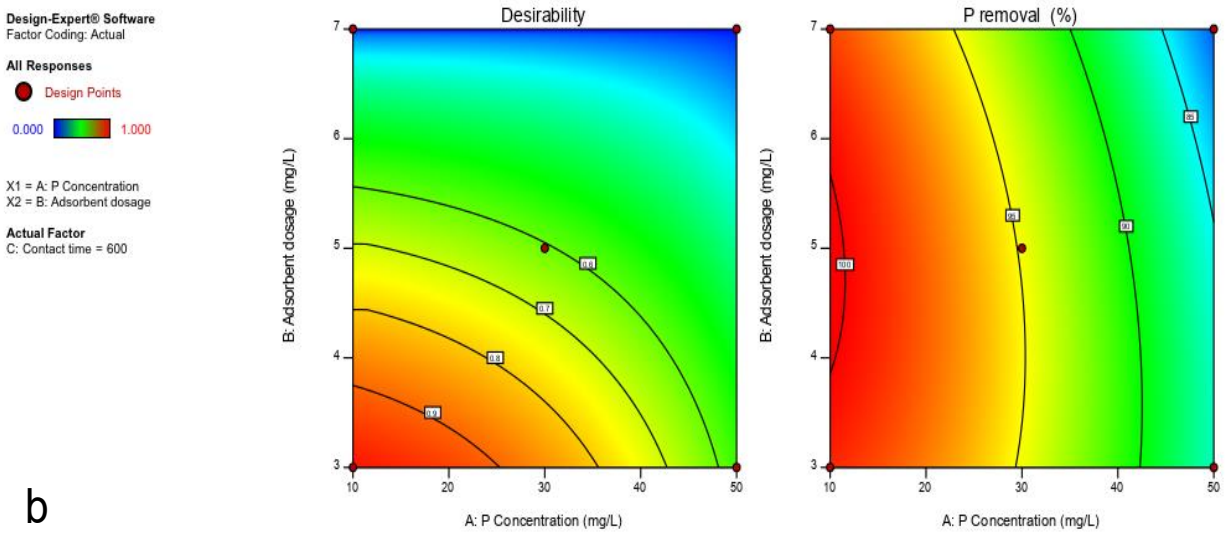

Figure 3.7 Effect of the adsorbent dosage on the P removal under the minimum and maximum contact times of a) 120 and b) 600 minutes respectively. Colour gradient indicates percent removal with red being 100% and blue being 0%.

In total, 8 kinds of media (consisting of novel, innovative materials) were developed in order to investigate the effect of the allophanic soil material, sawdust, pH of sawdust and the biochar on the phosphorous removal from wastewater in a SiBAR-CBA reactor. The Central Composite Design (CCD) method was utilised to design the experiments for each media, with 4 variables and 4 responses. The data was analysed with the Response Surface Methodology (RSM) software in order to monitor the effect of the variable changes in the responses. Finally, ANOVA was run for each experiment to determine the best operating details of the system and to choose the best media for removing P from the wastewater in the bioreactors. Table 4 shows the ALLODUST (comprising Horotiu soil material) removed P under optimum conditions for the different contamination zones. In total, 90 reactors for H-ALLODUST, 90 for the C-ALLODUST, 20 for the H-ALLOCHAR and 20 for the C-ALLOCHAR (Total of 220+ (16 control samples) reactors) were run to find the optimum media for the P removal, under the optimal operational conditions of the reactors; being lowest contact time and lowest aeration rate. Also in order to record the effect of each part of the media in P removal two control samples was run for each optimum condition.

Table 3.4 Optimization of the different developed media for P removal from wastewater, where H-in ALLODUST and ALLOCHAR refers to Horotiu, and C in C-ALLODUST refers to Craigieburn respectively.

	SD_{pH}	Aeration rate (L min^{-1})	Contact time (min)	P removal
		1- 50 (mg L^{-1}) – Low range		
H-ALLODUST	2.5	1.5	42.52	99.86
C-ALLODUST	5.68	1.5	447	100
H-ALLOCHAR	-	4.86	398	96.69
C-ALLOCHAR	-	4.68	385	100
		51-175 (mg L^{-1}) – Mid-range		
H-ALLODUST	4.21	7.49	450	79.12
C-ALLODUST	4.02	7.49	450	76.97
H-ALLOCHAR	-	4.35	450	60.11
C-ALLOCHAR	-	4.56	450	67.9
		176-300 (mg L^{-1}) – High-range		
H-ALLODUST	5.80	7.5	450	85.13
C-ALLODUST	2.29	7.5	450	69.31
H-ALLOCHAR	-	4.39	450	64.65
C-ALLOCHAR	-	5.0	450	57.97

3.3.2 Phosphorous Removal by H-ALLODUST

The results indicated that the phosphorous removal of H-ALLODUST was significantly affected by all four system variables. Moreover, central composite design was used to determine the interactive effects of the variables. The corresponding results are shown in Table 3.5.

Utilising the three-dimensional response surface curves and contours, the optimum values of the variables for P removal from the wastewater were determined. Figure 3.8 displays the response surface and contours of the P removal rate as a function of P concentration and contact time as independent variables while the sawdust pH and aeration rate are considered as the actual factors for the low-range P concentration to the high-range P concentration. The response surface of the P removal rate gradually decreased when the contact time and the P concentration increased from 30 to 450 min and 50 to 300 mg L^{-1} respectively when the system contained up to 50 mg L^{-1} phosphorous. Figure 3.8a illustrates the highest P removal with 99.86% when the P concentration was 50 mg L^{-1} and contact time was 30 minutes.

Table 3.5 Optimization of the different developed media for P removal from wastewater, utilising RSM and the Central Composite Design.

H-ALLODUST (HOROTIU base)								
Run	**Factor 1 A: Sawdust pH**	**Factor 2 B: Contact time (min)**	**Factor 3 C: Aeration rate (L min^{-1})**	**Factor 4 D: P Concentration (mg L^{-1})**	**Response 1 P removal (%)**	**DO (mg L^{-1})**	**EC (µS/cm)**	**pH**
1	2	450	1.5	300	55.39	9.62	1205	8.17
2	6	450	4.5	175	50.59	9.50	756	7.75
3	6	240	4.5	175	43.55	7.63	802	9.24
4	4	450	1.5	300	55.76	9.65	1211	8.05
5	2	30	7.5	300	53.1	9.37	1218	7.66
6	4	30	7.5	300	64.75	9.37	1228	7.62
7	6	30	4.5	175	37.61	9.37	896	7.35
8	4	30	1.5	50	94.76	7.19	376	9.55
9	4	30	1.5	300	41.33	8.95	1206	7.37
10	2	450	1.5	50	95.34	7.12	432	9.00
11	2	240	4.5	175	67.33	9.30	803	7.64
12	6	240	7.5	175	66.06	9.26	788	7.60
13	6	240	1.5	175	38.82	9.49	864	7.59
14	6	240	4.5	175	45.32	7.61	802	9.19
15	2	30	7.5	50	99.86	7.25	460	10.36
16	6	240	4.5	175	44.01	7.55	804	9.21
17	4	450	1.5	50	90.96	7.20	378	8.95
18	2	30	1.5	50	97.04	7.19	369	9.95
19	6	240	4.5	300	54.04	9.27	1208	8.08
20	4	450	7.5	300	79.8	9.71	1201	8.26
21	2	450	7.5	50	94.44	7.33	470	8.91
22	6	240	4.5	175	43.87	7.65	805	9.28
23	2	30	1.5	300	44.95	9.18	1210	7.53
24	6	240	4.5	175	43.21	7.60	803	9.25
25	4	450	7.5	50	95.22	7.30	466	8.90
26	4	30	7.5	50	97	7.25	397	9.53
27	2	450	7.5	300	58.05	9.66	1194	8.23
28	6	240	4.5	175	42.5	7.55	807	9.21
29	4	240	4.5	175	43.09	9.26	767	7.58
30	6	240	4.5	50	43.2	7.68	798	9.25

When the adsorbent is mixed with 50 mg L-1 to 300 mg L-1 P, (Figure 3.8), the system needs to be run with the highest contact time and the aeration rate for optimum operating conditions. The P removal was 79.12% for the mid-range zone by H-ALLODUST pH: 4.21 and 85.13% for the high-range zone by H-ALLODUST pH: 5.82 in 450 minutes. The adsorption amount for the blank Horotiu soil was just 52% and 41% in the mid-range and high-range P concentration while it could adsorb the 100% of the P in the low-range reactors.

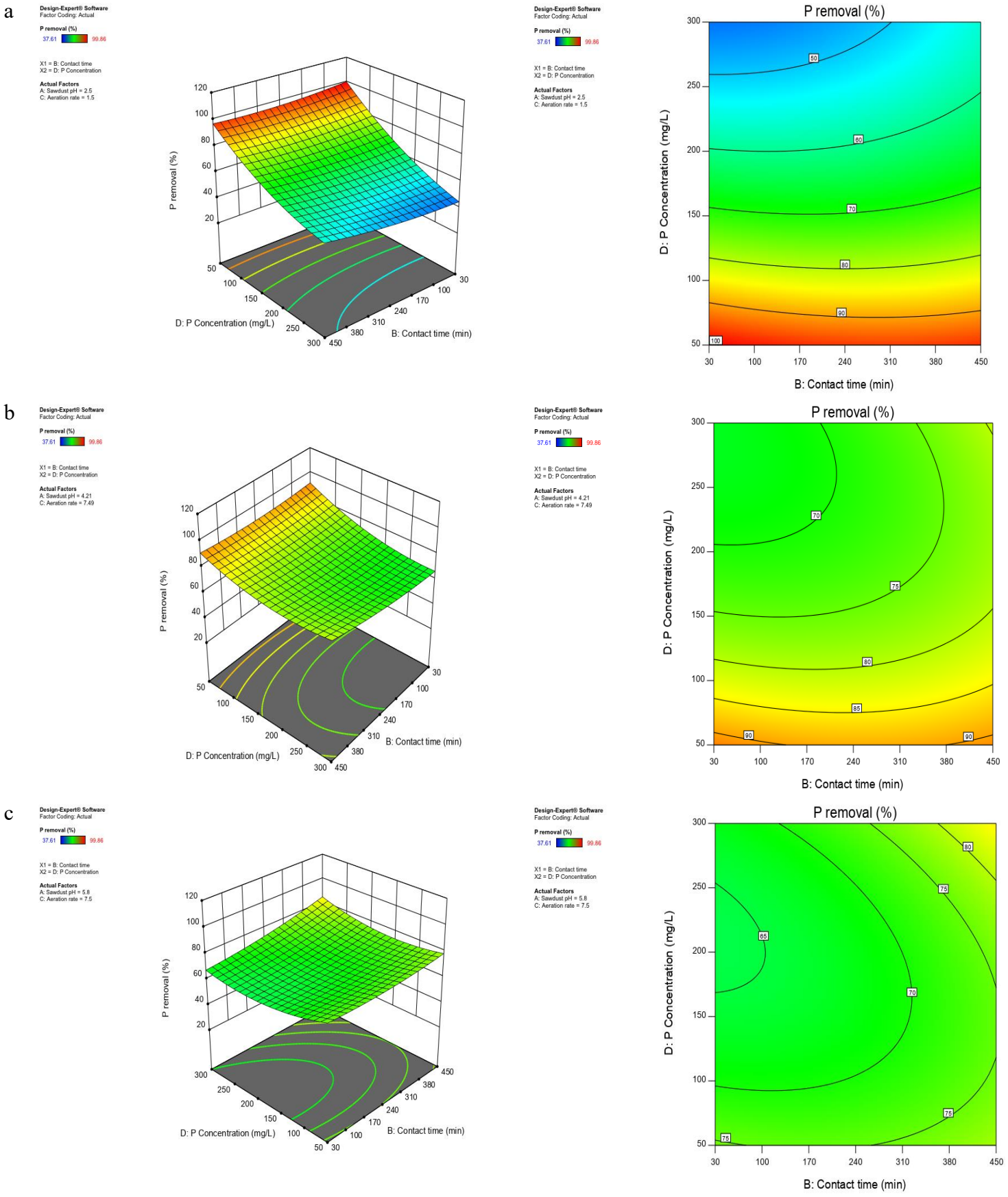

Figure 3.8 The response surface plots and corresponding contour plots of the optimized design for the a) low- range (1-50 mg L^{-1}), b) mid- range (51-175 mg L^{-1}), and c) high-range (176-300 mg L^{-1}) P removal efficiency as a function of contact time and P concentration.

Different clay minerals react with phosphate based on their physical and chemical properties. Kaolinite and goethite are often cemented together in a binary association and used as a mixture (GKM) and also an association (GKA), to enhance the soil phosphate adsorption capacity (Wei et al., 2014). Both goethite and kaolinite minerals are pH dependent and their adsorption capacity is highly dependent on the surface properties of the adsorbents. Montmorillonite's surface area and pore volumes when enhanced by the Zr^{4+} and Zr^{4+} / Al^{3+} treatment. Zr^{4+} / Al^{3+} showed a more significant ability to adsorb phosphate by 17.2 mg P g^{-1} under acidic conditions. The inorganic-bentonite modification was facilitated by Fe and Al (L.-g. Yan et al., 2010). The interlayer spacing and pore volumes were increased significantly: 4 g L^{-1} of the Al-bentonite at pH=3 could adsorbed up to 60 mg L^{-1} phosphate in 6 hr.

Phoslock® (lanthanum (La) modified bentonite), has been recognized as one of the most powerful medias to adsorb phosphate in aqueous solutions (Boers et al., 1992; Haghseresht et al., 2009; Reitzel, Jensen, et al., 2013; Robb et al., 2003; Ross et al., 2008; van Oosterhout & Lürling, 2013; Vopel et al., 2009), with acidic conditions favouring Phoslock® adsorption behaviour. Haghseresht et al. (2009) showed a 30% drop in adsorption capacity when pH increased to 9.0 from 5.0. It was reported that Phoslock® can't control the SRP concentration higher than 0.047 mg P L^{-1} and the reason is the interaction between La and humic acids (Lürling & van Oosterhout, 2013; Reitzel, Jensen, et al., 2013) even in the ratio of 220:1 of Phoslock® : P. Also, the pH dependency of the Phoslock® is not routine and is reversible. The results presented here show that H-ALLODUST could remove a notable amount of the P from wastewater in a wide range of non-acidic pH (Table 3.5) and short contact time. Also, the optimum adsorbent dosage to remove up to 300 mg L^{-1} of the phosphorous was just 3 g L^{-1}.

3.3.3 Adsorption Mechanisms

3.3.3.1 Allophane adsorption mechanism

Different soil properties are known as the main factors for phosphorus adsorption; pH (Ige et al., 2007), extractable Al and Fe(J. Kang et al., 2009), organic C(Ige et al., 2007), and clay content(Shoji & Ono, 1978). It has been reported that the allophanic soils adsorb the phosphate anion (Beck et al., 1999) with nano-ball allophane minerals being the adsorption agents (M Abdalla Elsheikh et al., 2009; Johan et al., 1997). Because of the Al-OH and Al–H_2O functional groups present on the surface of allophane minerals (Kasama et al., 2004), allophanic soils have more potential to adsorb the phosphate anions compared to the other

clay minerals such as kaolinite and montmorillonite with very high SSA and CEC. In the structure of allophane, the aluminol groups are only located at the pores of the wall of the hollow spherules (Henmi & Huang, 1985). Storing the organic carbon and phosphate adsorption are the main characteristics of the allophane spherules.

The surface complexation (specific adsorption) and proton transfer reactions of metals and ligands are the processes which cause the surface charge of the iron hydroxides (Stumm & Morgan, 2012). This surface property is one of the more important factors in the reaction of the anions and mineral surfaces during the adsorption mechanism. The anionic adsorption governs the ligand exchange mechanism, in which the water dipoles desorption is one of the main consequences (Hiemstra & Van Riemsdijk, 1996; Stumm, 1992). The exchange of the surface hydroxyl groups with the ligands (There is always a competition between ligands and OH^- for occupation of the binding sites) is the main process for the formation of the surface complex which its extension is completely depends on the solution pH (Hanrahan, 2010; Mohajeri et al., 2019). The inner sphere complexes which are known as the solute complexes and also surface complexes are formed during the adsorption of the anions by the minerals.

The physical-chemical characteristics of anions such as ionic radius, bulk diffusion coefficient, hydration energy, and solubility and how they interact with the different adsorbent surfaces determine the adsorption/selective mechanism of a treatment system. The other effective factor on the adsorption efficiency is the anions immobilization onto the adsorbent which is completely dependent on the pore sizes of the adsorbent. So, the anions hydrated dimensions and the adsorbent pore sizes are the factors which need to be considered in an adsorption system. The selective anionic adsorption is the outcome of this limiting factor. Also, the anions and adsorbent surface form inner-outer sphere complexes and electrostatic or hydrogen bonding need to be considered. Considering all these factors, the selective anionic adsorption does not completely follow the radius properties and charge. The sulphate behaviour is an example where they can form complexes on Al and Fe oxides and hydroxide with different charges when compared to fluoride, sulphate has a greater radius (Sposito, 1984). The investigation of the anions behaviour close to the depletion region is limited by the hydrated anion radius. This region is different in size for each mineral and adsorbent (Manciu & Ruckenstein, 2003). The translocation of the water molecules present in the hydrated anion

with metals is weak and completely ephemeral. The long-range electrostatic forces are the only attraction force between adsorbent surface and hydrated anions with large hydrated radius such as phosphate. The covalent bond is associated between the anions with smaller hydrated radius which can form the inner sphere complexes (Langmuir, 1997). The anions interaction with mineral surfaces which results in the adsorption is completely affected by iron oxide and hydroxide and its surface charge. The surface complexation of ligands and metals and proton transfer are the processes which appoint this charge (Stumm & Morgan, 2012). The water dipole desorption happens during the anionic adsorption which is controlled by the exchange of ligands (Hiemstra & Van Riemsdijk, 1996; Stumm, 1992).

3.3.3.2 Sawdust adsorption mechanism

The sawdust principal adsorption mechanisms are known as hydrogen bonding and ion exchange. The sawdust complex characteristics and the adsorption behaviour of the components when in contact with the ions are the factors which support this idea. The active ion exchange sawdust compounds are mainly the hydroxyl groups from the cell walls as well as the lignin and cellulose, that is, the polymeric material. Sawdust modification can enhance the adsorption properties of sawdust. Other researchers have successfully modified sawdust to enhance the binding ability (Benyoucef & Amrani, 2011; Shukla et al., 2002) resulting in the introduction and adjustment of more N-, S-, and P-containing groups which are extractive groups of the sawdust. These groups have electron donating behaviour while the phosphate is behaving as an electron acceptor. Based on these concepts the ion exchange mechanism could be considered as the main adsorption process in a system containing sawdust. The P ions present in the wastewater can be adsorbed by a solid media through the surface complexes formed between the P and the adsorbed ligands while the sawdust acid treatment can add more active sites on the surface (Figure 3.9). The physical adsorption mechanism by functional groups is the other considerable contaminant retention behavior of the sawdust. The surface activation and pores development was due to the acidic treatment of the sawdust.

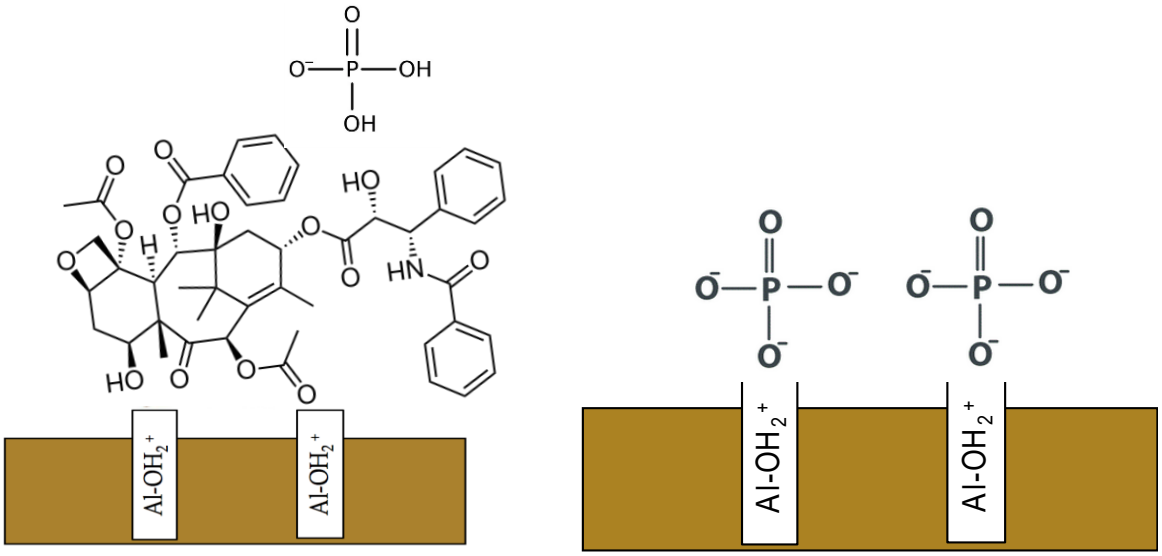

Figure 3.9 Sawdust role in P adsorption in the presence of the Allophane.

One of the most effective factors on the sawdust adsorption capacity is the dosage used in the treatment system based on the type of the contaminant and its concentration. For most cases, the lower adsorbent dosage is preferable. In this case all the surface sites are available and exposed for retention of contaminants and the surface saturation can happen faster which results in an enhancement of the system's adsorption capacity. On the other hand, the higher energy sites become unavailable when using the high adsorbent dosage. As a consequence, most of the lower energy sites become occupied which drops the total adsorption capacity of the system.

3.3.4 Fourier Transform Infrared Spectroscopy (FTIR) analysis

The FTIR result is presented in Figure 3.10. The presence of the allophane mineral in the media can be concluded from the band in 1028 and 816 cm^{-1} which belongs to strong Si–O–Si v_a and also the 524 and 480 cm^{-1} Si–O–Al which is an out-of-plane bending (Bishop et al., 2013; Levard et al., 2012; Parfitt et al., 1980; Russell et al., 1981). The bands at 1485 cm^{-1} can be represent the O_3–Si–OH and 688 cm^{-1} the presence of the H_2O. The weak bands belong to the OH v_s happen at more than 3600 cm^{-1}. Two bands of 688 and 500 cm^{-1} represent the allophane and opaline silica with a disordered structure while the 688 cm^{-1} band belongs only to the adobes. An increase at 1156 cm^{-1}, and 1052 cm^{-1} bonds can be seen due to the lignin structure. A strong aromatic ring stretch, phenylpropanoid polymer deformation (methyl and (methyl and methylene), glycosidic linkage, and vibrational stretching are indicative of a number of methylene, glycosidic linkage, and vibrational stretching are indicative of a number of bonds

which are present in the lignin (Adapa et al., 2009). Following P adsorption, Figure 3.10 illustrates that the binding energy belonging to the -OH groups (Si-OH, Al-OH) dropped because of the hydrogen bond formation between the P ions and the adsorbent (Iyoda et al., 2012; Opiso et al., 2009). Also the bonding between P ions and oxygen in hydroxyl groups resulted in the wavelength decrease of the hydroxyl groups which made the –OH binding energy weaker. So, due to the different binding changes and shift the interaction of the P ions with allophane and sawdust structure can be seen from the FTIR analysis.

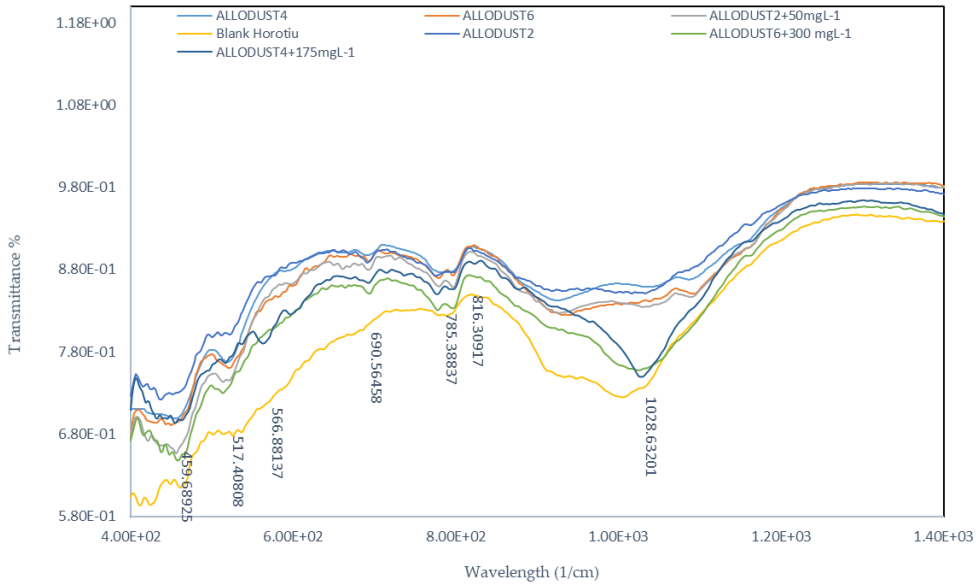

Figure 3.10 Fourier transform infrared spectroscopy (FTIR) of H-ALLODUST in different sawdust pH before and after P adsorption.

3.3.5 X-Ray powder Diffraction (XRD) analysis

The changing in the microstructure of clay minerals is one of the consequences of the interaction between contaminants and clay soil which impact the clay particle forces. XRD was used to analyse the soil structural

Figure 3.11 presents the result of the X-ray diffraction of the Horotiu soil material and H-ALLODUST at different sawdust pH values before and after interaction with phosphorous. According to the presented data, the main peaks intensity dropped while P presented in the structure of the media in high concentration. While the high concentration of phosphate adsorbed by the ALLODUST, the P ions concentration increased in the pore fluid and led the change in the structure which made it flocculated. That change didn't happen in the low range of phosphate concentration which adsorbed on the surface by the reactive sites and was

significantly lower than the adsorption capacity of the media. The peak intensity of the flocculated soils is lower than the dispersive ones. The presence of sawdust improved the peak intensity of the media in the presence of 300 mg L^{-1} phosphorous. So, the results of the SmartChem P analysis agree with the XRD diffraction results. It must be noticed that the peak position is not affected by increasing the P concentration of the pore fluid but just affects the peak intensity

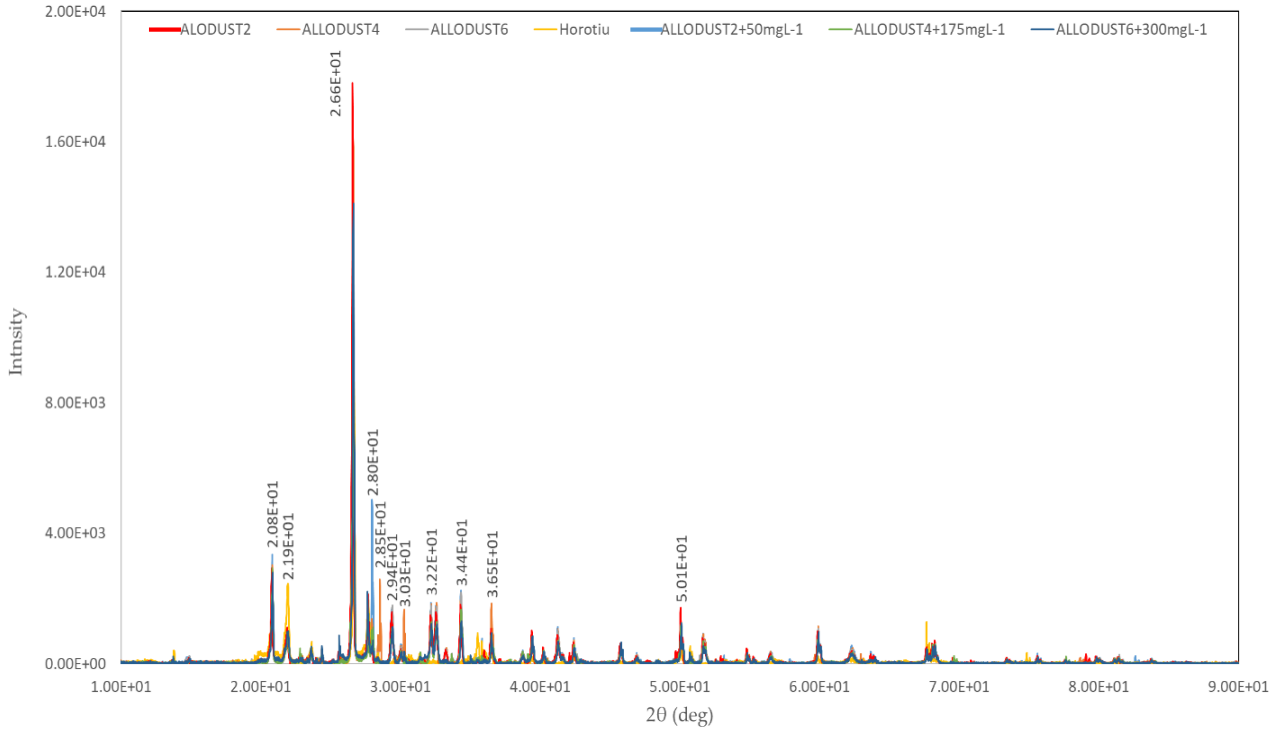

Figure 3.11 Changes of the peak intensity of the optimum and the blank samples (XRD).

3.3.6 Chemical Oxygen Demand (COD) analysis

Non-biodegradable organic matters (NBOM) are controlling the COD amount of an effluent. During the treatment process, it's essential to decrease the amount of the NBOMs in order to control the COD concentration to meet the guidelines (Rodrıguez et al., 2004). Soil minerals make several complexes with different properties when in contact with organic compounds, inorganic cations, water, silicate layers and organic molecules are all effective factors.

Recently, different studies have been conducted concerning sawdust application to remove different contaminations from wastewater. In a wastewater treatment process the main factors affecting the COD concentration in the effluent are the microorganisms, aquatic plants,

and wood based materials. So, it's essential to report the COD concentration and its changes during the process while using a bio-waste as a media in the removal process (Argun et al., 2007). So, the main objective of this part of the experiment was to quantify the effect of sawdust on the COD in the solution with different P concentrations and the other operational variables (such as contact time and aeration rate) (Table 3.6).

Table 3.6 Experimental variables for the COD changes as the result.

Run	Factor 1 A: Sawdust pH	Factor 2 B: Contact time min	Factor 3 C: Aeration rate L min^{-1}	Factor 4 D: P Concentration mg L^{-1}	COD mg L^{-1}
1	2	450	1.5	300	45
2	6	450	4.5	175	25
3	6	240	4.5	175	36
4	4	450	1.5	300	15
5	2	30	7.5	300	40
6	4	30	7.5	300	30
7	6	30	4.5	175	32
8	4	30	1.5	50	26
9	4	30	1.5	300	31
10	2	450	1.5	50	33
11	2	240	4.5	175	51
12	6	240	7.5	175	32
13	6	240	1.5	175	37
14	6	240	4.5	175	34
15	2	30	7.5	50	29
16	6	240	4.5	175	37
17	4	450	1.5	50	23
18	2	30	1.5	50	29
19	6	240	4.5	300	18
20	4	450	7.5	300	14
21	2	450	7.5	50	32
22	6	240	4.5	175	35
23	2	30	1.5	300	44
24	6	240	4.5	175	36
25	4	450	7.5	50	32
26	4	30	7.5	50	20
27	2	450	7.5	300	40
28	6	240	4.5	175	36
29	4	240	4.5	175	41
30	6	240	4.5	50	19

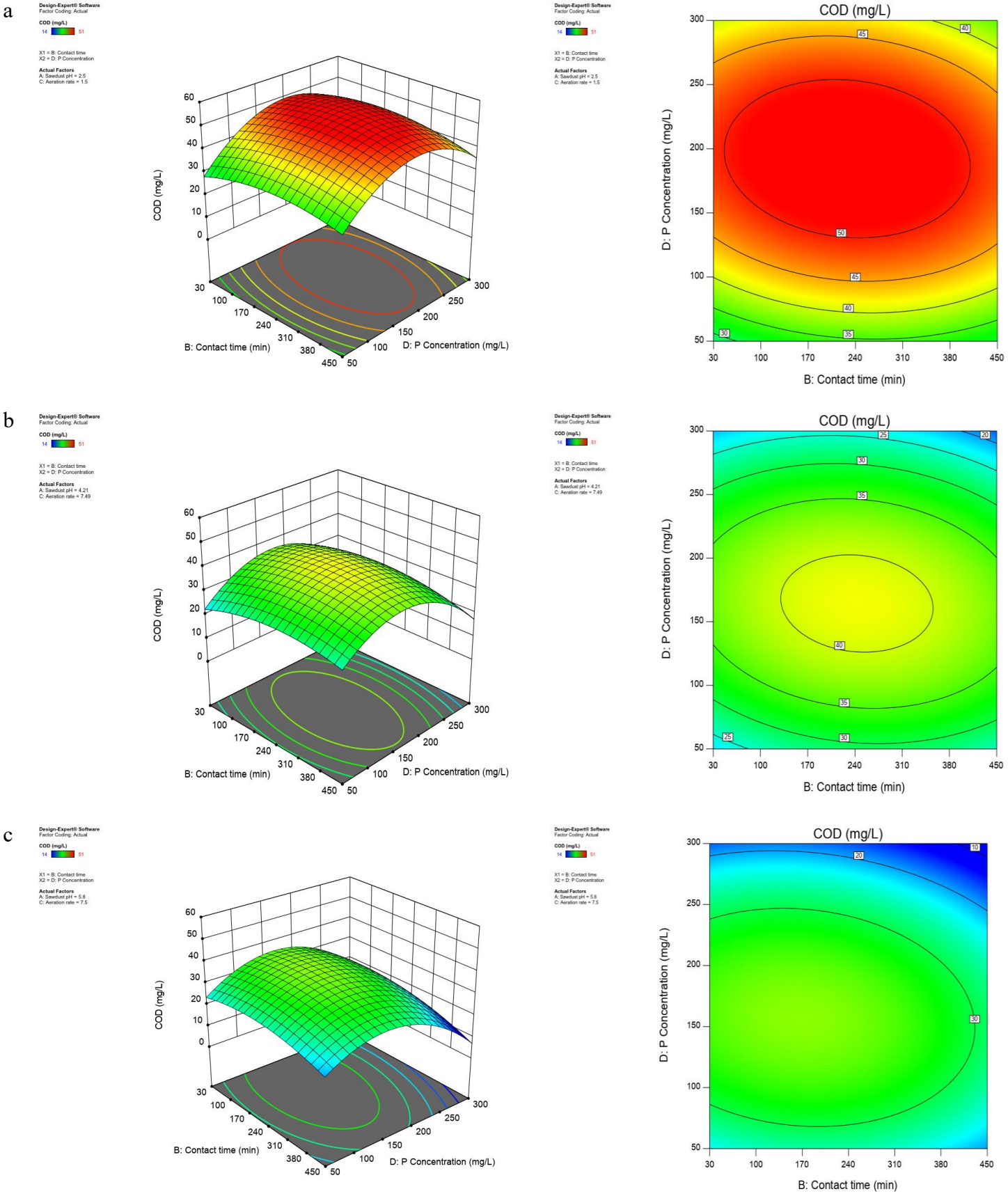

Figure 3.12 The response surface plots and corresponding contour plots of the optimized design for the a) low-range (1-50 mg L^{-1}), b) mid-range (51-175 mg L^{-1}), and c) high-range (176-300 mg L^{-1}) COD as a function of contact time and P concentration.

Figure 3.12 illustrates the trend of COD amounts for the different optimized conditions. The main objective of this experiment was to monitor the COD content and the changing trend of the optimized samples for each contamination range from low to high, after the P adsorption. The maximum COD amount occurred with the H-ALLODUST $_{pH:2}$ with 51 mg L^{-1} when mixed with the mid-range (175 mg L^{-1}) P contamination and run with 4.5 L min^{-1} aeration rate for 240 min. This result is in parallel with the P adsorption optimization while the H-ALLODUST$_2$ showed the highest removal efficiency for the low-range of P. The COD amount of the same media was only 29 mg L^{-1} for the low-range P concentration (50 mg L^{-1}) when run with 1.5 L min^{-1} aeration rate for only 30 min. So, the optimized operational conditions also contained the lowest COD after P adsorption. The mid-range optimized media (SD_{pH}:4.21 and Aeration rate:7.49) at the highest contact time (450 min) contained between 35 mg L^{-1} to 40 mg L^{-1} COD which was not the lowest but a good range when mixed with the 175 mg L^{-1} phosphorous. The COD amount for the high-range P concentration was only between 14 mg L^{-1} to 18 mg L^{-1} when the system was run at its optimized condition for this range of P. The COD could increase up to 45 mg L^{-1} with the other operational conditions remaining constant in this contamination range.

From these results, it can be stated that under acidic conditions of the media, both Horotiu and sawdust functional groups obtained a positive charge on the surface while the charge became negative under alkali conditions. So, adsorption efficiency of the organic matter which has a negative charge is high under acidic situations. Conversely, for the acidic treatment of sawdust, HCl was used to increase the proportion of active surfaces and to prevent the elution of tannin compounds that would stain the treated water and that would greatly increase COD. However, in parallel with increasing the P concentration from 50 mg L^{-1} to 175 mg L^{-1} the COD amount incurred as an incremental leap; but with increasing the anion concentration to 300 mg L^{-1} the COD amount decreased. So, the acidic treatment and protonation of the sawdust surface could be known as a method to control the COD concentration of the effluent.

3.3.7 Scanning Electron Microscope (SEM)

The results of the morphological study are illustrated in Figure 3.13 – 3.14.

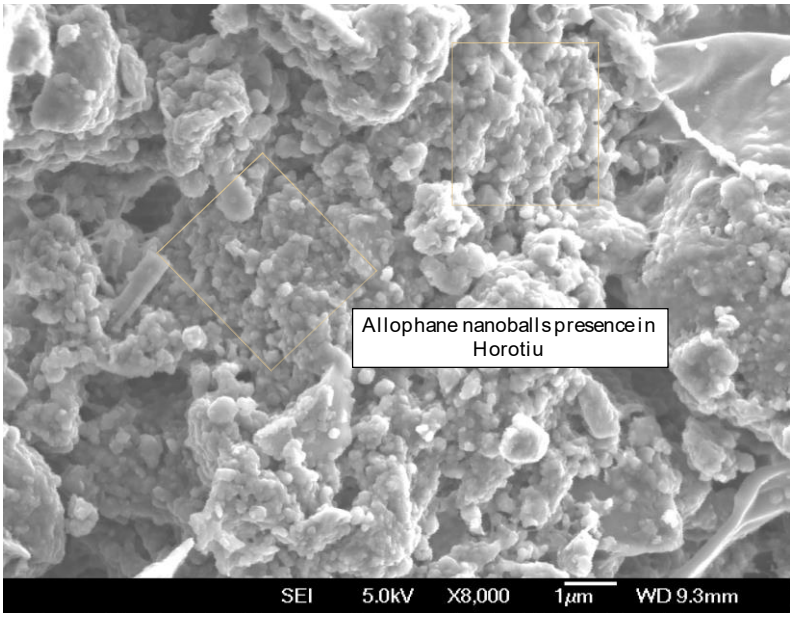

Figure 3.13 Scanning Electron Microscopy (SEM) of Horotiu.

The binding materials between the soil and media particles couldn't be resolved under optical magnification. The SEM images of the Horotiu soils and H-ALLODUST showed that silty structural units were dominant in the Horotiu soil. Also, allophane particles were the likely origin of the gel-like material observed. Three gravity sedimentation process were conducted and then the deposited materials were used for the morphology study (Figure 3.13). The clay size particles are still merged into each other, and the increased resolution shows that the binder is formed of globular agglomerates of spherical particles with outer diameters of approximately 5 nm, which corresponds to the morphology and dimensions of allophane particles (Bishop et al., 2013; Calabi-Floody et al., 2011; Levard et al., 2012; Rennert et al., 2014; Wada & Wada, 1977). These aggregates were observed on both Horotiu soil and H-ALLODUST media before and after the P adsorption.

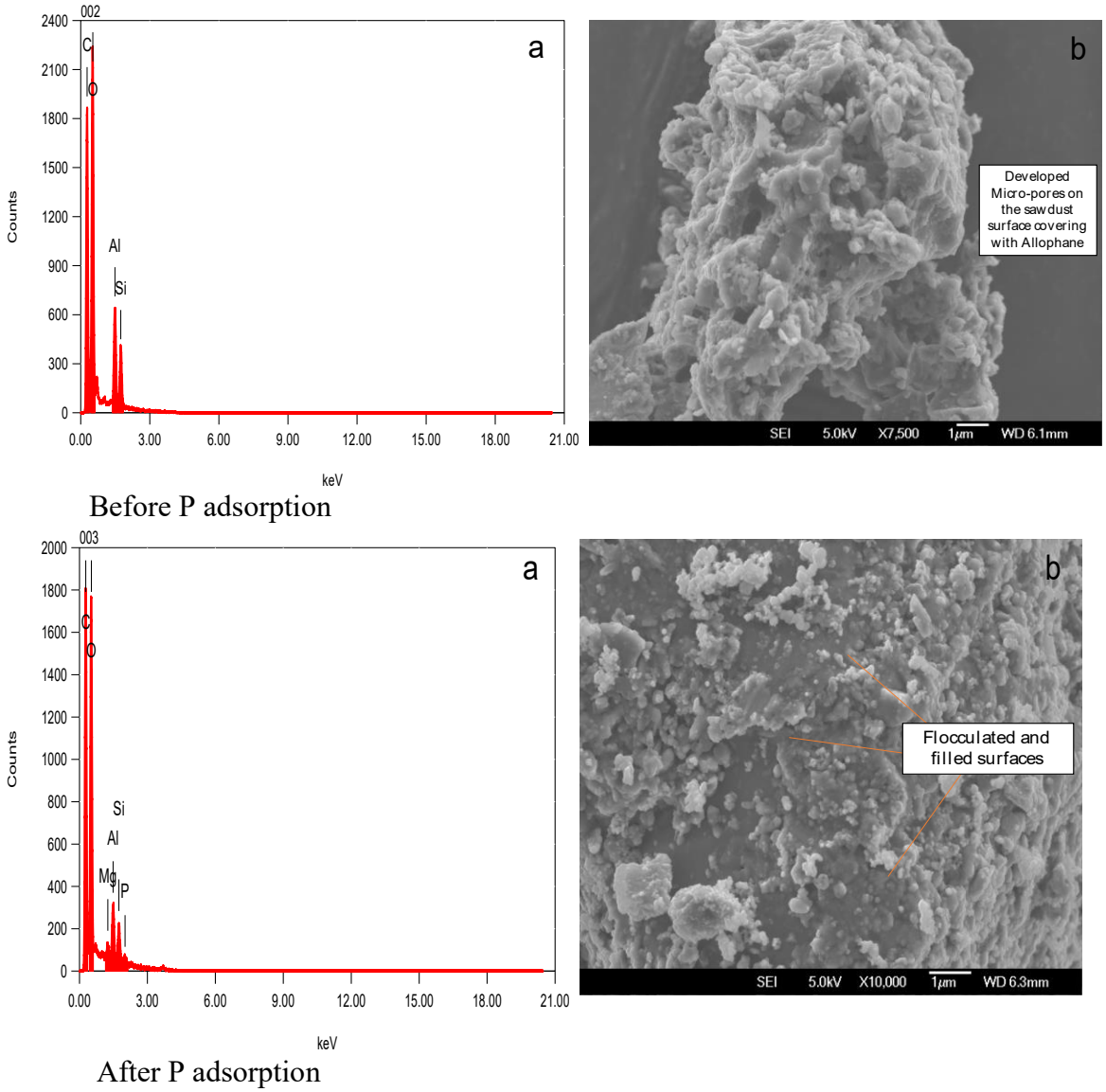

Figure 3.14 a) Energy-Dispersive Spectroscopy (EDS), and b) Scanning Electron Microscopy (SEM) of ALLODUST$_2$ before and after P adsorption.

The purpose of the sawdust acidic treatment was to increase the surface activity. The surface was activated resulting in well-developed pores and covered by the allophane nano particles (Figure 3.14 a). The acidic treatment was effective in achieving and activating the surface of the raw sawdust. The developed pores and channels on the sawdust particles are due to the elimination of filaments. SEM images of the media after the P adsorption (H-ALLODUST+50 mg L^{-1} P) demonstrates that the flocculated particles and filled pores can be seen while the allophanic particles are still present on the surface which is parallel with the adsorption results (Figure 3.14 b). The H-ALLODUST adsorbed almost all the P in the solution and still had the

capacity to adsorb more P from the wastewater. In addition, the EDS graphs demonstrate the presence of the P on the media surface (Figure 3.14 b).

3.3.8 Optimization and Statistical Analysis

The correlation between the variables sawdust pH, contact time (min), aeration rate ($L.min^{-1}$), and P concentration ($mg\ L^{-1}$) and the two important process responses, P removal (%) and COD ($mg\ L^{-1}$) was analyzed by response surface methodology (RSM). Several model terms were preferred to achieve the best fit in a particular model. The development of mathematical equations where predicted results (Y) were evaluated as a function of the sawdust pH (X_1), contact time (X_2), aeration rate (X_3), and P concentration (X_4) was permitted by central composite design (CCD). The sum of a constant four first order effects (terms in X_1, X_2, X_3 and X_4), six interaction effect (X_1X_2, X_1X_3, X_1X_4, X_2X_3, X_2X_4, X_3X_4), and four second-order effects ($X_1^{2,}$ $X_2^{2,}$ $X_3^{2,}$ X_4^{2}) were the factors which the calculation conducted based on them as shown in equation (1) and Table 3. Based on the parameter estimation, the following quadratic polynominal equation (19) is given to correlate the relationship between the four factors and the P removal rate.

$$\text{P removal} = +152.42941-3.65946X_1-0.053889X_2-13.39301X_3 \\ 0.499988X_4+0.005881X_1X_2+0.954583\ X_1X_3 +0.042907\ X_1X_4 -0.000652X_2X_3 +0.000137\ X_2X_4 \\ +0.008308X_3X_4 -1.61891X_1^{\,2} +0.000052\ X_2^{\,2}+1.18366\ X_3^{\,2} +0.000437\ X_4^{\,2} \quad (19)$$

Where Y is P removal percentage and X_1, X_2, X_3, and X_4 are the coded values of sawdust pH, contact time, aeration rate and P concentration, respectively.

Table 3.7 Model statistic details.

Std. Dev.	6.85	**R^2**	0.9510
Mean	62.70	**Adjusted R^2**	0.9053
C.V. %	10.92	**Predicted R^2**	0.7157
		Adeq Precision	13.3729

The model can be considered significant based on the Model F-value of 20.79. The chance of the occurrence of this F-value due to the noise is only 0.01%. Also, it can be concluded that the model terms are significant based on the P-values less than 0.0500. In this case the significant model terms represent as A, C, D, AC, AD, C^2. Values greater than 0.1000 indicate

the model terms are not significant. Also, the Lack of Fit F-value of 78.72 implies the Lack of Fit is significant. The chance of the occurrence of this Lack of Fit to the noise is only 0.01% (Table 3.7 and Table 3.8).

The Predicted R^2 of 0.7157 is in reasonable agreement with the Adjusted R^2 of 0.9053; i.e. the difference is less than 0.2. Adeq Precision measures the signal to noise ratio. A ratio greater than 4 is desirable. The model ratio of 13.373 indicates an adequate signal, and this model can be used to navigate the design space. The optimum conditions for the H-ALLODUST were determined for different P contamination zones (Table 3.4).

Table 3.8 ANOVA for Quadratic model

Source	Sum of Square	df	Mean Square	F-value	p-value	
Model	13653.06	14	975.22	20.79	< 0.0001	significant
A-Sawdust pH	417.70	1	417.70	8.90	0.0093	
B-Contact time	159.84	1	159.84	3.41	0.0847	
C-Aeration rate	731.54	1	731.54	15.60	0.0013	
D-P Concentration	2481.47	1	2481.47	52.90	< 0.0001	
AB	48.81	1	48.81	1.04	0.3239	
AC	262.43	1	262.43	5.59	0.0319	
AD	920.49	1	920.49	19.62	0.0005	
BC	2.70	1	2.70	0.0575	0.8137	
BD	207.14	1	207.14	4.42	0.0529	
CD	155.31	1	155.31	3.31	0.0888	
A^2	189.33	1	189.33	4.04	0.0629	
B^2	13.86	1	13.86	0.2955	0.5947	
C^2	294.03	1	294.03	6.27	0.0243	
D^2	120.97	1	120.97	2.58	0.1291	
Residual	703.60	15	46.91			
Lack of Fit	699.16	10	69.92	78.72	< 0.0001	significant
Pure Error	4.44	5	0.8881			
Cor Total	14356.65	29				

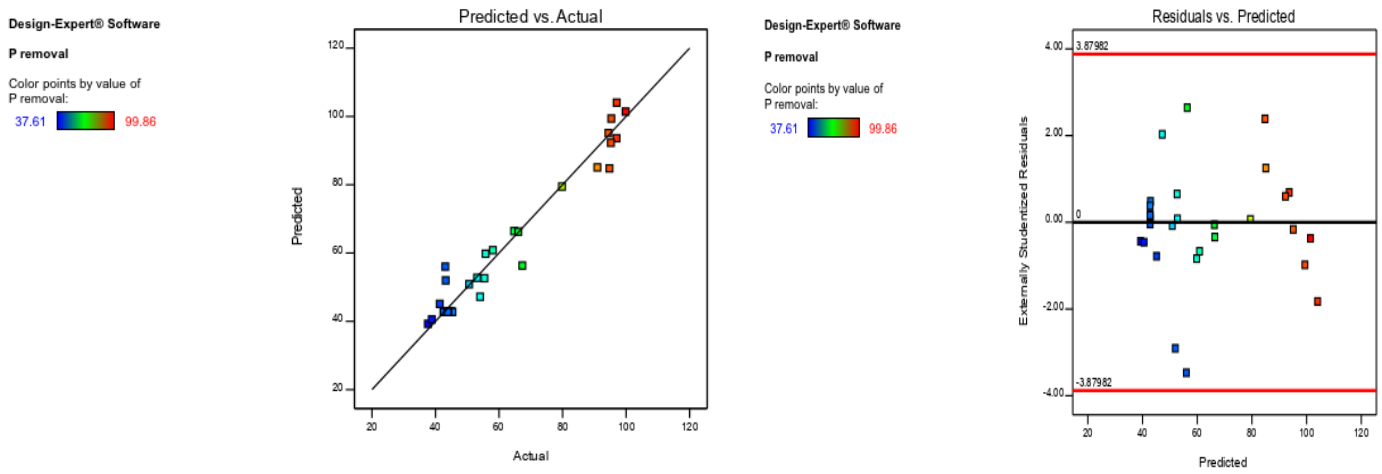

Figure 3.15 Design-expert plot; predicted vs. actual values plot for P removal – Residuals vs. Predicted.

All the models were significant at the 5% confidence level due to the probability < 0.05. In the quadratic models R^2 values close to 1 were favourable and an acceptable modification of the model can be concluded with a high value of the R^2. The ratio of sum of squares due to regression (SSR) to total sum of squares (SST) was indicated by the correlation coefficient (R^2) which presented the total variation in the response predicted by the model. Adequate precision compared the range of the predicted values at the design points to the mean prediction error. The sufficient agreement between the values achieved from the model and the real data is illustrated clearly in Figure 3.15.

3.4 Conclusions

The phosphorus removal efficiency of our innovative material (ALLODUST) augmented SiBAR was carried out using a low to high range of P concentrated agricultural wastewater. Utilising wastewater containing higher than permissible discharge limits of P also allowed us to investigate the morphology and microstructural changes along with the adsorption capacity of the media when it's mixed with a very high P concentration. The overarching aim of our research was to develop a low-cost and sustainable adsorbent media material which can adsorb a high concentration of phosphorus at the lowest contact time and minimal energy consumption. The P removal rate of 99.86% when the P concentration was up to 50 mg L^{-1} in 30 minutes by $ALLODUST_{2.50}$ and 85.13% for P concentration up to 300 mg L^{-1} P by H-$ALLODUST_{5.82}$ in 450 minutes demonstrated the high capacity of the ALLODUST to remove P from agriculturally sourced wastewater, under optimum operating conditions.

Chapter 4

Optimising the phosphorous adsorption/desorption capacity of ALLODUST

4.1 Introduction

The main aim of this chapter is to investigate the adsorption capacity and the process from the experimental point of view and optimizing (by response surface methodology (RSM)) of phosphate onto the innovative material ALLODUST. The media is designed to control contaminated natural and point sources which have a high concentration of phosphate. ALLODUST is a composite material based on the Horotiu soil and bio-wastes. An elution experiment was utilised to investigate the adsorption cycle capacity of the media. After seven continuous cycles, ALLODUST could still adsorb a high concentration of the phosphate with only 13% desorption. Both Freundlich and Langmuir adsorption isotherms were used to describe the adsorption behaviour of the ALLODUST while in contact with phosphate contaminated water. The Brunauer–Emmett–Teller (BET) experiment could support the high adsorption capacity of the ALLODUST while the total pore volume was increased by 70% compared to Horotiu soil itself.

ALLODUST is a composite media which contains allophanic clay minerals and bio-waste (Mohajeri et al., 2020). The 3 g L^{-1} of ALLODUST could remove 100% of P up to 50 mg L^{-1} in 30 minutes with the lowest aeration rate (1.5 L min^{-1} / low turbulence). Herein, we describe a study on the phosphate adsorption/desorption on ALLODUST during six cycles with different phosphate concentrations and how the adsorption fits the isotherms. In addition, the pH, EC, and DO were monitored to study the optimum condition of phosphate adsorption by ALLODUST. Also, the physical and chemical surface characteristics of the ALLODUST are presented in this chapter.

4.2 Materials and Methods

4.2.1 Wastewater Sampling and Analysis

Multiple water samples from the *Ararira LII* River, Lincoln have been obtained for continuous monitoring. The samples were collected from the centre of the river and from the surface at

a depth of 35 cm and transferred immediately to a chilly bin in the field to avoid any changes in the sample properties due to biological reactions. The samples were then transported to the laboratory and placed in a 4° C fridge (APHA 2005). At the time of sampling, the water pH, temperature (°C), electrical conductivity (µs cm^{-1}) and dissolved oxygen (mg L^{-1}) were determined by a HACH (HQD portable metre) probe on site. All the quality analysis was carried out in accordance with the Standard Water and Wastewater Examination Methods-American Public Health Association (APHA, 1998). The characteristics of water are given in Table 4.1. The phosphate concentration was set by spiking with K_2HPO_4 in various concentration zones from 50 mg L^{-1} up to 300 mg L^{-1} in separate batches.

Table 4.1 Water characteristics sampled from the *Araria LII* river.

Characteristics	Value
NTU	1.85
Total Nitrogen (TN)	3.6 mg L^{-1}
Ammonical Nitrogen (AN)	0.005 mg L^{-1}
Nitrate	19.31 mg L^{-1}
Dissolved Reactive Phosphate (DRP)	0.0143 mg L^{-1}
Total Phosphate (TP)	0.03 mg L^{-1}
Electrical Conductivity (EC)	288 µs cm^{-1}
Dissolved Oxygen (DO)	8.24 mg L^{-1}
Temperature (at time of sampling)	16.0 °C
pH	6.81

4.2.2 ALLODUST Preparation and Characterisation

According to the results presented in Chapter 3, the H-ALLODUST was the most efficient media in P adsorption in a wide range of the concentration. The H-ALLODUST was prepared according to the methodology described in section 3.2.2. The XRF analysis was conducted to obtain the major oxide, trace elements, and the main elements of the ALLODUST and the results are presented in Table 4.3 – 4.5. The sample was oven-dried at 110°C. The loss of ignition was obtained by Gravimetric method and the major oxides were measured by Borate fusion (XRF) method. The powder briquette (XRF) method was hired to measure the trace elements, Sc, Ba, Ce, La, and multi-elements. All the analysis were conducted by SPECTRACHEM ANALYTICAL Verum Group.

Table 4.2 Chemical characteristics of Horotiu soil used as the base of H-ALLODUST.

Characteristics	Horotiu
pH	5.7
Carbon (mg kg^{-1})	3.3
Nitrogen (mg kg^{-1})	0.27
CEC (meq $100g^{-1}$)	17
Sum Bases	4.09
SSA (m^2 g^{-1})	15.02
Pore Volume (cm^3 g^{-1})	0.031

Table 4.3 XRF major oxides analysis of ALLODUST.

SAMPLE	Fe_2O_3	MnO	TiO_2	CaO	K_2O	SO_3	P_2O_5	SiO_2	Al_2O_3	MgO	Na_2O	LOI	SUM
ALLODUST	2.55	0.07	0.32	20.20	0.69	0.72	0.13	48.72	9.81	1.02	1.28	14.24	99.74

LOI = loss on ignition at 1000°C for 1 hour.
Results are expressed as weight % on oven dried (110° C) basis.

Table 4.4 ALLODUST trace element analysis.

SAMPLE	As	Ba	Ce	Cr	Cu	Ga	La	Nb	Ni	Pb	Rb	Sc	Sr	Th	U	V	Y	Zn	Zr
ALLODUST	7	248	49	77	<1	11	30	6	21	11	27	7	1367	7	3	33	19	54	138

Values are expressed as mg/kg.

Table 4.5 X-ray multi-element analysis of ALLODUST.

Carbon	C	_	**Zinc**	Zn	0.005	**Iodine**	I	nd
Fluorine	F	nd	**Gallium**	Ga	nd	**Caesium**	Cs	nd
Sodium	Na	0.950	**Germanium**	Ge	nd	**Barium**	Ba	0.022
Magnesium	Mg	0.615	**Arsenic**	As	nd	**Lanthanum**	La	nd
Aluminium	Al	5.19	**Selenium**	Se	nd	**Cerium**	Ce	_
Silicon	Si	22.8	**Bromine**	Br	0.002	**Hafnium**	Hf	_
Phosphorus	P	0.057	**Rubidium**	Rb	0.002	**Tantalum**	Ta	nd
Sulphur	S	0.638	**Strontium**	Sr	0.131	**Tungsten**	W	nd
Chlorine	Cl	0.021	**Yttrium**	Y	0.003	**Rhenium**	Re	_
Potassium	K	0.573	**Zirconium**	Zr	0.013	**Osmium**	Os	_
Calcium	Ca	14.4	**Niobium**	Nb	nd	**Iridium**	Ir	_
Scandium	Sc	nd	**Molybdenum**	Mo	nd	**Platinum**	Pt	_
Titanium	Ti	0.192	**Rhodium**	Rh	_	**Gold**	Au	_
Vanadium	V	nd	**Palladium**	Pd	_	**Mercury**	Hg	nd
Chromium	Cr	0.006	**Silver**	Ag	_	**Thallium**	Tl	nd
Manganese	Mn	0.054	**Cadmium**	Cd	nd	**Lead**	Pb	nd
Iron	Fe	1.78	**Indium**	In	_	**Bismuth**	Bi	nd
Cobalt	Co	nd	**Tin**	Sn	nd	**Thorium**	Th	nd
Nickel	Ni	0.004	**Antimony**	Sb	nd	**Uranium**	U	nd
Copper	Cu	nd	**Tellurium**	Te	_	**Total**		47.5

Values are weight % nd = not detected – = not measured
100% - Total = sum of unmeasured elements [e.g.H,B,C,N,O]

4.2.3 Adsorption/Desorption

In order to determine the phosphate release risk by the ALLODUST, a cycle of adsorption/desorption was implemented. The optimum adsorbent dosage (3 g L^{-1}) was mixed with the wastewater containing different ranges of concentration in a 50 mL centrifuge tube with three replicants. A (blank) tube was run with solution only, to determine the amount of phosphate which have adsorbed to the filter and tube surfaces. To inhibit microbial activity, three droplets of Chloroform were applied to each tube. Then, the tubes were shaken for different times according to the designed contact time and centrifuged by 3800 rpm for 10 min. The supernatant was passed through a 0.45 µm membrane filter. When the supernatant has been extracted after an adsorption process, 25 mL of saturated NaCl solution at pH 7.0 was added to the tubes to extract the adsorbed phosphate. NaCl is a salt solution of higher ionic strength and is able to remove polymeric bonds and strong binding impurities. The solution was then removed, and this cycle repeated twice. Then, to replace the adsorbed phosphate, 25 mL 0.01 mol L^{-1} KCl solution was added at pH 7.0 The tubes were shaken, centrifuged, and then concentration determined as above (X. Yan et al., 2013; Xiaoyan Yang et al., 2019). The concentration of phosphates in the solutions is known as desorbed phosphate. This cycle was repeated several times until the media's adsorption capacity dropped significantly (Abdala et al., 2012).

4.2.4 Point of zero charge (pH_{zpc})

This experiment was conducted to find the pH at which the net charge of the ALLODUST surface as an adsorbent was equal the zero. The media was collected and a uniform size was obtained by a mechanical grinding of material and sieving through mesh 200. The media was washed with distilled water and was kept in dilute HCl for 24 h so that the final washing showed no further change in pH. The ALLODUST was dried by in an oven at 70- 72 °C; cooled and stored in an air tight container. pH_{zpc} was determined by the Rivera-Utrilla et al method (Rivera-Utrilla et al., 2001). In a 100 mL flask, 50 mL of 0.01 M NaCl solution was placed. Using either NaOH or HCl (0.1 N) containing 0.15 g of dry air, the pH was then modified to successive initial values between 2 and 12. The final pH was determined and plotted against the initial pH after a contact time of 24 h. The pH at which the curve crosses the line pH (final) = pH (initial) is taken as the pH_{zpc}.

4.2.5 Experimental design (CCD-RSM)

The Central Composite Design (CCD) and Response Surface Methodology (RSM) method from DOE software (Design Expert 11-Stat-Ease) were used to model the experimental conditions by evaluating the relation between the variables (i.e. sawdust pH, aeration rate, contact time and phosphate concentration) and the responses (percentage P removal, EC, DO, and pH) (Table 3.5).

The design consisted of k_2 factorial points completed by 2k axial points and a centre point, where k is the number of variables. By employing (equation 4.1) and the associated variables, it was possible to optimize the operational design to predict the best and desirable value of the responses.

$$\boldsymbol{Y = (\beta_0 + \varepsilon) + \sum_{i=1}^{k} \beta_i X_i + \sum_{i=1}^{k} \beta_{ii} X^2 + \sum_{i_i<j}^{k} \sum_{j}^{k} \beta_{ij} X_i X_j + \cdots + e} \quad (4.1)$$

Where, Y: response; X_i and X_j: variables; β_0 : constant coefficient; β_j, β_{jj}, and β_{ij} : interaction coefficients of linear, quadratic and second-order terms, respectively; k: number of studied factors; e: error).

4.2.6 Adsorption kinetic analysis

Adhesion of atoms, ions, biomolecules, or molecules of gas, liquid, or dissolved solids to a surface is refered to as adsorption (Aziz et al., 2012):

$$\boldsymbol{qe = \frac{(C_o C_e)V}{M}} \quad (4.2)$$

Where $\boldsymbol{qe}$ is the sum of solute adsorbed per unit weight of adsorbent (mg g^{-1}), $\boldsymbol{Co}$ is the initial adsorbate concentration, $\boldsymbol{Ce}$ is the equilibrium adsorbate concentration (mg L^{-1}), $\boldsymbol{V}$ is the volume of solution (L), and $\boldsymbol{M}$ is the adsorbent mass (g). In this analysis, Langmuir and Freundlich isotherms were used to demonstrate the characteristics of ALLODUST.

4.2.6.1 Langmuir Isotherm

Surface adsorption on a solid is divided into two broad categories: physisorption and chemisorption. Physisorption is an unspecific loose bond of the adsorbate to the solid via van der Waals – type interactions. Multilayer adsorption is possible and easily disrupted by rising temperatures. Chemisorption requires a more precise bonding of the adsorbate to the solid. (Altig, 2013).

$$\frac{x}{m} = \frac{abCe}{(1+bCe)} \quad (4.3)$$

Where x/m is the mass of the adsorbate adsorbed per unit mass of adsorbent (mg adsorbate per g activated carbon), *a* and *b* are the empirical constants, and *Ce* is the equilibrium concentration of adsorbate in the solution after adsorption (mg L^{-1}).

4.2.6.2 Freundlich Isotherm

Freundlich isotherm adsorption is a curve that compares the concentration of a solution on an adsorbent's surface to the concentration of the solute in the liquid with which it is in contact (Aziz et al., 2012). The Freundlich equation can be written as follows:

$$\frac{X}{M} = K_f C_e^{1/n} \quad (4.4)$$

Where K_f is a constant indicative of the relative adsorption capacity of the adsorbent ($mg^{1-\left(\frac{1}{n}\right)} \quad L^{\frac{1}{n}} \quad g^{-1}$) and n is a constant indicative of the intensity of the adsorption.

4.3 Results and Discussions

4.3.1 Elution Analysis

The desorption properties of an adsorbent could be an essential factor relevant to the adsorbed element recovery as well as the adsorbent itself (Kuzawa et al., 2006; Lata et al., 2015). The high desorption rate of an adsorbent can be considered as either an advantage or disadvantage. In a closed and controllable water treatment system which the operator can have access to the media after the adsorption process, a high rate of desorption would be favourable in order to recover the adsorbent and the adsorbed element. On the other hand, when an adsorbent is used as a media for the freshwater remediation, the high desorption rate can lead to the release of the adsorbed contamination to the environment again. Assessing the adsorption capacity in different cycles and a low desorption rate was the main target to in the development of the ALLODUST. In order to study the adsorption-desorption cycles of the media, six cycles were performed as presented in Figure 4.1-4.3. The P adsorption capacity of the ALLODUST declined by 6%, 36%, and 15.7% when the 50, 175, and 350 mg L^{-1} of P was added to the system at each cycle. This shows that the ALLODUST has a very high adsorption capacity and can perform for a long period of time even in an environment with a high concentration of P.

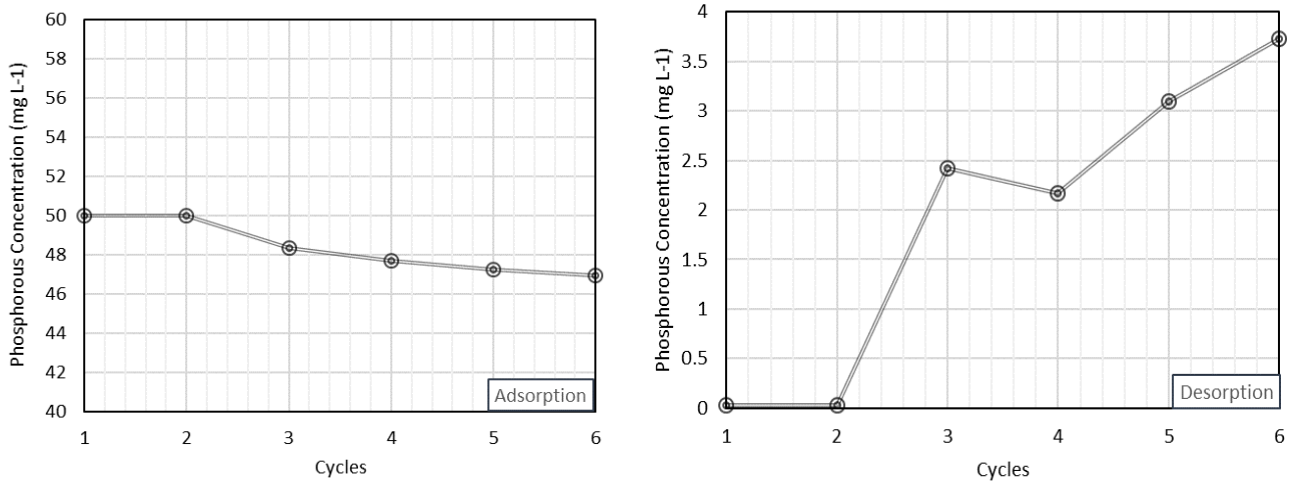

Figure 4.1 Adsorption/desorption cycles of the ALLODUST in the presence of 50 mg L^{-1} of phosphate.

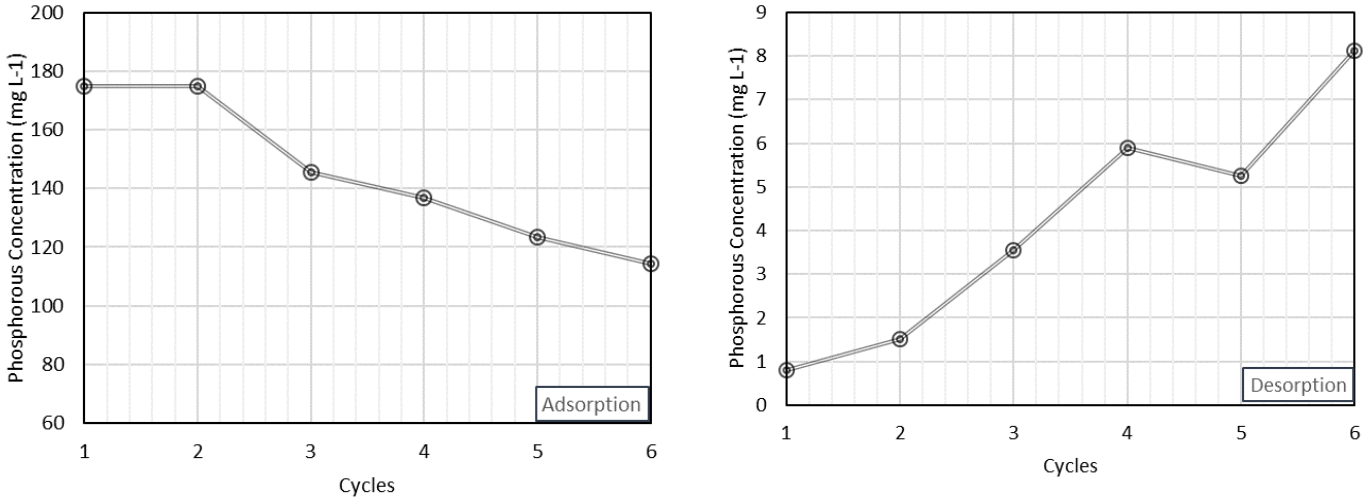

Figure 4.2 Adsorption/desorption cycles of the ALLODUST in the presence of 175 mg L^{-1} of phosphate.

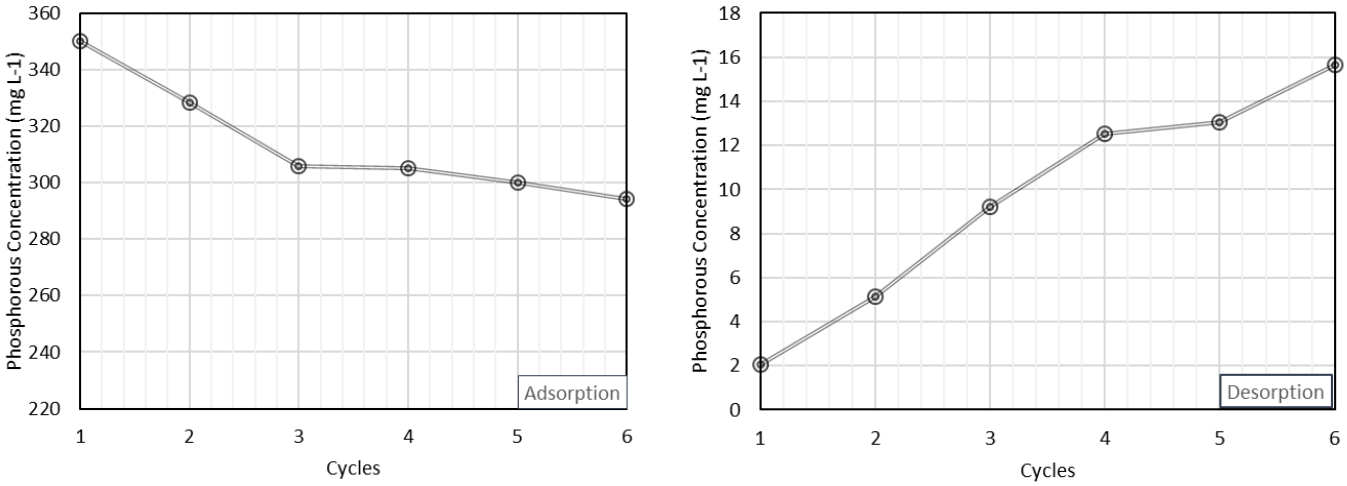

Figure 4.3 Adsorption/desorption cycles of the ALLODUST in the presence of 350 mg L^{-1} of phosphate.

After the first adsorption cycle, the ALLODUST demonstrated the same P adsorption capacity when the concentration is up to 175 mg L^{-1} while ALLODUST could adsorb 6% less P compared to the first interaction in a system containing 350 mg L^{-1} of P. From the first to the sixth cycle, the P desorption increased from 0% to 8% and from 0.57% to 4.68% for concentrations from 10 to 175 mg L^{-1} respectively. This amount was from 0.58% to 4.57% for the ALLODUST when in contact with 350 mg L^{-1} of P. The negative impacts of the desorbing agent and also the loss of media weight during desorption cycle may be one of the key reasons for the decrease in adsorption capability. It can generally be concluded that both the ALLODUST has a reusability potential with high adsorption and low desorption capacities. This would make the ALLODUST a safe media for sustainable USE in natural water body remediation.

4.3.2 Adsorption Isotherms

In equation 4.2, qe is calculated from equation 4.1 and by using the adsorption experiment data. By calculation the other factors in the equation and also the constant values a linear relationship and a plot of values for 1/qe versus values of 1/Ce was obtained. Figure 4.4 represents the relationship between 1/qe and 1/Ce for ALLODUST in C_0: 300 mg L^{-1}. The slope of the best fit line will be considered as K:ab and the values of a and b were calculated from the intercept. The data for the Langmuir isotherm are given in the Figure 4.4.

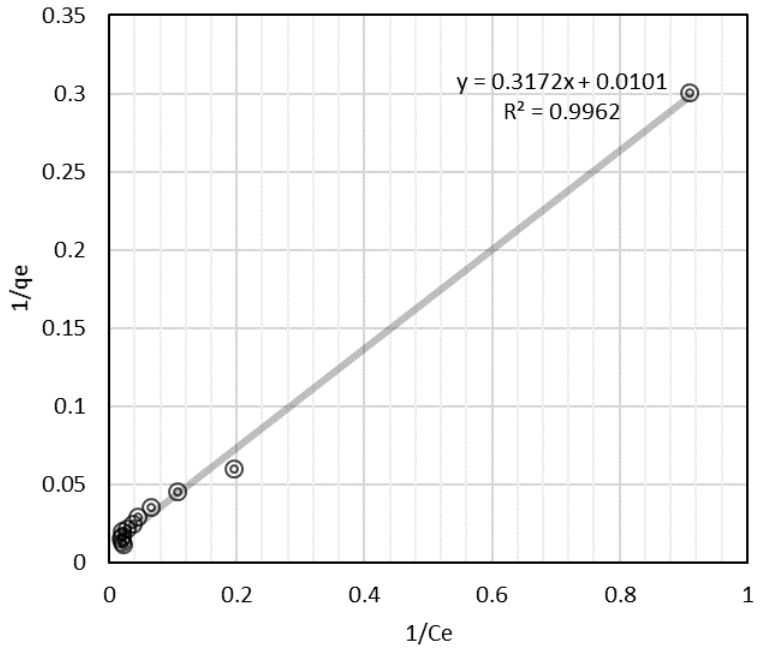

Figure 4.4 Langmuir isotherm regression for the P adsorption by ALLODUST (Q (mg g^{-1}): 85.14, b: 0.03, R2: 0.99, RL: 0.1, Isotherm type: favourable).

Regression analysis of the data for different initial concentrations fitted well in Langmuir adsorption isotherm. The Langmuir adsorption isotherms at different initial concentrations are often linear (R2: very close to 1).

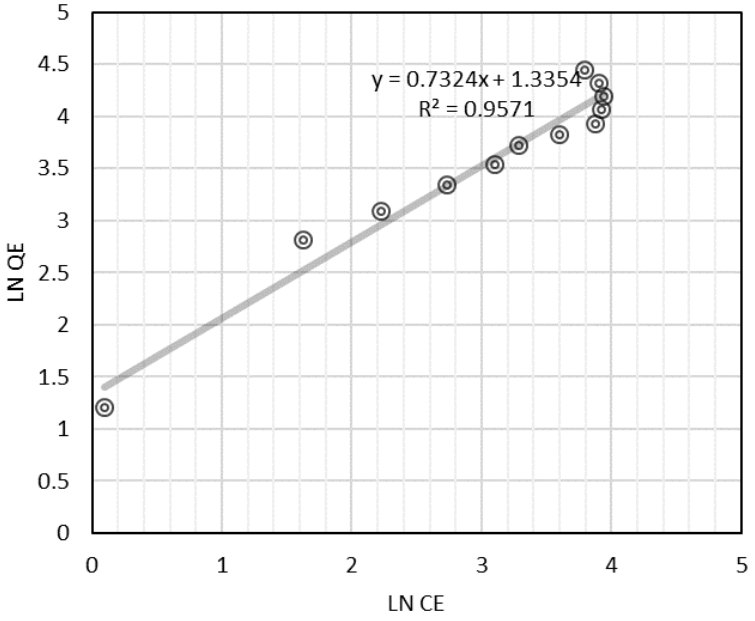

Figure 4.5 Freundlich isotherm regression for the P adsorption by ALLODUST (Kf (mg g^{-1} (L/mg)1/n): 5.53, 1/n: 0.72, R2: 0.95).

By taking the Ln from the both sides of the Freundlich isotherm it can be transferred to a linear equation 4.4 (Khayyun & Mseer, 2019; Wilhelm & Beam, 1999). When Ln (Ce) is plotted on x-axis and Ln (qe) on the y-axis, the best fit straight line has a slope of N and Ln (Kf) in the intercept. The Freundlich isotherm mostly applies to an adsorption system with a low concentration of the contaminant in equilibrium (Ce). The calculated n from the Freundlich isotherm and the laboratory data show 1.39 which indicates a good efficiency for the P adsorption by ALLODUST (Anton et al., 2020; Mckay et al., 1982). As it can be seen from Figure 5, the plot of the Ln (qe) vs Ln (Ce) is linear and the adsorption data obeyed the Freundlich adsorption isotherm. The constants values are Kf: 5.53, and n: 1.39 for the initial concentration of 300 mg L^{-1}. The regression analysis of data as shown in Figure 5, which is well matched for the various initial concentrations with the Freundlich adsorption isotherm. The value of n for several radionuclides to be adsorbed is always significantly different from 1, in so much that nonlinear isotherms are observed. Due to the high R^2 value, the Langmuir model in this analysis is a better predicator than the Freundlich model.

4.3.3 ALLODUST Charge characteristics

The zero point of charge is a basic definition of a mineral surface, which is the position where the maximum concentration of anionic surface sites is equivalent to the total concentration of cationic surface sites, so most sites are similar to neutral hydroxides. Throughout the pH above ZPC the adsorbent surface becomes negatively charged and the surface will engage in the processes of cation adsorption and cation exchange. In the other side, if the solution's pH is below ZPC, the surface has a net positive value, and the surface absorbs anions and participates in reactions of anion exchange.

Any arrangement of mineral and mineral crystals has zero point of charge. The charge formed on the surfaces of the oxides is transient charge since it relies on the pH. This form of load is comparatively lower than the permanent charge of clay minerals. In the case of ALLODUST, the pH as indicated below (Figure 4.6) is favourable for adsorption of chemical anions. So when the solution's pH is below the ZPC, the ALLODUST surface may be anticipated to participate in the phosphate adsorption cycle. This should be taken into consideration that although the solution's pH reaches ZPC, the other ALLODUST adsorption processes such as physical adsorption are also involved.

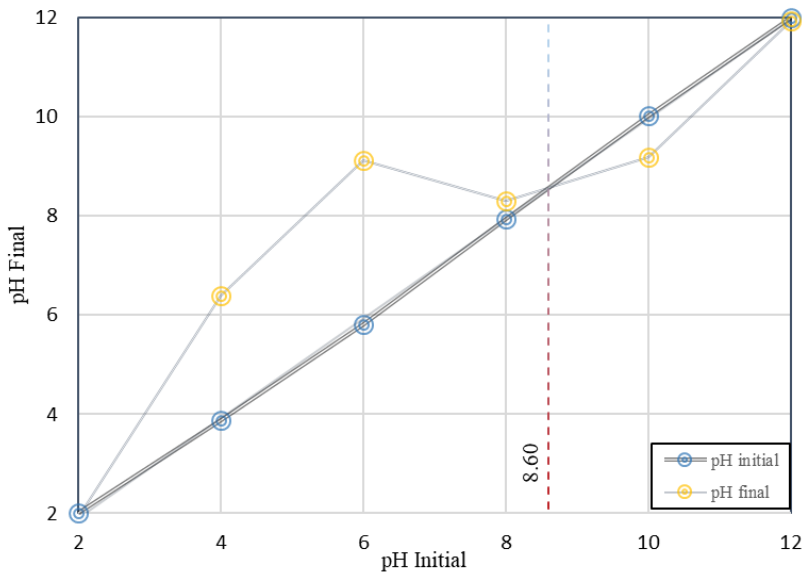

Figure 4.6 pH of zero point of charge (pH_{ZPC}) of the ALLODUST.

4.3.4 DO, pH, and EC correlations with adsorption capacity

High concentrations of dissolved oxygen in the aeration tank during the reacting phase resulted in minimal sludge biomass growth, which is a vital factor. The reactors were supplied with oxygen from a fine bubble air diffuser to maintain a dissolved oxygen concentration above 3 mg L^{-1} and it can be seen from Figure 4.7 that DO concentration increased by presenting more phosphate in the wastewater. Throughout the reaction phase, high concentrations of dissolved oxygen in the aeration tank resulted in reduced development of sludge biomass which is a critical element. The reactors were supplied with oxygen from a fine bubble air diffuser to retain a concentration of dissolved oxygen over 3 mg L^{-1} and it can be shown from Figure 4.7 that the concentration of DO increased with a higher initial concentration of phosphate in the wastewater(Aziz, Aziz, Yusoff, et al., 2011).

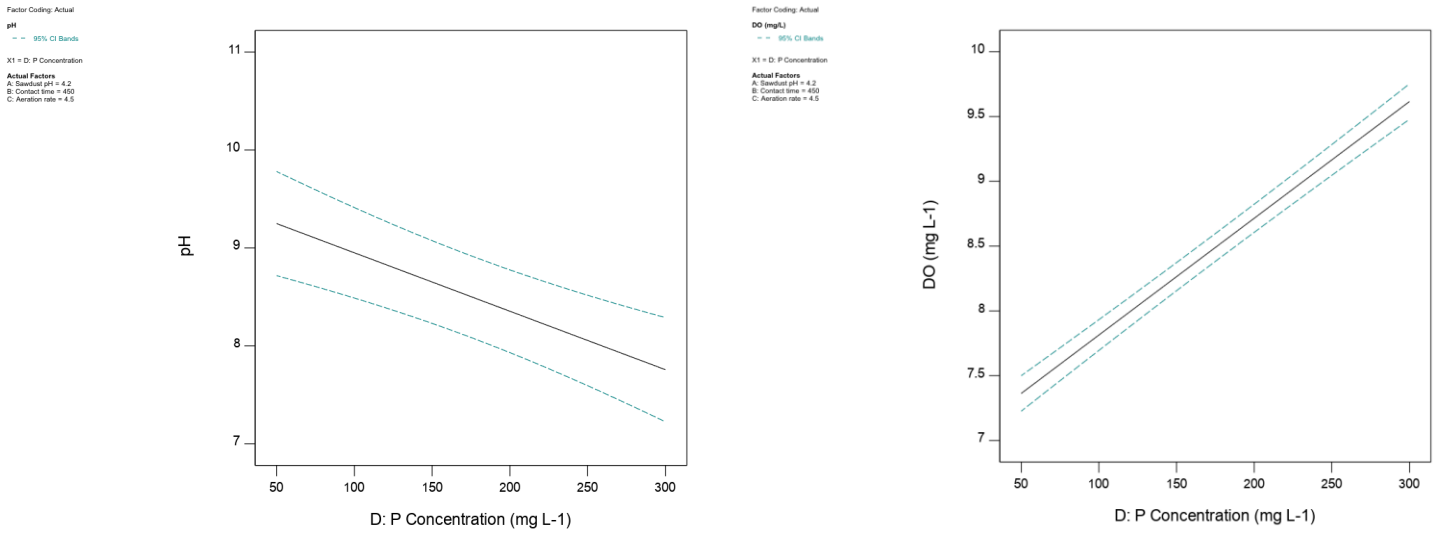

Figure 4.7 pH and DO values at the optimum operational details in the presence of different phosphate concentration.

A high pH level results in a substantial reduction of the clay's adsorption potential against phosphate ions in the interaction between soil (clay) minerals and phosphate. The adsorption of phosphate to iron oxides and hydroxides tended to decrease with a pH increase. The propagation of potentials and electrical charges near to the surface of metal oxides and hydroxides primarily relies on the adsorption and desorption of protons; pH has a major impact on the properties of surface adsorbent particles. Protonation and deprotonation at the hydroxyl sites on the surface of the metal hydroxides may occur in aqueous solution.

According to the pH ZPC value, ALLODUST surface is charged positively at pH less than 7.40 which favours phosphate ion adsorption. At alkaline pH values, the rapid decrease in phosphate elimination is due to the impact of hydroxyl ions on competition. After increasing phosphate adsorption on the ALLODUST surface, the pH of solution is predicted to rise, due to the contribution of phosphate negative charges. When the pH decreases, hydroxyl groups slowly dissociate and the surface charge on the beads is negative and strengthens electrostatic activity between these groups and the iron ions, which can bind phosphates. There can also be precipitation of Al^{3+} and Fe^{3+} at elevated initial phosphate concentrations and low pH, resulting in mineral phases such as variscite, $AlPO_4 \cdot 2H_2O$ and strengite, $FePO_4 \cdot 2H_2O$ (Gustafsson et al., 2012).

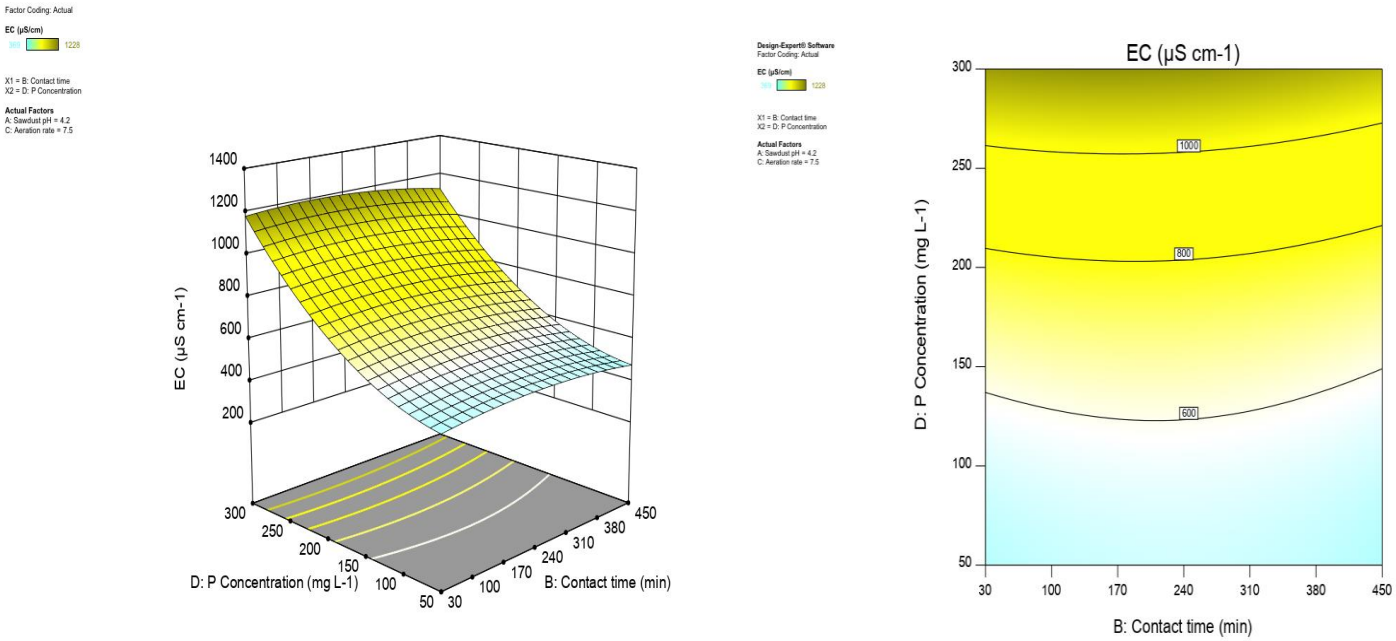

Figure 4.8 Electrical Conductivity (EC) values at the optimum operational details in the presence of different phosphate concentration.

High concentration of the ions leads to increasing in the electrical conductivity of the water. The electrical current is transported by the ions in solution, the conductivity increases as the concentration of ions increases. As it was expected high initial phosphate concentration caused high EC value in the water. As it can be seen from Figure 4.8 the EC value was not time dependent because the most of the ions were adsorbed during the first 30 minutes.

4.3.5 Brunauer–Emmett–Teller (BET)

In an adsorption process, the surface characteristics such as specific area and pore size are amongst the key factors. Table 4.6 shows the results of the BET experiment on the ALLODUST before and after the P adsorption. The surface area of the Horotiu as the base mineral of the ALLODUST is 15.02 $m^2 g^{-1}$. This value is compares favourably with the other clay minerals like the kaolinite which is reported at approximately 12.27 $m^2 g^{-1}$ (Macht et al., 2011). The ALLODUST SSA had not dropped significantly due to the replacement of some soil minerals with other materials such as sawdust. On the other hand, it can be seen that the pore volumes and sizes were increased by 66% and 69.5% respectively. The acidic treatment of the sawdust as previously expected contributes to activate the surface and also pore development. For this study the optimal acid treatment of the wood bio-waste was at pH=5.87. The particle size often influences the surface region directly and intra-particle diffusion analysis indicates that the adsorption intensity is strongly determined by the particle size. Reduction in particle size can result in increased surface area and thus increased adsorption potential and capability on the sawdust's outer surface. At the other hand, it is interesting to remember the effect of the probability of intra-particle diffusion from the outer surface through the inner sections and the pores of the substance.

The diffusional resistance to mass transfer is lesser for fine particles. The ALLODUST surface area after the P adsorption was decreased significantly while the pore size changed slightly to the lower number. It can be proved that the surface complexes, ligand exchange and the hydroxyl groups on the surface play the main role in the P adsorption compare to the pores which can contribute to the adsorption process by the physical mechanisms as well as providing a desirable space for the anaerobic microorganisms and PAOs.

Table 4.6 Surface characteristics of the ALLODUST – results of the BET experiment.

	HOROTIU	ALLODUST-B	ALLODUST-A
Surface Area ($m^2 g^{-1}$)			
Single point surface area at p/p = 0.250089228	14.59	13.85	1.70
BET Surface area	15.02	14.68	1.78
Langmuir surface area	21.85	21.42	2.64
t-Plot external surface area	2.02	15.01	1.83
BJH adsorption cumulative surface area of pores between 17.0 A and 3000 A width	11.51	18.19	1.97
BJH desorption cumulative surface area of pores between 17.0 A and 3000 A width	15.81	21.67	2.53
Pore Volume ($cm^3 g^{-1}$)			
Single point adsorption total pore volume of pores less than 1445.854 A width at p/p = 0.986432810	0.031313	0.099095	0.010358
t-Plot micropore volume	0.000844	0.000477	0.000051
BJH adsorption cumulative volume of pores between 17.0 A and 3000 A width	0.030087	0.099370	0.010425
BJH desorption cumulative volume of pores between 17.0 A and 3000 A width	0.032566	0.099328	0.010394
Pore Size (nm)			
Adsorption average pore width (4V/A by BET)	83.3582	273.9764	232.0559
BJH adsorption average pore width (4V/A)	104.521	218.575	211.081
BJH desorption average pore width (4V/A)	82.370	183.365	164.022
ALLODUST-B: Before P adsorption			
ALLODUST-A: After P adsorption			

4.3.6 Optimization and Statistical Analysis

The final experimental result – P removal % - with various operation conditions was analysed using RSM in order to determine a specific operation system that could lead to the optimum removal of phosphate at the highest concentration. The resulting responses from optimizing the phosphate removal is given in Figure 4.9. The optimized conditions were the sawdust pH of 5.9, contact time of 450 min, and aeration rate of 7.5 L min^{-1} which would result in 85.14% of P removal in 300 mg L^{-1} initial concentration. Also, it can be seen that the DO, pH and EC values of the system in this condition will be 9.68 mg L^{-1}, 7.8, and 1115 µs cm^{-1}.

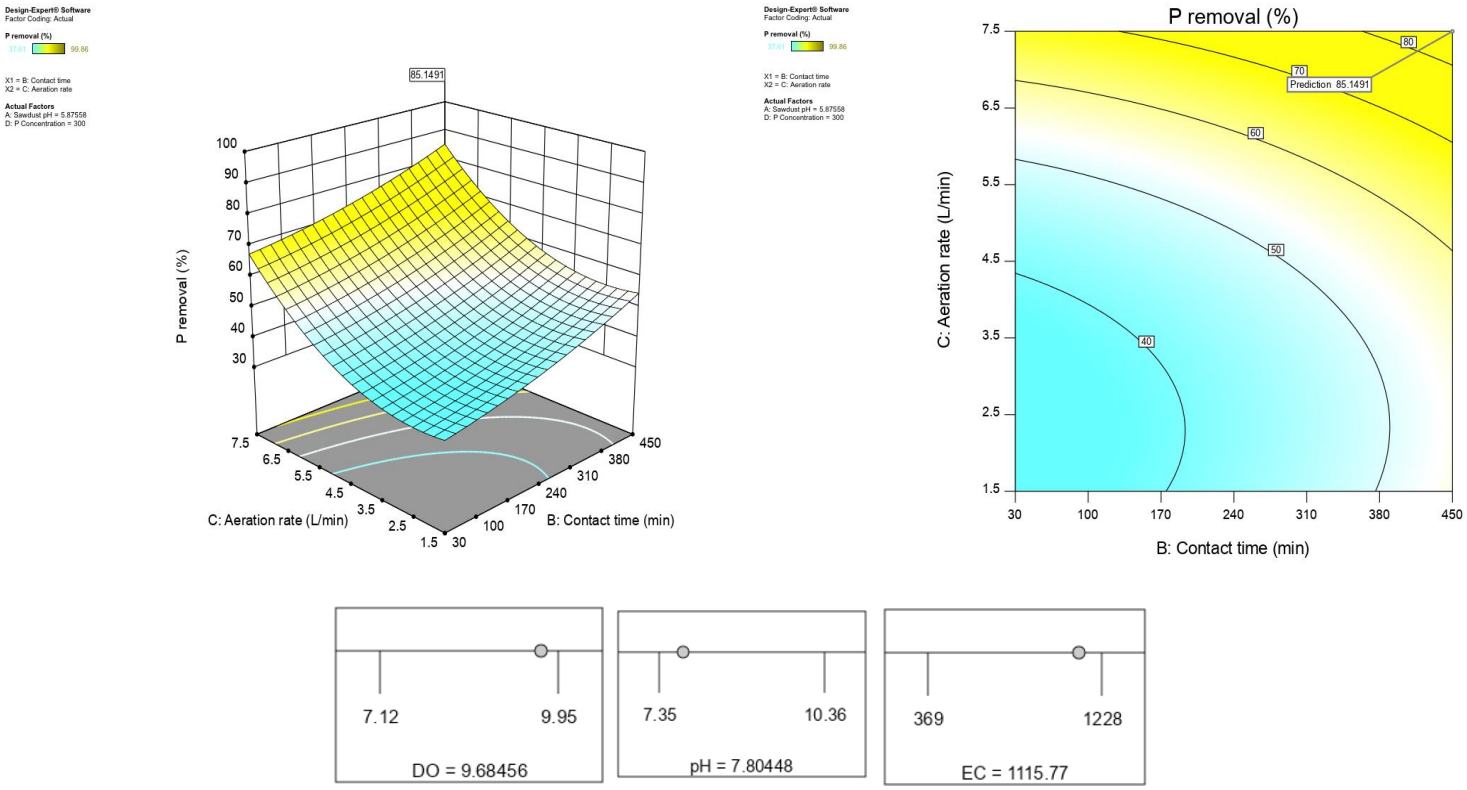

Figure 4.9 Optimum operational variables to achieve the highest removal efficiency in the max phosphate concentration.

4.4 Conclusions

In this research, the ALLODUST function in removing the phosphate from aqueous solution was optimized. Also, the adsorption/desorption capacity of the ALLODUST was monitored in different six cycles in order to evaluate the function of this media for the use as a long term filtration system. The adsorption capacity increased with an increase in all the variables such as contact time and the aeration rate (high turbulence). Also, the optimized pH of the solution in the presence of high concentration of phosphate as an anion without any chemical treatment was 7.8 which is below the pH ZPC. The Langmuir isotherm model was more effecive than the Freundlich model at describing the phosphate adsorption on ALLODUST. In conclusion, this result proves that the high adsorption capacity of the ALLODUST in a fixed mode, which the legacy phosphate release could be expected; is in the lowest amount when it's been used as a filter for the drainage pipes, fluidized media for the reactors, or floating media on phosphate contaminated surface water bodies.

Chapter 5

ALLODUST augmented activated sludge single batch anaerobic reactor (AS-SBAnR) for high concentration nitrate removal

5.1 Introduction

Excessive fertilizer application , oxidation of nitrogenous waste products, and point source pollution from agricultural and urban wastewater have led to surface and groundwater contamination and is now a critical global issue (Seitzinger et al., 2010). Changing land use and excessive application of artificial fertilisers are among the main reasons for increased nitrate concentrations in freshwaters over the past two decades (Karanasios et al., 2010). Nitrate is known as the most important anionic contaminant present in water bodies, partly because of its high solubility potential (Weigelhofer & Hein, 2015). Its high concentrations in ground water can pose a serious risk to the quality of drinking water supplies (Cheng et al., 1997; Y. H. Huang & Zhang, 2004). Public health can be affected negatively by high nitrate concentrations in drinking water sources, specifically infants (methemoglobinemia or blue baby syndrome) which nitrate can be one of a number of co-factors which causing the disease (Fewtrell, 2004), and the potential formation of carcinogenic nitrosamines (Shuval & Gruener, 2013). Also high concentration of nitrate cause eutrophication which can harm waterways and water bodies. The maximum contaminant level (MCL) for nitrate (as NO_3-N) has been set to 10 mg L^{-1} by the U.S. Environmental Protection Agency (U.S. EPA), while the World Health Organization (WHO) and European Economic Community (EEC) drinking water limit is 11.3 mg L^{-1}. The latter has been adopted by most countries as their regulatory limit (GROUNDWATER, 2013; Organization, 2003; WHO, 1985).

Synthetic nitrogen use in New Zealand (NZ) rose from 4.25 to 25.38 million kg yr^{-1} and the estimated amount of nitrogen leached into surface water has increased to 29 percent between 1990 to 2012 (Environment, 2017b). This magnitude of increase in the use of synthetic nitrogen is not only a threat to freshwaters, but also contributes to the country's green-house gas (GHG) emission inventory (R. Xu et al., 2019). N_2O concentration increased by the rate of 0.87 ppb/year from 1996 to 2016 linked to an increased use of nitrogen-based

fertilisers in New Zealand which is a serious threat to climate according to its contribution and affect in GHG concerns (Environment, 2017a). Recent model estimates suggest that only 68.2% of NZ river concentration meet the Australian and NZ Guidelines for Fresh and Marine Water Quality (ANZECC) trigger values of nitrate contamination for slightly disturbed upland ecosystems (upland and lowland) of 11.3 mg L^{-1} (as NO_3-N) (NIWA, 2017). At the same time, the long-term global warming potential of N_2O is 265 times that of CO_2 (Myhre et al., 2013; Pachauri et al., 2014); it is also the main threat to the ozone layer in the 21st century (Ravishankara et al., 2009).

Removing nitrate from wastewater using conventional treatment methods is often not practical. It's low potential for co-precipitation and adsorption means that most common approaches that rely on coagulation and filtration for removal are often ineffective (Weigelhofer & Hein, 2015). Nitrate removal technologies can be generally divided into two categories: physical-chemical nitrate removal and biological nitrate reduction. The physical and chemical methods are well-established and based on separation (Giwa et al., 2017), ion exchange (Palko et al., 2018), chemical oxidation (He et al., 2015) and chemical reduction (J. Xu et al., 2017). By considering the main aspects of the treatment processes such as simplicity, efficiency, and cost-effectiveness, nitrate elimination methods are preferred to the separation-based methods. Biological nitrate removal is recognized as a preferred method over physico-chemical methods (J.-H. Kim et al., 2008).

Biological nitrate removal through denitrification (forthwith, "biological denitrification", BD) is accomplished by denitrifying bacteria under anaerobic conditions. Hence, controlling dissolved oxygen (DO) concentration is the most important factor for BD. The exact optimal DO concentration for this purpose varies between microorganisms; however Aziz, Aziz, Yusoff, et al. (2011) showed that it is generally less than 1 mg L^{-1} . Nitrate removal from contaminated water can be achieved through BD directly in aquifers or in the vadose zone (*in situ*), or after withdrawal of water (*ex situ*) (GROUNDWATER, 2013). The *in situ* BD treatment techniques can usually only be applied to restricted geological conditions, due to the risk of clogging, slow water flow rates in aquifers and the difficulty associated with controlling substrate distribution (Della Rocca et al., 2007). *Ex situ* BD treatments most commonly employ bioreactors to assist the denitrification by providing microorganisms with a carbon source in an anaerobic environment. The complete denitrification cycle leads to a complete reduction of NO_3^- to N_2.

The treatment processes can be categorized according to the means by which the denitrifying organisms are propagated, with “suspended growth” and “attached growth” being the two most common. Fixed Film Denitrification is an attached growth process that employs microorganisms attached to a media that provides a high specific surface area for the development of bacterial community biofilms (Mohseni-Bandpi et al., 2013). These can then be deployed in packed bed and fluidized bed reactors, as well as bio-filters and membrane bioreactors. The high denitrification rate and low clogging and channelling risk have made fluidized bed reactors the most preferred design. Media that have been used to promote attached growth recently mainly have included polymeric (polyurethane) elements (Chu & Wang, 2011; Feng et al., 2012) which their environmental and health threats (isocyanates, cancer, asthma, and lung damage) have been well documented (Lithner et al., 2011).

When considering treatment options, denitrification that produces N_2O is not preferred. These conditions can arise because of low dissolved oxygen, high nitrite accumulation, change in optimal pH or temperature, fluctuation in C/N ratio, and short solid retention time (Thakur & Medhi, 2019). However, the occurrence of this can be mitigated by hiring sequential bioreactors and bio-scrubbers to provide a desirable and controllable reaction environment. What is not known is what material can be used to boost the control of N_2O emission while the treatment system is addressing a high concentration of the nitrate.

The aim of this chapter is to design a novel media together with a sequencing batch reactor in order to manipulate anaerobic, aerobic and anoxic conditions to improve the nitrate removal while minimizing N_2O production.

5.2 Materials and Methods

5.2.1 Wastewater Sampling and Analysis

Several water samples were collected from the *Ararira LII* river, Lincoln for regular monitoring (Figure 5.1). The samples were collected from the centre of the river and at a depth of 35 cm from the surface and were immediately moved to a chilly bin at field to prevent any changes in the sample properties due to the biological reactions. The samples then moved and stored in a fridge at 4°C (APHA 2005). Water pH, temperature (°C), electrical conductivity ($\mu s\ cm^{-1}$) and dissolved oxygen ($mg\ L^{-1}$) were determined on site at the time of sampling by a HACH probe (HQD portable meter).

Figure 5.1 Water sampling from *Ararira LII* river.

All the quality analysis was conducted in accordance with the Standard Methods for the Examination of Water and Wastewater – American Public Health Association (APHA 2005). The water characteristics are presented in Table 5.1. The nitrate concentration was fixed in different batches by spiking with KNO_3 in different concentration zones from 10 mg L^{-1} to 110 mg L^{-1}.

Table 5.1 Water characteristics sampled from the *LII river*.

Characteristics	Value
NTU	1.85
Total Nitrogen (TN)	3.6 mg L^{-1}
Ammonical Nitrogen (AN)	0.005 mg L^{-1}
Nitrate	19.31 mg L^{-1}
Dissolved Reactive Phosphorous (DRP)	0.0143 mg L^{-1}
Total Phosphorous (TP)	0.03 mg L^{-1}
Electrical Conductivity (EC)	288 µs cm^{-1}
Dissolved Oxygen (DO)	8.24 mg L^{-1}
Temperature (at time of sampling)	16.0 °C
pH	6.81

5.2.2 Bioreactor Designing (Couple Bottom Aeration-CBA)

Ten sequencing batch reactors (SBR) units were used for the experiment. The SBR consists of a transparent column made of clear Plexiglas for easier process monitoring and UPVC base and cap parts (Figure 5.2 – 5.3). Couple bottom aeration (CBA) was used to ensure optimal mixing efficiency of the air and water. The total volume of the reactors was 2000 mL, with

1500 mL working volume. All ten reactors were run under the same environmental conditions and at the same time. Two air pumps were used for the recycling of the headspace gas and aerating/stirring the system. The reactor headspace was sampled for N_2O through a butyl rubber septum on the top of each column. All reactors were tested for gas and water tightness before use. Nitrogen gas was used to purge O_2 from the reactors. The running details of the SBR (see below) were programmed and controlled using a data logger (CR850-Campbellsci). An air flow meter was used to control the aeration rates of the reactors. This SBR allows both the application of mixing and aeration process. This experimental design was chosen to allow for easy applicability and for simultaneous operation. This would avoid environmental condition changes during the experimental run time.

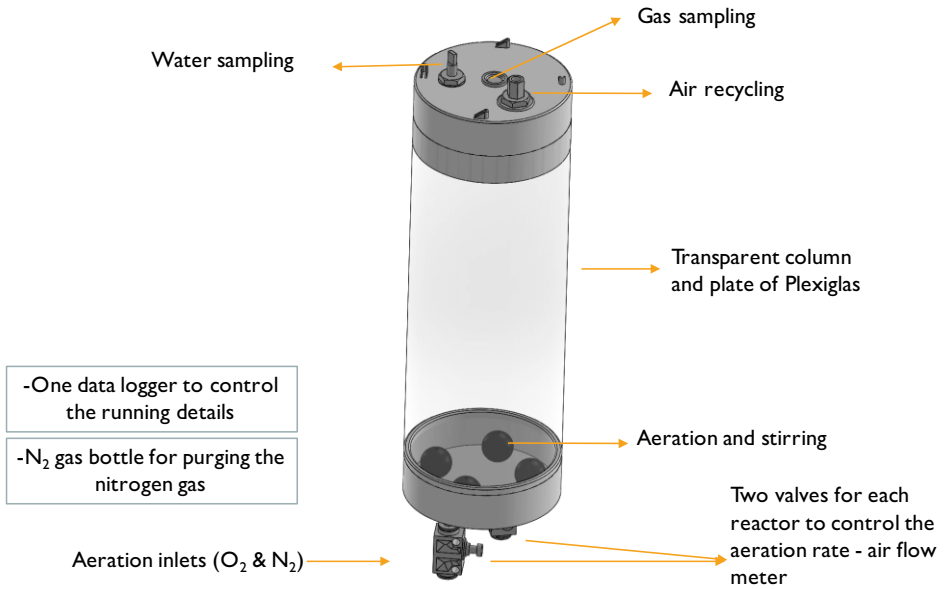

Figure 5.2 The schematic of lab-scaled couple bottom aeration (CBA) reactor.

Different operational variables were considered in the design of an optimum treatment system. The sawdust pH (2, 4, and 6), aeration rate (0.5, 4, and 7.5 L min^{-1}), contact time (2, 12, and 22 h) and adsorbent dosage (3, 7.5, 12 g L^{-1}) at different nitrate concentrations (10, 60, and 110 mg L^{-1}) were introduced to the system as the variables. To analyse the nitrate removal process, four dependent parameters were selected: N removal percentage; Chemical Oxygen Demand (COD); Electrical Conductivity (EC); and pH) were measured as the design responses. The timing of fill and mix (20 min), draw and idle (10 min), and settle (90 min) were set as a constant value for all reactor runs (Aziz, Aziz, & Yusoff, 2011; Aziz et al., 2012; Mahvi et al., 2004). The average mixed liquor suspended solid (MLSS) of all the reactors was set to

2500 mg L^{-1} for the blank sludge reactors and 5700 mg L^{-1} for the optimum ALLODUST contained reactors. The mixed liquor volatile suspended solid (MLVSS) concentration was 1825 mg L^{-1} to 1930 mg L^{-1} for the sludge reactor while this amount was 4380 mg L-1 for ALLODUST + activated sludge design. The SRT was calculated 14 days based on a preliminary study and a batch experiment according to the bioreactor solid (sludge + ALLODUST) and wasted plus effluent solids. This study was performed based on the fill and react method. The fill, react, settle, draw, and idle phases process occurred in a single reactor. The reaction time is the contact time which was different for different designs and was considered as one of the variables. The fill, settle, and draw and idle time for all the reactors were 15, 90, and 10 minutes respectively. All the effluents experienced a 2 h aeration as a clarification process.

Figure 5.3 Bioreactor set-up. Recycling the headspace by air pumps.

5.2.3 Experimental design (RSM-CCD)

Central composite design (CCD) and the response surface methodology (RSM) method from DOE software (Design Expert 11-Stat-Ease) were used to model the experimental conditions by evaluating the association between the variables (*i.e.* pH of the sawdust, aeration rate, contact time and nitrate concentration) and the responses (% N removal and N_2O concentration). The design consisted of k_2 factorial points completed by 2k axial points and a centre point, where k is the number of variables. By employing equation 5.1 and the associated variables, it was possible to optimize the operational design to predict the best and desirable value of the responses.

$$\boldsymbol{Y} = (\boldsymbol{\beta_0} + \varepsilon) + \sum_{i=1}^{k} \boldsymbol{\beta_i X_i} + \sum_{i=1}^{k} \boldsymbol{\beta_{ii} X^2} + \sum_{i_i<j}^{k} \sum_{j}^{k} \boldsymbol{\beta_{ij} X_i X_j} + \cdots + \boldsymbol{e} \quad (5.1)$$

Where, Y: response; X_i and X_j: variables; β_0 : constant coefficient; β_j, β_{jj}, and β_{ij} : interaction coefficients of linear, quadratic and second-order terms, respectively; k: number of studied factors; e: error).

5.2.4 Nitrate removal analysis

ALLODUST was developed to investigate the effect of the media on the fluidized bed reactor efficiency in nitrate removal in the presence of returned activated sludge (RAS). Contact time (h), sawdust pH, initial nitrate concentration (mg L^{-1}) and the adsorbent dosage (g L^{-1}) were chosen as the experiment variables. The CCD was utilised to design the experiments with 4 variables and nitrate removal (%) and the N_2O concentration (mg L^{-1}) as the main responses. COD, DO, EC, and pH were measured as the control responses (Table 5.2). Then the data was analysed with Response Surface Methodology (RSM) in order to investigate the effect of the variable changes in the responses. Finally, ANOVA was used for each experiment to find the optimum operational details to gain the best responses. In total, 90 reactors for (three replicates) was run to find the optimum condition for the N removal with the minimum N_2O emission. Table 5.3 presented the ALLODUST efficiency in nitrate removal under different operational conditions. The optimal operational condition of the reactors was determined by the lowest contact time and N_2O emission, with the highest nitrate removal. Also in order to record the effect of each part of the media on N removal, two control samples was run in each optimum condition. The aeration rate of 4.5 L min^{-1} was chosen for all the reactors. The N_2 gas was purged to the system for 20 minutes to make the reactors zero oxygen and favourable for the anaerobic condition. The headspace gas was recycled and pumped to the system again in the anaerobic reactors to make the agitation. One oxygen sensor was used to make sure about the reactors condition during the process.

The nitrate concentration was measured using the Alpkem FS3000 – twin channel analyser. Nitrate was analysed based on the cadmium reduction method-coil (OTCR –open tubular cadmium reactor) by initial reduction of nitrate to Nitrite-N. An azo dye compound is formed by the reaction of nitrite with sulphanilamide/NED. Then, a spectrophotometer was used to determine the compound's intensity.

Table 5.2 Optimization of the different developed media for N removal from wastewater.

Characteristics	pH	Carbon (mg kg^{-1})	Nitrogen (mg kg^{-1})	CEC (meq $100g^{-1}$)	Sum Bases	SSA (m^2 g^{-1})	Pore Volume (cm^3 g^{-1})
Horotiu	5.7	3.3	0.27	17	4.09	15.02	0.031
Craigieburn	6.2	3.8	0.26	17.9	0.87	12.48	0.027

In order to increase the removal rate and the system efficiency, 10% of returned activated sludge (RAS) was added to the system after acclimatization for 10 days. This was to increase the anaerobic bacterial community and utilising the area and the surface morphology which are provided by the ALLODUST material in the system. Biological denitrification is known to provide a high waste disintegration rate. The RAS is added to the reactor and then mixed with the wastewater by the aeration method (utilising the reactor's headspace air). The RAS is reused after sedimentation and returned to the aeration tank. The activated sludge method uses heterotrophic bacteria communities that utilise the organic carbon in the wastewater as an energy source; thus, producing a high-quality effluent. Aggregation of particles as microorganisms grow is the main principal behind RAS usage in a wastewater treatment process (Q. He et al., 2018). The activated sludge (pH: 7.17; EC: 735 µS cm^{-1}; DO: 0.22 mg L^{-1}) employed in this study was sampled from the Bromley Waste Water Treatment Plant, Christchurch, NZ. It was collected in a 25 L container, preserved with glycerol and stored at -20 °C between sampling and collection. Liquid sodium acetate was used as the energy source. The amount of the sodium acetate calculated based on the Equations 2.11 – 2.17 and was 0.238 g for 1 g nitrate removal (Figure 5.4). C/N ratio was 5-8 during the experiment.

In order to ensure system adaptation to the experimental condition, a 10 day-old activated sludge acclimatization was conducted. 1080 ml of activated sludge (90%) was mixed with 120 ml (10%) of the collected wastewater. After the completion of the reaction and settling phase, 120 ml of the supernatant was removed. The next cycle run was with the addition of 120 ml wastewater to the reactor (Aziz, Aziz, Yusoff, et al., 2011). At the end, the activated sludge was used as seed material in the treatment system.

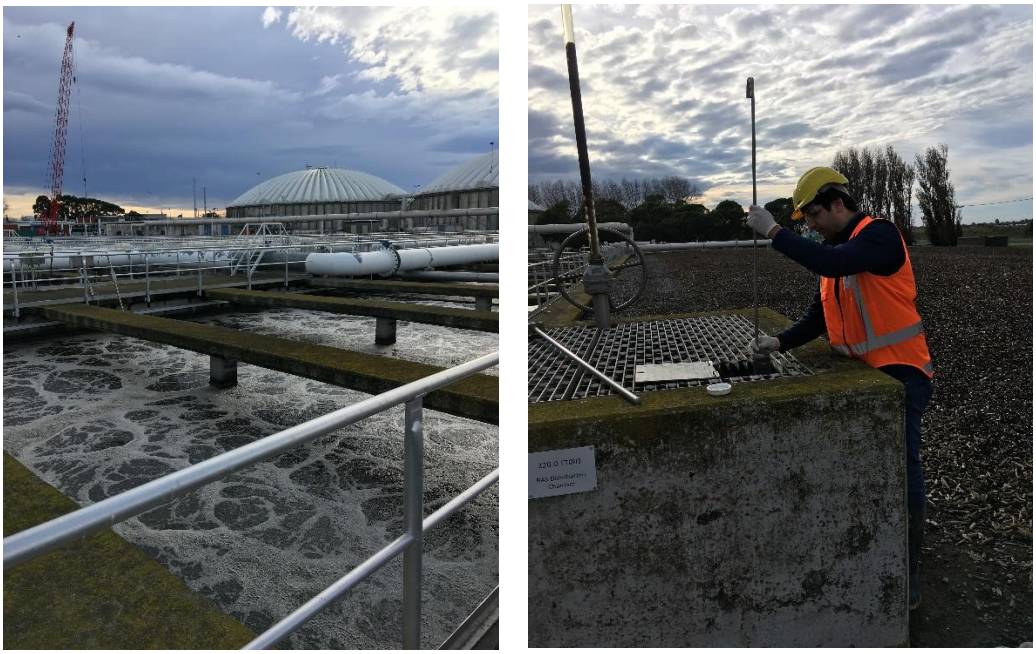

Figure 5.4 Sludge sampling from Bromley wastewater treatment plant.

5.2.5 Gas Sampling and Analysis

Gas sampling was carried out after the anaerobic process was completed. In order to enable nitrous oxide analysis, the headspace gas was collected into glass vials that were previously filled with compressed air. A rubber septum which was fitted in the vial's lid was used seal the samples. A 20 ml glass syringe was used as a sampler, whereby the needle was attached to a three-way stop-cock (no. 2C6201, Baxter Healthcare Corp., Waukegan, IL).

In order to avoid the syringe becoming contaminated with the other reactor's headspace and atmosphere air, it was flushed a couple of times with atmospheric air and then with headspace air during each sampling process. In order to prevent external air from contaminating the samples, the samples were over-pressurized. A minimum 10 ml gas samples were collected and injected into the pre-evacuated *Exetainer* vials with 6 ml volume (Labco Ltd., High Wycombe, UK). A double-ended needle was used to reduce the vials to ambient pressure immediately before analysis. The gas samples were analysed on automated GC (Model 8610C, SRI Instruments, California, USA) with automated Gilson GX-271 auto samplers (Gilson Inc, MI, USA). The GC were configured with two Haysep-D™ packed columns (6' X 1/8") in series as the analytical column and one Haysep-D™ as a pre column. An electron Capture Detector (ECD)

was used for nitrous oxide quantification. The radioactive 63Ni source sealed inside the ECD detector emits electrons (beta particles) which collide with and ionize the make-up gas (10% methane in argon) and carrier gas (nitrogen) molecules. Detection limit for N_2O was 0.07 mg L^{-1} (70ppb) with a quantitation range up to 1000mg L^{-1} (v/v).

5.3 Results and Discussion

5.3.1 Nitrate Removal by ALLODUST

It was concluded that the nitrate removal/reduction by ALLODUST was significantly affected by four factors. The sawdust pH, aeration rate, contact time and the initial P concentration. As hypothesized, the application of ALLODUST to the sludge bed reactor in the lab-scale AS-SBAnR significantly increased the removal of nitrate, resulting in a higher eliminating efficiency compared to the control. The allophanic soil material and sawdust greatly increased the nitrate reduction rate especially during the first 12 h, with an average 87.38% removal from the low to high range of contamination, compared with a 21.18% decrease in the control (Table 5.3). Sawdust pH did not show a significant effect on the system efficiency. In addition, RSM with a CCD had calculated the interactive effects of all variables.

Table 5.3 Optimization of the different developed media for N removal from wastewater.

ALLODUST+RAS (*C* : Control – Samples without ALLODUST)*										
No	**N.Con (mg L^{-1})**	**C.T (hrs)**	**Dosage (g L^{-1})**	**SD $_{pH}$**	**N removal (%)**	**N_2O (mg L^{-1})**	**COD (mg L^{-1})**	**DO (mg L^{-1})**	**EC (µs/cm)**	**pH**
1	110	2	12	2	12	0.148	409	0.75	2950	11.83
2	10	2	12	6	8.01	0.143	145	0.86	2112	11.75
3	60	12	7.5	4	88.9	1.378	295	0.53	2760	11.89
4	60	12	7.5	4	87.42	1.335	288	0.74	2730	12.03
5	110	2	3	2	10.2	0.09	469	0.93	1989	11.53
6	10	2	3	2	8.7	0.455	152	5.79	1046	11.36
7	60	2	7.5	4	17.63	0.152	304	0.78	2340	11.79
8	110	2	3	6	12.43	0.524	387	1.46	1702	11.21
9	60	22	7.5	4	19.75	0.533	260	0.97	2830	12.03
10	60	12	7.5	4	90.04	1.186	238	0.89	2760	11.91
11	60	12	7.5	4	92.14	2.17	299	0.65	2760	11.95
12	60	12	7.5	4	91.52	2.826	310	0.77	2750	12.01
13	10	22	3	2	9.05	0.378	124	1.31	1417	11.75
14	110	22	12	2	10.6	0.241	422	0.86	3280	12.03
15	10	2	3	6	8.03	0.142	157	0.69	1197	11.49
16	110	22	3	2	12.68	1.429	391	1.15	2077	11.71
17	10	2	12	2	6.6	0.109	164	2.05	2125	11.75
18	10	22	12	6	8.3	0.173	165	0.76	2610	12.00
19	110	12	7.5	4	72.2	1.69	435	0.72	3220	11.83
20	10	12	7.5	4	100	1.756	146	0.81	2340	11.87
21	60	12	7.5	4	90.23	1.69	307	0.62	2730	11.94
22	60	12	12	4	78.5	2.094	228	0.87	2910	11.9
23	60	12	7.5	6	82.88	1.744	306	0.78	2800	11.82
24	10	22	12	2	4.7	0.136	141	0.79	2450	11.92
25	110	22	3	6	12.94	0.96	411	0.76	2190	11.74
26	110	22	12	6	14.61	0.106	374	0.67	3500	12.07
27	10	22	3	6	0	0.742	137	0.85	1223	11.68
28	60	12	7.5	2	98.12	2.113	304	0.98	2680	11.80
29	110	2	12	6	12.53	0.224	438	1.14	2870	11.72
30	60	12	3	4	100	2.829	265	0.72	1678	11.48
C1	10	2	-	-	20.05	83.82	290	0.40	428	7.55
C2	10	2	-	-	16.80	84.12	307	0.32	230	7.27
C3	60	2	-	-	21.18	67.74	350	0.83	858	7.12
C4	60	2	-	-	16.26	43.78	293	0.36	626	7.36
C5	110	2	-	-	13.40	88.24	299	0.47	1248	7.11
C6	110	2	-	-	10.99	64,86	296	0.32	1058	6.93
C7	10	12	-	-	18.38	75.42	357	0.52	452	6.68
C8	10	12	-	-	18.37	84.61	251	0.19	195	6.84
C9	60	12	-	-	17.33	85.96	348	0.11	721	7.43
C10	60	12	-	-	17.52	78.65	336	0.12	532	7.48
C11	110	12	-	-	18.21	84.72	307	0.08	1084	7.64
C12	110	12	-	-	18.95	81.35	355	0.12	969	7.55
C13	10	22	-	-	0	N/A	376	0.44	497	5.29
C14	10	22	-	-	0	N/A	277	0.71	284	4.83
C15	60	22	-	-	1.5	N/A	288	0.45	876	5.14
C16	60	22	-	-	15.6	N/A	403	0.51	683	4.81
C17	110	22	-	-	11.14	N/A	305	0.52	1294	5.15
C18	110	22	-	-	9.30	N/A	261	0.67	1111	4.66

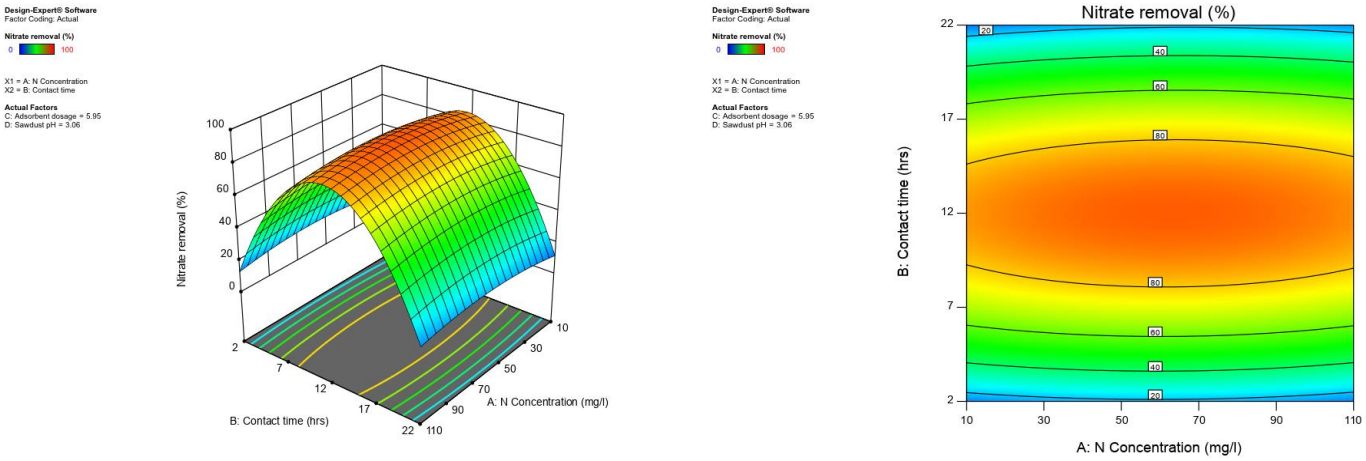

Figure 5.5 The response surface plots and corresponding contour plots of the optimized design for the N removal efficiency as a function of sawdust pH=3.06 and Adsorbent dosage=5.95.

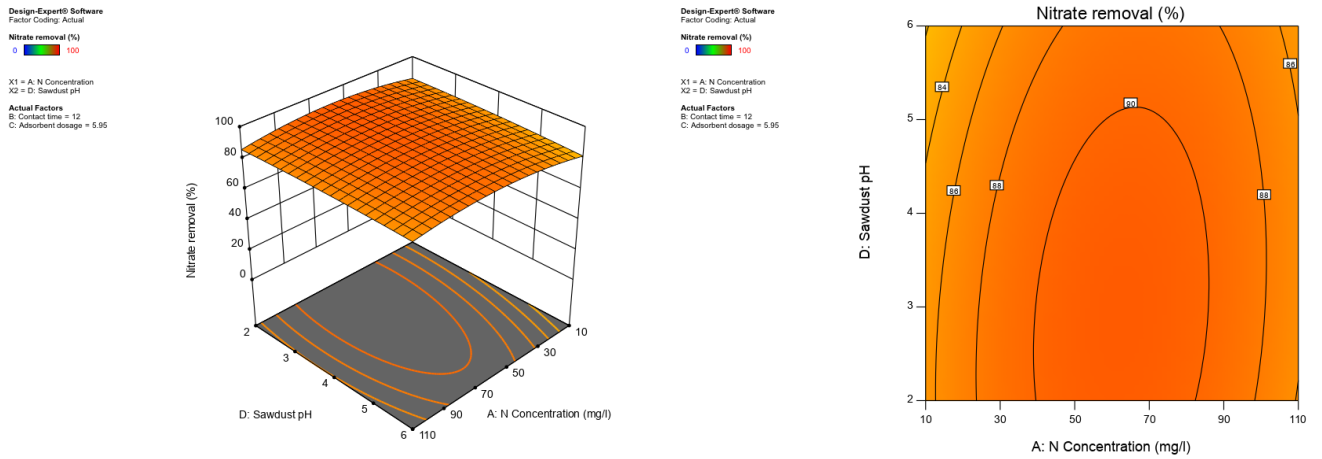

Figure 5.6 The response surface plots and corresponding contour plots of the optimized design for the effect of sawdust pH on N removal efficiency in optimum condition.

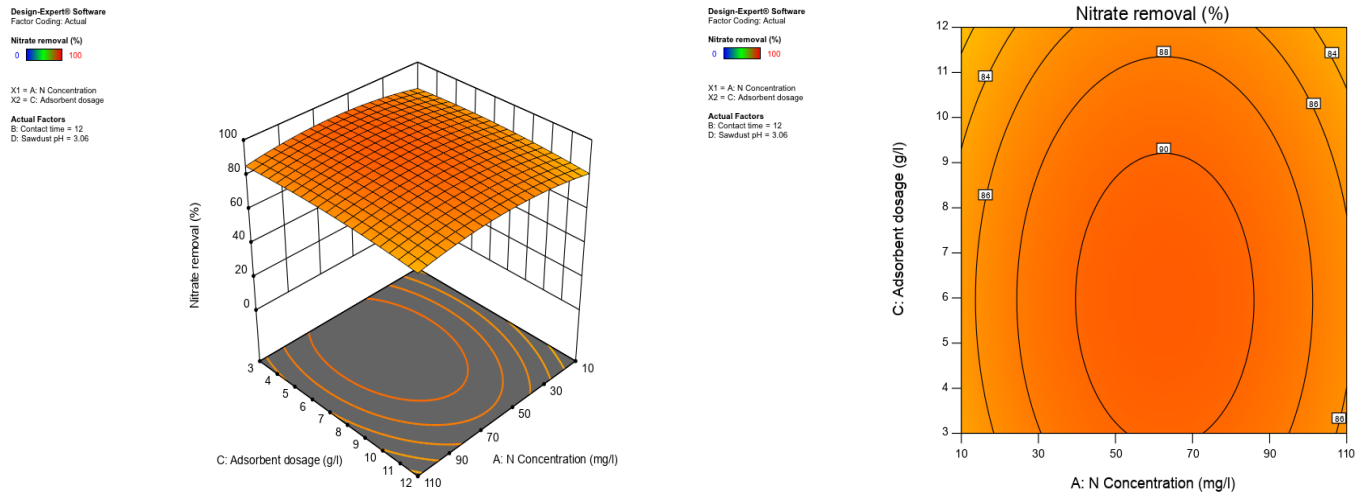

Figure 5.7 The response surface plots and corresponding contour plots of the optimized design for the effect of adsorbent dosage on N removal efficiency in optimum condition.

Given that the ALLODUST media had a significant effect on nitrate removal, the data indicated the effect of the media on the nitrate reduction. Consequently, the additional removal efficiency of the AS-SBAnR can be considered an enhancement of the system performance by ALLODUST to result in a step-change in the permanent removal efficiency of the reactors. Denitrification is the main nitrate mechanism of nitrate removal and increase in denitrifying bacterial communities will result in an increase in nitrate removal(Mohseni-Bandpi et al., 2013; Z. Zhang et al., 2018). Both the allophanic material and the sawdust played a major role in the nitrate removal mechanism. The allophanic soil material is a porous media with a high soil microbial population in anaerobic respiration; denitrification uses nitrate (NO_3^-) as a terminal electron acceptor in the respiratory electron transport chain. Also sawdust will provide an additional habitat for microbial colonization. Surface protonation by a chemical-acidic treatment lead to the development of positive surface charge density and also provided more microsites and nanosites which enhanced the specific surface area favourable for the microorganism's growth. Ions, water, and organic compounds can be retained by the polar sites on the surface (Kookana et al., 2011).

Dissimilatory nitrate reduction or denitrification is reduction of the nitrate to nitrogen gas. New cell biomass, and hydroxyl ion occurred in the system as the main nitrate reduction products mediated by ALLODUST. This cycle triggered an increase in pH which was not considered a critical issue. Nitrate acts as a terminal electron acceptor instead of oxygen and under anaerobic conditions, induces the production of adenosine triphosphate (ATP). These electrons provided by specific inorganic and organic electron donors in both autotrophs and heterotrophs (Ashok & Hait, 2015; Lew et al., 2012). During denitrification, nitrate is consumed as electron acceptors for the oxidation of organic electron donors, and involves energy conservation. The organisms which gained energy by electron transformation from donor to acceptor applied this for the synthesis of new cell mass and maintenance of existing cell mass. The ALLODUST media provided a surface area and micro-pores, to significantly enhance the growth of bacterial biofilm. All these reactions occur only under anaerobic conditions, while denitrification can be facilitated by a number of species of bacteria under aerobic conditions (Burghate & Ingole, 2014). *Paracoccus* is a type of bacteria which can survive in different environments and enable the denitrification process under aerobic conditions. Nitrate removal by biological denitrification occurred in the system due to heterotrophic bacteria which used liquid sodium acetate as an organic carbon source. In

contrast, methanol is most widely used compared to the other carbon sources but produces a lower bacterial cell yield (Hamlin et al., 2008; Weigelhofer & Hein, 2015). *Pseudomonas* and *Bacillus* are the most common heterotrophic denitrifiers which degrade organic carbon to obtain energy for the growth and reproduction (Brezonik, 2013). In order for cell synthesize and performing the respiration and anabolism, both nitrate and organic carbon need to be participate (Rezvani et al., 2019).

The increased number of positive charges, through electrostatic attraction, adsorbed more negatively charged nitrate anions. The acid treatment protonation was a convenient and proven technique for eliminating nitrate from wastewater as well as efficient in removing other contamination from wastewater (Yin et al., 2007). This modification method is generally performed on adsorbents derived from agricultural and industrial residue, which are low-cost substances. This surface modification approach would therefore be cost-effective and fit for purpose.

Through the three-dimensional response surface curves and contours, the optimum values of the variables for eliminating N from the wastewater were evaluated (Table 5.4). Figures 5.5-5.7 present the N removal rate response surface and contours as a result of N concentration and contact time as independent variables; the sawdust pH and ALLODUST dosage were considered as the actual factors for the low-high range N concentration. After optimisation of the system it was found that there was not a significant difference in nitrate removal efficiency for the different concentration ranges. So, the average of the variables was considered for all the nitrate concentrations. These Figures 5.5-5.7 show the impact of the contact time on the system's N elimination capacity. The response surface of the N removal rate gradually increased when the contact time increased from 2 to 12hrs and then dropped if the reactor was run for 22 hrs. The initial N concentration was another effective factor. The N removal rate increased when the concentration of nitrate increased from 10 mg L^{-1} to 60 mg L^{-1}. However, it gradually decreased while the initial nitrate concentration increased up to 110 mg L^{-1}.

When the adsorbent was in contact with 10 mg L^{-1} nitrate, the system could remove 85.46% of the nitrate in the 11.95 hrs contact time and 4.5 L min^{-1} aeration rate and the efficiency of the system enhanced when the nitrate concentration increased up to the 60 mg L^{-1}. If the reactors ran with the same operational conditions the nitrate removal rate dropped to 86.47%

in the presence of the 110 mg L^{-1} nitrate in the wastewater; this was the highest removal rate for this range of nitrate concentration. In order to optimise the adsorbent dosage, a reduction in the quantity of media usage in the system was trialled. In a large scale design, using less media would be desirable, as it will decrease the project cost and also generate less residual waste after the treatment process.

Table 5.4 Optimum results for different ranges of Nitrate concentration.

Characteristics	Low Range	Mid-Range	High Range
Nitrate Concentration (mg L^{-1})	1-10	11-60	61-110
Contact time (hrs)	11.95	11.98	12.03
Adsorbent dosage (g L^{-1})	5.4	5.82	6.28
Sawdust pH	2.0	2.82	3.71
Nitrate removal (%)	85.46	91.13	86.47
N_2O Concentration (mg L^{-1})	1.67 for 10	2.02 for 60	1.80 for 110
Chemical Oxygen Demand (COD) (mg L^{-1})	277.42	232	257.35
Dissolved Oxygen (DO) (mg L^{-1})	2.50	1.43	0.76
Electrical Conductivity (EC) (µs cm^{-1})	353.23	396.80	145.72
pH	11.71	11.81	11.84

5.3.2 N_2O Emission Analysis

The activated sludge control treatment created significantly more N_2O than any other treatments which contained the ALLODUST material during the experimental period. The bioreactors which contained ALLODUST showed higher nitrate removal while having the minimum N_2O emission compared to the control (without ALLODUST). The control bioreactors containing just activated sludge and had almost 80% more N_2O emissions compared to the reactors containing ALLODUST. This indicated that the ALLODUST media performed a significant role in the system to achieve a sustainable solution for removal of high concentration of nitrate from wastewater. It is important to note that the results of nitrous oxide emissions need to be considered in the context of the sealing ability of the laboratory-scaled bioreactors and the open gas exchange with the AS-SBAnR field-scale atmosphere will lead to varied results. During the denitrification process, it's expected that the nitrous oxide consumption occurs in conjunction with the nitrous oxide production. The very low N_2O concentration that was observed in the reactors containing ALLODUST might be the result of N_2O diffusion back into the aqueous phase from the headspace, during the denitrification process. So, it will be available to the bacterial communities on the media's surface for the

reduction to N_2 by denitrifiers. The high specific surface area, pore sizes and the porous structure of the media could enhance the N_2O emission control.

The system response to the N_2O emission during the nitrate removal is presented in Figure 5.8-5.10. The highest gas emission occurred during the system run of 12 h for all ranges of the nitrate concentration; this was the optimum contact time for the nitrate removal. Nitrate removal of 2.02 mg L^{-1} N_2O for 60 mg L^{-1} was the highest concentration of the optimum designs. Figure 5.9 illustrates that the sawdust pH did not affect the system proficiency according to the N_2O emission. Figure 5.10 shows the highest N_2O emission attributed to the lowest ALLODUST containing reactor. While a lower quantity of the media will decrease the treatment cost, it is important to control the N_2O emissions during the wastewater treatment. The optimum adsorbent dosage (5.95 g L^{-1}) was the first point which the contour jumped out from the red zone. The higher media usage led to less gaseous N_2O emission, but the difference was only 10% which is not economical to use according to the waste management and operational affairs.

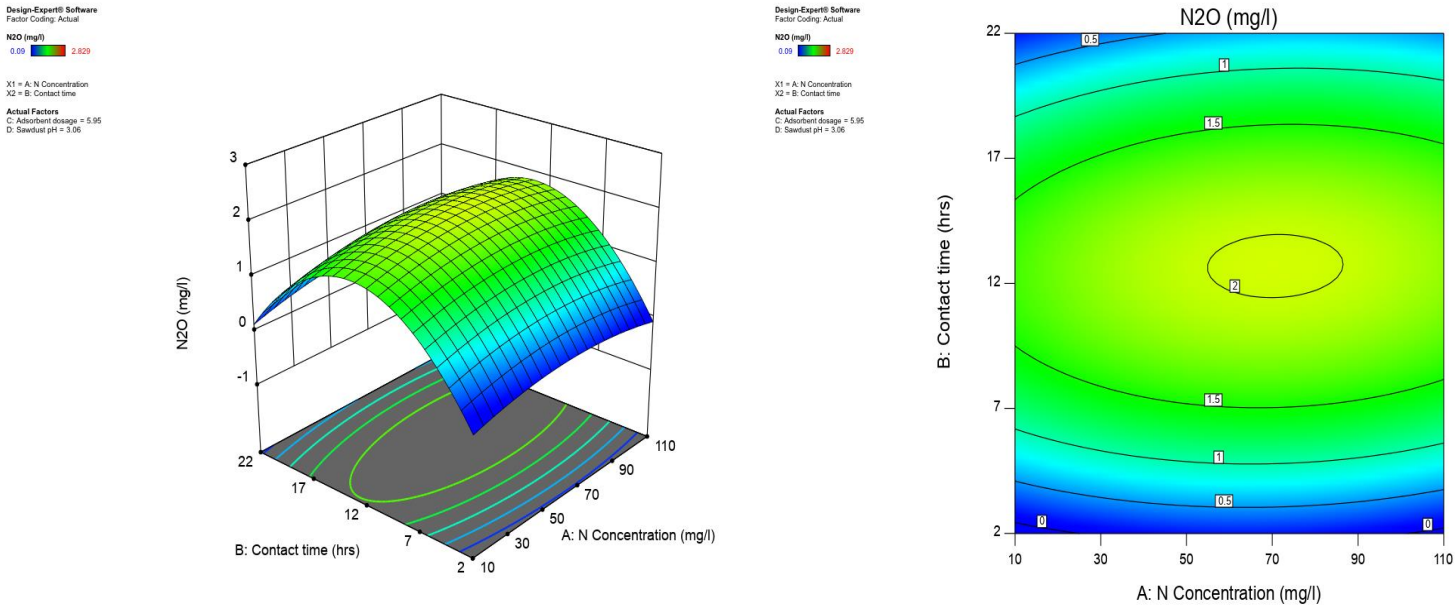

Figure 5.8 The response surface plots and corresponding contour plots of the optimized design for the N_2O emission as a function of sawdust pH=3.06 and Adsorbent dosage=5.95.

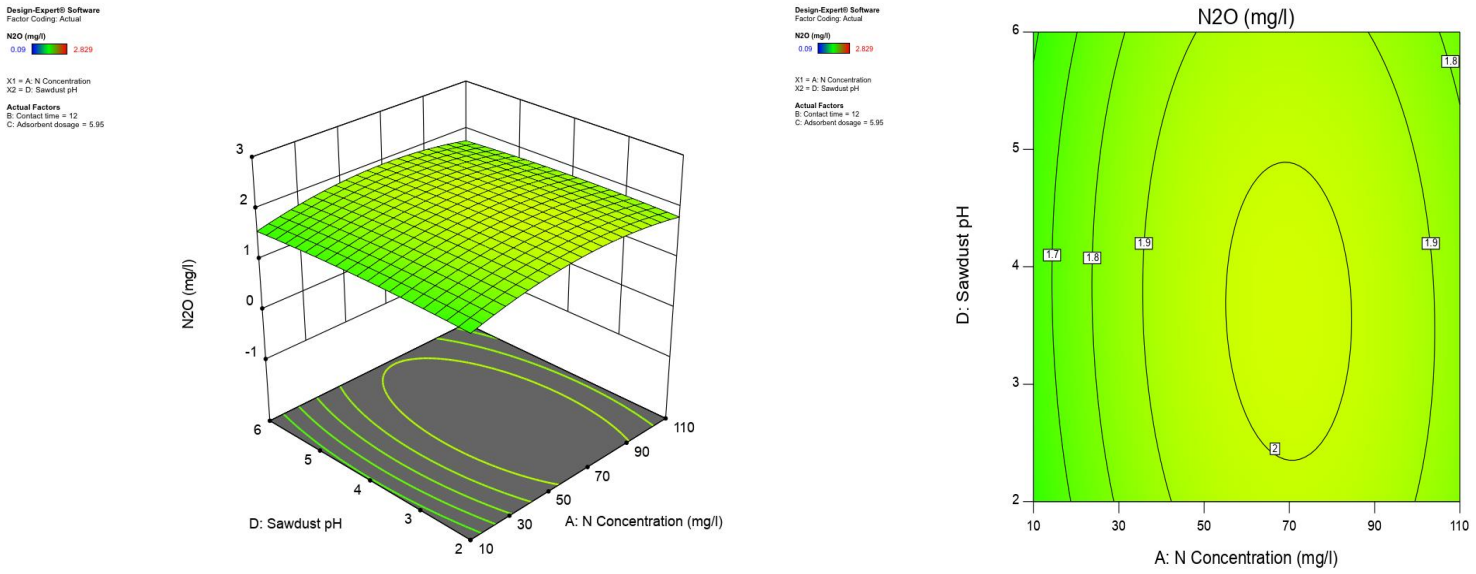

Figure 5.9 The response surface plots and corresponding contour plots of the optimized design for the effect of sawdust pH on N_2O emission in optimum condition.

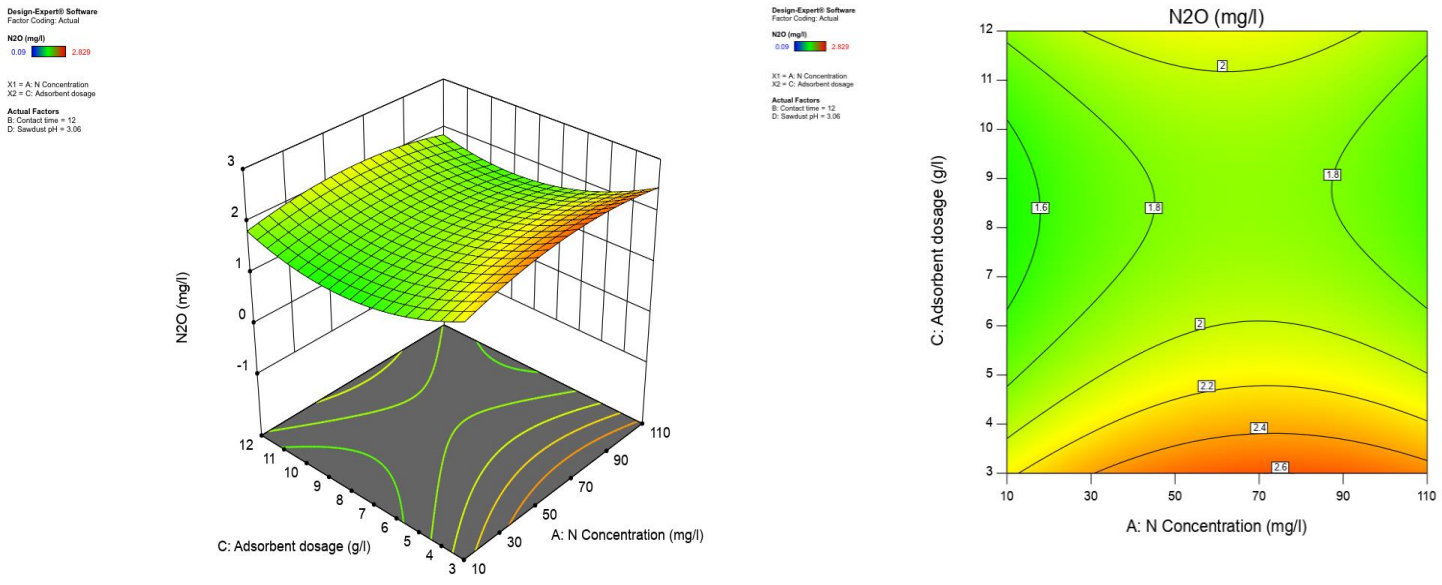

Figure 5.10 The response surface plots and corresponding contour plots of the optimized design for the effect of adsorbent dosage on N_2O emission in optimum condition.

5.3.3 Scanning Electron Microscope (SEM)

The samples were coated with carbon by EMS 150T ES at 62A and 80 mm distance with three pulses @ 3 seconds/pulse. The morphology study was operated by SEM JEOL JSM 7000F at 5KV and WD6mm for imaging. The morphological study results are shown in Figure 5.11 and Figure 5.12.

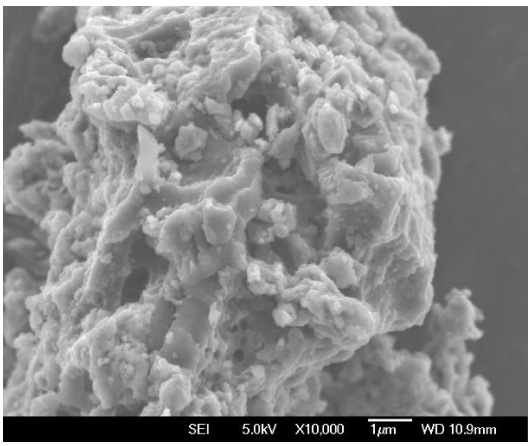

Figure 5.11 Scanning Electron Microscopy (SEM) of developed ALLODUST.

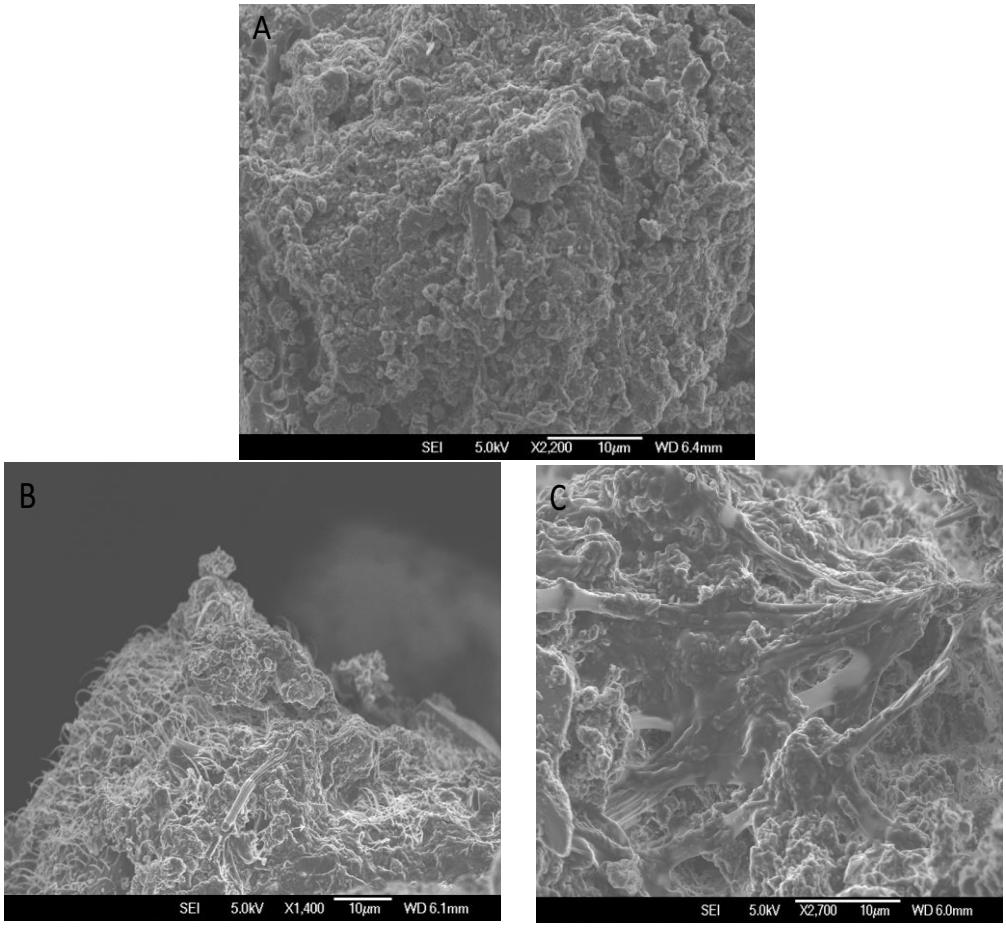

Figure 5.12 Scanning Electron Microscopy (SEM) ALLODUST$_2$ after N reduction: A) without RAS and B), C), with RAS, showing bacterial biofilm growth.

In order to activate the surface, the acidic sawdust treatment was used in the SEM study. The activated surface exhibited well-developed pores and were covered by the allophane nano particles (Figure 5.11). The anaerobic sites which developed on the media surface and the

adsorption capacity of the untreated sawdust was enhanced by the acidic treatment. The results of the removal of filaments are the hollow channels and pores on the sawdust particles.

The result of carrying out the SEM of the media after the N adsorption is shown in Figure 5.12A. The media which was subjected to the 50 mg L^{-1} nitrate without the RAS demonstrated weak bacterial activity. Most of the spaces are filled with the adsorbed nitrate ions and the cations presented in the wastewater which can make a bridge mechanism for the nitrate adsorption on the negatively charged surfaces and the adsorption sites; in addition, the surface structure is flocculated. The bacterial biofilm growth is visible in the media which was enriched with the RAS and subjected to the same concentration of the nitrate (Figure 5.12B and Figure 5.12C).

The ALLODUST SEM images showed that there is a binding agent between particles which couldn't be resolved with the regular magnification of 20X-30,000X. Because allophane was the likely origin for the gel-like substance observed; the morphology study using SEM was conducted to identify nanostructures in the soil. The silt particle morphology is however dominant. Figure 5.11 shows the surface of the deposited particles after three gravity sedimentation processes: the particles of clay size are still combined and at greater magnification, the increased resolution showing that the binding agent is composed of globular agglomerates of spherical particles with outer diameters of approximately 5 nm. This concurs with the structure of allophane (Bishop et al., 2013; Calabi-Floody et al., 2011; Levard et al., 2012; Rennert et al., 2014; Wada & Wada, 1977). On both HOROTIU soil and ALLODUST, these aggregates were observed before and after removal of N.

5.3.4 Chemical Oxygen Demand (COD)

The COD measurement was conducted during the experiment as a measure of a pollutants in the wastewater and the treated water. The COD concentration of the samples were determined by COD digestion vials, High range, Reactor digestion method (HACH-method 8000) and a HACH spectrophotometer (DR 3800). In this series of the experiments, as Figure 5.13 shows, the COD concentration increased in the system by increasing the initial concentration of the nitrate. The results show that 5.95 g of prepared ALLODUST material can decrease COD concentration to 11 % in the presence of the same nitrate concentration compare to the sludge treatment method only. Also, it can be seen from Figure 5.13, that the ALLODUST dosage in the removal system is not a factor in increasing the COD concentration

during the nitrate removal. The additional plant biomass is an effective factor to shorten the adaption period for denitrification in the nitrate removal system which is in agreement with the findings of Wen et al. (2010). Such additional biomass can increase the effluent COD concentration which may then exceed the effluent standard. In a denitrification system the main COD consumers are the methane-producing bacteria (47.3 -61.0%) and the sulphate-reducing bacterial (20.6 – 26.0%), while the denitrifying bacteria's contribution in the COD consumption is the minimum (8.4 – 9.2%) (Y. Chen et al., 2014). This fact demonstrates that in the case of using plant biomass such as sawdust in a denitrifying system, the excessive carbon source could be ineffective due to the excessive carbon source provided by plant biomass in the initial stage.

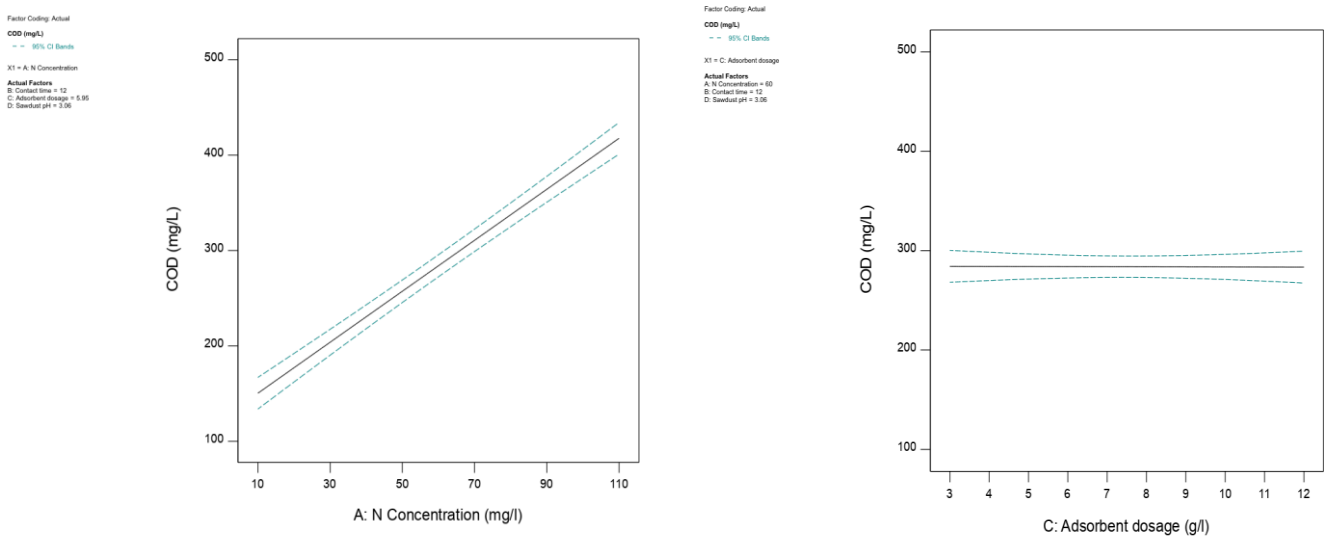

Figure 5.13 COD changes according to the nitrate concentration in the optimum condition and the effect of the adsorbent dosage on the COD concentration.

5.3.5 Optimization and Statistical Analysis

It was found that the nitrate eliminating in AS-SBAnR in the presence of ALLODUST was significantly affected by four factors: N concentration; contact time; adsorbent dosage and sawdust pH. Therefore, RSM with a central composite design evaluated the interactive results of these variables. The following quadratic polynominal equation was used based on the estimate of the parameter to compare the interaction between the four factors and the rate of elimination of N.

$$Y = -23.09965+0.226530X_1+17.36082X_2+0.868884X_3+0.366789X_4+0.001620X_1X_2 - 0.000094X_1X_3 +0.007338X_1X_4 +0.005222X_2X_3 -0.014625X_2X_4 +0.116528X_3X_4 - 0.002133X_1^2 -0.727422X_2^2-0.107763X_3^2-0.233048X_4^2 \quad (5.2)$$

Where Y is N removal rate and X_1, X_2, X_3, and X_4 are the coded values of N concentration, contact time, adsorbent dosage and sawdust pH, respectively.

The equation can be used in terms of actual variables to make predictions about the reaction of each factor for given amounts. Here the amounts for each factor should be defined in the original units. This equation should not be used to calculate each factor's relative impact because the coefficients are scaled to match each factor's units and the intercept is not at the centre of the design space.

Table 5.5 Model statistic details.

	N	N_2O		N	N_2O
Std. Dev.	7.65	0.4244	**R^2**	0.9809	0.8781
Mean	42.02	0.9832	**Adjusted R^2**	0.9631	0.7643
C.V. %	18.19	43.17	**Predicted R^2**	0.9155	0.6774
			Adeq Precision	15.7538	8.4263

The Predicted R^2 of 0.9809 and 0.8781 are in reasonable agreement with the Adjusted R^2 of 0.9631 and 0.7643 for nitrate and N_2O respectively; i.e (Table 5.5), the difference is less than 0.2. Adeq Precision measures the signal to noise ratio. A ratio greater than 4 is desirable. The model ratio for nitrate of 15.754 and for N_2O of 8.4263 indicates an adequate signal. This model can be used to navigate the design space. The Model F-value implies the models are significant. There is only a 0.01% chance that an F-value this large could occur due to noise. P-values less than 0.05 indicate model terms are significant.

Table 5.6 ANOVA for Quadratic model.

Source	Sum of Square		df		Mean Square		F-value		p-value	
	N	N_2O	N	N_2O	N	N_2O	N	N_2O	N	N_2O
Model	45010.35	19.47	14	14	3215.03	1.39	55.00	7.72	<0.0001	0.0002
A-N.Con	15.68	0.1055	1	1	15.68	0.1055	0.2683	0.5856	0.6121	0.4560
B-Contact time	0.6806	0.4083	1	1	0.6806	0.4083	0.0116	2.27	0.9155	0.1530
C-Ads.dosage	18.36	0.9684	1	1	18.36	0.9684	0.3141	5.38	0.5834	0.0350
D-Sawdust pH	9.27	0.0065	1	1	9.27	0.0065	0.1587	0.0359	0.6960	0.8523
AB	10.50	0.0856	1	1	10.50	0.0856	0.1796	0.4749	0.6777	0.5013
AC	0.0072	0.0795	1	1	0.0072	0.0795	0.0001	0.4414	0.9913	0.5165
AD	8.61	0.0029	1	1	8.61	0.0029	0.1474	0.0162	0.7064	0.9005
BC	0.8836	0.3209	1	1	0.8836	0.3209	0.0151	1.78	0.9038	0.2019
BD	1.37	0.0118	1	1	1.37	0.0118	0.0234	0.0653	0.8804	0.8017
CD	17.60	1.0E-6	1	1	17.60	1.0E-6	0.3011	5.5E-6	0.5913	0.9982
A^2	73.67	0.1783	1	1	73.67	0.1783	1.26	0.9899	0.2792	0.3355
B^2	13709.61	6.99	1	1	13709.6	6.99	234.55	38.82	< 0.0001	<0.0001
C^2	12.34	0.5874	1	1	12.34	0.5874	0.2111	3.26	0.6525	0.0911
D^2	2.25	0.0084	1	1	2.25	0.0084	0.0385	0.0465	0.8470	0.8322
Residual	876.76	2.70	15	15	58.45	0.1802				
Lack of Fit	861.96	0.7370	10	10	86.20	0.0737	29.12	0.1875	0.0008	0.9880
Pure Error	14.80	1.97	5	5	2.96	0.3931				
Cor Total	45887.11	22.17	29	29						

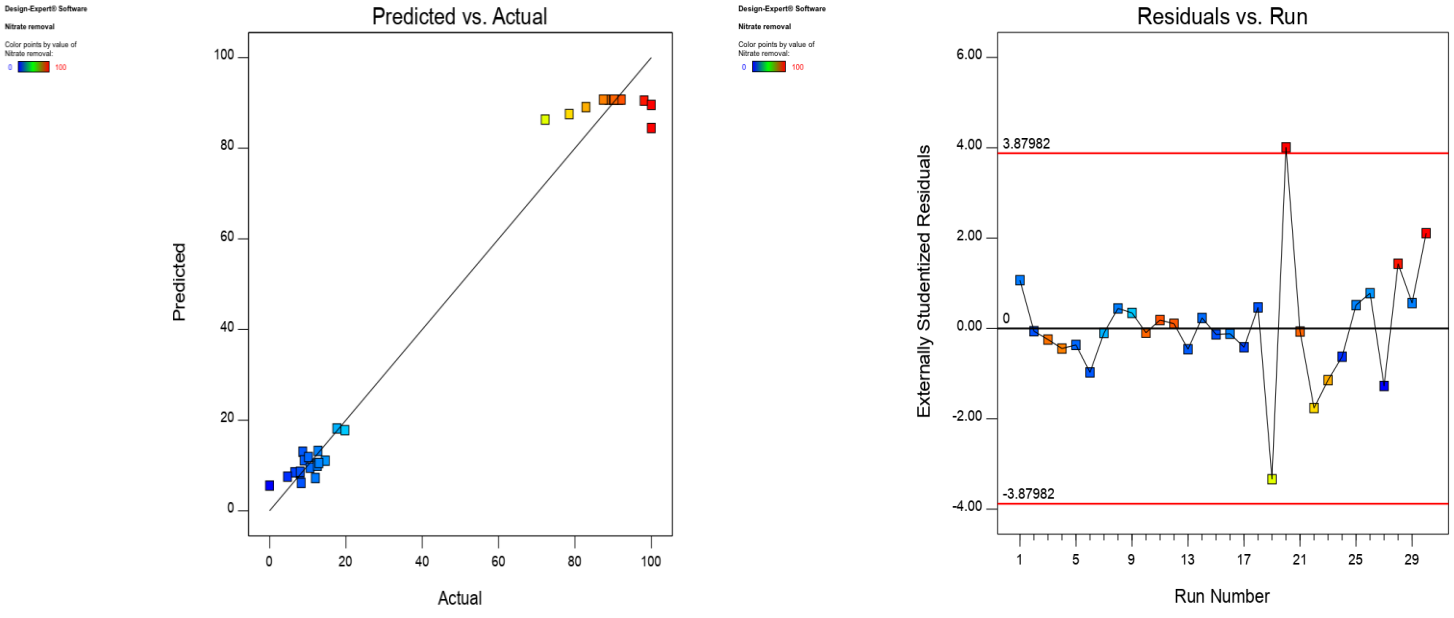

Figure 5.14 Design-expert plot; predicted vs. actual values plot for N removal – Residuals vs. Predicted.

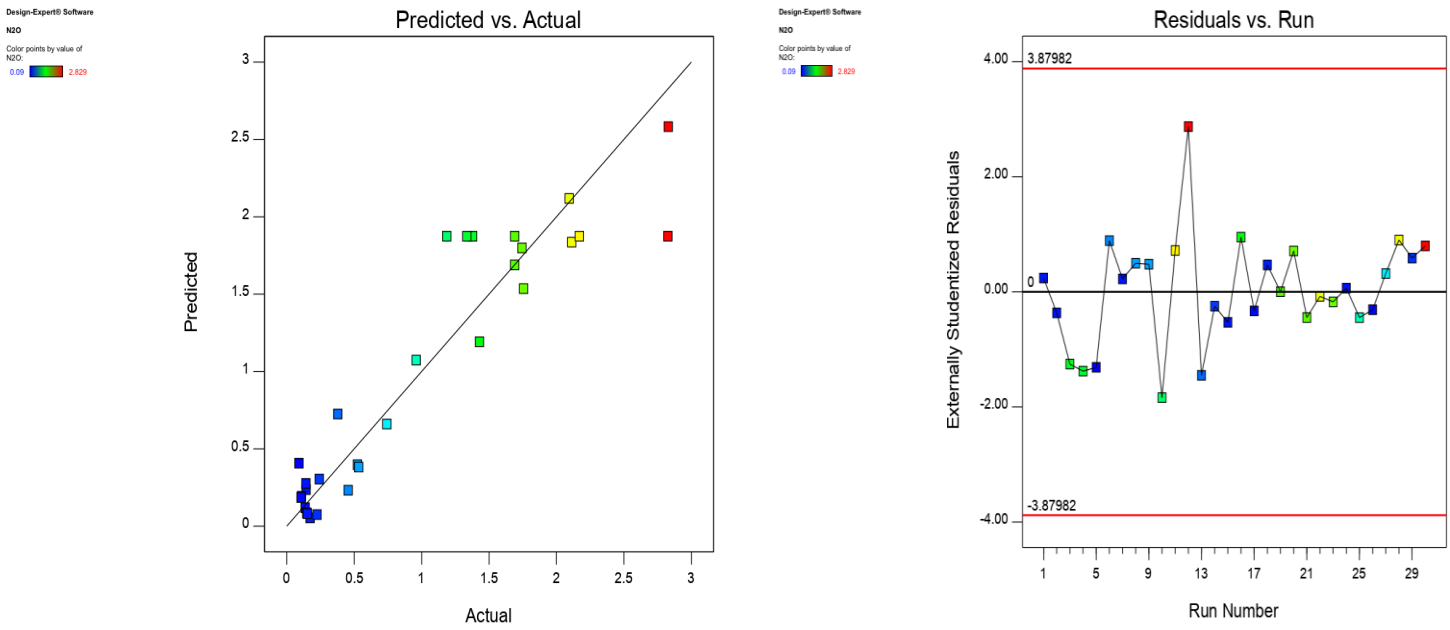

Figure 5.15 Design-expert plot; predicted vs. actual values plot for N_2O emission – Residuals vs. Predicted.

According to the probability value (less than 0.05), all models were significant at the 5% confidence level. R^2 values close to 1 were favourable, and a high R^2 coefficient ensured acceptable modification of the quadratic model to fit the experimental data. Figure 5.14 and Figure 5.15 show the predicted versus actual-value plots of the response parameters for the N removal and the N_2O emission respectively. These plots signified a sufficient agreement between the real data and the values achieved from the models.

5.4 Conclusions

This experiment highlights the potential of the innovative ALLODUST media material to enhance the AS-SBAnR functionality for nitrate removal and N_2O emission control. The role of ALLODUST in the treatment system was significant while the contact time was dropped by 12 hrs. The system efficiency was increased by almost 77% and 80% for nitrate removal and N_2O emission respectively, compared to the activated sludge system. The ALLODUST media is a low cost and sustainable approach to remove N from agricultural wastewater. Further studies are recommended to investigate the ability of ALLODUST media to remediate wastewater containing other contaminants such as heavy metals and pharmaceuticals.

Chapter 6

Nitrate and phosphorous removal from waterbodies by floating treatment wetland (FTW) using *Carex virgata*

6.1 Introduction

Eutrophication is a major global threat to the ecological quality of surface waterways and freshwater's ecosystems. Nutrients such as N and P enter surface water bodies due to increasing human activities such as agricultural and dairy farming, often resulting in excessive algae/macrophyte growth, resulting in oxygen loss and aquatic mortality in the water bodies. Moreover, there are also risks to human health from the toxin-excreting blue-green algae. Floating Treatment Wetlands (FTWs), also known as Constructed Floating Wetlands (CFWs) are artificial or vegetated floating islands, in contrast to natural floating wetlands which occur around the world (Van Duzer, 2004). The potential of the CFWs for stormwater management was addressed by Headley and Tanner (2012) and the expression Floating Emergent Macrophyte Wetlands (FTWs) was given. The development of (sub)surface wetlands for the treatment of different forms of wastewater, including urban wastewater, acid mine drainage, industrial wastewater, agriculture and storm water runoff as well as livestock effluent, has become a common method to minimise nutrient loading to surface waters (Keizer-Vlek et al., 2014; Y.-F. Lin et al., 2002; Y. F. Lin et al., 2002). The modest construction costs, relatively low energy usage and maintenance demands, and the wildlife habitat improvement are some of the advantages of the FTWs.

The Floating Treatment Wetlands (FTWs) system is formed by adaptive plants developed on a buoyant infrastructure, which floats on a water body. The upper sections of the plant emerge and mostly stay above the water level, whilst the roots reach down into the water base, forming a substantial root network below water level. Therefore, the plant grows hydroponically and directly consumes nutrients from the surrounding water (Headley & Tanner, 2012; Hubbard, 2010). Creation of an expansive and robust root system is vital for the FTW functionality. The roots act as a natural filter while the physical and bio-chemical removal mechanisms will be activated by the bio-films which are attached to the roots (Dodkins &

Mendzil, 2014; Li & Li, 2009). Floating Treatment Wetlands (FTWs) doesn't impact on any land usage and can be a solution for the water quality management in the areas which are limited by land availability. In the case of a contaminated lake or pond, the FTWs adapt to the water level fluctuations (WLFs) of the water body. It will also have an influence on the aesthetic value of the local environment by providing a desirable habitat for fish, birds, and invertebrates. All these characteristics make it an extremely valuable water and wastewater quality management technique.

Carex virgate is a frost tolerant plant which is used in swamp and wetland restorations, drain margins, seepages and wet pastures. *Carex Virgata* has been used for road run off treatment in New Zealand (Borne et al., 2013; Cao & Zhang, 2014). There are also three floating aquatic plants like water hyacinth (*Eichhornia crassipes*), water lettuce (*Pistia stratiotes*), and duckweed (*Lemna-ceae*) which can reduce nutrient concentrations in wastewater without using any supportive mat infrastructure (Hubbard, 2010). However, these plants are also deemed a threat in temperate waters due to their immense colonisation potential, i.e., the oxygen concentration in water can be significantly decreased by the decomposing plant material and they can kill species present in the water; the dense growth of free floating plants beside the indigenous species can cause blockages in the hydraulic system of the waterways (Keizer-Vlek et al., 2014). The quality of pond water, stormwater, urban lake water, and dairy manure effluent have been improved recently by FTWs (Weragoda et al., 2012). This water treatment method has been used for a wide range of contaminants and there are several researchers which have reported on the efficiency of the nutrient removal by FTWs (De Stefani et al., 2011; Revitt et al., 1997; Vymazal, 2007). The biological and physio-chemical mechanisms play the main role in nutrient removal and the effect of the vegetation on the overall nutrient removal has been reported (Keizer-Vlek et al., 2014) however more research is needed to quantify the effect of different initial nutrient concentrations on the vegetation and the plants ability to uptake the contaminants from the water. Therefore, the main aim of this research is to quantify the nitrate and phosphorous removal in different ranges of initial concentration and the effect of that initial concentration on the vegetation and the removal efficiency. Also the contribution of the plant uptake to overall removal capacity of FTWs is discussed.

6.2 Materials and methods

6.2.1 Experimental design

The experiment was carried out by setting up a batch mesocosm experiment in the Lincoln University glasshouse nursery. The duration of the experiment was 3 months. The mesocosms used consisted of twenty 20 L polyethylene buckets with a surface opening of 0.08 m^2 which were placed in the glasshouse randomly (Figure 1). Four buckets were planted with *Carex virgata* for each range of the nutrient concentration (low-average-high) and four buckets as a control. The water used in the buckets was sampled from the *Ararira (LII)* catchment, Lincoln. After filling the buckets, 2 cm thick Styrofoam was used as the covering mat. Three holes were created in the Styrofoam cover providing the space for the hydroponic pots. A HQD HACH portable probe was used for measuring the pH, Dissolved Oxygen (DO), and Electrical Conductivity (EC) during the experiment. In order to provide the essential trace elements and the minimum amount of the nutrients 0.0125 mL L^{-1} of a trace element fertilizer (Yates "Thrive" Fertilizer Trace Element Liquid – commercially available from Yates ltd; K, Fe, Mn, B, Cu, Zn, and Mo); 4 mg L^{-1} nitrate, and 0.25 mg L^{-1} phosphorous was spiked. The KNO3 and K_2HPO_4 were purchased from Merck.

Figure 6.1 Experiment set-up.

10 mL water samples were collected from each of the buckets. The biofilm attached to the inner surface and bottom of the buckets were brought into suspension by stirring prior to sampling. The water samples and the *Ararira (LII)* river water sample were analysed to measure the nitrate and phosphorous level of each bucket before adjusting the contaminant

concentration. The nutrient concentration was analysed by SMARTCHEM 200 - Murphy-Riley (Murphy & Riley, 1962) method for the PO_4-P and Vanadium (III) reduction (Braman & Hendrix, 1989) method for the concentration. The nitrate and phosphorous removal experiment was conducted in three ranges of contamination. Low-range buckets were set up by adding 10 mg d^{-1} L^{-1} NO_3-N and 0.5 mg d^{-1} L^{-1} PO_4-P. These amounts were 20 mg d^{-1} L^{-1} NO_3-N and 1 mg d^{-1} L^{-1} PO_4-P for average range and 30 mg d^{-1} L^{-1} NO_3-N and 1.5 mg d^{-1} L^{-1} PO_4-P for high-range. The N and P concentration is provided in Table 1 after the first round of the nutrient addition.

Table 6.1 Nutrient concentrations in the bucket after the first addition.

	Nitrate-nitrogen mg L^{-1}	Phosphate mg L^{-1}
Blank	5.69 ± 0.01	0.26 ± 0.02
C.V $_{max}$	31.49 ± 0.01	1.5 ± 0.02
C.V $_{average}$	21.49 ± 0.01	1.0 ± 0.02
C.V $_{min}$	11.49 ± 0.01	0.5 ± 0.02
Ararira (LII)	19.31 ± 0.01	0.03 ± 0.02

The Carex Virgate plants (root-trainer) were supplied by Southernwoods ltd, New Zealand. The pot mix adhering to the roots was washed off thoroughly by RO water and the root was brushed with a soft brush and rinsed with DI water to remove all the small particles captured between the roots. Then, the plants were placed in the plastic hydroponic pots to support the plant's weight during the experiment and to avoid their failure because of any increase in plant weight. Three shoots of each plant were tagged and their length were measured before the experiment. From the supplied batch, ten plants were chosen randomly and prepared to determine the nutrient level of the roots and shoots, roots and shoots length and plant biomass at the start of the experiment. Each bucket was planted with three Carex virgata through the holes in the Styrofoam. Also, the microclimatic condition of the glasshouse location during the experiment is presented in Table 2.

Table 6.2 Weather conditions from Dec 20/2019 to March 20/2020 in Lincoln (Source: wunderground/metservice)

	Max Temp(°C)	Min Temp(°C)	Average Temp(°C)	Total rainfall (mm)	Average Dew point(°C)	Humidity (%)
Month1	31.11	16.67	24.16	3.302	10.88	70.58
Month2	34.44	22.22	28.47	23.114	11.62	71.04
Month3	28.88	15.55	21.80	58.674	9.17	74.66

6.2.2 Water analysis

Water samples were taken weekly to measure the NO_3-N and PO_4-P concentration. Prior to each sampling event, the pH, DO, and EC were measured using the HQD HACH portable probe. The water level in each bucket was monitored during the week and they were refilled by topping up to volume with the *Ararira (LII)* river water when the water volume dropped below the 80%. Water levels dropped due to evaporation and transpiration. Two samples were taken before and after the water top up in order to consider the effect of that in the nutrient removal efficiency. The presence of sufficient nutrient concentration in each bucket was determined by sampling during the week from random buckets selected on a random basis. Thrive Yates, KNO_3, and K_2HPO_4 solutions were used to bring the concentration up to the minimum nutrient level of 4 mg L^{-1} N and 0.25 mg L^{-1} P (Keizer-Vlek et al., 2014). The water level in each bucket was determined on the last day of the experiment and the final nutrient level was measured. Table 3 presents the total nutrient addition to each series of the buckets.

Table 6.3 Overview per treatment of the total amount of NO_3 – N and PO_4-P added to each tank during the experiment.

	Nitrate-nitrogen mg L^{-1}	Phosphate mg L^{-1}
Blank	4.2 ± 0.01	0.25 ± 0.02
C.V $_{max}$	480 ± 0.01	24 ± 0.02
C.V $_{ave}$	320 ± 0.01	16 ± 0.02
C.V $_{min}$	160 ± 0.01	8.0 ± 0.02

6.2.3 Plant analysis

All the plants were removed from the buckets. The remaining water in the buckets was drained through a 200 mesh to separate the algae from the water. Also, the algae attached to each bucket was removed and placed in an aluminium container then air dried for further biomass, N, and P analysis. The roots and shoots were separated and the mass was measured. The total biomass was reported per each bucket. Then they moved to an oven at 70°C for several days until they completely dried. The dried roots and shoots were grounded using a plant grinder and analysed for N and P by Rapid Max N and Varian 5110 ICP-OES respectively. The samples were digested using nitric acid (69%) and 30% hydrogen peroxide and CEM MARS Xpress used as the microwave digester. The average wet and dried weight of the plants before

the experiment were calculated based on the ten randomly selected *Carex virgata* at the start of the experiment. The roots and shoots condition is presented in Figure 2 before harvesting.

6.2.4 Removal Capacity

The removal capacity of the plants was calculated based on the initial N and P concentration in each bucket, the nutrient addition during the experiment, and the final nutrients concentration in each bucket. The working volume of each bucket was considered 18 L and multiplied by the difference of the total N and P added during the experiment, and the initial concentration of N and P in the buckets to calculate the total removal capacity in each contaminant range. The plants contribution to the total removal (nutrient uptake) was calculated. The dry weight at the start and end of the experiment was multiplied by the N and P concentrations present in the plant's tissues. The same process was performed for the algae created in each of the buckets according to the nutrient concentration.

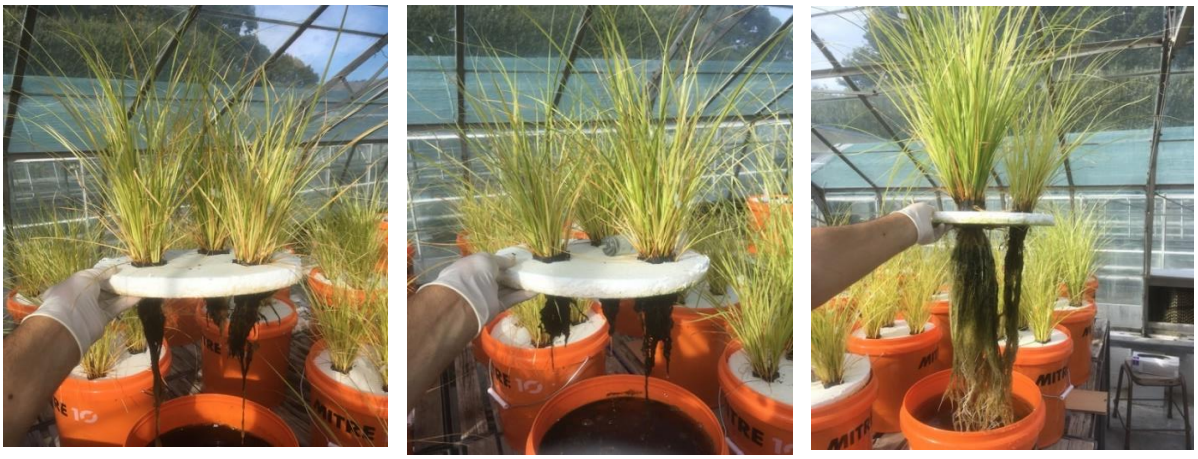

Figure 6.2 The final roots and shoots condition for each range of the nutrient concentration before the harvesting.

6.3 Results and Discussions

6.3.1 Nitrate and phosphorous removal

The total nitrate and phosphorous removal efficiency of each treatment differed during the experimental period (Figure 3). Based on the percentage of the contamination, the removal of both TN and TP was highest in the minimum treatment while this amount was the highest for maximum treatment for mg removal in each m^2 (Figure 3-4). For all the treatments and both the TN and TP removal the difference between the control and removal efficiencies was

not significant. The removal capacity of *Carex virgata* while in contact with the lower range of TN and TP was higher compared to the same condition but with a higher initial concentration. The removal efficiency was highest in the minimum treatment (88 %), followed by the average (67%) and maximum (68%). This amount for the control was below 5% for all the treatments. The TP removal from the wastewater by *Carex virgata* was 99.75%, 99.06%, and 93.88% for the minimum, average, and maximum treatments respectively while the highest decrease TP concentration in the control samples belonged to average treatment with 7.75%.

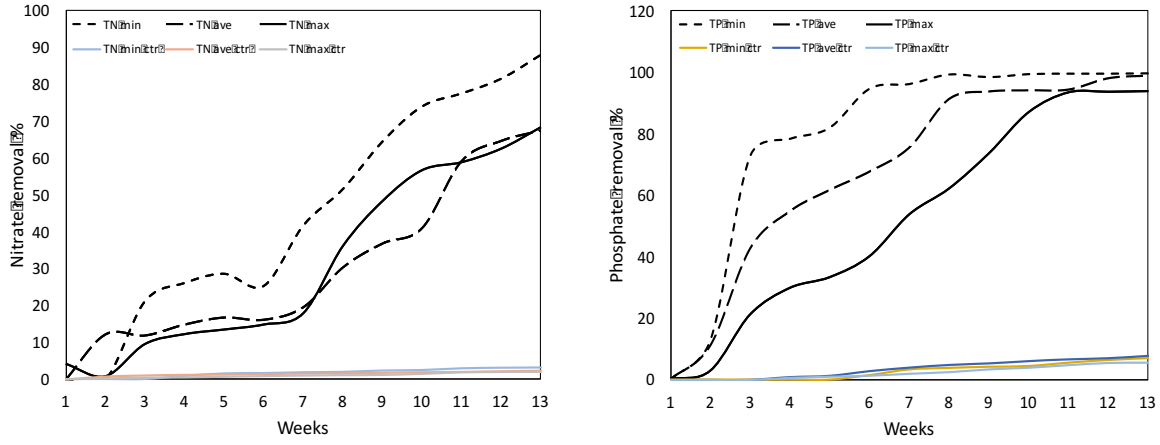

Figure 6.3 Removal of nitrate and phosphate (%) from the mesocosms during the experiment.

The percentage of TN removal by *Carex virgata* was significantly higher than in the control treatments for all the contamination ranges. Although, the TP removal efficiency of the *Carex virgata* in the minimum treatment was significantly higher during the first weeks but maximum treatment reached the level of the minimum treatment at the end. However, according to the initial concentration for each of the treatments and the total percentage of the removal at the end of the experiment the removal efficiency of the maximum treatment is significantly higher than the minimum and average in each m^2 of the contaminated water (Figure 4).

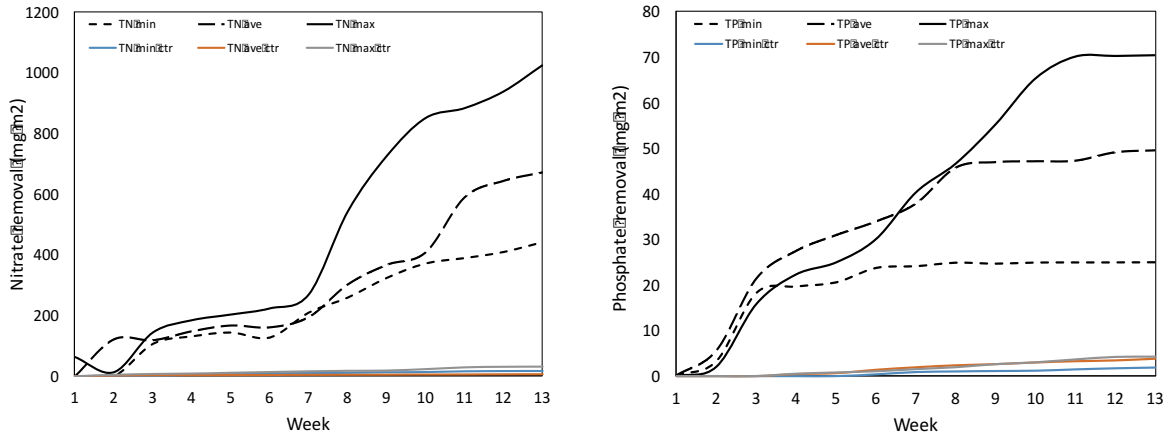

Figure 6.4 Removal of nitrate and phosphate (mg m^{-2}) from the mesocosms during the experiment.

The highest total removal of the nutrients from the buckets planted with Carex virgata was 228 mg N $m^{-2}d^{-1}$ and 15.60 mg P $m^{-2}d^{-1}$ during the time of the experiment (90 days) and belonged to the maximum treatment. However, the maximum treatment couldn't remove high percentage of the available nutrient but because of having access to a higher nutrient level in the water, could reach higher total removal. So, it was considered as the highest removal efficiency of the FTW system planted with Carex virgata. The removal efficiency for the FTW's planted with Carex virgata were very high in this study (68% to 88% for the nitrate and 94% to 99% for the phosphate) in comparison with the results mentioned by Winston et al. (2013). As the authors mentioned, reducing TN (36% and 59%), TP (36% and 57%), was the highest removal rate of the FTW planted with Carex stricta in a field scale. However, comparing these two research projects is very difficult because there are various environmental factors which can affect the removal efficiency of the system such as loading rate and the study scale. In the study conducted by Keizer-Vlek et al. (2014), the removal efficiency for the FTWs planted by *Typha* reported high rates with 57% removal of TN but the point is that the absolute nutrient removal was low due to a low nutrient load. In this study, we designed three different nutrient concentration ranges by adding different concentrations of the nitrate and phosphate to the buckets during the experiment time and maintained at approximately 4 mg N L^{-1} and 0.25 mg P L^{-1} same as the amount which the control buckets received. The efficiency of the system was described based on the removal rate in milligram per day as suggested by Headley and Tanner (2012). According to the different variables which affect the removal efficiency directly in the FTWs studies, it's hard and challenging to compare the effectiveness of the different studies. This is due to the different experiment designs and

set up: like batch or continuous to nutrient loading, control situation, reaction time, soil presence on the mat, age of the plants and roots and shoots length at the start of the experiment. These are all different factors with fundamental effects on the final result and system efficiency.

6.3.2 Physiochemical properties

Based on the DO concentration presented in Figure 5 the condition for all the buckets remained aerobic during the experiment. Because we were not using soil media in this study, we didn't expect dissolved organic matter leaching to the wastewater, which normally contributes to biochemical oxygen demand and as a result, a decrease in DO over time. One of the main factors which contributed to DO decrease was additional respiration by heterotrophic bacteria within the biofilm attached to the roots. High concentrations of dissolved oxygen during the first weeks of the experiment was because of the high nutrient load and resulted in minimal algae biomass growth. The buckets were not supplied with oxygen to maintain a dissolved oxygen concentration. The DO concentration decreased by more nutrient uptake by plants over the time. The DO reduction over the time of the experiment was because the plants are able to leak oxygen through their roots. The total oxygen released by the roots were more than outweighed by the oxygen demand imparted by the respiration of heterotrophic bacteria within the root associated biofilms.

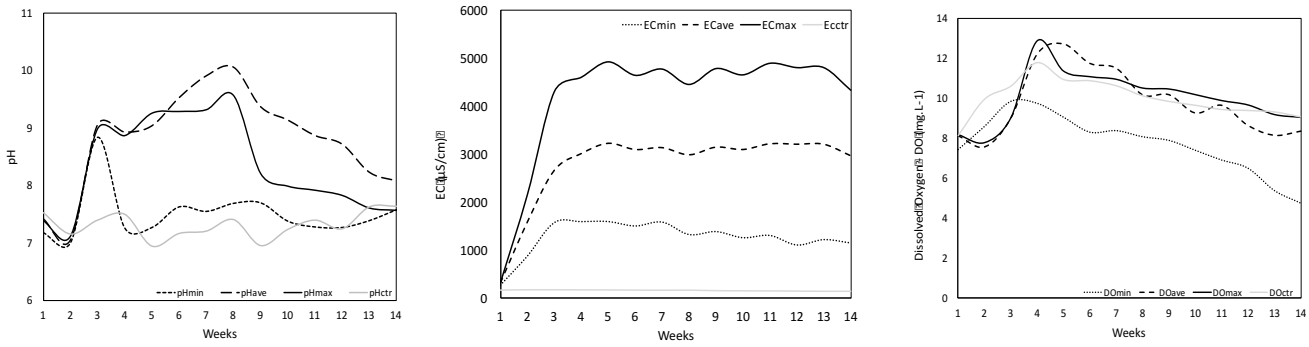

Figure 6.5 Dissolved oxygen (DO), electrical conductivity (EC), and pH values of different treatments during the experiment.

High concentration of the ions leads to an increase in the electrical conductivity of the water. The electrical current is transported by the ions in solution, the conductivity increases as the concentration of ions increases. As expected, the high initial nutrient concentration caused

high EC value in the wastewater. As can be seen from Figure 5, the EC value increased dramatically during the first three weeks due to adding nutrients to the water and then reached to a steady trend after being stable and plants started to uptake the nutrients from the wastewater. This is parallel with the nutrient removal results in Figure 3, where the plants uptake started to be more than the nutrient load in the water. As can be seen from Figure 5, the maximum treatment is in the higher level of the EC while the minimum treatment started to tend to a lower level after week 7.

All the treatment had higher pH during the experiment than the control. The low pH in the treatments could be attributed to the release of root exudates that may include organic acids, phenolic compounds and sugars from the rhizosphere (Blossfeld et al., 2011).

6.3.3 Plant growth and uptake

The biomass of the plants increased during the experiment and the nutrient uptake. This amount was almost tripled for the minimum treatment and the increase in the biomass was the result of an increase in the plant's shoots rather than the roots for all the treatments. The absolute increase in the biomass for the average and the maximum treatments was low compared to the minimum treatment. At the start of the experiment, average *Carex virgata* biomass was 19.61 g and the root biomass was higher than the shoot with the ratio of root:shoot = 1.45. After the experiment and harvesting the plants, the shoot biomass was higher than the root for all the treatments with the highest amount of shoot:root = 3.92 for the minimum treatment.

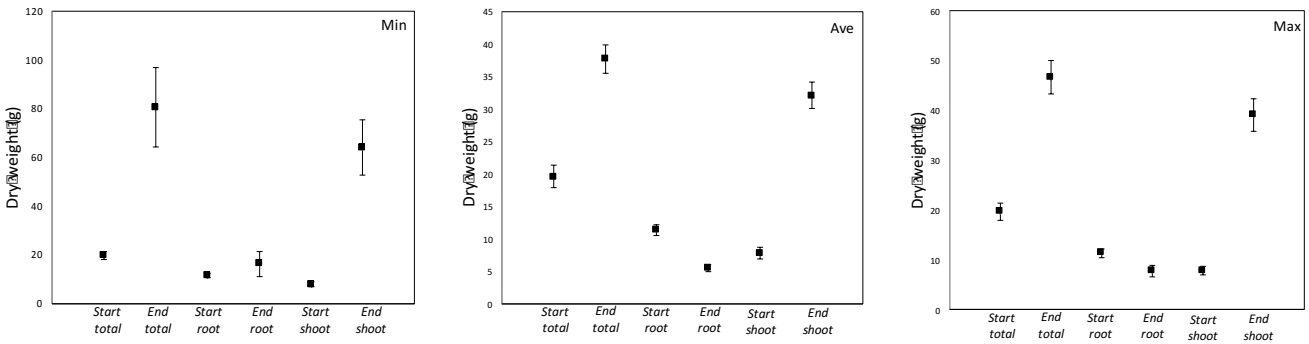

Figure 6.6 Dry weight of Carex virgata in the mesocosms at the start and end of the experiment for different treatments.

At the start of the experiment the average tissue concentration of TN was higher in roots than in the shoots (Figure 7). Also, the TP concentration was slightly more in the roots compare to the shoots for all the treatments. At the end of the experiment, the average tissue concentration of TN and TP increased in the roots for the minimum treatment than the shoots and the differences between average root and shoot tissue concentration of TN was the highest. This trend was the same by increasing the concentration of the nitrate in the wastewater but the differences between average root and shoot tissue concentration of TN and TP became smaller. This is because of the higher average root tissue concentration at the end of the experiment for the minimum treatment. The most remarkable result was that the minimum treatment experienced higher increase in the biomass and weight and also the root, shoot, and average tissue concentration of TN amongst all the treatment while the other treatments had higher nutrient concentration available in the wastewater to uptake. This trend was higher in TP by increasing the phosphorous concentration in the buckets.

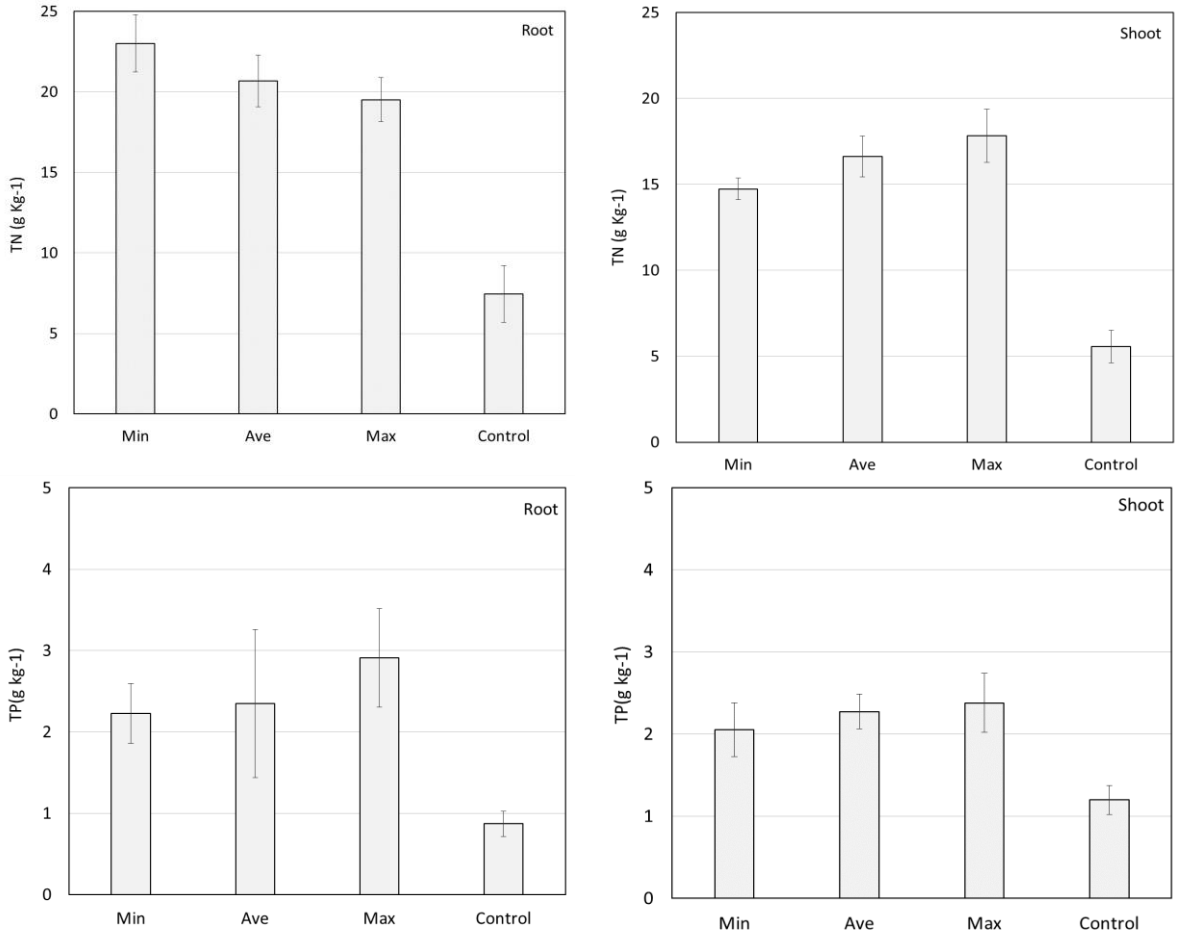

Figure 6.7 Average plant tissue concentrations of TN and TP in shoots and roots.

Average TN and TP plant uptake by Carex virgata was significantly different between different treatments. The plant participation in the nitrate and phosphate removal from the wastewater belonged to the minimum treatment where the plants faced to a lower initial and final nutrient concentration. The Carex virgata nitrate uptake was 58.8% higher than the average and 46.7% than the maximum treatments. This amount was 60.8% higher than the average treatment and 34.9% higher than the maximum treatment for the phosphate. This result was expected according to the changes in the shoot and root mass during and at the end of the experiment (Figure 8). Average TN and TP plant uptake in the minimum treatment was three times higher for shoots than roots, despite lower tissue concentrations in shoots. So, in determining the total plant nutrient uptake; the biomass increase was more important than plant tissue concentrations (Keizer-Vlek et al., 2014).

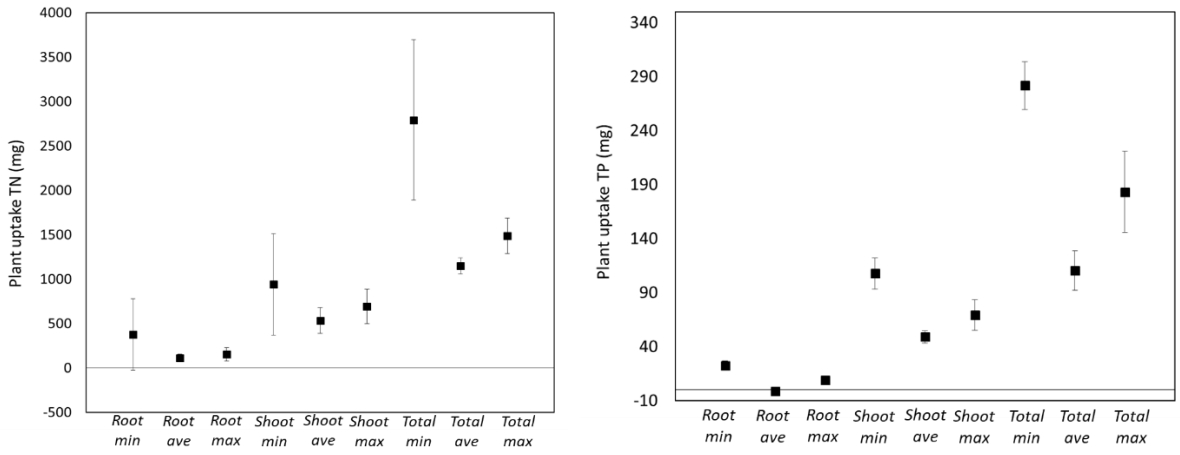

Figure 6.8 Estimated amount of TN and TP assimilated in shoots and roots tissues of Carex virgata during the experiment.

In the minimum treatment of the *Carex virgata*, plant uptake on average accounted for 87% TN and 81% TP of the total TN and TP removal during the experiment (Figure 8). It's important to be notified that the standard deviation (SD) for the minimum treatment was very high in TN. The plant uptake contribution in TN decreased to the 82% and 83.5% for the average and the maximum treatments respectively. Also, the plant uptake contribution in TP dropped to 63.5% for average and 74.2% for maximum treatments. The differences between the shoot and root's biomass was increased for the average and maximum treatments and also the difference in the contribution in nutrient uptake between the shoots and roots from the

wastewater was highest for the maximum treatment in TN and for the minimum treatment in TP.

Figure 6.9 Shoots and roots condition of different treatments after harvesting.

Carex virgata showed significant results in removing nitrate and phosphate from wastewater in different nutrient loading during the experiment time. The high removal rate of TN and TP from the wastewater was the result of relatively high increase in the *Carex virgata* biomass in all the treatments. The average shoot length of the *Carex virgata* in the minimum treatment, after harvesting was 41 ± 4 cm and increased by almost two times while this amount for the average and the maximum treatments was 32.5 ± 5 and 32.0 ± 3 for the average and maximum treatments respectively. The plant P uptake in this study was significantly more than the previous studies (Spangler et al., 2019; Tanner & Headley, 2011) which could be attributed to the nutrient load during the experiment. For the minimum treatment the N removal was 28 times and P removal was 14 times higher than the control which these numbers were (30 and 13 times) and (35 and 14 times) higher for the N and P removal of average and maximum treatments compared to the control respectively. On average, 87% of the nitrate and 81% of the phosphate removal belonged to the plant uptake in the tissues. Based on the results in this study we can say that FTWs planted with *Carex virgata* and receiving the nutrient load in the range of the minimum treatment is an effective method to remove nitrate and phosphate from the contaminated water bodies and wastewater. The other plants were used in the FTW system by other researchers and had different results in N and P removal. The *Cyperus papyrus* was known as the main factor for N and P removal, contributed by 69.5% to TN and 88.8% to TP removal in a FTW system (Kyambadde et al., 2004). On the other hand, for the species

Miscanthidium violaceum plant contribution in nutrient removal was only 15.8% of TN and 30.7% of TP. According to Borne (2014), the plant uptake did not contribute significantly to the overall TP removal from a contaminated pond.

The results presented in this study indicate that *Carex virgata* contributed in the TN and TP removal significantly from wastewater. The N and P uptake of different plant species reported by Tanner and Headley (2011) in mg (N,P) m^2 d^{-1}. The TP uptake rate of 15.60 mg P $m^{-2}d^{-1}$ is much higher than the *Iris* of 5.57 mg P $m^{-2}d^{-1}$ and *Juncus edgariae* of 5.2 mg P $m^{-2}d^{-1}$(Tanner & Headley, 2011). However, a higher uptake rates reported for *Cyperus ustulatus* of 8.50 mg P $m^{-2}d^{-1}$. The P uptake capacity of a FTW planted with *J. effusus* reported 1.69 g P m^{-2} (White & Cousins, 2013) but the experiment lasted for 5 months instead of 90 days. Because of low bioavailable N and P in the water, a number of researches reported very low P uptake by plants (C.-Y. Wang et al., 2015). The TN uptake rate *of Carex virgata* (20.5 g N m^{-2}) was comparable to the uptake rate for Iris (18.6 g N m^{-2}) (Keizer-Vlek et al., 2014), *Canna flaccida* (16.8 g N m^{-2}), and for *J. effusus* (28.5 g N m^{-2}) reported by (White & Cousins, 2013).

6.3.4 Algae analysis

The floating algae tissue concentration of TN and TP increased from minimum to maximum treatments and the average TN uptake did not differ significantly between the treatments (Figure 10). But this amount was increased significantly for the TP by increasing the phosphorous concentration in the wastewater. The nutrient uptake by algae in the control treatment was very low because the control treatment received the optimum nutrient concentration during the experiment and was uptake was mostly by the plant.

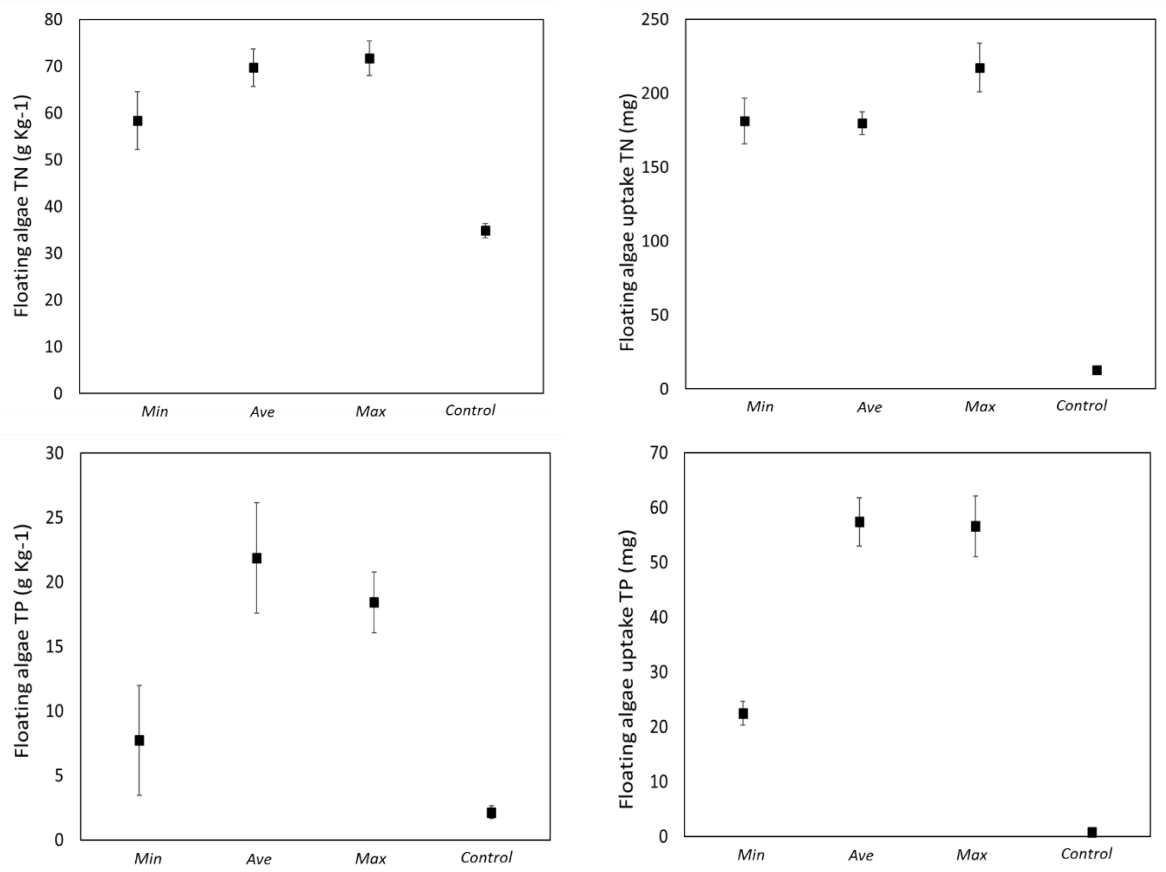

Figure 6.10 Total amount of TN and TP assimilate in floating algae tissue per treatment

6.4 Other N and P removal mechanisms and factors

The plant uptake was a part of the total removal as described before. The 87% of nitrate uptake and 82% of the phosphate was the highest plant nutrient uptake from the minimum treatment. The other factor that should be considered is the algae nutrient uptake and its participation in the total removal. But, this amount was only 5% and less than the TN and TP removal in the system. So, a big portion of the total removal remain unexplained. The mechanisms which could be considered are plant-mediated processes and biofilm (Stewart et al., 2008). Also, under controlled aeration and organic carbon addition to the system, floating mat matrixes can contribute to the total nutrient removal by microbially mediated nutrient removal such as nitrification, denitrification and P adsorption (Keizer-Vlek et al., 2014; Stewart et al., 2008). However, the TN and TP removal from the controlled buckets which covered by Styrofoam was very low in this study and it could be concluded that the biofilm present in the buckets didn’t have an effective participation in the total removal in the planted buckets. The

similar result was concluded by Tanner and Headley (2011) and Keizer-Vlek et al. (2014) which suggest that the floating mat does not have direct and significant effect on the total nutrient removal in a FTW system. The sorption and sedimentation processes can be considered as potential processes by enhancing the nutrient removal in a planted FTW system. These processes are affected by bioactive compounds release by roots and changes in the physico-chemical conditions(Tanner & Headley, 2011). In this study, as the sediment that settled to the bottom of the buckets was suspended before each sampling, the phosphorous removal couldn't follow this explanation. The decrease in the dissolved oxygen level during that time might be an effective factor in N removal. Dissolved oxygen concentration was measured continuously during the time of experiment for different treatments and reported in Figure 5. The control buckets had always been in a saturated condition but the DO of the other treatments started to decrease after week 4. The water in the minimum treatment was close to the hypoxia condition according to the reduced dissolved oxygen. The aerobic decomposition of the organic matter and respiration of plant biofilm was suggested as the main reason of the reduce DO concentration beneath FTWs (Keizer-Vlek et al., 2014; Tanner & Headley, 2011; White & Cousins, 2013), with a high amount of nitrate entering the FTW system and low level of DO result in loss of nitrogen because of denitrification(White & Cousins, 2013).

6.5 Conclusions

The results from this chapter shows that the FTW treatment system using *Carex virgata* can be applied in a contaminated pond by using a wide range of nutrient load and preventing the growth of the excessive algae in surface of the water. The overall nutrient uptake of the FTW treatment system planted with *Carex virgata* was 228 mg N m^{-2} d^{-1} and 15.60 mg P m^{-2} d^{-1} from the water during the experiment. These value were dramatically higher than the nutrient removal in the control buckets, i.e, 35 times higher for TN removal and 16 times higher for TP removal. The role of the plant uptake in the FTW treatment system was the major factor in uptake of nitrate and phosphate from wastewater. i.e, 87% of TN and 82% of TP removal resulted from plant uptake. According to the nutrient removal results, the FTW treatment system can handle a wide range of the nutrient load entering the pond daily but high concentration of the nitrate and phosphate accumulated in the system can lead to an anaerobic condition and result in the dead roots. So, harvesting the plant material should be a correct FTW system practice.

Chapter 7

General discussion and conclusion

7.1 General overview

Nitrate and phosphate have been known as the most important anionic contaminants present in waterways and agricultural related industries which cause serious environmental and health problems.

This PhD thesis evaluated a sustainable and near market water processing design for adsorbing the high concentration of phosphate and reducing the high concentration of nitrate from a contaminated treatment pond:

- Developing a novel media from natural sources and bio wastes with high phosphate adsorption capacity by providing desirable adsorption active sites for phosphorous adsorption and high surface area and pores volume/size for microbial biofilm growth to reducing the nitrate. The wastewater process was designed based on a fluidised bioreactor.

- Designing a bioreactor which can provide both aerobic and anaerobic conditions. This reactor was designed in order to provide stirring without using any agitator; aerating and oxidizing when it's required; and degassing when an anaerobic condition is needed.

- Designing a floating treatment wetland (FTW) by using a native plant to remove the remaining nutrients which are present in the effluent. The effect of different nutrient loadings on plant uptake and biomass was monitored.

A series of physiochemical experiments on the developed media and water/air quality analysis in conjunction with engineering designs evaluated the potential for these proposed process design to reduce N and P concentration from highly contaminated wastewater containing a maximum 120 mg L^{-1} nitrate-nitrogen and 300 mg L^{-1} phosphate.

7.2 Summary of results and conclusions

7.2.1 Chapter 3: Powdered ALLODUST/ALLOCHAR augmented single batch aerobic reactor (SiBAR) for high concentration phosphorous removal

Chapter 3 examined the phosphorous removal capacity of two novel developed media ALLODUST/ALLOCHAR in a fluidized aerobic batch reactor. This chapter also determined the effect of different operational details and variables on the designed process performance by conducting a series of water and solid quality analysis. It was hypothesised that a specific dosage of ALLODUST or ALLOCHAR would remove a high concentration of phosphorous from wastewater by an adsorption mechanism in a short contact time. The overarching aim of my research is to develop a low-cost and sustainable adsorbent media material which can adsorb a high concentration of phosphorus at the lowest contact time and minimal energy consumption.

P undergoes several geo-chemical processes in soil such as solubilization, complexation, adsorption, and precipitation that determine its mobility and fate. These chemical processes are a complex function of several soil properties including: Al and Fe oxide form and content; the amount and form of silicate clays; and $CaCO_3$ content. The reaction of P and soil minerals was considered as the basis of the main adsorption mechanism for ALLODUST and ALLOCHAR .

The phosphorus removal efficiency of ALLODUST augmented SiBAR was higher than ALLOCHAR at the same dosage. Utilising wastewater containing higher than permissible discharge limits of P also allowed us to investigate the morphology and microstructural changes along with the adsorption capacity of the media when it's mixed with a very high P concentration. The P removal rate of 99.86% when the P concentration was up to 50 mg L^{-1} in 30 minutes by $ALLODUST_{2.50}$ and 85.13% for P concentration up to 300 mg L^{-1} P by H-$ALLODUST_{5.82}$ in 450 minutes demonstrated the high capacity of the ALLODUST to remove P from agriculturally sourced wastewater, under optimum operating conditions.

As it was explained before, while the EBPR process is one of the most popular phosphorous removal methods, it is facing a number of challenges. The changes in influent concentration, VFAs/TP ratio, and pH can make significant changes in the removal efficiency of the EBPR process. So, adsorption is a prefereable method for P removal from wastewater and waterways.

One of the most popular and trending medias used to adsorp phosphorous from aqueous solutions is Phoslock®. It has been reported that even in the ratio of 220:1 Phoslock® : P, Phoslock® can't control the SRP concentration higher than 0.047 mg P L^{-1}. After investigating Phoslock® performance in different lakes at different pH values a minimum of 200:1 adsorbent dosage was suggested, since 100:1 was insufficient for even concentrations below 0.001 mg P L^{-1}. Moreover, pH dependency of the Phoslock® is reversible. In comparison, ALLODUST (by removing up to 300 mg L^{-1} and over a wide range of pH) showed an efficient performance in adsorbing phosphate from wastewaters and waterways. The 3 g L^{-1} adsorbent dosage and several cycle workability was the other factor which signifies this process as resource-efficient and therefore sustainable.

As it can be seen from the adsorption results, varying the pH of the sawdust (as the biowaste used in the ALLODUST development process) can have an effect on the resultant ALLODUST pH, surface and structure characteristics, and lignin/cellulose/hemicellulose content. The pH of ALLODUST can also have an effect at the end of the process on the adsorption efficiency of the system under different initial P concentrations. Moreover, sawdust affects the COD concentration in the effluent in a similar way as the microorganisms and aquatic plants (reported in Chapter 6). The COD monitoring was one of the main factors in this process in which results showed that the acidic treatment and protonation of the sawdust surface could be employed as a method to control the COD concentration of the effluent.

The SiBAR was the other positive aspect of this research in regards to phosphate adsorption. The design of the reactor was significant to ensure the success of the process. The CBA method was used to remove the mechanical agitator from the system and to provide aeration and stirring for the system at a same time.This resulted in an ability to shift from a higr aeration rate, more turbulance to a lower aeration rate lower turbulance in the water, when required. So the reaction tank and aeration tank processes were all provided by SiBAR-CBA. Also, by purging nitrogen gas to the reactors and applying degasification process the headspace air was recycleable by the air pumps in order to providing anoxic conditions in the reactors, when required. The contact time of minimum 30 min and maximum 450 min showed that P removal by ALLODUST in a fluidized bed reactor (SiBAR) is a fast process even at very high P concentrations. Also the aeration rate of maximum 7.5 L min^{-1} was another positive point of this method; which demonstrates that the method does not need a high aeration rate for

optimum functionality. The morphology study of the ALLODUST before and after reaction with different concentration of P showed that how the soil and biowaste structure changed during the adsorption process while the EDS result of the same surface demonstrated the presence of P on the flocculated surfaces and filled pores.

7.2.2 Chapter 4: Optimizing the phosphorous adsorption/desorption capacity of ALLODUST

Chapter 3 showed that ALLODUST has a higher P adsorption efficiency compared to ALLOCHAR. Different factors played a role in the P adsorption capacity of the developed media. In order to optimize the process, a series of experiments were conducted in Chapter 4. The evaluation of the ALLODUST as a long term filteration system was evaluated by monitoring its function during several adsorption/desorption cycles.

The point of zero charge was determined for ALLODUST to optimize the pH of the system. The optimized pH of the solution in the presence of high concentration of phosphate as an anion without any chemical treatment was 7.8 which is below the pH_{zpc}.

Dissolved oxygen (DO) concentration is a vital factor in minimizing sludge biomass growth. The DO concentration for all the reactors was kept above 3 mg L^{-1} and DO concentration increased by releasing more phosphate in the wastewater. It was also demonstrated that a high pH and alkaline condition results in a substantial reduction of the clay's adsorption potential against phosphate ions. According to the pH_{zpc} value, the ALLODUST surface is positively charged at pH less than 7.40 which favours phosphate ion adsorption. It also needs to be considered that after increasing phosphate adsorption on the ALLODUST surface, the pH of the solution is predicted to rise due to the contribution of phosphate negative charges. As expected, a high initial phosphate concentration caused a correspondingly high EC value in the water; the EC value was not time dependent because the most of the ions were adsorbed during the first 30 minutes.

In order to describe the equilibrium between adsorbate and adsorbent system the Langmuir and Freundlich isotherms were analysed. The Langmuir isotherm model was better than the Freundlich model at describing the phosphate adsorption on ALLODUST and regression analysis of the data for different initial concentrations fitted well with the Langmuir adsorption isotherm. The BET experiment was conducted to monitor the surface area and pore size

development in ALLODUST. The pore volumes and sizes were increased by 66% and 69.5% respectively. The acidic treatment of the sawdust as previously expected contributes to creating an active surface and also pore development and was demonstrated to be one of the major factors in moderating the surface area and pore size development of ALLODUST compare to the Horotiu soil. The major oxides, trace elements and multi elements of ALLODUST presented in this chapter can support the P adsorption mechanism which is described in Chapter 3.

In conclusion, these results prove the high adsorption capacity of the ALLODUST in a fixed mode (the legacy phosphate release could be expected in the lowest amount) when it's been used as a filter for drainage pipes, fluidized media for the reactors, or floating media on phosphate contaminated water bodies.

7.2.3 Chapter 5: ALLODUST augmented activated sludge single batch anaerobic reactor (AS-SBAnR) for high concentration nitrate removal

The effectiveness of a novel biological denitrification using ALLODUST was evaluated in this chapter and the results compared to the conventional activated sludge process. The newly developed media (ALLODUST), was evaluated for enhanced NO_3^--N removal from agricultural wastewater for a range of initial N concentration. It was hypothesised that ALLODUST contributed to the microbial biofilm growth and enhanced the denitrification rate of the system. Also, reducing the N_2O emission from the system during denitrification under anaerobic condition was the other objective of the experiments presented in this chapter. From the results of these experiments, it was apparent that the application of ALLODUST is effective in increasing the nitrate removal rate during a biological nutrient removal process (BNR) and also it can help the system to enhance the N_2O emission control. Low ALLODUST dosage (5.95 g L^{-1}) removed 87% of the NO^-_3-N from the wastewater within 12 h. Further exploration revealed that the same amountof the media was optimal for decreasing N_2O emissions from the anaerobically activated sludge reactor by 80%. Compared to the other N removal technologies and methods such as sulphur-based autrotrophic denitrification process (biological), nano zero-valent iron oxide (adsorption), and hydrogenotrophic process, ALLODUST augmented activated sludge had notable advantages. Although N concentrations removed by this process was notable, its important to note that the sulphur-based autrotrophic denitrification produces 7.54 mg sulphate per one mg of nitrate removal and

acid, while thiosulphate generated 35% more sulphate in the system which affect the treated water quality and another process should be considered to remove the side effects of this method. In contrast, the ALLODUST augmented activated sludge process is a reliable and "green" technology according to the ALLODUST components. The only waste that can be considered for this process is the sludge which can be returned to the system as a returned activated sludge.

NZVI is one of the most popular adsorbents to remove nitrate. The major disadvantages of using NZVI include a narrow working pH, low reactivity due to its intrinsic passive layer, a reactivity loss with time due to the precipitation of metal hydroxides and metal carbonates, and low selectivity under anoxic conditions. On the other hand, the ALLODUST augmented activated sludge process showed a wide range of working pH, long term operation by keeping the same removal efficiency due to the development of the bacterial biofilm on the ALLODUST surfaces and in the pores after each cycle, and high operational efficiency in the anoxic condition. Employing a hydrogenotrophic approach is the most sustainable and efficient nitrate removal method, but it still has limitations in the target concentrations, pH, and energy cost.

New cell biomass, and hydroxyl ions were present in the system as the main NO^{-}_{3}-N reduction mediated by ALLODUST. This cycle triggered an increase in pH which was not considered a critical issue. The other effective factor in removing nitrate from wastewater was the adsorption mechanism. The increased number of positive charges, through electrostatic attraction, adsorbed more negatively charged NO^{-}_{3}-N anions. The acid treatment protonation was a convenient and proven technique for eliminating NO^{-}_{3}-N from wastewater as well as efficient in removing other contamination products from wastewater.

During the denitrification process, it's expected that nitrous oxide consumption occurs in conjunction with nitrous oxide production. The very low N_2O concentration that was observed in the reactors containing ALLODUST might be the result of N_2O diffusion back into the aqueous phase from the headspace, during the denitrification process. So, it will be available to the bacterial communities on the media's surface for the reduction to N_2 by denitrifiers. The high specific surfacearea, pore sizes and the porous structure of the media could enhance the N_2O emission control. The N_2O analysis during the developed process through a comprehensive study can be a key topic for future research.

7.2.4 Chapter 6: Nitrate and phosphorous removal from waterbodies by floating treatment wetland (FTW) using *Carex virgata*

In this chapter, the nutrient removal efficiency of a FTW was evaluated. The results from this chapter shows that the FTW treatment system using *Carex virata* can be applied in a contaminated treatment pond or water body, and can treat a wide range of nutrient load (both N and P) and also prevent the growth of excessive algae on the water. The optimum nutrient uptake of the FTW treatment system planted with *Carex virgata* was 228 mg N m^{-2} d^{-1} and 15.60 mg P m^{-2} d^{-1} from the water in maximum nutrient load during the experiment. These values were notably higher than the nutrient removal in the control buckets, i.e, 35 times higher for TN removal and 16 times higher for TP removal. The role of plant uptake in the FTW treatment system was the major component in uptake of nitrate and phosphate from wastewater. i.e, 87% of TN and 82% of TP removal resulted due to plant uptake. According to the nutrient removal results, the FTW treatment system can handle a wide range of the nutrient load entering a water body or pond daily. However, a high concentration of nitrate and phosphate accumulating in the system can lead to anaerobic conditions and result in dead roots. So, it is recommended that harvesting of the plants should be a recommended FTW system practice, to maintain the efficiency of the FTW system. The harvested plants and the ALLODUST can be used as a soil conditioner to improve water holding capacity, a source of nutrients and can also enhance the soil structure. The harvested plant will be effectively an organic N and P fertilizer.

The biomass of the plants increased during the experiment and increased with nutrient uptake. The increase in the biomass was the result of an increase in the plant's shoots rather than the roots for all the treatments. The algae nutrient uptake and participation in the total N and P removal was less than 5% and negligible. Plant-mediated processes and biofilms are considered as the mechanism to remove the TN and TP difference between the total amount and plant uptake capacity. Also, under controlled aeration and organic carbon addition to the system, floating mat matrixes can contribute to the total nutrient removal by microbially-mediated nutrient removal such as nitrification, denitrification and P adsorption. But in our study we showed that the floating mat and biofilm present in the buckets didn't have an effective participation in the total nutrient removal in the planted buckets. The sorption and sedimentation processes can be considered as potential processes by enhancing the nutrient removal in a planted FTW system. These processes are affected by bioactive compounds

released by roots and changes in the physiochemical conditions. In this study, as the sediment that settled to the bottom of the buckets, suspended before each sampling, the phosphorous removal couldn't follow this explanation.

7.3 General Conclusions

In this research, a novel media from natural resources was developed and its efficiency in P adsorption and N reduction was evaluated in a series of four experiments ranging from laboratory simulations to mesocosm experiments.

All the physiochemical experiments along with morphological study tracked the quality of the developed media according to the target contaminants. The desirable physical structure was to develop a media with a high SSA, pore volume, pore sizes, and adsorption sites and also adjusting chemical conditions for optimum functionality to achieve the research objectives.

The ALLODUST augmented SiBAR showed a significant P adsorption capacity which was 76% - 100% in the P concentration range of 1-300 mg L^{-1}. The adsorption process happened in a short contact time (30 – 450 min), at a low-medium aeration rate (1.5 – 7.5 L min^{-1}), and a low adsorbent dosage (3 g L^{-1}) with a high buffering capacity under different adsorption cycles. In order to evaluate ALLODUST in its capacity to be used as filter media, the desorption capacity of the ALLODUST was also examined (Chapter 4). The high capacity of the ALLODUST in not releasing the adsorbed phosphate is another positive point of this treatment system. While phosphate recovery is an important target in many current research projects, the target of this particular methodology was to investigate the use of a low cost adsorbent for a high period of time in a removal system for freshwater bodies rather than focusing on contaminant release due to changes in environmental conditions. After 6 cycles of the adsorption/desorption, ALLODUST released only 16% of the adsorbed phosphate and maintained a high adsorption capacity with 85% of the first cycle in the highest concentration. Recently, many studies have been done to investigate new processes for higher P removal efficiency from wastewater. For example, the removal efficiency of P in two studies have shown to have been increased significantly. But the point to consider is that the limited initial concentration and acidic environment have made the use of them limited (Chapter 2) (Haghseresht et al., 2009; Yang et al., 2020).

From the preliminary results of experiments in Chapter 5, it was apparent that the application of ALLODUST just by itself in removing (reducing) the nitrate is not as effective as the application of the same media in adsorbing the phosphate. So, ALLODUST augmented AS-SBAnR was used to remove the N from wastewater at high concentrations. ALLODUST can increase the N removal efficiency of the conventional activated sludge system by 77% and also reduce the N_2O emission from the system by 80%. This process occurred using twice the amount of the ALLODUST that was needed for the P adsorption, which was 5.95 g L^{-1}.

The focus of the research in this thesis was to reduce the nutrient level to be in a safe zone for use in land application, irrigation and plant uptake. Three different contamination loads of N and P were applied to a series of the hydroponics in a mesocosm experiment and the results showed that the effluent quality in a low-range contamination zone (chapter 6) is the optimum range to use if the effluent flows to surface waterways directly. However, the FTW system can handle a wide range of the nutrient load entering a controlled water body or treatment pond on a daily basis.

7.4 Recommendations for future research

The key recommendations for future research and study are:

1. Synthesize a pure nano allophanic clay in order to increase the SSA and adsorption sites by adjusting positive charge on the surface. A series of physiochemical experiments will be needed to evaluate the quality of synthesize and also the nano material formation.

2. Use the ALLODUST and ALLOCHAR as an adsorbent in a fluidized reactor and choose different heavy metals at different concentrations in order to determine the efficiency of the treatment system to extract heavy metals.

3. Determine different concentration of trace elements and add it as a variable to the existing set up, bioreactor, and nutrient (N and P) concentration. The target of this study will be to evaluate the selectivity of ALLODUST between different heavy metals, P, and N in different conditions and variables. Also, explore the effect of the heavy metals on the denitrification rate of the system and the N reduction capacity of the ALLODUST/ALLOCHAR augmented activated sludge.

4. Use the ALLODUST/ALLOCHAR in a column study to evaluate the removal capacity of the filtering media while subjected to different concentration, flow rate, etc.

5. Set up a simulation study of the treatment system using engineering software such as Ansys Fluent, to model and simulate a three phase bioreactor and optimising the operational detail.

Appendix A

The upscale (commercialized) design of the treatment system

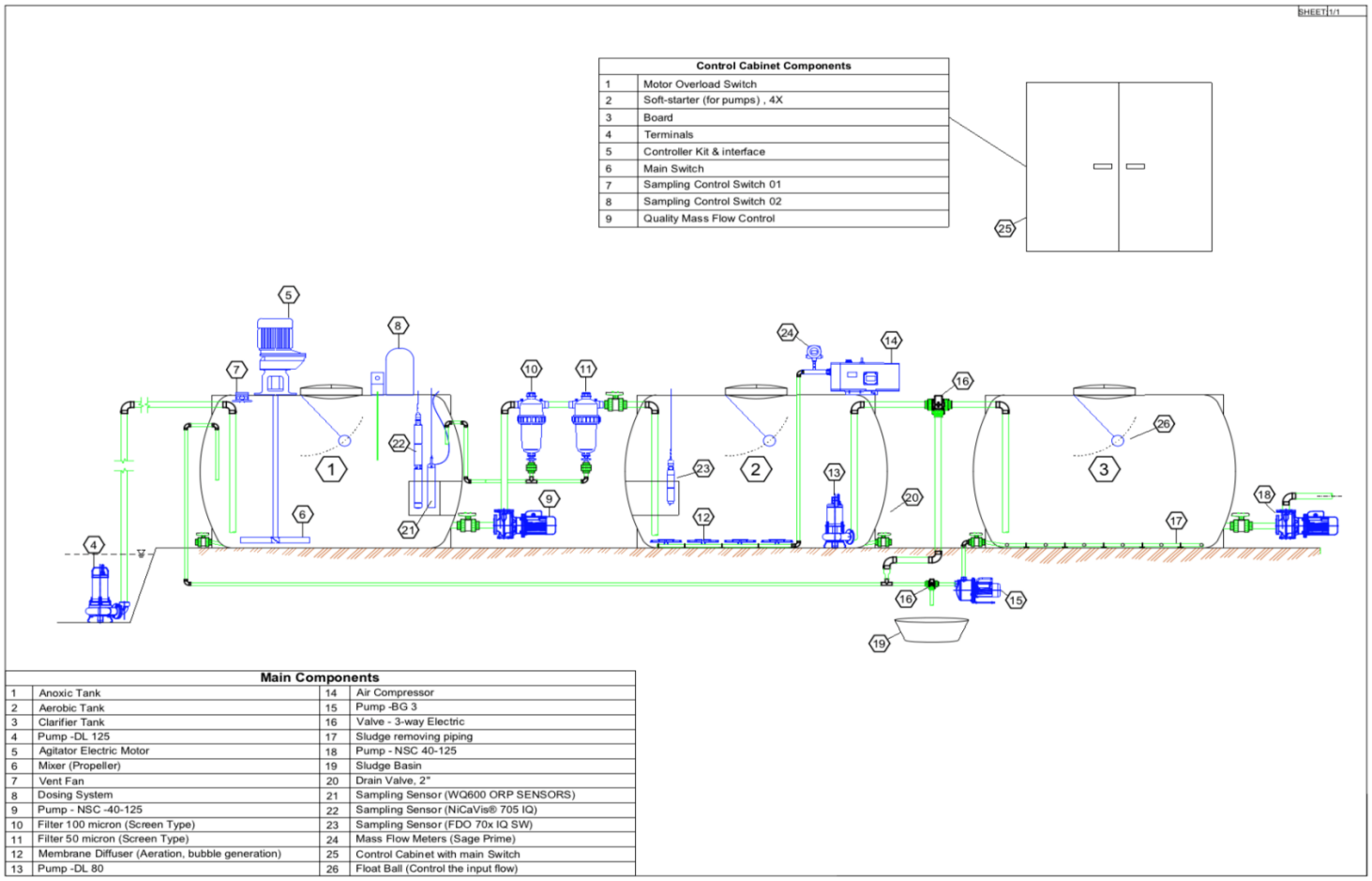

Main Components			
1	Anoxic Tank	14	Air Compressor
2	Aerobic Tank	15	Pump -BG 3
3	Clarifier Tank	16	Valve - 3-way Electric
4	Pump -DL 125	17	Sludge removing piping
5	Agitator Electric Motor	18	Pump - NSC 40-125
6	Mixer (Propeller)	19	Sludge Basin
7	Vent Fan	20	Drain Valve, 2"
8	Dosing System	21	Sampling Sensor (WQ600 ORP SENSORS)
9	Pump - NSC -40-125	22	Sampling Sensor (NiCaVis® 705 IQ)
10	Filter 100 micron (Screen Type)	23	Sampling Sensor (FDO 70x IQ SW)
11	Filter 50 micron (Screen Type)	24	Mass Flow Meters (Sage Prime)
12	Membrane Diffuser (Aeration, bubble generation)	25	Control Cabinet with main Switch
13	Pump -DL 80	26	Float Ball (Control the input flow)

LINCOLN UNIVERSITY
TE WHARE WĀNAKA O AORAKI

Components of SBR Unit

Row	Components	Description	Specification	Quantity	Price (USD)
1	Anoxic Tank	1st Tank	HDPE , Tank Capacity (litres): 3000 Standard Outlet: 2 " LxWxH: 2240 x 1460 x 1470 (mm) Lid (mm): 455	1	1,012.44
2	Aerobic Tank	2nd Tank, Aerating	Same	1	1,012.44
3	Clarifier Tank	3rd Tank, final step	Same	1	1,012.44
4	Pump	Pond to Anoxic Tank	Lowara- DL 125 , Power: 1.5kW Free passage: 50mm DN: 50mm Weight: 27.0kg Unit without floatswitch, fitted with 10 meters of cable and supplied with a 2" discharge elbow DL: Series name 125: Impeller size	1	1,307.39

5	Agitator	in Anoxic Tank	1.0 HP, 240V , 180 RPM, (Motor+Gear+Shaft+Propeller <35 kg)	1	550.00
6	Mixer	in Anoxic Tank	High Density Plastic only (D = 55 cm)	1	65.00
7	Vent Fan	in Anoxic Tank	16x16, 24V	1	95.00
8	Dosing System	in Anoxic Tank	Dosing Pumps, Controller, Probes, Dosing Tanks (with agitator)	1	1,100.00
9	Pump - NSC 40-125	Anoxic Tank to Aeration Tank	Speed: 2900rpm Power: 400V, Three Phase (3~), 50Hz, Power:1.5 kW Weight: 35kg	1	1,357.00
10	Filter (Screen Type)	Anoxic Tank to Aeration Tank	100 micron , 2" T type	1	470.00
11	Filter (Screen Type)	Anoxic Tank to Aeration Tank	50 micoron, 2" T type	1	700.00
12	Membrane Diffuser (Aerating)	in Aeration Tank	9"	5	175.00

13	Pump - DL 80	in Aeration Tank - to Clrifier Tank	Family code: 8C Part No: 107560060XXXUAA Power: 0.6kW Free passage: 45mm DN: 50mm Weight: 19.5kg Unit without floatswitch, fitted with 10 meters of cable DL: Series name 80: Impeller size A: Version Three Phase	1	902.70
14	Air Compressor	in Aeration Tank	DTN 41 ,52.2 m3/hr, Installed motor output [kW] (for Compressor 1.5 kW)	1	3,088.01
15	Pump - BG 3	Clarifier Tank to Anoxic Tank	BG : Series name Three phase (400/3/50) Inlet: Rp 1Â¼, Outlet: Rp 1 Part no: 107320060 0.37kW Weight: 10kg	1	566.40
16	Sludge Removing	in Aeration Tank,	1.3" pipine PE	4	-

17	Pump - NSC 40-125	Clarifier Tank to Farm	Speed: 2900rpm Power: 400V, Three Phase (3~), 50Hz, Power:1.5 kW Weight: 35kg	1	1,357.00
18	Sludge Basin	non-Active Sludge	Portable (is not Issued)	1	-
19	Sampling Unit	in Clarifier Tank		1	20.00
20	Control Cabinet with main switch	Control all mechanical units: - Pumps, (4x) - Agitator (1x) - Compressor, (1) - Valve, (1x) - Dosing system (1x)	Components: - Motor overload Switch - Soft-starter - Board - Terminals - Controller kits & interface - Main switch	1	5,600.00
21	Sensor - Sampling	in Anoxic Tank (input Sampling)	Global Water **WQ600-O ORP** Sensor Output: 4-20 mA ,Range: -500 to +500mV ,Accuracy: 2% of full scale Maximum Pressure: 40 psi, Operating Voltage: 10-36VDC Current Draw: 0.2 mA plus sensor output , Warm Up Time: 3 seconds minimum , Operating Temperature: -40 to +55°C Size: Online: 39.4 cm L x 6.3 cm Dia.(end cap)	1	1,415.32

			Weight: Online: 22 oz (623 g) * Extra Cable is required		
22	Sensor - Sampling	in Anoxic Tank (output Sampling)	**NiCaVis® 705 IQ** **UV IQ sensor for NO2, NO3 and carbons, 1mm** Flow rate ≤ 3 m/s , Pressure Resistance: Maximum 1 bar (incl. sensor connection cable) Electrical connections: 2-wire shield cable with quick fastener to sensor , Electromagnetic Compatibility: EN 61326. Class B. FCC Class A Intended for indispensable operation Certifications: CE , Mechanical: Housing: Titan Grade 2. PEEK, Window: Sapphire glass , Protection class: IP 68 , Weight (without cable): Approx. 8.82 lb (4 kg)	1	30,549.75
23	Sensor - Sampling	in Aeration Tank (DO sensor (Galvanic))	YSI P2030 2030-4 G Pro2030 Field Galvanic DO 4 Meter Dissolved Oxygen % air saturation- 0 to 500% air saturation Dissolved Oxygen (mg/L)-0 to 50 mg/L Conductivity-0 to 200 mS/cm Salinity-0 to 70 ppt Total Dissolved Solids (TDS)-0 to 100 g/L TDS constant range .30 to 1.00 (.65 default) Temperature--5 to 55°C Barometer-500 to 800 mmHg		1,727.00
24	Quality Mass Flow Meters	in Aeration Tank	Sage Prime – Quality Mass Flow Meters	1	1,300.00

25	Valves (Drain)	All Tanks,	PE Ball Valve	5	50.00
26	Valve 3-way Electric	Change way between Sludge Basin & Anoxic Tank	S4 PVC-U Electric Actuator EO510	3	160.00
27	Valve 2-way Electric				
28	Pipe & Fitting	All tank interfaces	2" and 1.3" Depends on arrangement & workshop PE is preferred		450.00
			Inc. Tax	**Total**	**25,493.15 - 56,042.90**

References

Abdala, D. B., Ghosh, A. K., da Silva, I. R., de Novais, R. F., & Venegas, V. H. A. (2012). Phosphorus saturation of a tropical soil and related P leaching caused by poultry litter addition. *Agriculture, ecosystems & environment, 162*, 15-23.

Acevedo, B., Oehmen, A., Carvalho, G., Seco, A., Borrás, L., & Barat, R. (2012). Metabolic shift of polyphosphate-accumulating organisms with different levels of polyphosphate storage. *Water Research, 46*(6), 1889-1900.

Adapa, P. K., Karunakaran, C., Tabil, L. G., & Schoenau, G. J. (2009). Potential applications of infrared and Raman spectromicroscopy for agricultural biomass. *Agricultural Engineering International: CIGR Journal*.

Aghamohammadi, N., bin Abdul Aziz, H., Isa, M. H., & Zinatizadeh, A. A. (2007). Powdered activated carbon augmented activated sludge process for treatment of semi-aerobic landfill leachate using response surface methodology. *Bioresource technology, 98*(18), 3570-3578.

Ahmed, F. N., & Lan, C. Q. (2012). Treatment of landfill leachate using membrane bioreactors: A review. *Desalination, 287*, 41-54.

Alimohammadi, V., Sedighi, M., & Jabbari, E. (2016). Response surface modeling and optimization of nitrate removal from aqueous solutions using magnetic multi-walled carbon nanotubes. *Journal of environmental chemical engineering, 4*(4), 4525-4535.

Anton, J. M. C., Oliver-Villanueva, J. V., Pastor, J. V. T., Jiménez, M. D. R., Romero, J. A. G., & Cuquerella, J. M. (2020). Reduction of Phosphorous from Wastewater Through Adsorption Processes Reusing Wood and Straw Ash Produced in Bioenergy Facilities. *Water, Air, & Soil Pollution, 231*(3), 1-12.

ANZECC, A. (2000). Australian and New Zealand guidelines for fresh and marine water quality. *Australian and New Zealand Environment and Conservation Council and Agriculture and Resource Management Council of Australia and New Zealand, Canberra*, 1-103.

APHA, A. (1998). WEF "Standard methods for the examination of water and wastewater 20th edition". *American Public Health Association, Washington, DC*.

Argun, M. E., Dursun, S., Ozdemir, C., & Karatas, M. (2007). Heavy metal adsorption by modified oak sawdust: Thermodynamics and kinetics. *Journal of hazardous materials, 141*(1), 77-85.

Ashok, V., & Hait, S. (2015). Remediation of nitrate-contaminated water by solid-phase denitrification process—a review. *Environmental Science and Pollution Research, 22*(11), 8075-8093.

Aslan, S., & Turkman, A. (2006). Nitrate and pesticides removal from contaminated water using biodenitrification reactor. *Process Biochemistry, 41*(4), 882-886.

Aziz, S. Q., Aziz, H. A., & Yusoff, M. S. (2011). Optimum process parameters for the treatment of landfill leachate using powdered activated carbon augmented sequencing batch reactor (SBR) technology. *Separation Science and Technology, 46*(15), 2348-2359.

Aziz, S. Q., Aziz, H. A., Yusoff, M. S., & Bashir, M. J. (2011). Landfill leachate treatment using powdered activated carbon augmented sequencing batch reactor (SBR) process: Optimization by response surface methodology. *Journal of hazardous materials, 189*(1-2), 404-413.

Aziz, S. Q., Aziz, H. A., Yusoff, M. S., Mojiri, A., & Amr, S. S. A. (2012). Adsorption isotherms in landfill leachate treatment using powdered activated carbon augmented sequencing batch reactor technique: statistical analysis by response surface methodology. *International Journal of Chemical Reactor Engineering, 10*(1).

Bagherifam, S., Komarneni, S., Lakzian, A., Fotovat, A., Khorasani, R., Huang, W., . . . Wang, Y. (2014). Highly selective removal of nitrate and perchlorate by organoclay. *Applied Clay Science, 95*, 126-132.

Başar, C. A. (2006). Applicability of the various adsorption models of three dyes adsorption onto activated carbon prepared waste apricot. *Journal of hazardous materials, 135*(1-3), 232-241.

Bashar, R., Gungor, K., Karthikeyan, K., & Barak, P. (2018). Cost effectiveness of phosphorus removal processes in municipal wastewater treatment. *Chemosphere, 197*, 280-290.

Beck, M., Robarge, W., & Buol, S. (1999). Phosphorus retention and release of anions and organic carbon by two Andisols. *European journal of soil science, 50*(1), 157-164.

Benyoucef, S., & Amrani, M. (2011). Removal of phosphorus from aqueous solutions using chemically modified sawdust of Aleppo pine (Pinus halepensis Miller): kinetics and isotherm studies. *The Environmentalist, 31*(3), 200-207.

Bhatnagar, A., Kumar, E., & Sillanpää, M. (2010). Nitrate removal from water by nano-alumina: Characterization and sorption studies. *Chemical Engineering Journal, 163*(3), 317-323.

Bishop, J. L., Ethbrampe, E. B., Bish, D. L., Abidin, Z. L., Baker, L. L., Matsue, N., & Henmi, T. (2013). Spectral and hydration properties of allophane and imogolite. *Clays and Clay Minerals, 61*(1), 57-74.

Blossfeld, S., Gansert, D., Thiele, B., Kuhn, A. J., & Lösch, R. (2011). The dynamics of oxygen concentration, pH value, and organic acids in the rhizosphere of Juncus spp. *Soil biology and biochemistry, 43*(6), 1186-1197.

Boers, P., Van der Does, J., Quaak, M., Van der Vlugt, J., & Walker, P. (1992). Fixation of phosphorus in lake sediments using iron (III) chloride: experiences, expectations. In *Restoration and Recovery of Shallow Eutrophic Lake Ecosystems in The Netherlands* (pp. 211-212): Springer.

Borgnino, L., Giacomelli, C. E., Avena, M. J., & De Pauli, C. P. (2010). Phosphate adsorbed on Fe (III) modified montmorillonite: Surface complexation studied by ATR-FTIR spectroscopy. *Colloids and Surfaces A: Physicochemical and Engineering Aspects, 353*(2-3), 238-244.

Borne, K. E. (2014). Floating treatment wetland influences on the fate and removal performance of phosphorus in stormwater retention ponds. *Ecological engineering, 69*, 76-82.

Borne, K. E., Fassman, E. A., & Tanner, C. C. (2013). Floating treatment wetland retrofit to improve stormwater pond performance for suspended solids, copper and zinc. *Ecological engineering, 54*, 173-182.

Bourke, S. A., Iwanyshyn, M., Kohn, J., & Hendry, M. J. (2019). Sources and fate of nitrate in groundwater at agricultural operations overlying glacial sediments. *Hydrology and Earth System Sciences, 23*(3), 1355-1373.

Bouwer, H. (2000). Integrated water management: emerging issues and challenges. *Agricultural water management, 45*(3), 217-228.

Bowes, M., Jarvie, H., Halliday, S. J., Skeffington, R., Wade, A., Loewenthal, M., . . . Palmer-Felgate, E. (2015). Characterising phosphorus and nitrate inputs to a rural river using high-frequency concentration–flow relationships. *Science of the Total Environment, 511*, 608-620.

Bozorgpour, F., Ramandi, H. F., Jafari, P., Samadi, S., Yazd, S. S., & Aliabadi, M. (2016). Removal of nitrate and phosphate using chitosan/Al2O3/Fe3O4 composite nanofibrous adsorbent: comparison with chitosan/Al2O3/Fe3O4 beads. *International journal of biological macromolecules, 93*, 557-565.

Braman, R. S., & Hendrix, S. A. (1989). Nanogram nitrite and nitrate determination in environmental and biological materials by vanadium (III) reduction with chemiluminescence detection. *Analytical chemistry, 61*(24), 2715-2718.

Brenner, A., & Argaman, Y. (1990). Effect of feed composition, aerobic volume fraction and recycle rate on nitrogen removal in the single-sludge system. *Water Research, 24*(8), 1041-1049.

Brettar, I., Labrenz, M., Flavier, S., Bötel, J., Kuosa, H., Christen, R., & Höfle, M. G. (2006). Identification of a Thiomicrospira denitrificans-like epsilonproteobacterium as a catalyst for autotrophic denitrification in the central Baltic Sea. *Appl. Environ. Microbiol., 72*(2), 1364-1372.

Brezonik, P. L. (2013). *Denitrification in natural waters.* Paper presented at the Proceedings of the conference on nitrogen as a water pollutant.

Brown, N., & Shilton, A. (2014). Luxury uptake of phosphorus by microalgae in waste stabilisation ponds: current understanding and future direction. *Reviews in Environmental Science and Bio/Technology, 13*(3), 321-328.

Brown, P., Jefcoat, I. A., Parrish, D., Gill, S., & Graham, E. (2000). Evaluation of the adsorptive capacity of peanut hull pellets for heavy metals in solution. *Advances in Environmental Research, 4*(1), 19-29.

Buj, I., Torras, J., Rovira, M., & de Pablo, J. (2010). Leaching behaviour of magnesium phosphate cements containing high quantities of heavy metals. *Journal of hazardous materials, 175*(1-3), 789-794.

Burghate, S., & Ingole, N. (2014). Biological denitrification-a Review. *J Environ Sci Comput Sci Eng Technol, 14*, 009-028.

Cai, X., Gao, Y., Sun, Q., Chen, Z., Megharaj, M., & Naidu, R. (2014). Removal of co-contaminants Cu (II) and nitrate from aqueous solution using kaolin-Fe/Ni nanoparticles. *Chemical Engineering Journal, 244*, 19-26.

Calabi-Floody, M., Bendall, J. S., Jara, A. A., Welland, M. E., Theng, B. K., Rumpel, C., & de la Luz Mora, M. (2011). Nanoclays from an Andisol: extraction, properties and carbon stabilization. *Geoderma, 161*(3-4), 159-167.

Cao, W., & Zhang, Y. (2014). Removal of nitrogen (N) from hypereutrophic waters by ecological floating beds (EFBs) with various substrates. *Ecological engineering, 62*, 148-152.

Cengeloglu, Y., Tor, A., Ersoz, M., & Arslan, G. (2006). Removal of nitrate from aqueous solution by using red mud. *Separation and Purification Technology, 51*(3), 374-378.

Chatterjee, S., & Woo, S. H. (2009). The removal of nitrate from aqueous solutions by chitosan hydrogel beads. *Journal of hazardous materials, 164*(2-3), 1012-1018.

Chen, D., Dai, T., Wang, H., & Yang, K. (2016). Nitrate removal by a combined bioelectrochemical and sulfur autotrophic denitrification (CBSAD) system at low temperatures. *Desalination and Water Treatment, 57*(41), 19411-19417.

Chen, D., Yang, K., & Wang, H. (2016). Effects of important factors on hydrogen-based autotrophic denitrification in a bioreactor. *Desalination and Water Treatment, 57*(8), 3482-3488.

Chen, Y., Wen, Y., Zhou, J., Tang, Z., Li, L., Zhou, Q., & Vymazal, J. (2014). Effects of cattail biomass on sulfate removal and carbon sources competition in subsurface-flow constructed wetlands treating secondary effluent. *Water Research, 59*, 1-10.

Cheng, I. F., Muftikian, R., Fernando, Q., & Korte, N. (1997). Reduction of nitrate to ammonia by zero-valent iron. *Chemosphere, 35*(11), 2689-2695.

Chitrakar, R., Tezuka, S., Sonoda, A., Sakane, K., Ooi, K., & Hirotsu, T. (2006). Phosphate adsorption on synthetic goethite and akaganeite. *Journal of Colloid and Interface Science, 298*(2), 602-608.

Cho, D.-W., Chon, C.-M., Kim, Y., Jeon, B.-H., Schwartz, F. W., Lee, E.-S., & Song, H. (2011). Adsorption of nitrate and Cr (VI) by cationic polymer-modified granular activated carbon. *Chemical Engineering Journal, 175*, 298-305.

Chu, L., & Wang, J. (2011). Comparison of polyurethane foam and biodegradable polymer as carriers in moving bed biofilm reactor for treating wastewater with a low C/N ratio. *Chemosphere, 83*(1), 63-68.

Creamer, A. E., & Gao, B. (2016). Carbon-based adsorbents for postcombustion CO2 capture: a critical review. *Environmental science & technology, 50*(14), 7276-7289.

Cydzik-Kwiatkowska, A., & Zielińska, M. (2016). Bacterial communities in full-scale wastewater treatment systems. *World Journal of Microbiology and Biotechnology, 32*(4), 66.

Davis, M. (2018). Greenhouse gas emissions from saturated riparian buffers and woodchip bioreactors.

De Stefani, G., Tocchetto, D., Salvato, M., & Borin, M. (2011). Performance of a floating treatment wetland for in-stream water amelioration in NE Italy. *Hydrobiologia, 674*(1), 157-167.

Della Rocca, C., Belgiorno, V., & Meriç, S. (2007). Overview of in-situ applicable nitrate removal processes. *Desalination, 204*(1-3), 46-62.

Demiral, H., & Gündüzoğlu, G. (2010). Removal of nitrate from aqueous solutions by activated carbon prepared from sugar beet bagasse. *Bioresource technology, 101*(6), 1675-1680.

Di Capua, F., Milone, I., Lakaniemi, A.-M., Lens, P. N., & Esposito, G. (2017). High-rate autotrophic denitrification in a fluidized-bed reactor at psychrophilic temperatures. *Chemical Engineering Journal, 313*, 591-598.

Di Capua, F., Pirozzi, F., Lens, P. N., & Esposito, G. (2019). Electron donors for autotrophic denitrification. *Chemical Engineering Journal, 362*, 922-937.

Ding, Y., Sun, W., Yang, W., & Li, Q. (2017). Formic acid as the in-situ hydrogen source for catalytic reduction of nitrate in water by PdAg alloy nanoparticles supported on amine-functionalized SiO2. *Applied Catalysis B: Environmental, 203*, 372-380.

Dodkins, I., & Mendzil, A. (2014). Enterprise Assist: Floating Treatment Wetlands.

Doltabadi, M., Alidadi, H., & Davoudi, M. (2016). Comparative study of cationic and anionic dye removal from aqueous solutions using sawdust-based adsorbent. *Environmental Progress & Sustainable Energy, 35*(4), 1078-1090.

Dong, S., & Wang, Y. (2016). Characterization and adsorption properties of a lanthanum-loaded magnetic cationic hydrogel composite for fluoride removal. *Water Research, 88*, 852-860.

Duyar, A., Ozdemir, S., Akman, D., Akgul, V., Sahinkaya, E., & Cirik, K. (2018). Optimization of sulfide-based autotrophic denitrification process in an anaerobic baffled reactor. *Journal of Chemical Technology & Biotechnology, 93*(3), 754-760.

El Ouardi, M., Qourzal, S., Alahiane, S., Assabbane, A., & Douch, J. (2015). Effective removal of nitrates ions from aqueous solution using new clay as potential low-cost adsorbent. *Journal of Encapsulation and Adsorption Sciences, 5*(04), 178.

Elsheikh, M. A., Matsue, N., & Henmi, T. (2009). Effect of Si/Al ratio of allophane on competitive adsorption of phosphate and oxalate. *International Journal of Soil Science, 4*(1), 1-13.

Elsheikh, M. A., Muchaonyerwa, P., Johan, E., Matsue, N., & Henmi, T. (2018). Mutual Adsorption of Lead and Phosphorus onto Selected Soil Clay Minerals. *Advances in Chemical Engineering and Science, 8*(02), 67.

Ensie, B., & Samad, S. (2014). Removal of nitrate from drinking water using nano SiO2–FeOOH–Fe core–shell. *Desalination, 347*, 1-9.

Environment, N. Z. s. M. f. t. (2017a). Greenhouse gas concentrations. Retrieved from http://archive.stats.govt.nz/browse_for_stats/environment/environmental-reporting-series/environmental-indicators/Home/Atmosphere-and-climate/greenhouse-gas-concentrations.aspx

Environment, N. Z. s. M. f. t. (2017b). Trends in nitrogen leaching from agriculture. http://archive.stats.govt.nz/browse_for_stats/environment/environmental-reporting-series/environmental-indicators/Home/Fresh%20water/nitrogen-leaching-agriculture.aspx

Eroglu, E., Agarwal, V., Bradshaw, M., Chen, X., Smith, S. M., Raston, C. L., & Iyer, K. S. (2012). Nitrate removal from liquid effluents using microalgae immobilized on chitosan nanofiber mats. *Green Chemistry, 14*(10), 2682-2685.

Feng, Q., Wang, Y., Wang, T., Zheng, H., Chu, L., Zhang, C., . . . Xing, X.-H. (2012). Effects of packing rates of cubic-shaped polyurethane foam carriers on the microbial community and the removal of organics and nitrogen in moving bed biofilm reactors. *Bioresource technology, 117*, 201-207.

Fernández, E., Grilli, A., Alvarez, D., & Aravena, R. (2017). Evaluation of nitrate levels in groundwater under agricultural fields in two pilot areas in central Chile: a hydrogeological and geochemical approach. *Hydrological Processes, 31*(6), 1206-1224.

Fewtrell, L. (2004). Drinking-water nitrate, methemoglobinemia, and global burden of disease: a discussion. *Environmental health perspectives, 112*(14), 1371-1374.

Foo, K., & Hameed, B. (2009). An overview of landfill leachate treatment via activated carbon adsorption process. *Journal of hazardous materials, 171*(1-3), 54-60.

Foote, K. J., Joy, M. K., & Death, R. G. (2015). New Zealand dairy farming: milking our environment for all its worth. *Environmental management, 56*(3), 709-720.

Fu, C.-C., Tran, H. N., Chen, X.-H., & Juang, R.-S. (2020). Preparation of polyaminated Fe3O4@ chitosan core-shell magnetic nanoparticles for efficient adsorption of phosphate in aqueous solutions. *Journal of Industrial and Engineering Chemistry, 83*, 235-246.

Fu, F., Dionysiou, D. D., & Liu, H. (2014). The use of zero-valent iron for groundwater remediation and wastewater treatment: a review. *Journal of hazardous materials, 267*, 194-205.

Gao, Q., Wang, C.-Z., Liu, S., Hanigan, D., Liu, S.-T., & Zhao, H.-Z. (2019). Ultrafiltration membrane microreactor (MMR) for simultaneous removal of nitrate and phosphate from water. *Chemical Engineering Journal, 355*, 238-246.

Gao, Y., Zhang, W., Gao, B., Jia, W., Miao, A., Xiao, L., & Yang, L. (2018). Highly efficient removal of nitrogen and phosphorus in an electrolysis-integrated horizontal subsurface-flow constructed wetland amended with biochar. *Water Research, 139*, 301-310.

George, A., Radhakrishnan, K., & Nair, A. J. (2018). Adsorption of perchlorate using cationic modified rice husk. In *Emerging Trends in Engineering, Science and Technology for Society, Energy and Environment* (pp. 573-578): CRC Press.

Gieseke, A., Arnz, P., Amann, R., & Schramm, A. (2002). Simultaneous P and N removal in a sequencing batch biofilm reactor: insights from reactor-and microscale investigations. *Water Research, 36*(2), 501-509.

Giwa, A., Dufour, V., Al Marzooqi, F., Al Kaabi, M., & Hasan, S. (2017). Brine management methods: Recent innovations and current status. *Desalination, 407*, 1-23.

Greenan, C. M., Moorman, T. B., Parkin, T. B., Kaspar, T. C., & Jaynes, D. B. (2009). Denitrification in wood chip bioreactors at different water flows. *Journal of Environmental Quality, 38*(4), 1664-1671.

GROUNDWATER, B. O. (2013). INTRODUCTION TO IN SITU BIOREMEDIATION OF GROUNDWATER.

Guan, X., Sun, Y., Qin, H., Li, J., Lo, I. M., He, D., & Dong, H. (2015). The limitations of applying zero-valent iron technology in contaminants sequestration and the corresponding countermeasures: the development in zero-valent iron technology in the last two decades (1994–2014). *Water Research, 75*, 224-248.

Günther, S., Trutnau, M., Kleinsteuber, S., Hause, G., Bley, T., Röske, I., . . . Müller, S. (2009). Dynamics of polyphosphate-accumulating bacteria in wastewater treatment plant microbial communities detected via DAPI (4', 6'-diamidino-2-phenylindole) and tetracycline labeling. *Appl. Environ. Microbiol., 75*(7), 2111-2121.

Gustafsson, J. P., Mwamila, L. B., & Kergoat, K. (2012). The pH dependence of phosphate sorption and desorption in Swedish agricultural soils. *Geoderma, 189*, 304-311.

Hagemann, N., Kammann, C. I., Schmidt, H.-P., Kappler, A., & Behrens, S. (2017). Nitrate capture and slow release in biochar amended compost and soil. *PloS one, 12*(2), e0171214.

Haghseresht, F., Wang, S., & Do, D. (2009). A novel lanthanum-modified bentonite, Phoslock, for phosphate removal from wastewaters. *Applied Clay Science, 46*(4), 369-375.

Hamlin, H., Michaels, J., Beaulaton, C., Graham, W., Dutt, W., Steinbach, P., . . . Main, K. (2008). Comparing denitrification rates and carbon sources in commercial scale upflow denitrification biological filters in aquaculture. *Aquacultural engineering, 38*(2), 79-92.

Hanrahan, G. (2010). *Modelling of pollutants in complex environmental systems* (Vol. 2): ILM Publications.

Hashem, A., Akasha, R., Ghith, A., & Hussein, D. (2007). Adsorbent based on agricultural wastes for heavy metal and dye removal: A review. *Energy Educ. Sci. Technol, 19*, 69-86.

Hashimoto, Y., Kang, J., Matsuyama, N., & Saigusa, M. (2012). Path analysis of phosphorus retention capacity in allophanic and non-allophanic andisols. *Soil Science Society of America Journal, 76*(2), 441-448.

He, Q., Chen, L., Zhang, S., Wang, L., Liang, J., Xia, W., . . . Zhou, J. (2018). Simultaneous nitrification, denitrification and phosphorus removal in aerobic granular sequencing batch reactors with high aeration intensity: Impact of aeration time. *Bioresource technology, 263*, 214-222.

He, S., Huang, Q., Zhang, Y., Wang, L., & Nie, Y. (2015). Investigation on direct and indirect electrochemical oxidation of ammonia over Ru–Ir/TiO2 anode. *Industrial & Engineering Chemistry Research, 54*(5), 1447-1451.

He, Y., Lin, H., Dong, Y., Li, B., Wang, L., Chu, S., . . . Liu, J. (2018). Zeolite supported Fe/Ni bimetallic nanoparticles for simultaneous removal of nitrate and phosphate: synergistic effect and mechanism. *Chemical Engineering Journal, 347*, 669-681.

Headley, T., & Tanner, C. C. (2012). Constructed wetlands with floating emergent macrophytes: an innovative stormwater treatment technology. *Critical Reviews in Environmental Science and Technology, 42*(21), 2261-2310.

Henmi, T., & Huang, P. (1985). Removal of phosphorus by poorly ordered clays as influenced by heating and grinding. *Applied Clay Science, 1*(1-2), 133-144.

Hewitt, A. E. (2010). New Zealand soil classification. *Landcare research science series*(1).

Hiemstra, T., & Van Riemsdijk, W. H. (1996). A surface structural approach to ion adsorption: the charge distribution (CD) model. *Journal of Colloid and Interface Science, 179*(2), 488-508.

Holan, Z., & Volesky, B. (1994). Biosorption of lead and nickel by biomass of marine algae. *Biotechnology and Bioengineering, 43*(11), 1001-1009.

Hu, Z., Srinivasan, M., & Ni, Y. (2001). Novel activation process for preparing highly microporous and mesoporous activated carbons. *Carbon, 39*(6), 877-886.

Huang, W., Chen, J., He, F., Tang, J., Li, D., Zhu, Y., & Zhang, Y. (2015). Effective phosphate adsorption by Zr/Al-pillared montmorillonite: insight into equilibrium, kinetics and thermodynamics. *Applied Clay Science, 104*, 252-260.

Huang, Y.-T., Lowe, D. J., Churchman, G. J., Schipper, L. A., Cursons, R., Zhang, H., . . . Cooper, A. (2016). DNA adsorption by nanocrystalline allophane spherules and nanoaggregates, and implications for carbon sequestration in Andisols. *Applied Clay Science, 120*, 40-50.

Huang, Y. H., & Zhang, T. C. (2004). Effects of low pH on nitrate reduction by iron powder. *Water Research, 38*(11), 2631-2642.

Hubbard, R. K. (2010). Floating vegetated mats for improving surface water quality. In *Emerging Environmental Technologies, Volume II* (pp. 211-244): Springer.

Huno, S. K., Rene, E. R., van Hullebusch, E. D., & Annachhatre, A. P. (2018). Nitrate removal from groundwater: a review of natural and engineered processes. *Journal of Water Supply: Research and Technology-Aqua, 67*(8), 885-902.

Ige, D., Akinremi, O., & Flaten, D. (2007). Direct and indirect effects of soil properties on phosphorus retention capacity. *Soil Science Society of America Journal, 71*(1), 95-100.

Isoyama, M., & Wada, S.-I. (2007). Remediation of Pb-contaminated soils by washing with hydrochloric acid and subsequent immobilization with calcite and allophanic soil. *Journal of hazardous materials, 143*(3), 636-642.

Iyoda, F., Hayashi, S., Arakawa, S., John, B., Okamoto, M., Hayashi, H., & Yuan, G. (2012). Synthesis and adsorption characteristics of hollow spherical allophane nano-particles. *Applied Clay Science, 56*, 77-83.

Jabari, P., Munz, G., & Oleszkiewicz, J. A. (2014). Selection of denitrifying phosphorous accumulating organisms in IFAS systems: comparison of nitrite with nitrate as an electron acceptor. *Chemosphere, 109*, 20-27.

Ji, H., Wu, W., Li, F., Yu, X., Fu, J., & Jia, L. (2017). Enhanced adsorption of bromate from aqueous solutions on ordered mesoporous Mg-Al layered double hydroxides (LDHs). *Journal of hazardous materials, 334*, 212-222.

Jiang, H., Chen, P., Luo, S., Tu, X., Cao, Q., & Shu, M. (2013). Synthesis of novel nanocomposite Fe3O4/ZrO2/chitosan and its application for removal of nitrate and phosphate. *Applied Surface Science, 284*, 942-949.

Johan, E., Matsu, N., & Henmi, T. (1997). Phosphate adsorption on nano-ball allophane and its molecular orbital analysis. *Clay science, 10*(3), 259-270.

Justin, P., & Kelly, D. (1978). Growth kinetics of Thiobacillus denitrificans in anaerobic and aerobic chemostat culture. *Microbiology, 107*(1), 123-130.

Kalaruban, M., Loganathan, P., Shim, W., Kandasamy, J., Naidu, G., Nguyen, T. V., & Vigneswaran, S. (2016). Removing nitrate from water using iron-modified Dowex 21K XLT ion exchange resin: Batch and fluidised-bed adsorption studies. *Separation and Purification Technology, 158*, 62-70.

Kang, D., Yu, X., & Ge, M. (2017). Morphology-dependent properties and adsorption performance of CeO2 for fluoride removal. *Chemical Engineering Journal, 330*, 36-43.

Kang, J., Hesterberg, D., & Osmond, D. L. (2009). Soil organic matter effects on phosphorus sorption: a path analysis. *Soil Science Society of America Journal, 73*(2), 360-366.

Kapoor, A., & Viraraghavan, T. (1997). Nitrate removal from drinking water. *Journal of environmental engineering, 123*(4), 371-380.

Karan, S., Kidmose, J., Engesgaard, P., Nilsson, B., Frandsen, M., Ommen, D., . . . Pedersen, O. (2014). Role of a groundwater–lake interface in controlling seepage of water and nitrate. *Journal of hydrology, 517*, 791-802.

Karanasios, K., Vasiliadou, I., Pavlou, S., & Vayenas, D. (2010). Hydrogenotrophic denitrification of potable water: a review. *Journal of hazardous materials, 180*(1-3), 20-37.

Kasama, T., Watanabe, Y., Yamada, H., & Murakami, T. (2004). Sorption of phosphates on Al-pillared smectites and mica at acidic to neutral pH. *Applied Clay Science, 25*(3-4), 167-177.

Keizer-Vlek, H. E., Verdonschot, P. F., Verdonschot, R. C., & Dekkers, D. (2014). The contribution of plant uptake to nutrient removal by floating treatment wetlands. *Ecological engineering, 73*, 684-690.

Kelso, B. H., Smith, R. V., & Laughlin, R. J. (1999). Effects of carbon substrates on nitrite accumulation in freshwater sediments. *Appl. Environ. Microbiol., 65*(1), 61-66.

Kesaano, M., & Sims, R. C. (2014). Algal biofilm based technology for wastewater treatment. *Algal Research, 5*, 231-240.

Keshvardoostchokami, M., Babaei, S., Piri, F., & Zamani, A. (2017). Nitrate removal from aqueous solutions by ZnO nanoparticles and chitosan-polystyrene–Zn nanocomposite: Kinetic, isotherm, batch and fixed-bed studies. *International journal of biological macromolecules, 101*, 922-930.

Khajeh, M., Laurent, S., & Dastafkan, K. (2013). Nanoadsorbents: classification, preparation, and applications (with emphasis on aqueous media). *Chemical reviews, 113*(10), 7728-7768.

Khalil, A. M., Eljamal, O., Amen, T. W., Sugihara, Y., & Matsunaga, N. (2017). Optimized nano-scale zero-valent iron supported on treated activated carbon for enhanced nitrate and phosphate removal from water. *Chemical Engineering Journal, 309*, 349-365.

Khanal, S. K. (2008). Biohydrogen production: Fundamentals, challenges, and operation strategies for enhanced yield. *Anaerobic biotechnology for bioenergy production: principles and applications*, 189-219.

Khayyun, T. S., & Mseer, A. H. (2019). Comparison of the experimental results with the Langmuir and Freundlich models for copper removal on limestone adsorbent. *Applied Water Science, 9*(8), 170.

Khosravi, R., Eslami, H., Zarei, A., Heidari, M., Baghani, A. N., Safavi, N., . . . Adhami, S. (2018). Comparative evaluation of nitrate adsorption from aqueous solutions using green and red local montmorillonite adsorbents. *Desalination and Water Treatment, 116*, 119-128.

Kim, B.-K., Baek, K., & Yang, J.-W. (2004). Simultaneous removal of nitrate and phosphate using cross-flow micellar-enhanced ultrafiltration (MEUF). *Water Science and Technology, 50*(6), 227-234.

Kim, J.-H., Guo, X., & Park, H.-S. (2008). Comparison study of the effects of temperature and free ammonia concentration on nitrification and nitrite accumulation. *Process Biochemistry, 43*(2), 154-160.

Kim, Y.-S., Lee, Y.-H., An, B., Choi, S.-A., Park, J.-H., Jurng, J.-S., . . . Choi, J.-W. (2012). Simultaneous removal of phosphate and nitrate in wastewater using high-capacity anion-exchange resin. *Water, Air, & Soil Pollution, 223*(9), 5959-5966.

King, A., Boyle, D., Jensen, V., Fogg, G., & Harter, T. (2012). Groundwater Remediation and Management for Nitrate (Technical Report 5). In *Addressing Nitrate in California's Drinking Water with*

a Focus on Tulare Lake Basin and Salinas Valley Groundwater. Report for the State Water Resources Control Board Report to the Legislature: Center for Watershed Sciences, University of California Davis.

Koilraj, P., & Kannan, S. (2010). Phosphate uptake behavior of ZnAlZr ternary layered double hydroxides through surface precipitation. *Journal of Colloid and Interface Science, 341*(2), 289-297.

Kookana, R. S., Sarmah, A. K., Van Zwieten, L., Krull, E., & Singh, B. (2011). Biochar application to soil: agronomic and environmental benefits and unintended consequences. In *Advances in agronomy* (Vol. 112, pp. 103-143): Elsevier.

Krapp, A., David, L. C., Chardin, C., Girin, T., Marmagne, A., Leprince, A.-S., . . . Daniel-Vedele, F. (2014). Nitrate transport and signalling in Arabidopsis. *Journal of experimental botany, 65*(3), 789-798.

Kumar, P. S., Prot, T., Korving, L., Keesman, K. J., Dugulan, I., van Loosdrecht, M. C., & Witkamp, G.-J. (2017). Effect of pore size distribution on iron oxide coated granular activated carbons for phosphate adsorption–Importance of mesopores. *Chemical Engineering Journal, 326*, 231-239.

Kurniawan, T. A., Lo, W.-h., & Chan, G. Y. (2006). Physico-chemical treatments for removal of recalcitrant contaminants from landfill leachate. *Journal of hazardous materials, 129*(1-3), 80-100.

Kurt, M., Dunn, I., & Bourne, J. (1987). Biological denitrification of drinking water using autotrophic organisms with H2 in a fluidized-bed biofilm reactor. *Biotechnology and Bioengineering, 29*(4), 493-501.

Kuzawa, K., Jung, Y.-J., Kiso, Y., Yamada, T., Nagai, M., & Lee, T.-G. (2006). Phosphate removal and recovery with a synthetic hydrotalcite as an adsorbent. *Chemosphere, 62*(1), 45-52.

Kyambadde, J., Kansiime, F., Gumaelius, L., & Dalhammar, G. (2004). A comparative study of Cyperus papyrus and Miscanthidium violaceum-based constructed wetlands for wastewater treatment in a tropical climate. *Water Research, 38*(2), 475-485.

Landry, C. J., Koretsky, C. M., Lund, T. J., Schaller, M., & Das, S. (2009). Surface complexation modeling of Co (II) adsorption on mixtures of hydrous ferric oxide, quartz and kaolinite. *Geochimica et Cosmochimica Acta, 73*(13), 3723-3737.

Langmuir, D. (1997). Aqueous environmental. *Geochemistry Prentice Hall: Upper Saddle River, NJ*.

Lata, S., Singh, P., & Samadder, S. (2015). Regeneration of adsorbents and recovery of heavy metals: a review. *International Journal of Environmental Science and Technology, 12*(4), 1461-1478.

Lee, H. S., & Volesky, B. (1997). Interaction of light metals and protons with seaweed biosorbent. *Water Research, 31*(12), 3082-3088.

Lee, K.-C., & Rittmann, B. E. (2002). Applying a novel autohydrogenotrophic hollow-fiber membrane biofilm reactor for denitrification of drinking water. *Water Research, 36*(8), 2040-2052.

Lee, S. Y., Choi, J.-W., Song, K. G., Choi, K., Lee, Y. J., & Jung, K.-W. (2019). Adsorption and mechanistic study for phosphate removal by rice husk-derived biochar functionalized with Mg/Al-calcined layered double hydroxides via co-pyrolysis. *Composites Part B: Engineering, 176*, 107209.

Lehmann, J., & Joseph, S. (2009). Biochar systems. *Biochar for Environmental Management: Science and Technology*, 147-181.

Levard, C., Doelsch, E., Basile-Doelsch, I., Abidin, Z., Miche, H., Masion, A., . . . Bottero, J.-Y. (2012). Structure and distribution of allophanes, imogolite and proto-imogolite in volcanic soils. *Geoderma, 183*, 100-108.

Lew, B., Stief, P., Beliavski, M., Ashkenazi, A., Svitlica, O., Khan, A., . . . Green, M. (2012). Characterization of denitrifying granular sludge with and without the addition of external carbon source. *Bioresource technology, 124*, 413-420.

Li, R., Morrison, L., Collins, G., Li, A., & Zhan, X. (2016). Simultaneous nitrate and phosphate removal from wastewater lacking organic matter through microbial oxidation of pyrrhotite coupled to nitrate reduction. *Water Research, 96*, 32-41.

Li, R., Wang, J. J., Zhou, B., Awasthi, M. K., Ali, A., Zhang, Z., . . . Mahar, A. (2016). Enhancing phosphate adsorption by Mg/Al layered double hydroxide functionalized biochar with different Mg/Al ratios. *Science of the Total Environment, 559*, 121-129.

Li, W., & Li, Z. (2009). In situ nutrient removal from aquaculture wastewater by aquatic vegetable Ipomoea aquatica on floating beds. *Water Science and Technology, 59*(10), 1937-1943.

Lin, Y.-F., Jing, S.-R., Lee, D.-Y., & Wang, T.-W. (2002). Nutrient removal from aquaculture wastewater using a constructed wetlands system. *Aquaculture, 209*(1-4), 169-184.

Lin, Y. F., Jing, S. R., Lee, D. Y., & Wang, T. W. (2002). Removal of Solids and Oxygen Demand from Aquaculture Wastewater with a Constructed Wetland System in the Start-Up Phase. *Water Environment Research, 74*(2), 136-141.

Lithner, D., Larsson, Å., & Dave, G. (2011). Environmental and health hazard ranking and assessment of plastic polymers based on chemical composition. *Science of the Total Environment, 409*(18), 3309-3324.

Liu, C., Shi, W., Li, H., Lei, Z., He, L., & Zhang, Z. (2014). Improvement of methane production from waste activated sludge by on-site photocatalytic pretreatment in a photocatalytic anaerobic fermenter. *Bioresource technology, 155*, 198-203.

Liu, H., Li, M., Chen, T., Chen, C., Alharbi, N. S., Hayat, T., . . . Sun, Y. (2017). New synthesis of nZVI/C composites as an efficient adsorbent for the uptake of U (VI) from aqueous solutions. *Environmental science & technology, 51*(16), 9227-9234.

Liu, J., Cao, J., Hu, Y., Han, Y., & Zhou, J. (2017). Adsorption of phosphate ions from aqueous solutions by a CeO2 functionalized Fe3O4@ SiO2 core-shell magnetic nanomaterial. *Water Science and Technology, 76*(11), 2867-2875.

Liu, W.-T. (2006). Nanoparticles and their biological and environmental applications. *Journal of bioscience and bioengineering, 102*(1), 1-7.

Loe, B. (2012). *Estimating nitrogen and phosphorous contributions to water from discharges that are consented and permitted activities under NRRP* (R12/18). Retrieved from https://api.ecan.govt.nz/TrimPublicAPI/documents/download/3857470

Lürling, M., & van Oosterhout, F. (2013). Case study on the efficacy of a lanthanum-enriched clay (Phoslock®) in controlling eutrophication in Lake Het Groene Eiland (The Netherlands). *Hydrobiologia, 710*(1), 253-263.

Machida, M., Yoo, P., & Amano, Y. (2019). Adsorption of nitrate from aqueous phase onto nitrogen-doped activated carbon fibers (ACFs). *SN Applied Sciences, 1*(4), 323.

Macht, F., Eusterhues, K., Pronk, G. J., & Totsche, K. U. (2011). Specific surface area of clay minerals: Comparison between atomic force microscopy measurements and bulk-gas (N2) and-liquid (EGME) adsorption methods. *Applied Clay Science, 53*(1), 20-26.

Mahvi, A. H., Mesdaghinia, A., & Karakani, F. (2004). Feasibility of continuous flow sequencing batch reactor in domestic wastewater treatment. *American J App Sci, 1*(4), 348-353.

Malakootian, M., Yaghmaeian, K., Hashemi, S. Y., & Farpoor, M. H. (2019). Evaluation of Clay Soil Efficacy Carrying Zero-Valent Iron Nanoparticles to Remove Nitrate From Aqueous Solutions. *Journal of Water Chemistry and Technology, 41*(1), 29-35.

Manciu, M., & Ruckenstein, E. (2003). Specific ion effects via ion hydration: I. Surface tension. *Advances in colloid and interface science, 105*(1-3), 63-101.

Martin, H. G., Ivanova, N., Kunin, V., Warnecke, F., Barry, K. W., McHardy, A. C., . . . Szeto, E. (2006). Metagenomic analysis of two enhanced biological phosphorus removal (EBPR) sludge communities. *Nature biotechnology, 24*(10), 1263-1269.

Mazarji, M., Aminzadeh, B., Baghdadi, M., & Bhatnagar, A. (2017). Removal of nitrate from aqueous solution using modified granular activated carbon. *Journal of Molecular Liquids, 233*, 139-148.

Mckay, G., Blair, H., & Gardner, J. (1982). Adsorption of dyes on chitin. I. Equilibrium studies. *Journal of applied polymer science, 27*(8), 3043-3057.

Mdlalose, L., Balogun, M., Setshedi, K., Chimuka, L., & Chetty, A. (2019). Adsorption of phosphates using transition metals-modified bentonite clay. *Separation Science and Technology, 54*(15), 2397-2408.

Meis, S., Spears, B. M., Maberly, S. C., O'Malley, M. B., & Perkins, R. G. (2012). Sediment amendment with Phoslock® in Clatto Reservoir (Dundee, UK): investigating changes in sediment elemental composition and phosphorus fractionation. *Journal of environmental management, 93*(1), 185-193.

Mena-Duran, C., Kou, M. S., Lopez, T., Azamar-Barrios, J., Aguilar, D., Dominguez, M., . . . Quintana, P. (2007). Nitrate removal using natural clays modified by acid thermoactivation. *Applied Surface Science, 253*(13), 5762-5766.

Mielcarek, A., Rodziewicz, J., Janczukowicz, W., & Thornton, A. (2015). The feasibility of citric acid as external carbon source for biological phosphorus removal in a sequencing batch biofilm reactor (SBBR). *Biochemical Engineering Journal, 93*, 102-107.

Mirkin, C. A., Letsinger, R. L., Mucic, R. C., & Storhoff, J. J. (1996). A DNA-based method for rationally assembling nanoparticles into macroscopic materials. *Nature, 382*(6592), 607-609.

Mohajeri, P., Smith, C., Selamat, M., & Abdul Aziz, H. (2018). Enhancing the adsorption of lead (II) by bentonite enriched with pH-adjusted meranti sawdust. *Water, 10*(12), 1875.

Mohajeri, P., Smith, C. M., Chau, H. W., & Lehto, N. (2020). Powdered ALLODUST/ALLOCHAR Augmented Single Batch Aerobic Reactor (SiBAR) for High Concentration Phosphorous Removal from Agricultural Wastewater. *Journal of Water Process Engineering, 36*, 101301.

Mohajeri, P., Smith, C. M., Chau, H. W., Lehto, N., Azimi, A., & Farraji, H. (2019). Adsorption behavior of Na-bentonite and nano cloisite Na+ in interaction with Pb (NO3) 2 and Cu (NO3) 2· 3H2O contamination in landfill liners: Optimization by response surface methodology. *Journal of environmental chemical engineering, 7*(6), 103449.

Mohan, D., Sarswat, A., Ok, Y. S., & Pittman Jr, C. U. (2014). Organic and inorganic contaminants removal from water with biochar, a renewable, low cost and sustainable adsorbent–a critical review. *Bioresource technology, 160*, 191-202.

Mohseni-Bandpi, A., Elliott, D. J., & Zazouli, M. A. (2013). Biological nitrate removal processes from drinking water supply-a review. *Journal of environmental health science and engineering, 11*(1), 35.

Mohsenipour, M., Shahid, S., & Ebrahimi, K. (2015). Nitrate adsorption on clay kaolin: batch tests. *Journal of Chemistry, 2015*.

Mojiri, A., Aziz, H. A., Zaman, N. Q., Aziz, S. Q., & Zahed, M. A. (2014). Powdered ZELIAC augmented sequencing batch reactors (SBR) process for co-treatment of landfill leachate and domestic wastewater. *Journal of environmental management, 139*, 1-14.

Mojiri, A., & Branch, I. K. (2011). Review on membrane bioreactor, ion exchange and adsorption methods for landfill leachate treatment. *Aust. J. Basic Appl. Sci, 5*(12), 136.

Moon, H. S., Chang, S. W., Nam, K., Choe, J., & Kim, J. Y. (2006). Effect of reactive media composition and co-contaminants on sulfur-based autotrophic denitrification. *Environmental pollution, 144*(3), 802-807.

Mubita, T., Dykstra, J., Biesheuvel, P., Van Der Wal, A., & Porada, S. (2019). Selective adsorption of nitrate over chloride in microporous carbons. *Water Research, 164*, 114885.

Murphy, J., & Riley, J. P. (1962). A modified single solution method for the determination of phosphate in natural waters. *Analytica chimica acta, 27*, 31-36.

Muthu, M., Ramachandran, D., Hasan, N., Jeevanandam, M., Gopal, J., & Chun, S. (2017). Unprecedented nitrate adsorption efficiency of carbon-silicon nano composites prepared from bamboo leaves. *Materials Chemistry and Physics, 189*, 12-21.

Myhre, G., Shindell, D., Bréon, F.-M., Collins, W., Fuglestvedt, J., Huang, J., . . . Mendoza, B. (2013). Anthropogenic and natural radiative forcing. *Climate change, 423*, 658-740.

Nabbou, N., Belhachemi, M., Boumelik, M., Merzougui, T., Lahcene, D., Harek, Y., . . . Jeguirim, M. (2019). Removal of fluoride from groundwater using natural clay (kaolinite): optimization of adsorption conditions. *Comptes Rendus Chimie, 22*(2-3), 105-112.

Neupane, G., & Donahoe, R. J. (2013). Leachability of elements in alkaline and acidic coal fly ash samples during batch and column leaching tests. *Fuel, 104*, 758-770.

Nguyen, T. M. P., Van, H. T., Nguyen, T. V., Ha, L., Vu, X. H., Pham, T., . . . Nguyen, X. (2020). Phosphate Adsorption by Silver Nanoparticles-Loaded Activated Carbon derived from Tea Residue. *Scientific Reports, 10*(1), 1-13.

Nguyen, T. T., Ngo, H. H., & Guo, W. (2013). Pilot scale study on a new membrane bioreactor hybrid system in municipal wastewater treatment. *Bioresource technology, 141*, 8-12.

Nicholls, H., & Osborn, D. (1979). Bacterial stress: prerequisite for biological removal of phosphorus. *Journal (Water Pollution Control Federation)*, 557-569.

Nodeh, H. R., Sereshti, H., Afsharian, E. Z., & Nouri, N. (2017). Enhanced removal of phosphate and nitrate ions from aqueous media using nanosized lanthanum hydrous doped on magnetic graphene nanocomposite. *Journal of environmental management, 197*, 265-274.

Nunell, G. V., Fernandez, M. E., Bonelli, P. R., & Cukierman, A. L. (2015). Nitrate uptake improvement by modified activated carbons developed from two species of pine cones. *Journal of Colloid and Interface Science, 440*, 102-108.

Obiri-Nyarko, F., Grajales-Mesa, S. J., & Malina, G. (2014). An overview of permeable reactive barriers for in situ sustainable groundwater remediation. *Chemosphere, 111*, 243-259.

Oehmen, A., Lemos, P. C., Carvalho, G., Yuan, Z., Keller, J., Blackall, L. L., & Reis, M. A. (2007). Advances in enhanced biological phosphorus removal: from micro to macro scale. *Water Research, 41*(11), 2271-2300.

Oh, S., Yoo, Y., Young, J., & Kim, I. (2001). Effect of organics on sulfur-utilizing autotrophic denitrification under mixotrophic conditions. *Journal of biotechnology, 92*(1), 1-8.

Omotosho, O. (2016). Mitigation of nitrate pollution in wastewater: A case study of the treatment of cassava processing effluent using cassava peel carbon material. *International Journal of Environmental, Chemical, Ecological, Geological and Geophysical Engineering, 9*, 399-404.

Opiso, E., Sato, T., & Yoneda, T. (2009). Adsorption and co-precipitation behavior of arsenate, chromate, selenate and boric acid with synthetic allophane-like materials. *Journal of hazardous materials, 170*(1), 79-86.

Organization, W. H. (2003). *Nitrate and nitrite in drinking-water: Background document for development of WHO Guidelines for Drinking-water Quality*. Retrieved from

Ota, K., Amano, Y., Aikawa, M., & Machida, M. (2013). Removal of nitrate ions from water by activated carbons (ACs)—influence of surface chemistry of ACs and coexisting chloride and sulfate ions. *Applied Surface Science, 276*, 838-842.

Pachauri, R. K., Allen, M. R., Barros, V. R., Broome, J., Cramer, W., Christ, R., . . . Dasgupta, P. (2014). *Climate change 2014: synthesis report. Contribution of Working Groups I, II and III to the fifth assessment report of the Intergovernmental Panel on Climate Change*: IPCC.

Padilla, G. N., Matsue, Naoto, & Henmi, T. (2002). Adsorption of sulfate and nitrate on nano-ball allophane. *Clay science, 11*(6), 575-584.

Palko, J. W., Oyarzun, D. I., Ha, B., Stadermann, M., & Santiago, J. G. (2018). Nitrate removal from water using electrostatic regeneration of functionalized adsorbent. *Chemical Engineering Journal, 334*, 1289-1296.

Pan, J., Gao, B., Song, W., Xu, X., Jin, B., & Yue, Q. (2019). Column adsorption and regeneration study of magnetic biopolymer resin for perchlorate removal in presence of nitrate and phosphate. *Journal of Cleaner Production, 213*, 762-775.

Parfitt, R. L., Furkert, R., & Henmi, T. (1980). Identification and structure of two types of allophane from volcanic ash soils and tephra. *Clays and Clay Minerals, 28*(5), 328-334.

Park, D., Yun, Y.-S., Jo, J. H., & Park, J. M. (2006). Biosorption process for treatment of electroplating wastewater containing Cr (VI): Laboratory-scale feasibility test. *Industrial & Engineering Chemistry Research, 45*(14), 5059-5065.

Parsa, M., Razip, b. S. M., Abdul, A. H., Hossein, V. A., & Hossein, F. (2019). Geoenvironmental behaviour of lead-contaminated clay with sawdust. *Environmental Geotechnics, 6*(7), 450-459. doi:10.1680/jenge.16.00030

Pearce, B. J., & Chertow, M. (2017). Scenarios for achieving absolute reductions in phosphorus consumption in Singapore. *Journal of Cleaner Production, 140*, 1587-1601.

Pietrzak, R., Wachowska, H., & Nowicki, P. (2006). Preparation of nitrogen-enriched activated carbons from brown coal. *Energy & fuels, 20*(3), 1275-1280.

Prado, B., Duwig, C., Escudey, M., & Esteves, M. (2006). Nitrate Sorption in a Mexican allophanic andisol using intact and packed columns. *Communications in soil science and plant analysis, 37*(15-20), 2911-2925.

Ra, C., Lo, K., Shin, J., Oh, J., & Hong, B. (2000). Biological nutrient removal with an internal organic carbon source in piggery wastewater treatment. *Water Research, 34*(3), 965-973.

Rahimi, Y., Torabian, A., Mehrdadi, N., & Shahmoradi, B. (2011). Simultaneous nitrification–denitrification and phosphorus removal in a fixed bed sequencing batch reactor (FBSBR). *Journal of hazardous materials, 185*(2-3), 852-857.

Rajeswari, A., Amalraj, A., & Pius, A. (2016). Adsorption studies for the removal of nitrate using chitosan/PEG and chitosan/PVA polymer composites. *Journal of Water Process Engineering, 9*, 123-134.

Ravishankara, A., Daniel, J. S., & Portmann, R. W. (2009). Nitrous oxide (N2O): the dominant ozone-depleting substance emitted in the 21st century. *science, 326*(5949), 123-125.

Reitzel, K., Andersen, F. Ø., Egemose, S., & Jensen, H. S. (2013). Phosphate adsorption by lanthanum modified bentonite clay in fresh and brackish water. *Water Research, 47*(8), 2787-2796.

Reitzel, K., Jensen, H. S., & Egemose, S. (2013). pH dependent dissolution of sediment aluminum in six Danish lakes treated with aluminum. *Water Research, 47*(3), 1409-1420.

Rennert, T., Eusterhues, K., Hiradate, S., Breitzke, H., Buntkowsky, G., Totsche, K. U., & Mansfeldt, T. (2014). Characterisation of Andosols from Laacher See tephra by wet-chemical and spectroscopic techniques (FTIR, 27Al-, 29Si-NMR). *Chemical Geology, 363*, 13-21.

Revitt, D., Shutes, R., Llewellyn, N., & Worrall, P. (1997). Experimental reedbed systems for the treatment of airport runoff. *Water Science and Technology, 36*(8-9), 385-390.

Rezvani, F., Sarrafzadeh, M.-H., Ebrahimi, S., & Oh, H.-M. (2019). Nitrate removal from drinking water with a focus on biological methods: a review. *Environmental Science and Pollution Research, 26*(2), 1124-1141.

Rivera-Utrilla, J., Bautista-Toledo, I., Ferro-García, M. A., & Moreno-Castilla, C. (2001). Activated carbon surface modifications by adsorption of bacteria and their effect on aqueous lead adsorption. *Journal of Chemical Technology & Biotechnology, 76*(12), 1209-1215.

Robb, M., Greenop, B., Goss, Z., Douglas, G., & Adeney, J. (2003). Application of Phoslock TM, an innovative phosphorus binding clay, to two Western Australian waterways: preliminary findings. In *The Interactions between Sediments and Water* (pp. 237-243): Springer.

Robertson, W. (2010). Nitrate removal rates in woodchip media of varying age. *Ecological engineering, 36*(11), 1581-1587.

Rodrıguez, J., Castrillon, L., Maranon, E., Sastre, H., & Fernandez, E. (2004). Removal of non-biodegradable organic matter from landfill leachates by adsorption. *Water Research, 38*(14-15), 3297-3303.

Ross, G., Haghseresht, F., & Cloete, T. E. (2008). The effect of pH and anoxia on the performance of Phoslock®, a phosphorus binding clay. *Harmful algae, 7*(4), 545-550.

Rouquerol, J., Rouquerol, F., Llewellyn, P., Maurin, G., & Sing, K. S. (2013). *Adsorption by powders and porous solids: principles, methodology and applications*: Academic press.

Russell, M., Parfitt, R., & Claridge, G. (1981). Estimation of the amounts of allophane and other materials in the clay fraction of an Egmont loam profile and other volcanic ash soils, New Zealand. *Soil Research, 19*(3), 185-195.

Saeed, T., & Sun, G. (2012). A review on nitrogen and organics removal mechanisms in subsurface flow constructed wetlands: dependency on environmental parameters, operating conditions and supporting media. *Journal of environmental management, 112*, 429-448.

Sakakibara, Y., & Kuroda, M. (1993). Electric prompting and control of denitrification. *Biotechnology and Bioengineering, 42*(4), 535-537.

Salam, M. A., Fageeh, O., Al-Thabaiti, S. A., & Obaid, A. Y. (2015). Removal of nitrate ions from aqueous solution using zero-valent iron nanoparticles supported on high surface area nanographenes. *Journal of Molecular Liquids, 212*, 708-715.

Sanchez Gomez, C., & Minamisawa, K. (2019). Nitrogen cycling in soybean rhizosphere: Sources and sinks of nitrous oxide (N2O). *Frontiers in microbiology, 10*, 1943.

Sanjay, M., Amit, D., & Mukherjee, S. (2013). Applications of adsorption process for treatment of landfill leachate. *Journal of Environmental Research and Development, 8*(2), 365.

Santana-Mayor, Á., Rodríguez-Ramos, R., Socas-Rodríguez, B., Asensio-Ramos, M., & Rodríguez-Delgado, M. Á. (2020). Carbon-based adsorbents. In *Solid-Phase Extraction* (pp. 83-127): Elsevier.

Schipper, L. A., Robertson, W. D., Gold, A. J., Jaynes, D. B., & Cameron, S. C. (2010). Denitrifying bioreactors—an approach for reducing nitrate loads to receiving waters. *Ecological engineering, 36*(11), 1532-1543.

Schmidt, C. A., & Clark, M. W. (2012). Efficacy of a denitrification wall to treat continuously high nitrate loads. *Ecological engineering, 42*, 203-211.

Seitzinger, S., Mayorga, E., Bouwman, A., Kroeze, C., Beusen, A., Billen, G., . . . Garnier, J. (2010). Global river nutrient export: A scenario analysis of past and future trends. *Global Biogeochemical Cycles, 24*(4).

Seliem, M. K., Komarneni, S., Byrne, T., Cannon, F. S., Shahien, M., Khalil, A., & El-Gaid, I. A. (2013). Removal of nitrate by synthetic organosilicas and organoclay: Kinetic and isotherm studies. *Separation and Purification Technology, 110*, 181-187.

Shoji, S., & Ono, T. (1978). Physical and chemical properties and clay mineralogy of Andosols from Kitakami, Japan. *Soil Science, 126*(5), 297-312.

Shrimali, M., & Singh, K. (2001). New methods of nitrate removal from water. *Environmental pollution, 112*(3), 351-359.

Shukla, A., Zhang, Y.-H., Dubey, P., Margrave, J., & Shukla, S. S. (2002). The role of sawdust in the removal of unwanted materials from water. *Journal of hazardous materials, 95*(1-2), 137-152.

Shuval, H. I., & Gruener, N. (2013). *Infant methemoglobinemia and other health effects of nitrates in drinking water.* Paper presented at the Proceedings of the Conference on Nitrogen as a Water Pollutant.

Smith, M., Cross, K., Paden, M., & Laban, P. (2016). Spring–Managing groundwater sustainably. *IUCN, Gland, Switzerland*.

Soares, M. (2000). Biological denitrification of groundwater. *Water, Air, and Soil Pollution, 123*(1-4), 183-193.

Sowmya, A., Das, D., Prabhakar, S., Kumar, M. M., Anbalagan, K., & Rajesh, M. (2019). Adsorption of perchlorate from water using quaternary ammonium-functionalized chitosan beads. *Environmental Progress & Sustainable Energy*, e13325.

Spangler, J. T., Sample, D. J., Fox, L. J., Albano, J. P., & White, S. A. (2019). Assessing nitrogen and phosphorus removal potential of five plant species in floating treatment wetlands receiving simulated nursery runoff. *Environmental Science and Pollution Research, 26*(6), 5751-5768.

Sposito, G. (1984). *The surface chemistry of soils*: Oxford university press.

Stewart, F. M., Muholland, T., Cunningham, A. B., Kania, B. G., & Osterlund, M. T. (2008). Floating islands as an alternative to constructed wetlands for treatment of excess nutrients from agricultural and municipal wastes–results of laboratory-scale tests. *Land Contamination & Reclamation, 16*(1), 25-33.

Stumm, W. (1992). *Chemistry of the solid-water interface: processes at the mineral-water and particle-water interface in natural systems*: John Wiley & Son Inc.

Stumm, W., & Morgan, J. J. (2012). *Aquatic chemistry: chemical equilibria and rates in natural waters* (Vol. 126): John Wiley & Sons.

Su, Y., Cui, H., Li, Q., Gao, S., & Shang, J. K. (2013). Strong adsorption of phosphate by amorphous zirconium oxide nanoparticles. *Water Research, 47*(14), 5018-5026.

Sun, S., Liu, J., Zhang, M., & He, S. (2020). Thiosulfate-driven autotrophic and mixotrophic denitrification processes for secondary effluent treatment: Reducing sulfate production and nitrous oxide emission. *Bioresource technology, 300*, 122651.

Tanner, C. C., & Headley, T. R. (2011). Components of floating emergent macrophyte treatment wetlands influencing removal of stormwater pollutants. *Ecological engineering, 37*(3), 474-486.

Taşkın, E. G., & Cuci, Y. (2019). Removal of Nitrate from Groundwater Using a Hydrogen-Based Membrane Biofilm Reactor: The Effects of Hydrogen Pressure and Hydraulic Retention Time. *J. BIOL. ENVIRON. SCI, 13*(38), 101-106.

Teimouri, A., Nasab, S. G., Vahdatpoor, N., Habibollahi, S., Salavati, H., & Chermahini, A. N. (2016). Chitosan/Zeolite Y/Nano ZrO2 nanocomposite as an adsorbent for the removal of nitrate from the aqueous solution. *International journal of biological macromolecules, 93*, 254-266.

Thakur, I. S., & Medhi, K. (2019). Nitrification and denitrification processes for mitigation of nitrous oxide from waste water treatment plants for biovalorization: Challenges and opportunities. *Bioresource technology*.

Tian, S., Jiang, P., Ning, P., & Su, Y. (2009). Enhanced adsorption removal of phosphate from water by mixed lanthanum/aluminum pillared montmorillonite. *Chemical Engineering Journal, 151*(1-3), 141-148.

Tofighy, M. A., & Mohammadi, T. (2012). Nitrate removal from water using functionalized carbon nanotube sheets. *Chemical Engineering Research and Design, 90*(11), 1815-1822.

Tsai, W.-T., & Jiang, T.-J. (2018). Mesoporous activated carbon produced from coconut shell using a single-step physical activation process. *Biomass Conversion and Biorefinery, 8*(3), 711-718.

Tyagi, S., Rawtani, D., Khatri, N., & Tharmavaram, M. (2018). Strategies for nitrate removal from aqueous environment using nanotechnology: a review. *Journal of Water Process Engineering, 21*, 84-95.

Uçar, D., Çokgör, E. U., & Şahinkaya, E. (2016). Evaluation of nitrate and perchlorate reduction using sulfur-based autotrophic and mixotrophic denitrifying processes. *Water Science and Technology: Water Supply, 16*(1), 208-218.

USEPA. (2013). INTRODUCTION TO IN SITU BIOREMEDIATION OF GROUNDWATER.

Van Duzer, C. A. (2004). *Floating Islands: A Global Bibliography: with an Edition and Translation of GC Munz's Exercitatio Academica de Insulis Natantibus (1711)*: Cantor Press.

Van Loosdrecht, M., Hooijmans, C., Brdjanovic, D., & Heijnen, J. (1997). Biological phosphate removal processes. *Applied Microbiology and Biotechnology, 48*(3), 289-296.

van Oosterhout, F., & Lürling, M. (2013). The effect of phosphorus binding clay (Phoslock®) in mitigating cyanobacterial nuisance: a laboratory study on the effects on water quality variables and plankton. *Hydrobiologia, 710*(1), 265-277.

Vasiliadou, I., Pavlou, S., & Vayenas, D. (2006). A kinetic study of hydrogenotrophic denitrification. *Process Biochemistry, 41*(6), 1401-1408.

Vopel, K., Gibbs, M., Hickey, C., & Quinn, J. (2009). Modification of sediment–water solute exchange by sediment-capping materials: effects on O2 and pH. *Marine and Freshwater Research, 59*(12), 1101-1110.

Vymazal, J. (2007). Removal of nutrients in various types of constructed wetlands. *Science of the Total Environment, 380*(1-3), 48-65.

Wada, S.-I., & Wada, K. (1977). Density and structure of allophane. *Clay Minerals, 12*(4), 289-298.

Walcarius, A., & Mercier, L. (2010). Mesoporous organosilica adsorbents: nanoengineered materials for removal of organic and inorganic pollutants. *Journal of Materials Chemistry, 20*(22), 4478-4511.

Wan, D., Liu, H., Liu, R., Qu, J., Li, S., & Zhang, J. (2012). Adsorption of nitrate and nitrite from aqueous solution onto calcined (Mg–Al) hydrotalcite of different Mg/Al ratio. *Chemical Engineering Journal, 195*, 241-247.

Wang, C.-Y., Sample, D. J., Day, S. D., & Grizzard, T. J. (2015). Floating treatment wetland nutrient removal through vegetation harvest and observations from a field study. *Ecological engineering, 78*, 15-26.

Wang, L., Tsang, D. C., & Poon, C.-S. (2015). Green remediation and recycling of contaminated sediment by waste-incorporated stabilization/solidification. *Chemosphere, 122*, 257-264.

Wang, T., Lin, J., Chen, Z., Megharaj, M., & Naidu, R. (2014). Green synthesized iron nanoparticles by green tea and eucalyptus leaves extracts used for removal of nitrate in aqueous solution. *Journal of Cleaner Production, 83*, 413-419.

Wang, X., Xing, L., Qiu, T., & Han, M. (2013). Simultaneous removal of nitrate and pentachlorophenol from simulated groundwater using a biodenitrification reactor packed with corncob. *Environmental Science and Pollution Research, 20*(4), 2236-2243.

Wang, X.-J., Xia, S.-Q., Chen, L., Zhao, J.-F., Renault, N., & Chovelon, J.-M. (2006). Nutrients removal from municipal wastewater by chemical precipitation in a moving bed biofilm reactor. *Process Biochemistry, 41*(4), 824-828.

Wang, Z., Fei, X., He, S., Huang, J., & Zhou, W. (2017). Comparison of heterotrophic and autotrophic denitrification processes for treating nitrate-contaminated surface water. *Science of the Total Environment, 579*, 1706-1714.

Wei, S., Tan, W., Liu, F., Zhao, W., & Weng, L. (2014). Surface properties and phosphate adsorption of binary systems containing goethite and kaolinite. *Geoderma, 213*, 478-484.

Weigelhofer, G., & Hein, T. (2015). Efficiency and detrimental side effects of denitrifying bioreactors for nitrate reduction in drainage water. *Environmental Science and Pollution Research, 22*(17), 13534-13545.

Wen, Y., Chen, Y., Zheng, N., Yang, D., & Zhou, Q. (2010). Effects of plant biomass on nitrate removal and transformation of carbon sources in subsurface-flow constructed wetlands. *Bioresource technology, 101*(19), 7286-7292.

Weragoda, S., Jinadasa, K., Zhang, D. Q., Gersberg, R. M., Tan, S. K., Tanaka, N., & Jern, N. W. (2012). Tropical application of floating treatment wetlands. *Wetlands, 32*(5), 955-961.

White, S. A., & Cousins, M. M. (2013). Floating treatment wetland aided remediation of nitrogen and phosphorus from simulated stormwater runoff. *Ecological engineering, 61*, 207-215.

WHO, C. D. (1985). Health hazards from nitrates in drinking-water.

Wilhelm, R., & Beam, P. (1999). Understanding variation in partition coefficient, Kd, values. *Environmental Protection Agency (EPA), Washington, DC*.

Winston, R. J., Hunt, W. F., Kennedy, S. G., Merriman, L. S., Chandler, J., & Brown, D. (2013). Evaluation of floating treatment wetlands as retrofits to existing stormwater retention ponds. *Ecological engineering, 54*, 254-265.

Wu, T. Y., Mohammad, A. W., Jahim, J. M., & Anuar, N. (2009). A holistic approach to managing palm oil mill effluent (POME): Biotechnological advances in the sustainable reuse of POME. *Biotechnology Advances, 27*(1), 40-52.

Xia, F., Yang, H., Li, L., Ren, Y., Shi, D., Chai, H., . . . Gu, L. (2019). Enhanced nitrate adsorption by using cetyltrimethylammonium chloride pre-loaded activated carbon. *Environmental technology*, 1-11.

Xu, J., Pu, Y., Qi, W.-K., Yang, X. J., Tang, Y., Wan, P., & Fisher, A. (2017). Chemical removal of nitrate from water by aluminum-iron alloys. *Chemosphere, 166*, 197-202.

Xu, R., Tian, H., Pan, S., Prior, S. A., Feng, Y., Batchelor, W. D., . . . Yang, J. (2019). Global ammonia emissions from synthetic nitrogen fertilizer applications in agricultural systems: Empirical and process-based estimates and uncertainty. *Global change biology, 25*(1), 314-326.

Xue, Y., Hou, H., & Zhu, S. (2009). Characteristics and mechanisms of phosphate adsorption onto basic oxygen furnace slag. *Journal of hazardous materials, 162*(2-3), 973-980.

Yan, L.-g., Xu, Y.-y., Yu, H.-q., Xin, X.-d., Wei, Q., & Du, B. (2010). Adsorption of phosphate from aqueous solution by hydroxy-aluminum, hydroxy-iron and hydroxy-iron–aluminum pillared bentonites. *Journal of hazardous materials, 179*(1-3), 244-250.

Yan, X., Wang, D., Zhang, H., Zhang, G., & Wei, Z. (2013). Organic amendments affect phosphorus sorption characteristics in a paddy soil. *Agriculture, ecosystems & environment, 175*, 47-53.

Yang, H., He, K., Lu, D., Wang, J., Xu, D., Jin, Z., . . . Chen, J. (2020). Removal of phosphate by aluminum-modified clay in a heavily polluted lake, Southwest China: Effectiveness and ecological risks. *Science of the Total Environment, 705*, 135850.

Yang, X., Chen, X., & Yang, X. (2019). Effect of organic matter on phosphorus adsorption and desorption in a black soil from Northeast China. *Soil and Tillage Research, 187*, 85-91.

Yang, X., Wan, Y., Zheng, Y., He, F., Yu, Z., Huang, J., . . . Gao, B. (2019). Surface functional groups of carbon-based adsorbents and their roles in the removal of heavy metals from aqueous solutions: a critical review. *Chemical Engineering Journal*.

Yang, Y., Zheng, Z., Ji, W., Yang, M., Ding, Q., & Zhang, X. (2019). The study of bromate adsorption onto magnetic ion exchange resin: Optimization using response surface methodology. *Surfaces and Interfaces, 17*, 100385.

Yidana, S. M., Banoeng-Yakubo, B., Aliou, A.-S., & Akabzaa, T. M. (2012). Groundwater quality in some Voltaian and Birimian aquifers in northern Ghana—application of mulitvariate statistical methods and geographic information systems. *Hydrological sciences journal, 57*(6), 1168-1183.

Yin, H., Yan, X., & Gu, X. (2017). Evaluation of thermally-modified calcium-rich attapulgite as a low-cost substrate for rapid phosphorus removal in constructed wetlands. *Water Research, 115*, 329-338.

Yin, Q., Ren, H., Wang, R., & Zhao, Z. (2018). Evaluation of nitrate and phosphate adsorption on Al-modified biochar: Influence of Al content. *Science of the Total Environment, 631*, 895-903.

Yin, Q., Wang, R., & Zhao, Z. (2018). Application of Mg–Al-modified biochar for simultaneous removal of ammonium, nitrate, and phosphate from eutrophic water. *Journal of Cleaner Production, 176*, 230-240.

Yoon, S.-Y., Lee, C.-G., Park, J.-A., Kim, J.-H., Kim, S.-B., Lee, S.-H., & Choi, J.-W. (2014). Kinetic, equilibrium and thermodynamic studies for phosphate adsorption to magnetic iron oxide nanoparticles. *Chemical Engineering Journal, 236*, 341-347.

Yoshino, H., Tokumura, M., & Kawase, Y. (2014). Simultaneous removal of nitrate, hydrogen peroxide and phosphate in semiconductor acidic wastewater by zero-valent iron. *Journal of Environmental Science and Health, Part A, 49*(9), 998-1006.

Youssef, A., Radwan, N., Abdel-Gawad, I., & Singer, G. (2005). Textural properties of activated carbons from apricot stones. *Colloids and Surfaces A: Physicochemical and Engineering Aspects, 252*(2-3), 143-151.

Zeng, R. J., Saunders, A. M., Yuan, Z., Blackall, L. L., & Keller, J. (2003). Identification and comparison of aerobic and denitrifying polyphosphate-accumulating organisms. *Biotechnology and Bioengineering, 83*(2), 140-148.

Zeng, Y., Walker, H., & Zhu, Q. (2017). Reduction of nitrate by NaY zeolite supported Fe, Cu/Fe and Mn/Fe nanoparticles. *Journal of hazardous materials, 324*, 605-616.

Zhang, B., Zhou, W., Zhao, H., Tian, Z., Li, F., & Wu, Y. (2016). Stabilization/solidification of lead in MSWI fly ash with mercapto functionalized dendrimer Chelator. *Waste Management, 50*, 105-112.

ZHANG, H., JIN, Z.-h., Lu, H., & QIN, C.-h. (2006). Synthesis of nanoscale zero-valent iron supported on exfoliated graphite for removal of nitrate. *Transactions of Nonferrous Metals Society of China, 16*, s345-s349.

Zhang, L., Wang, Z., Xu, X., Chen, C., Gao, B., & Xiao, X. (2019). Insights into the phosphate adsorption behavior onto 3D self-assembled cellulose/graphene hybrid nanomaterials embedded with bimetallic hydroxides. *Science of the Total Environment, 653*, 897-907.

Zhang, L., Zhou, Q., Liu, J., Chang, N., Wan, L., & Chen, J. (2012). Phosphate adsorption on lanthanum hydroxide-doped activated carbon fiber. *Chemical Engineering Journal, 185*, 160-167.

Zhang, Y., Wei, D., Morrison, L., Ge, Z., Zhan, X., & Li, R. (2019). Nutrient removal through pyrrhotite autotrophic denitrification: Implications for eutrophication control. *Science of the Total Environment, 662*, 287-296.

Zhang, Z., Han, Y., Xu, C., Ma, W., Han, H., Zheng, M., . . . Ma, W. (2018). Microbial nitrate removal in biologically enhanced treated coal gasification wastewater of low COD to nitrate ratio by coupling biological denitrification with iron and carbon micro-electrolysis. *Bioresource technology, 262*, 65-73.

Zhou, W., Sun, Y., Wu, B., Zhang, Y., Huang, M., Miyanaga, T., & Zhang, Z. (2011). Autotrophic denitrification for nitrate and nitrite removal using sulfur-limestone. *Journal of Environmental Sciences, 23*(11), 1761-1769.